LIVERPOOL POLYTECHNIC

DEPARTMENT OF PHYSICS

THESIS FOR THE DEGREE OF DOCTOR OF PHILOSOPHY

The Effect of Wind Turbulence on Noise Barrier Performance

Geoffrey William Burrows, B.Sc.

July 1985

This thesis is submitted to the Council for
National Academic Awards in partial fulfilment
of the requirements for the degree of
Doctor of Philosophy

Course of Advanced Studies

Whilst registered as a candidate for the degree for which this thesis is submitted, the author was not a registered candidate or enrolled student for another award of the CNAA or other institution.

In order to gain knowledge in subject areas related to this thesis, the following courses and conferences were attended.

Time Series Analysis Course
(ISVR, Southampton: September, 1981)

Microprocessor Applications in Acoustics
(Open University: July, 1980)

Institute of Acoustics Autumn Conference
(Windermere: 1979, 1980, 1984)

Outdoor Sound Propagation Conference
(Bedford College: March, 1982)

Constant Temperature Anememotery Course
(Cranfield Institute of Technology: May, 1981)

CONTENTS

Figure index v
Abstract viii

1 Introduction 1

1.1 Reasons for Present Work (p1)
1.2 Thesis Structure (p2)

2 Theorectical Aspects of Outdoor Sound Propagation (Excluding Meteorological Effects) 4

2.1 Horizontal Sound Propagation over Open Ground (p4)
2.1.1 Ground Effects - The Shadow Zone
2.1.2 Interfernce Effects
2.1.3 The Ground Wave
2.2 Barrier Effects (p12)
2.2.1 Transmission through the Barrier
2.2.2 Diffraction over the Barrier
(a) The semi-infinite Thin Screen
(b) Thin Screen Resting on a Rigid Surface
(c) Screen on Absorptive Surfaces
(d) Wedge shaped barriers and thick barriers
2.3 Resume (p27)

3 The Present state of knowledge of Meteorological Effects on Outdoor Sound Propagation 28

3.1 Bulk Effects of Wind (p28)
3.2 Bulk Effects of Temperature (p28)
3.3 Vertical Wind Gradients (p29)
3.3.1 The Effect of Vertical Wind Gradients on Unobstructed Sound Propagation
3.3.2 The Effects of Vertical Wind Gradients on Barrier Performance
3.4 Vertical Temperature Gradients (p33)
3.5 Microstructure of the Wind (p34)
3.5.1 Wind Turbulence Effects on Unobstructed Sound Propagation
3.5.2 The Effect of Wind Turbulence on Barrier Performance
3.6 The Microstructure of Air Temperature (p36)
3.7 Resume (p36)

4 The Experimental Design 38

4.1 General Design Requirements (p38)
4.1.1 Summary
4.2 Realisation of the Measurement Requirements (p43)
4.2.1 Geometrical Aspects
4.2.2 The Source Signal
4.2.3 The Acoustic Source
4.2.4 Microphone Measurement
4.2.5 Recording of the Acoustic Signals
4.2.6 Calibration of the Acoustic System
4.2.7 Wind Velocity Measurement
4.2.8 Wind Direction Determination
4.2.9 Air Temperature Measurement
4.2.10 Mobile Laboratory

4.3 Microphone Control (p49)
4.3.1 Microcomputer Interface Development
4.3.2 Software Development
4.4 Alternative Measurement Methods (p51)
4.5 Implications of the above for Scale Model Work (p53)

5 Details of the Measurement System 54

5.1 Source Signal (p54)
5.1.1 The Electronic Noise Generator
5.1.2 The Pure Tone Source
5.1.3 The Random Pure Tone Source
5.2 The Sound Source (p57)
5.2.1 The Loudspeaker
5.2.2 Equaliser
5.2.3 The Signal Gate
5.2.4 The Power Amplifier
5.2.5 The Band Pass Filter
5.3 Microphone Channels (p63)
5.3.1 The Autoranging Device
5.3.2 Automatic Operation of the Microphone Filters
5.4 The Twin Channel Capture Device (p66)
5.5 Anemometer (p68)
5.1.1 Digitisation of the Anemometer Signal
5.6 Wind Direction Indicator (p70)
5.7 The Electronic Thermometer (p71)
5.8 Overall Control of the Automatic Measurement System (p71)
5.9 Calculations (p76)
5.9.1 Sound Pressure Levels
5.9.2 Wind Speeds
5.9.3 Wind Turbulence
5.9.4 Wind Direction
5.9.5 Air Temperature
5.10 Data Storage (p81)

6 Validation of Measurement System 84
6.1 Acoustical Measurements (p84)
6.1.1 Calculation Software
6.1.2 Electrical Test Signals
6.1.3 Acoustical Signals
6.2 Meteorological Measurements (p100)
6.2.1 The Anemometer
6.2.2 Wind Direction Sensor
6.2.3 Electronic Thermometer

7 Modification of the Measurement System for Model Work 109

7.1 Modifications to the Acoustical System (p109)
7.2 Modifications to the Meteorological System (p110)
7.3 Additional Tests Required for Model Work (p110)
7.3.1 Measuring the Point Source Origin of a loudspeaker
7.3.2 Polar Diagrams
7.4 Validation of Automated Acoustical Measurements at Model Work (p121)
7.5 Choice of Covering for the Model Floor (p121)
7.5.1 Determination of Amplitude and Phase Changes on Reflection

8 Experiments 135

8.1 Field Experiments (p135)
8.1.1 Location
8.1.2 Open Propagation
8.1.3 Barrier Experiments
8.1.4 Use of a Tape Recorder with the Automatic Measurement System
8.2 Model Experiments (p165)
8.2.1 Modelling Wind Conditions
8.2.2 Construction
8.2.3 Model Procedures

9 The Results of Full Scale Experiments 151

10 The Results of Model Scale Experiments 177

11 Analysis of Results 186

11.1 Analysis Techniques (p186)
11.1.1 PET printouts
11.1.2 The DEC-20 Computer
11.1.3 The GENSTAT Package
11.1.4 Inspection of Graphical Representations
11.2 Analysis of Full Scale Results (p192)
11.2.1 Visible Trends and Tendencies in the Graphical Results of Chapter 9
11.2.2 A Study of the high turbulence level difference
11.2.2.1 Open Propagation
11.2.2.2 Barrier Present (Octave Bands)
11.2.2.3 Barrier Present (Pure Tones and Random Pure Tones)
11.2.3 The Observed Scatter of Level Difference Measurements
11.2.3.1 Low Turbulence Scatter ranges (unobstructed propagation/octave bands of noise)
11.2.3.2 Low turbulence Scatter Range (Barrier Present/Octave Bands of Noise/Source and Receivers above ground)
11.2.3.3 Low Turbulence Scatter Range (Barrier Present/Octave Bands of Noise/Source and Far Microphone at Ground Level)
11.2.3.4 Low Turbulence Scatter Range (Barrier Present/Pure Tones)
11.2.3.5 Low Turbulence Scatter Range (Barrier Present/Random Pure Tones)
11.2.4 Resume of the Observations Discussed in 11.2
11.2.5 Model Scale Results
11.2.5.1 Asymptotic Level Difference
11.2.5.2 Low Turbulence Limit of Level Difference Scatter

12 Conclusions and Suggestions for Further Work 217

12.1 Source/Receiver Grometries (p217)
12.2 Development of the Anemometry (p218)
12.3 Temperature Turbulence (p219)
12.4 The Use of an Impulse Sound Source (p219)
12.5 Air Turbulence in the Model (p220)
12.6 Computer Prediction of Observed Effects (p220)

References 221

Acknowledgements 225

Appendix A Control of Measurement Equipment 226

A.1 The Sound Source (p226)
A.1.2 The Band Pass Filter
A.1.3 The Electronic Gate
A.1.4 The Attenuator
A.2 The Digital Event Recorder (p230)
A.2.1 The Kemo Analogue Memory
A.2.2 The Datalab DL901 Transient Event Recorder
A.3 The Wind Direction Indicator (p241)
A.4 The Electronic Thermometer (p243)
A.5 Microcomputer Control of the PIA's (p244)

Appendix B Microcomputer Control of the PIA's 247

B.1 The MSC 6522 (p247)
B.1.1 The Processor Interface
B.1.2 The Peripheral Interface
B.1.3 In-built Features
B.2 The MCS 6532 (p260)

Appendix C Hot Wire Probe Calibration 261

Appendix D Typical Raw Data Printouts 263

Appendix E Programme Listing 275

FIGURE INDEX

2.1	Propagation Close to the ground (p5)
2.2	Excess Attenuation for propagation from a point source over mown grass(p9)
2.3	Semi-infinite thin screen(p18)
2.4	Four possible ray paths for a thin screen on a rigid ground (p18)
2.5	Thin screen grometrical parameters for Embleton's equation (p21)
2.6	Makaewa's Equivalet Screen (p24)
2.7	Pierce's Equivalent Barrier (p24)
2.8	Kurze's Wide Barrier approach (p26)
3.1	Variation of wind velocity and temperature in the vicinity of a flat ground surface (up to 10m) (p30)
3.2(a)	Refraction downward, (b) Refraction upward (p30)
3.3	DeJong - Stusnick wind effect model (p32)
4.1	Geometries used for Outdoor Experiments (p44)
4.2	Number of Captured Wavelengths (p45)
4.3	The Automatic Measurement System Block Diagram (p52)
5.1	Noise Generator Circuit Diagram (p55)
5.2	Sound Source Block Diagram (p58)
5.3	The Equadiser Circuit (p60)
5.4	Power Amplifier (p62)
5.5	Comparison of two VBF 22/05 filters with B&K Third octave filter set and ANSI Class III standard (p64)
5.6	Filter Set Solenoid Circuit Diagram (p67)
5.7	Wind Direction Sensor (a) Internal View (b) Showing Protective Cover and Battery Box (pp72-73)
5.8	Temperature Sensor Circuit Diagram (p74)
5.9	Flowchart for the RMS routine (p77)
5.10	Memory Map of Commodore System (By Blocks) (p82)
6.1	Integration Limits for standard deviation calculations (p87)
6.2	Standard deviation of pure tones with random phases (p89)
6.3	Sequence of Development of Automatic Acoustical Measurement System (p91)
6.4	Standard Deviation of 356 RMS levels vs. No. of waves measured, For continuous Octave Bands of Noise (Electrical) (p92)
6.5	Electrical Test Signal Standard Deviation Resuts (p94)
6.6	Standard Deviation of 256 RMS levels vs. No. of waves measured, For Gated Octave noise bands (Electrical) (p96)
6.7	Electrical Test Signal RMS Results (p97)
6.8	Standard Deviation vs. No. of waves captured for continuous Octave. Bands of Electrical Noise with Equaliser in Circuit (p98)
6.9	Instrumentation for Acoustic Tests at Leyland (p101)
6.10	Geometries for Acoustic Tests at Leyland (p102)
6.11	Standard Deviation of 256 RMS levels vs. No. of waves for Gated octave noise bands (Acoustical) (p103)
6.12	Anemometer Comparisons (p105)
7.1	On-axis response of electrostatic transducer (p112)
7.2	On-axis response of Piezo-electric tweeter (p114)
7.3	Arrangement used to determine Polar Response of Loudspeakers (p116)
7.3(b)	Polar Response of Loudspeakers (p117)
7.4	Method of mounting loudspeakers for model work (p119)
7.5	Response of Combined Loudspeaker Assembly (p120)
7.6	Response of Loudspeaker Assembly in Quasi-anechoic Laboratory (p122)
7.7	Vector Diagram of Direct and Reflected Wave over a plane reflective surface (p125)

7.8 Arrangement of Model Table for Reflection Coefficient Determinations (126
7.9 Constant phase triggering circuit for kemo Analogue Memory (p129)
7.10 Results of Reflection Coefficient Measurements for
(a) Felt, (b) Foam, (c) Melamine (pp131-132)
7.11 Amphitude Reflection Coefficient vs. Frequency for
(a) Felt, (b) Foam (p133)
7.12 Phase Change on reflection vs. Frequency for
(a) Felt, (b) Foam, (c) Melamine (p134)
8.1 Summary of Open Propagation Geometries (p138)
8.2 Barrier Construction (p139)
8.2(a) Summary of Barrier Geometries; Octave Bands of Noise. Source and Receivers above ground (p140)
8.2(b) Source and Far Receiver at Ground Level (p141)
8.3 Summary of Barrier Geometries; Pure Tones and Random Pure Tones (p142)
8.4 Nagra Playback Circuit (p146)
8.5 Arrangement for Model Investigations (p149)
9.1 Level difference vs. TN_{50} (pp153-157)
Full Scale; Octave bands; unobstructed propagation various frequencies and geometries
9.2.1 Level difference vs. TN_{50} (pp158-161)
Full Scale; octave bands; barrier present (source and receivers all above ground) Various frequencies and geometries
9.2.2 Level difference vs. TN_{50} (pp162-165)
Full scale; octave bands; barrier present (source and far receiver on the ground) Various frequencies and geometries
9.3 Level difference vs. TN_{50} (pp166-169)
Full scale; pure tones; barrier present. Various frequencies and geometries
9.4 Level difference vs. TN_{50} (pp170-176)
Full scale; random pure tones; barrier present. Various frequencies and grometries
10.2 Level difference vs TN_{500} (pp178-181)
Model scale; octave bands of noise; barrier present various frequencies and geometries
10.3 Level difference vs. TN_{500} (pp182-185)
Model scale; pure tones; barrier present Various frequencies and geometries
11 A typical PET printout of results (p187)
11.1 Level difference vs. Frequency for Octave bands of noise propagated over unobstructed grassland (p204)
11.2 Level Difference vs Frequency for Octave bands of noise propagated over a barrier (p205)
11.3 Level Difference vs. Frequency for Octave bands of noise propagated over a barrier (p206)
11.4 Level Difference vs. Frequency for pure tones propagated over a barrier (p207)
11.5 Level Difference vs. Frequency for random pure tones propagated over a barrier (p208)
11.6 Low turbulence scatter range vs. Frequency for octave noise bands propagated over unobstructed grassland (p204)
11.7 Low turbulence scatter range vs. Frequency for octave noise bands propagated over a barrier (p210)
11.8 Low turbulence scatter range vs. Frequency for octave noise band propagated over a barrier (p211)
11.9 Low turbulence scatter range vs. Frequency for pure tones propagated over a barrier (p212)

11.10 Low turbulence scatter range vs. Frequency for random pure tones propagated over a barrier (p213)
11.11 Model Scale: Level Difference vs. Full Scale equivalent frequency for Octave bands of noise propagated over a barrier (p214)
11.12 Model Scale: Level Differences vs. Full scale equivalent frequency for pure tones propagated over a barrier (p215)
11.13 Model Scale: Low turbulence scatter range vs. Full scale equivalent frequency for pure tones propagated over a barrier (p216)

A.1 Servicing of Kemo Analogue Memory (p234)
A.2 Analogue memory connections to PIA (p235)
A.3 Independant Triggering Modification to Kemo Analogue Memory (p236)
A.4 Servicing of Datalab DL901 Event Recorder (pp238-239)
A.5 Signals for Datalab DL901 Event Recorder (p240)
A.6 Wind Diretion Sensor Flowchart (p242)
A.7 Electronic Thermometer Flowchart (p243)
B.1 System RESET circuit (p250)
C.1 Typical Hot wire anemometer Calibration Curve (p262)

ABSTRACT

The Effect of Wind Turbulence on Noise Barrier Performance

G W Burrows

An investigation has been carried out into the effect of wind turbulence on the propagation of sound over open grassland both with, and without, a 2.4m high barrier present.

Sound bursts, derived from a variety of original signals, were generated using a horn loudspeaker and the resulting levels were measured using two variably positioned microphones, the further of which was placed at distances of up to 24m from the source. Simultaneous measurements were made of a variety of meteorological parameters. A microcomputer-based system was developed to control the experiments and store the measured data for subsequent retrieval and analysis.

As one of the approaches adopted in a search for visible evidence of correlation between various acoustical and meteorological parameters, the measured level difference for each sound burst was displayed graphically against the corresponding value of a particular measure of wind turbulence. For many combinations of measurement geometry and acoustic signal type, the data points fell, with a noticeable degree of consistency, within an envelope of characteristic shape. The shape implied that when the instant of transmission of a sound burst coincided with a low value of the measure of local turbulence, the apparent level difference was subject to considerable statistical fluctuation. This was the case both with and without the barrier present. As the turbulence increased, however, the propagating medium appeared to behave as a progressively more uniform and stable one and the observed scatter correspondingly reduced. The origin of this behaviour remains unclear; however the presence of the barrier, it was concluded, did not appear to modify this effect.

1 to 16 laboratory scale model experiments have been carried out to investigate the replication of the above effects and the results are reported.

CHAPTER 1

Introduction

Acoustical barriers are important in noise control engineering especially if the reduction of the noise level at source is difficult or impossible. They are designed to reduce the received noise by eliminating the direct path of sound from source to receiver, leaving the sound arriving by reflection from surrounding objects, refraction through the atmosphere and by diffraction around the barrier to contribute to the sound pressure level at the receiver.

Applications have been found indoors, for example, to separate operators from noisy machinery or in the lay-out of open-plan offices, and outdoors to limit motorway, airport or factory noise. In addition, built-up environments, local topography etc., may produce a barrier-like shielding effect.

With the aid of methematical formulae and acoustical scale model studies the physics of the diffraction of sound around noise barriers is well understood and can lead to confident prediction of indoor barrier performance especially for the case of a simple thin screen barrier.

1.1 Reasons for Present Work

There is evidence to show that the effects of wind and temperature profiles above the ground, coupled with atmospheric turbulence, significantly reduce the predictability of outdoor barrier performance.

There is a need to investigate the processes by which barrier performance can be degraded in outdoor applications. It is to be expected that such processes could then be taken into account in barrier design in order to predict their effectiveness more accurately. This requires that any phenomena which emerge as having significance in addition to the well-known effects of diffraction and transmission should be quantified, and if possible, reproduced to a representative degree in scale models.

At the time of writing, little work has been done on the effects of meteorological conditions on barrier performance so this project is primarily concerned with identifying anomolies in horizontal sonic propagation outdoors with and without a barrier in the propagation path. Such effects as are identified may, it is hoped, be relevant to particular meteorological phenomena in a qualitative or quantitative way. The intention is also to investigate the degree to which the effect is replicated at model scales. This would be expected to point the direction in which further more rigorous investigation lies.

1.2 Thesis Structure

This thesis is organised as follows. The second chapter contains a review of previous work pertaining to the current study including the theoretical background, concerning outdoor sonic propagation both with and without an obstructing noise barrier under static atmospheric conditions. Chapter 3 reviews the current understanding of how meteorology affects the phenomena discussed in Chapter 2.

In Chapter 4 the rationale for the approach adopted in this study is discussed and the requirements for the experimental system arising from that approach are outlined. Chapter 5 details the physical realisation of the requirements and Chapter 6 documents the evidence produced to ensure that the requirements of the experimental system were met.

The modifications to the above measurement system needed to perform scale model experiments are given in Chapter 7, which also contains descriptions of the additional vaildation tests required at model scale.

Chapter 8 includes details of the experiments performed at both full and model size, and the results of these are given in Chapter 9 and Chapter 10 respectively. The analysis of the results is discussed in Chapter 11. Chapter 12 suggest further work that could build on the present study and its findings.

Appendices are included to give details of the measurement system and how it was controlled that would be cumbersome in the main body of the thesis.

Relevant acknowledgements and a list of references are provided.

CHAPTER 2

Theoretical Aspects of Outdoor Sound Propagation (Excluding Meteorological Effects).

Sound propagation between a transmitter and receiver above the ground in the neighbourhood of a noise barrier, clearly involves the well-understood phenomena of transmission through the barrier, diffraction at the edges of the barrier, refraction through the air and reflections at the various surfaces involved, (i.e. the ground, barrier or nearby buildings) with the consequent introduction of interference effects. These are in addition to beam-spreading and other phenomena associated with horizontal propagation close to a finite-impedance surface that can give rise to the formation of shadow zones.

This chapter reviews in outline the present state of knowledge of these phenomena under static atmospheric conditions. The effect of meteorology on these phenomena is reviewed in the next chapter.

2.1 Horizontal Sound Propagation over Open Ground

This section reviews the present understanding of propagation phenomena in the absence of a barrier for a sound source and receiver close to the ground. The review paper by Piercy, Embleton and Sutherland (1) and by Embleton, Piercy and Olsen (2) are helpful references for this section.

2.1.1 Ground Effects - The Shadow Zone

Consider the case of a point source and receiver close to the ground as shown in Figure 2.1. The pressure, p, at the receiver, R, is given by the so-called Weyl-Van der Pol solution (3):

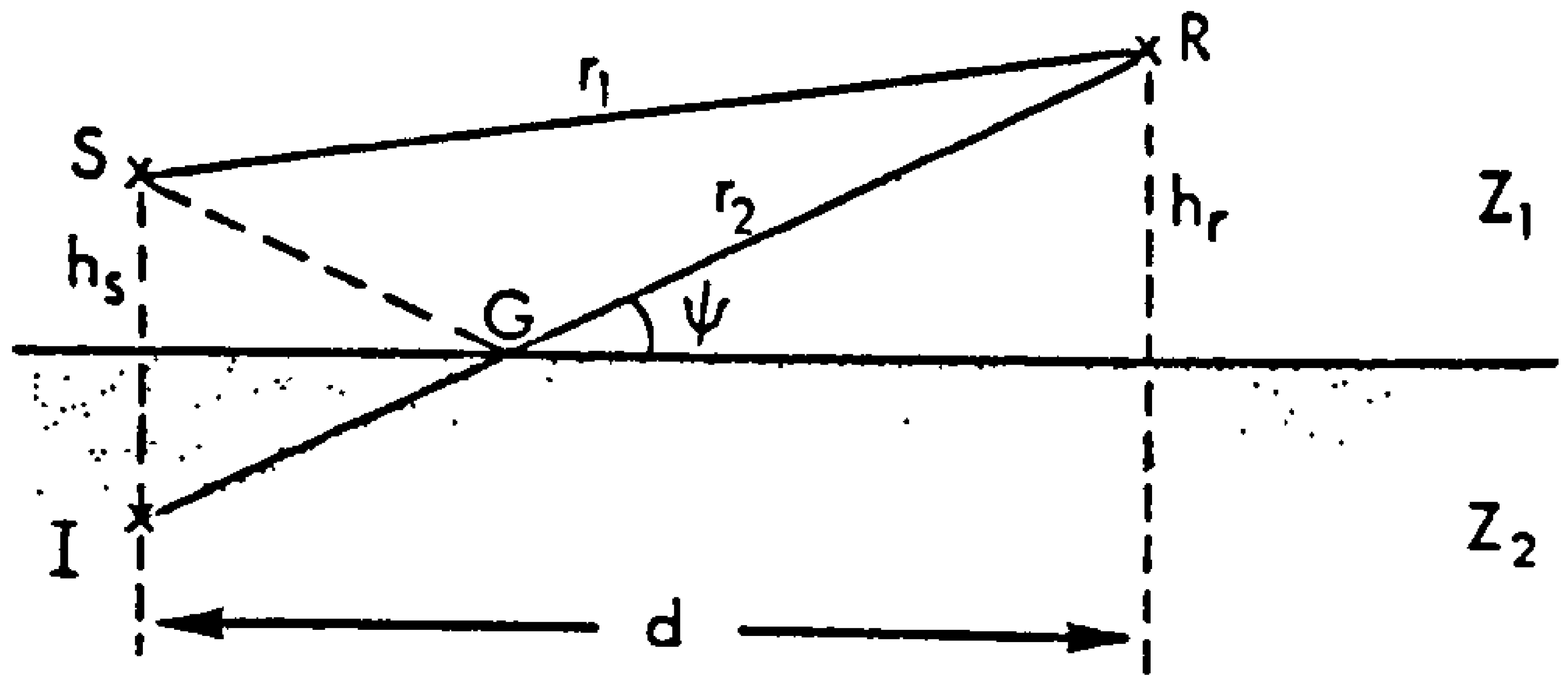

Fig. 2.1 Propagation close to the ground.

$$\frac{p}{p_o} = \frac{1}{r_1} \cdot \exp - ikr_1 + \frac{R_p}{r_2} \cdot \exp - ikr_2 + \frac{(1 - R_p)F}{r_2} \cdot \exp - ikr_2 \qquad (2.1)$$

where p_o = pressure at unit distance from the source

R_p = plane wave reflection coefficient

The amplitude factor, F, in the third term will be discussed later.

The first term represents the direct ray from source to receiver. The r in the denominator gives the classical attenuation due to spherical beam spreading of 6dB per doubling of distance.

The second term represents the reflected ray notionally from an image source in the ground, travelling a distance r_2 to the receiver. The plane wave reflection coefficient in this term is given by:

$$Rp = \frac{\sin \psi - Z_1/Z_2}{\sin \psi + Z_1/Z_2} \qquad (2.2)$$

where ψ = grazing angle (see Fig. 2.1)

Z_1 = characterisitic impedance of air

Z_2 = specific impedance of the ground.

In order to accommodate phase and amplitude change on reflection Z_2 and R_p. are represented as complex variables.

It can be seen that for an acoustically hard surface when Z_2 approaches ∞, at normal incidence R_p can approach unity. This gives rise to pressure doubling if the source is placed directly on the surface giving coherent reflection at all frequencies. Although Z_2 can be very large it can never reach infinity. This means that in the limit of very small grazing angles R_p will equal -1.

This gives a reflected wave that is 180° out of phase with the incident wave with no loss of amplitude. A cancellation of direct and reflected wave results and so the propagation of plane waves at grazing incidence to an impedance boundary is forbidden and a shadow zone is formed.

From equations (2.1) and (2.2) the attenuation in the shadow zone in excess of geometrical spreading is given by:

$$A_e = 20 \log \left[2 \sin \psi \left(Z_2/Z_1\right)\right], \text{ dB} \tag{2.3}$$

Such a shadow zone is **also** formed for point sources at distances where spherical wave fronts approximate plane waves.

<u>2.1.2 Interference Effects</u>

If the source and receiver are both above ground then there is a phase change between direct and reflected rays caused by a difference in path lengths which is additional to the phase change on reflection as described above. A simple geometric analysis of Fig. 2.1. reveals that the path length difference is given by:

$$P\,L\,D \approx 2\,h_s h_r/d \tag{2.4}$$

If the phase change on reflection is neglected (this would be valid only for acoustically hard surfaces) interference minima will occur when the path length difference is an odd number of half wavelengths. The frequency of the first minimum will increase with increasing separation or decreasing transducer height.

However, above about 1kHz grassland is effectively soft giving a phase change on reflection approaching 180° and so the interference minima appear at an even number of wavelengths. Below about 150 Hz the ground becomes reflective giving coherence of direct and reflected beams. Between the two regions is a broad minimum at $\sim$ 500 Hz characteristic of propagation over grassland. It is due to the shadow zone postulated above for source or receiver close to the ground. See Fig. 2.2.

Rasmussen (4) has compared theoretical predictions of sound pressure levels with results of measurements of sound propagation from a point source over grassland. He compares models for locally reacting ground that use one parameter (5,6), his own proposed model using two parameters and Thomassen's four parameter model (7).

All three models give reasonable agreement with measured data although it is noted that the two and four parameter models, both of which assume a porous ground surface backed by an acoustically hard sub-surface layer, predict interference minima more satisfactorily than the single parameter model. However, the two-layer models are less satisfactory at low frequency.

2.1.3 The Ground Wave

The third term in equation (2.1) is not as readily recognisable as the first two terms. It arises from the fact that the curvature of the wavefront changes with distance. The amplitude factor, F, in this term

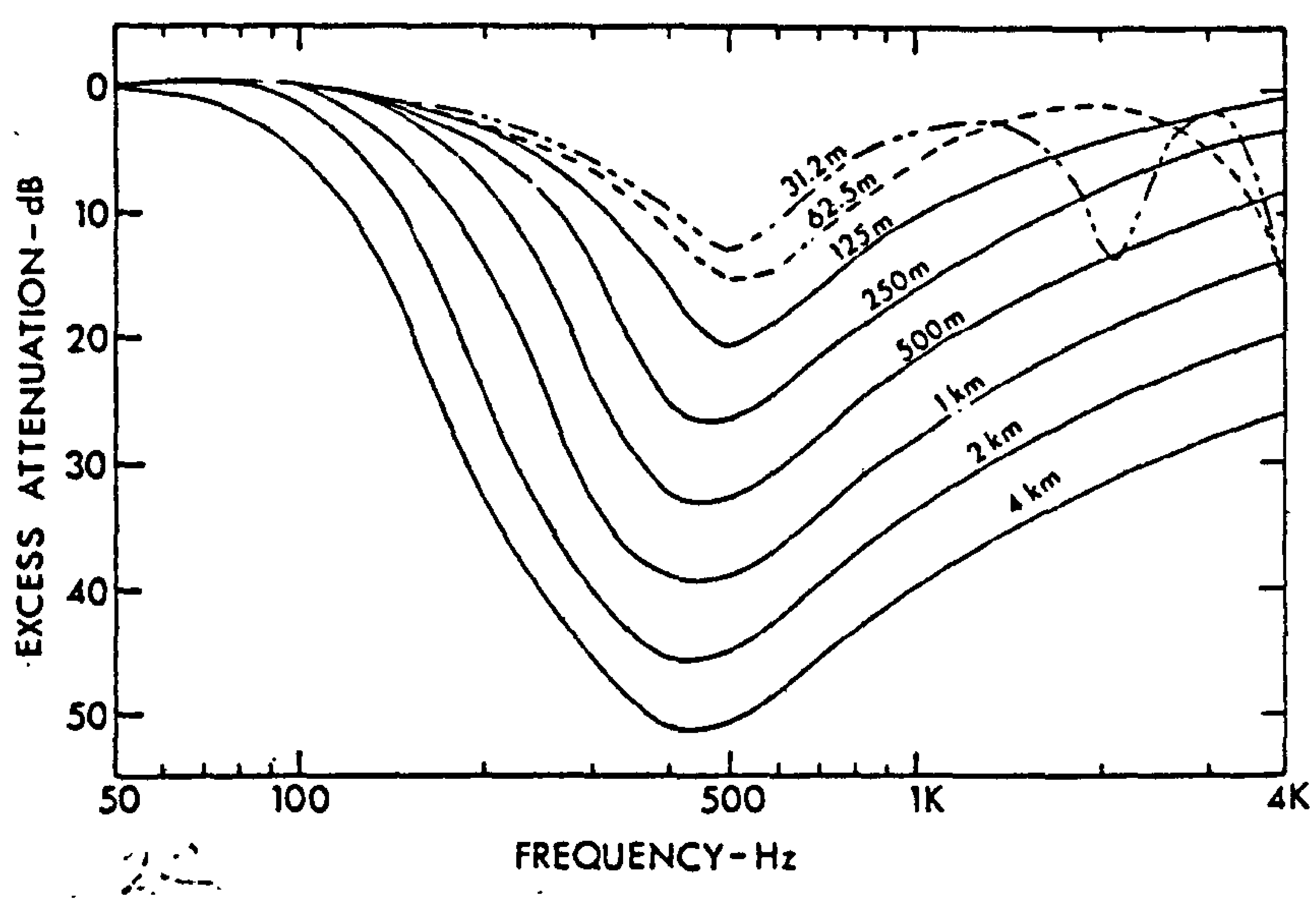

Fig. 2.2 Excess attenuation calculated for propagation from a point source over mown grass for h_s = 1.8 m, h_r = 1.5 m, and the distances of propagation, r_1, indicated. The excess attenuation is relative to that for the point source placed on a perfectly hard surface (Ref. (1))

is a complicated function dependant on a variable known as the numerical distance, W, which is given by:

$$W = \left(\frac{1}{2} ikr_1\right)\left(\sin\psi + \frac{Z_1}{Z_2}\right)^2 \tag{2.5}$$

The numerical distance is the propagation distance scaled to the impedance of the ground for a given frequency and grazing angle.

This third term predicts the existence of a ground wave capable of penetrating the shadow zone described earlier. Although the nature of the ground wave is as yet unclear, its dependance on physical variables is well understood from studies of radio wave propagation. For instance, for source and receiver on the ground it is well known (2) that at short distances ($W \ll 1$) the ground wave suffers no excess attenuation but at longer distances ($W \gg 1$) there is an attenuation of 6dB per doubling of distance. However, if the ground acoustic impedance has a finite phase angle, the amplitude of function F increases from the infinitely hard ground case in the area of $W \approx 1$. This is due to a surface wave which is coupled to the surface due to its reactive impedance but actually propagates in the air. The amplitude of the surface wave decreases exponentially with height according to:

$$p = p_o \exp\left[-X_2^2 kz \Big/ \left(R_2^2 + X_2^2\right)\right] \tag{2.6}$$

It can be seen that for small propagation distances the surface wave is very small. For $W \gg 1$ the amplitude again decreases because of the boundary losses which have an exponential dependance on distance. At $W = 1$ the surface wave adds to the ground wave giving an increased amplitude.

It should be noted that, for transducer heights of about 1-2 M, the ground wave needs only be considered for propagation distances greater than about 100 M. See for example Fig. 11 of Ref.(1).

The described effects for near-horizontal propagation above a finite impedance boundary have been used to predict the excess attenuation in practical situations. Attenborough (8) has used the theory to predict A-weighted excess attenuation of traffic over various surfaces including grassland, snow and sand. This work includes a review of available measurements of normal impedance for various surfaces.

Attention has been paid to propagation over ground on non-uniform composition. A numerical evaluation of the field above an impedance boundary has yielded predictions of excess attenuation when the surface beneath the propagation path comprises both hard and soft areas with a distinct boundary line separating the two areas, (9), and boundary integral equation methods have produced equations for sound propagation above an imhogeneous impedance plane (10).

2.2 Barrier Effects

This section reviews the published literature concerned with the phenomena associated with the introduction of a barrier in a sound propagation path such as that discussed above.

2.2.1 Transmission through the Barrier

The transmission loss (TL) of a panel is defined as the ratio of the incident power to the transmitted power and is related to the transmission coefficient, τ, a frequency-dependent characteristic of the panel, by

$$TL = 10 \log \left(\frac{1}{\tau} \right)$$

Below a frequency known as the critical frequency the transmission is largely dependant only on the surface mass, M_s, of the panel (i.e. the product of its density and thickness). The transmission loss for low frequency and normal incidence can be predicted by a version of the so-called "Mass Law" (11).

$$TL = 10 \log_{10} \left\{ 1 + \left(\frac{\omega M_s}{2 \rho c} \right)^2 \right\}$$

It can be seen that transmission loss increases by 6dB per doubling of surface mass and, for a given mass, by 6dB per doubling of frequency.

At the critical frequency the velocity of bending waves within the panel equals the velocity of sound in air. Incident sound at grazing incidence and at the critical frequency can, therefore, induce bending waves which radiate efficiently causing a dip in transmission loss. Bending wave velocity is inversely proportional to the panel thickness and so increasing barrier thickness will both increase surface mass and decrease the critical frequency.

Above the critical frequency the effect of surface mass is reduced, with transmission loss increasing only by 3dB per doubling of mass. Instead stiffness and internal damping become increasingly important.

2.2.2 Diffraction over the Barrier

The conventional study of diffraction of waves around obstacles is based on the Huygens-Fresnel principle first encountered in optics. Developments and extensions of this theory form the basis of the treatises discussed below. The review paper by Kurze (12) is a convenient primary source on this topic.

(a)The semi-infinite Thin Screen

This hypothetical barrier extends into infinity in depth below the free edge and length and is suspended in otherwise unobstructed space. It therefore represents the simplest physical situation since sound can arrive in the shadow zone of the barrier only by diffraction over the free edge at the top of the barrier. (See Fig. 2.3). Sommerfield produced an exact solution to the diffraction of a plane wave incident on a wedge; from this Kirchoff (13) and others derived an approximation for the case of a semi-infinite thin screen.

Keller produced another approximate solution from his geometrical theory of optics:

$$\Delta_k = -10 \log \left(8\pi^2 \frac{h}{\lambda} \tan \frac{\phi}{2}\right) - 10 \log\left[\frac{d^2}{d(A+B)}\right] \qquad (2.7)$$
$$- 20 \log \left[1 + \frac{\sin \phi/2}{\sin(\theta + \phi/2)}\right]$$

where the dependant variables are defined in Fig. 2.3. Stated in this form Kurze was able to demonstrate some potentially major errors in a chart developed by Redfearn (15) relating barrier attenuation to effective barrier height, h/λ, with diffraction angle as a parameter (See Ref 12 Fig 1).

The family of curves can be approximated to within 1 dB by:-

$$\Delta L_R = 20 \log \left\{ 2 \frac{\pi\left[(2h/\lambda)\tan\phi/2\right]^{1/2}}{\tanh \pi\left[(2h/\lambda)\tan\phi/2\right]^{1/2}} \right\} \qquad (2.8)$$

By extending Kirchoff's diffraction theory Makaewa (16) replaced this family of curves with a single curve based on the so-called Fresnel number N, which relates barrier attenuation to the path length difference in terms of half wavelengths between a sound ray travelling directly from source to receiver and a sound ray diffracted over the top of the barrier:

$$\Delta L_M = \left[10 \log \frac{\sqrt{2\pi N}}{\tanh \sqrt{2\pi N}} + 5\right] \quad \text{dB} \qquad (2.9)$$

$$\approx 10 \log (20N) \qquad \text{dB}$$

$$\text{where} \quad N = \frac{2\delta}{\lambda} = \frac{2}{\lambda}(A + B - d)$$

It can be seen that equation (2.9) is equivalent to the first term in (2.7). The second term in Keller's expression is significant if $A + B \gg d$, i.e. if the diffracted path length is much longer than the direct path length. The third term is small for small diffraction angles, but can reach a value of 6 dB for source and receiver close to the barrier.

Makaewa's curve finds widespread application as a design guide and also as the basis for further modification, such as Kurze and Anderson's chart for an incoherent line source (17).

(a)

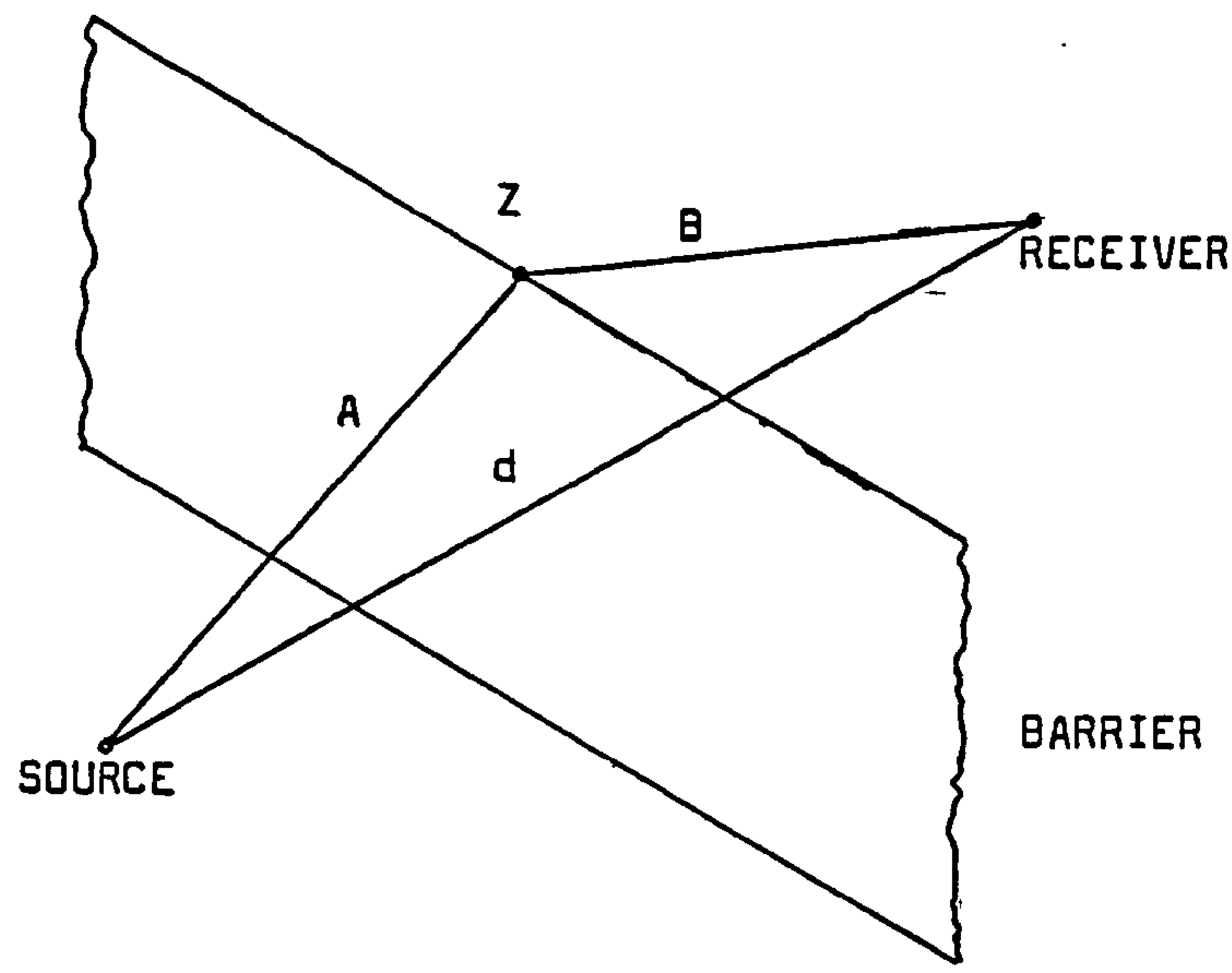

(b)

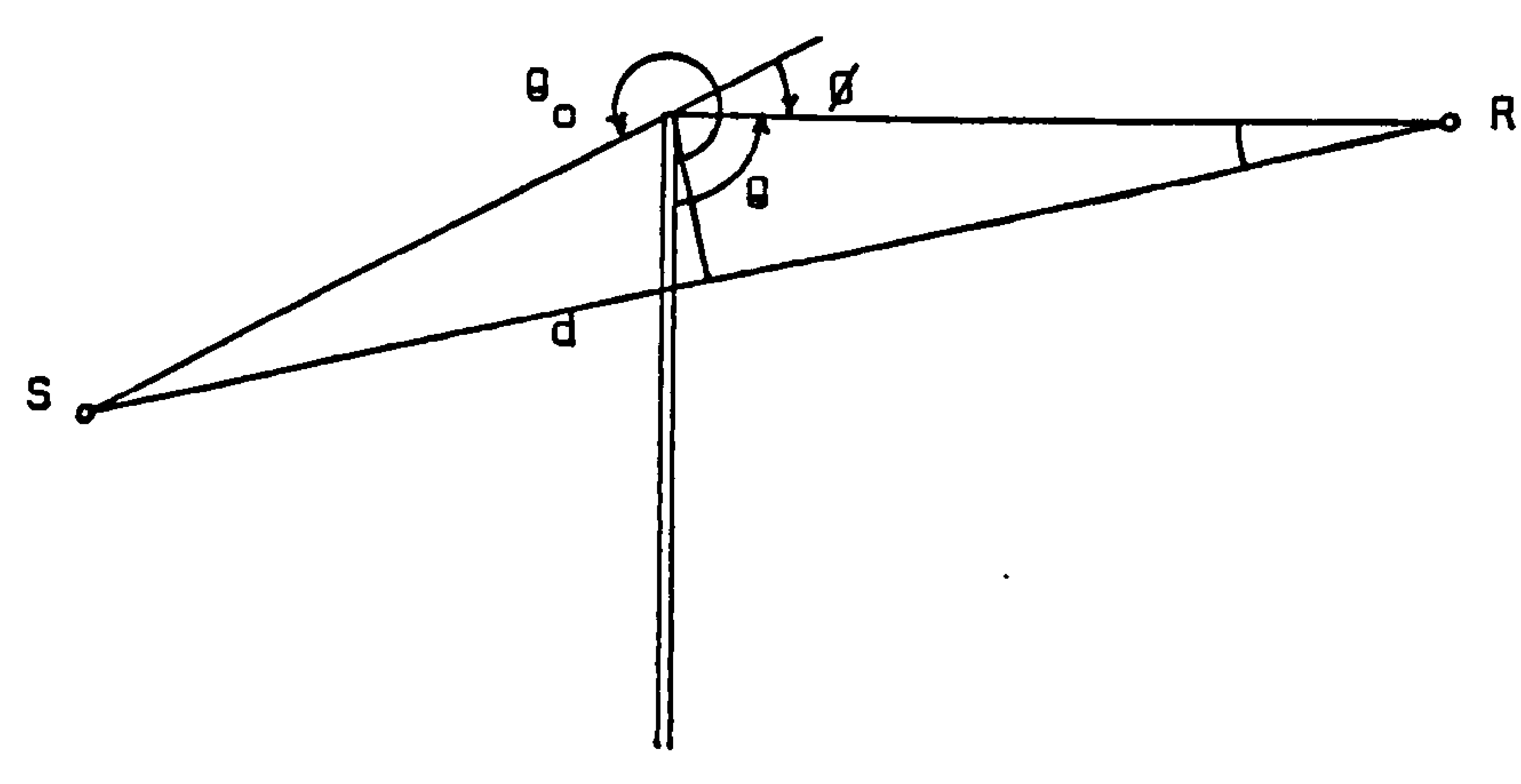

Fig. 2.3 Semi-infinite thin screen
(a) perspective view (b) projection on the Z=constant plane

(b) Thin Screen Resting on a Rigid Surface

The preceding section gives an insight into basic diffraction phenomena.

The case to be discussed now is a step towards a more practical case, for instance, when a screen is erected on concrete, tarmacadum or other rigid surfaces.

In the case of a simple, practical barrier sound may arrive at a receiver by four ray paths, that is with and without reflection from the ground on either side of the barrier. See Fig. 2.4. It is interesting to note that in a barrier-free situation, the introduction of a perfectly reflective ground will increase the level at the receiver at 6dB, assuming coherence between direct and reflected rays. Now, with a barrier interposed, the receiver level increases by 12dB on the introduction of the reflective plane. Therefore, the attenuation is 6dB less than the value predicted for a semi-infinite thin screen. That this is so can be appreciated by considering that a hypothetical screen of zero height above a reflective surface gives no attenuation but there is 6dB attenuation when the top of a semi-infinite screen lies on the direct ray path between source and receiver.

In order to simplify the analysis of barrier attenuation in the presence of a hard ground it is useful to consider the case of the source on the ground and the receiver near the ground and in the shadow zone. This reduces the rays arriving at the receiver to two, i.e. one directly from the top of the barrier and the other reflected from the ground. The Fresnel number introduced in the previous section pertains to the direct ray only. If the extra path length travelled by the reflected ray is δ', then the additional Fresnel number is given by $N' = 2\delta'/\lambda$, and the total Fresnel number is $N + N'$.

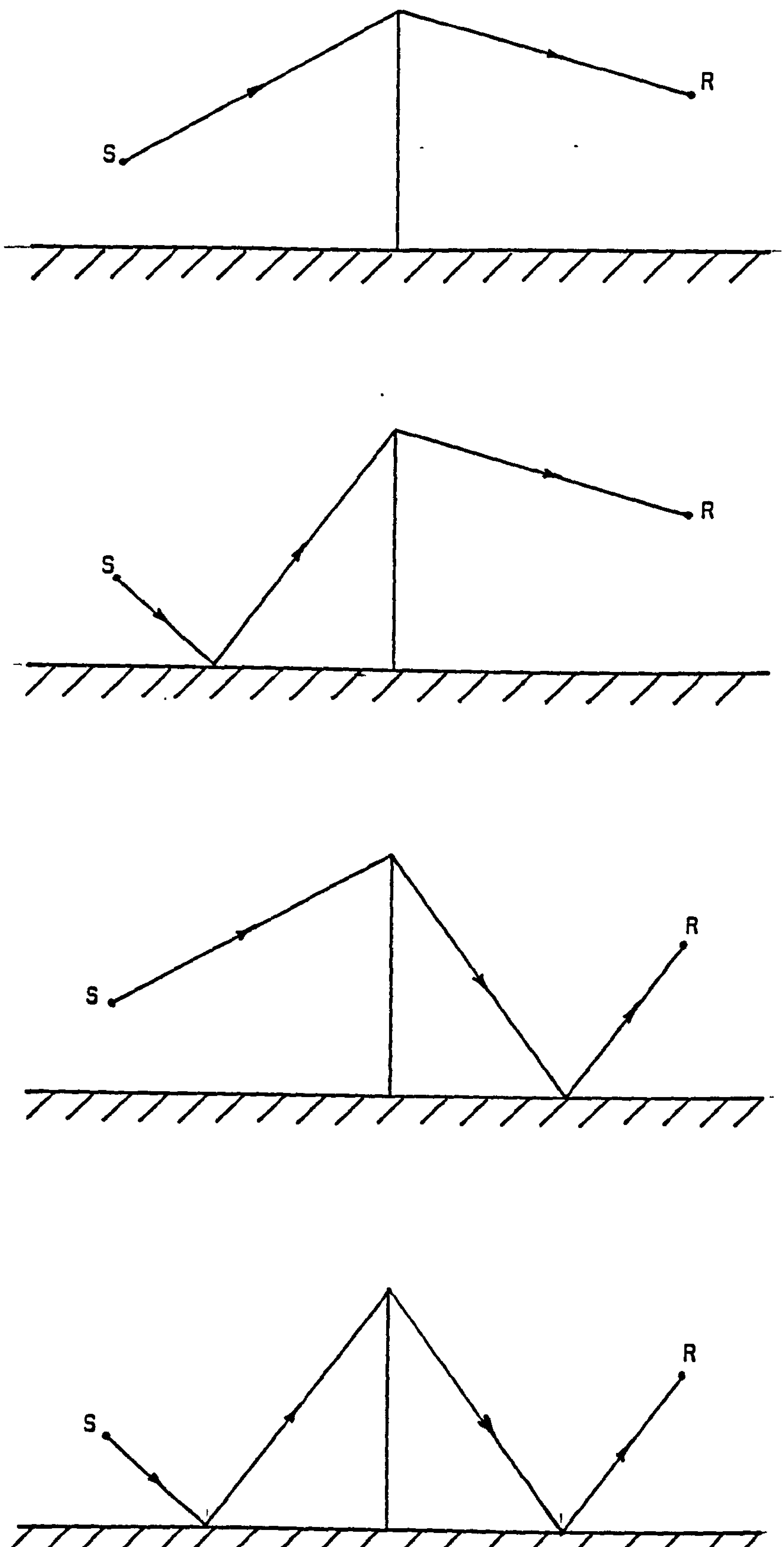

Fig. 2.4 Four possible ray paths for a thin screen on a rigid ground.

If the difference in attenuation due to beam spreading is negligible, then the pressure, p, at the receiver relative to a free-field pressure of p_o is given by:

$$\frac{p}{p_o} = 10^{-\Delta L(N)/20}\left\{1 + 10^{[\Delta L(N) - \Delta L(N+N')]/10} + 2 \times 10^{[\Delta L(N) - \Delta L(N+N')]/20} \cos(\pi N') \frac{\sin[(\Delta f/fm)\pi N']}{(\Delta f/fm)\pi N'}\right\}^{1/2} \qquad (2.10)$$

where fm = centre frequency and Δf = bandwidth of noise. The auto-correlation functions of a plane wave and band-limited noise appear as Cos (π N') and Sin X/X respectively.

This equation has the disadvantage that the free-field pressure may not always be known. Makaewa (16) proposed to overcome this problem by relating the receiver level to the level at the position of the top of the screen in the absence of the screen, however, experiments performed by Makaewa show fluctuating levels inconsistent with predictions. These have been attributed to interference effects at the top of the barrier causing erratic reference levels (12). It is, therefore, necessary to avoid sources of pure tone or even narrow band noise (1/3 octave, say) if this procedure is to be adopted. Broader bandwidths are needed for sufficient cancellation of interference effects, to reduce noise level fluctuations to about 2dB.

(c) Screen on Absorptive Surfaces

It is probable that the location of a noise barrier in a practical situation will involve, to some degree, reflections from a ground that cannot be considered as perfectly rigid. For instance, above about 150Hz grassland should be considered as having finite impedance.

Predictive procedures are similar to the case of a perfectly reflective ground but involve consideration of a complex reflection coefficient, affecting both amplitude and the phase of the reflected wave.

Under such conditions the introduction of a noise barrier can have adverse effects by interfering with the formation of a shadow zone (see section 2.1.1). For instance, if a barrier is placed such as to interrupt the ground reflection without substantially attenuating the direct ray, it could, paradoxically, increase the level at the receiver.

Addressing the problem of the prediction of barrier performance in the presence of a locally reactive ground, Embleton (18), adapted the Young-Rubinowicz diffraction formula, which was originally concerned with the field from a point source arriving behind an opaque screen containing a circular aperture, for use with a semi-infinite barrier. Referring to Fig. 2.5 Embleton's formula is:

$$\psi(R,t) = -\frac{k}{2\pi} \exp(-i\omega t)\, A \sin\phi \int_0^{\pi/2} \frac{\exp\{ik \sec\beta [A+\alpha]\} \cos^2\beta \, d\beta}{\alpha [B \sin^2\beta + \alpha - A \cos\phi \cos^2\beta]} \qquad (2.11)$$

where k = pressure amplitude at unit distance

β = angle LRB $\qquad \alpha = [A^2 \cos^2\beta + B^2 \sin^2\beta]^{1/2}$

The effects due to the presence of a finite impedance ground on the source side of the barrier can be taken into account by incorporating the amplitude coefficients of the Weyl-Van der Pol solution (2.1) into the pressure amplitude factor, K.

Similar expressions can be used to determine Kr, the amplitude of the reflected wave on the receiver side of the barrier.

(a)
(b)
(c)

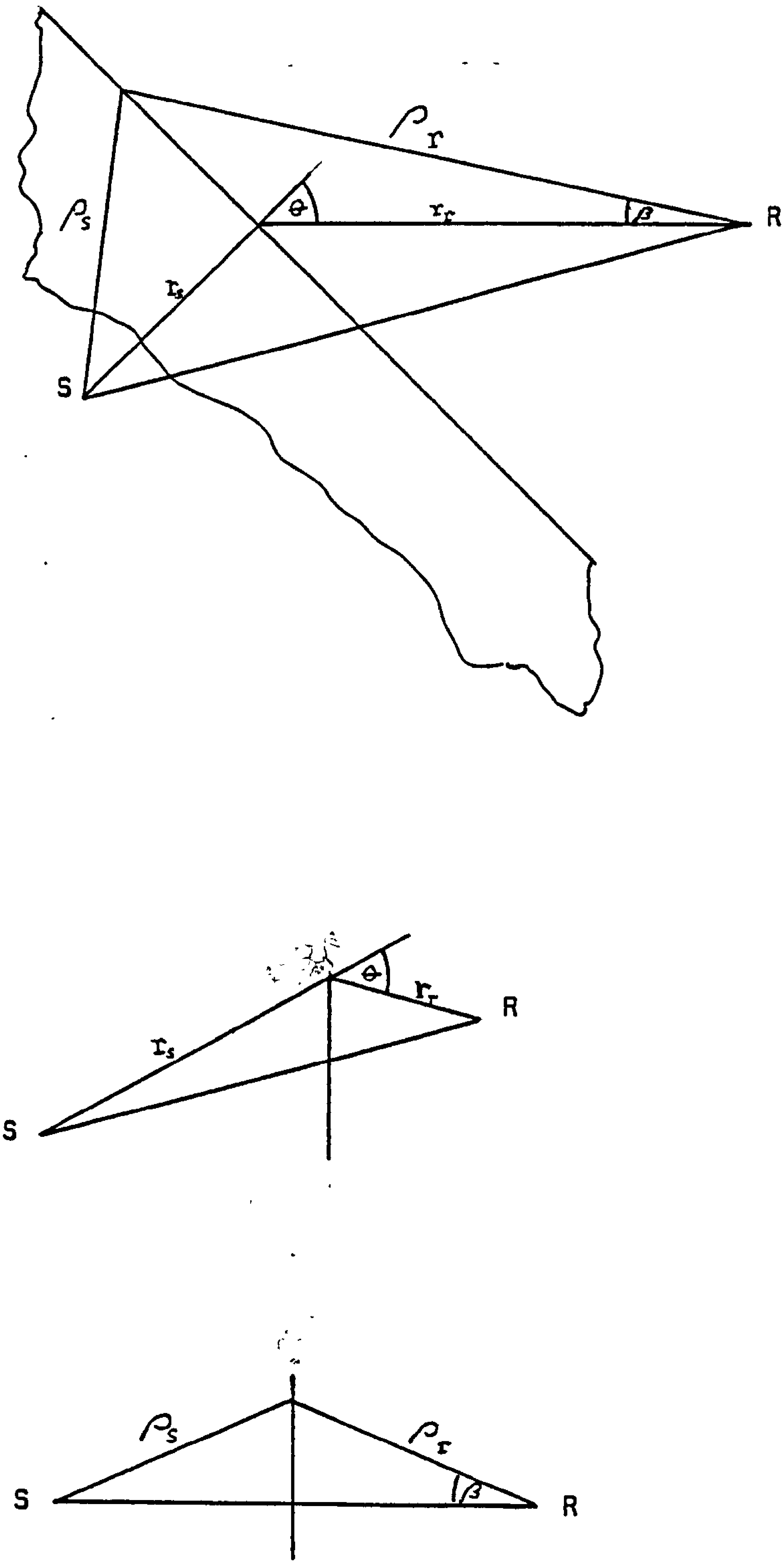

Fig. 2.5 Thin screen geometrical parameters for Embleton's equation (2.11). (a) perspective view (b) projection on z = constant plane, (c) projection on y = constant plane.

This solution has the advantage that it is suitable for computational techniques and can easily accommodate the effects of a ground wave and complex reflection coefficients. Oblique angles of incidence can be accounted for with the introduction of a linear offset term in the geometrical calculations.

Embleton's approach is one of five techniques used to predict diffraction of sound over barriers that are reviewed and compared in a paper by Isei, Embleton and Piercy (19). Particular attention is paid to the effect of a finite impedance ground on barrier performance. The theories compared are Keller, (14) and Kirchoff-Fresnel diffraction theories (13, 20), a modification of Macdonald's diffraction theory due to Kawai et al (21), a theory proposed by Thomasson (7, 22) based on Babinets Principle and Embleton's theory. The ground impedance model used in the calculation schemes other than that of Thomasson was that based on the work of Delaney and Bagley (5, 23), and developed by Chessell (6). Thomasson uses a four parameter model for ground impedance. Embleton's paper (18) gives details of the modification of a diffracted wave to include a ground reflection wave. It was found that the theories of Embleton and of Kawai were in close agreement with each other and with measured data for the case of a point source emitting pure tones and a particular geometry of source, barrier and receiver on an acoustically hard surface. Since the Kawai-Macdonald technique has a faster computing speed than that of Embleton, the former was developed to predict linear and A-weighted broadband sound pressure levels for line sources which gave good agreement with experimental data, especially compared with theories such as Makaewa's that take no account of interference phenomenon.

(d) Wedge shaped barriers and thick barriers

Continuing to move the discussion towards more practical barrier configurations, Makaewa (24), Pierce (25) and Kurze (12), have produced prediction techniques for wide barriers. Makaewa's approach was to replace a thick barrier with a notional equivalent thin screen such that the tangential raypaths to the barrier become the direct raypaths between the top of the screen and the source and the receiver, see Fig 2.6. There is no theoretical background for such an approach and clearly the technique is dubious for source and receiver close to the barrier.

Pierce approached the problem by first deriving a formula for the attenuation of a wave by a wedge. He then extended this to consider double-edged diffraction and hence proposed that an equivalent barrier used in assessing noise reduction by earth berms, hills, buildings etc. should be of trapezoidal cross-section and fit within the physical bounds of the real barrier using the grazing rays to derive the geometry, see Fig. 2.7.

His single-edged diffraction formula used, as a starting point, the geometrical optics theory of Keller, as stated in Part (a) of this section and yielded, for the receiver in the shadow zone:

$$\Delta L_p = \left(3 - 10\log\left\{[f(X_+)+f(X_-)]^2 + [g(X_+)+g(X_-)]^2\right\}\right)\,\mathrm{dB} \qquad (2.12)$$

where $f(x)$ and $g(x)$ are auxilliary Fresnel functions

$$\text{and } X_{+(-)} = \left(\frac{2r_r r_s}{\lambda L}\right)^{1/2}\left|\frac{\cos(\pi^2/\beta) - \cos[(\pi/\beta)(\theta_r + (-)\theta_s)]}{\pi/\beta\,\sin(\pi^2/\beta)}\right|$$

$$\text{and } L = \left((r_r + r_s)^2 + (z_r - z_s)^2\right)^{1/2}$$

β = free wedge angle

r_r, θ_r, z_r and r_s, θ_s, z_s are the cylindrical co-ordinates of source and receiver respectively.

Fig. 2.6 Maekawa's Equivalent Screen

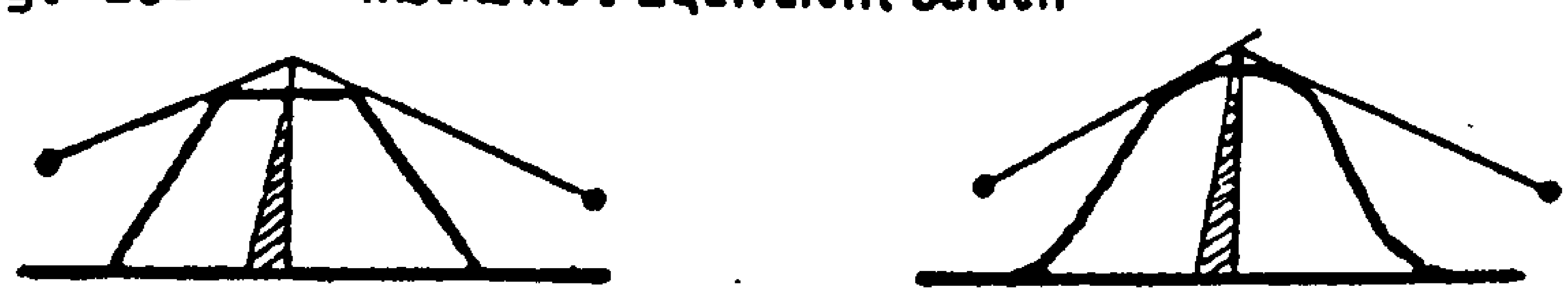

Trapezoidal Cross Section Earth Berm

Fig. 2.7 Pierce's Equivalent Barrier

Direct Application Equivalent Earth Berm Barrier

Fig. 2.6 and Fig. 2.7

The asymptotic expansion of this formula is similar to a result obtained by Jonasson (26).

For the special case of $\beta = 2\pi$ i.e. a thin screen, Pierce's results are in agreement with Redfearn's chart to within 1dB.

For the case of a three-sided wide barrier Pierce's equation becomes:

$$\Delta L_P = 20 \log \frac{L}{d} - 10 \log \left[f^2(Y_>) + g^2(Y_>)\right]\left[f^2(BY_<) + g^2(BY_<)\right] \text{ dB} \tag{2.13}$$

where B is a parameter characterising the barrier width and $Y_>$ and $Y_<$ are the greater and smaller parts of the quantities Y_S and Y_R, parameters for diffraction of sound over wide barriers.

Kurze proposed a double-diffraction formula which considers two single edge diffractions, one for a ray travelling from the source to a hypothetical receiver in the plane of the top of the barrier and at the same distance from the barrier top as the real receiver, and one for a similar ray travelling from a hypothetical source to the receiver (see Fig. 2.8).

In a model study by Ivey, et al, (27), the formulae of Pierce and of Kurze are compared. It is found that the more rigorous solution by Pierce is closer to the measurements.

In another scale model by Masiak (28) the prediction technique of Makaewa and of Pierce were compared. Below a Fresnel number of about 3, both these theories and experimental data are in good agreement. At higher Fresnel numbers it is shown that Pierce overestimates and Makaewa underestimates barrier attenuation, the discrepancy in each case being 2 or 3 dB for N $\approx$ 20.

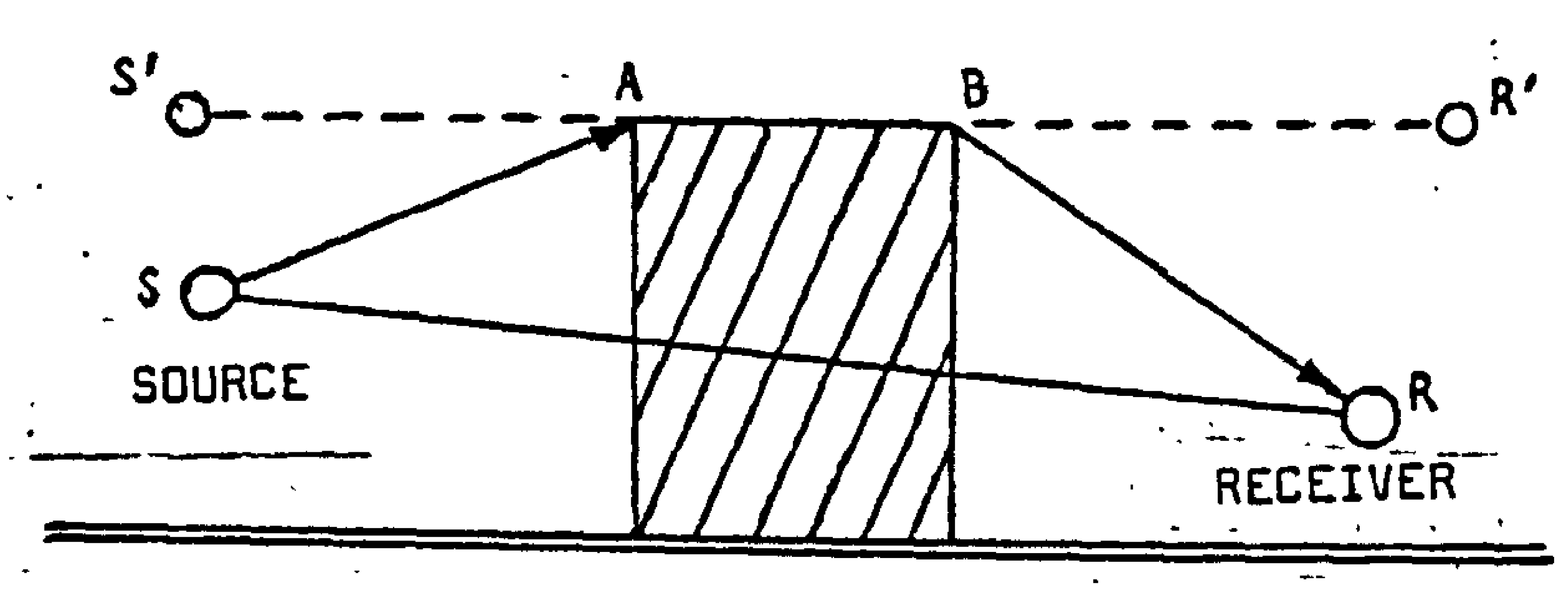

Fig. 2.8 Kurze's Wide Barrier approach.

2.3 Résumé

It is clear that there is a wealth of literature investigating sound propagation over open ground and barrier performance in static atmospheric conditions. The physical principles involved are well understood.

CHAPTER 3

The Present state of Knowledge of Meteorological Effects on Outdoor Sound Propagation

It is generally accepted (1) that wind and temperature effects can give rise to anomolies in sound propagation. The physical variables known to influence acoustical behaviour are the overall wind and temperature conditions, the gradient of wind and temperature with height above the ground and the microstructure of wind and temperature (i.e. atmospheric turbulence). Air humidity is neglected since there is no evidence to suggest that propagation of sound frequencies lower than about 15 kHz is affected by humidity.

This section outlines the known effects of each of the above meteorolgical phenomena on sonic propagation.

3.1 Bulk Effects of Wind

Wind velocity adds vectorially with the velocity of sound and, therefore, changes the wavelength of a sound signal of a fixed frequency. This implies that diffraction and interference phenomena will be affected. However, even a strong wind of about 30 ms^{-1} adds less than 10% to the speed of down wind propagation. Such a small change would only be evidenced in the position, but not the nature, of interference fringes. As long as the wind velocity is constant a non-fluctuating received sound pressure level is predicted.

3.2 Bulk Effects of Temperature

The speed of sound is proportional to the square root of absolute temperature and so a change in temperature can be expected to alter the wavelength of a sound wave of a certain frequency.

If the ambient temperature is $300^{o}K$ then a $10^{o}K$ fluctuation is a change of 3% giving a 1.7% change in wind speed. Although this will cause interference patterns to be shifted slightly, diffraction effects can not be reasonably expected to alter noticeably.

3.3 Vertical Wind Gradients

Piercy, Embleton and Sutherland, in their helpful review paper of 1977 (1) refer to the fact that wind velocity increases with increasing height within the boundary layer close to the ground according to the equation (29)

$$V_w = K_v \log \frac{Z}{Z_o} \tag{3.1}$$

This logarithmic variation of wind velocity, V_w, with height above the ground, Z, is caused by viscous drag with the constant, K_v , determined by the surface roughness and the mean wind velocity above this layer. The constant, Z_o, is a linear dimension representative of the size of obstacles on the surface.

3.3.1 The Effect of Vertical Wind Gradients on Unobstructed Sound Propagation

With a vertical wind profile as described above (see Fig. 3.1) geometrical (or ray) acoustics, as applied to the study of underwater acoustics, satisfactorily predicts refraction of the sound rays downwards for down wind propagation or upwards for upwind propagation with the consequent formation of shadow zones or focal points, (30, 31) see Fig. 3.2. There is no evidence to suggest that geometrical acoustics is inappropraite in this case. Clearly if even high wind velocities are about 10% of the velocity of sound the radius of curvature of refracted rays will be large and the effects will be significant only over large propagation distances, may be of the order of kilometres.

Fig. 3.1 Variation of wind velocity and temperature in the vicinity of a flat ground surface (upto $\sim$10 m)

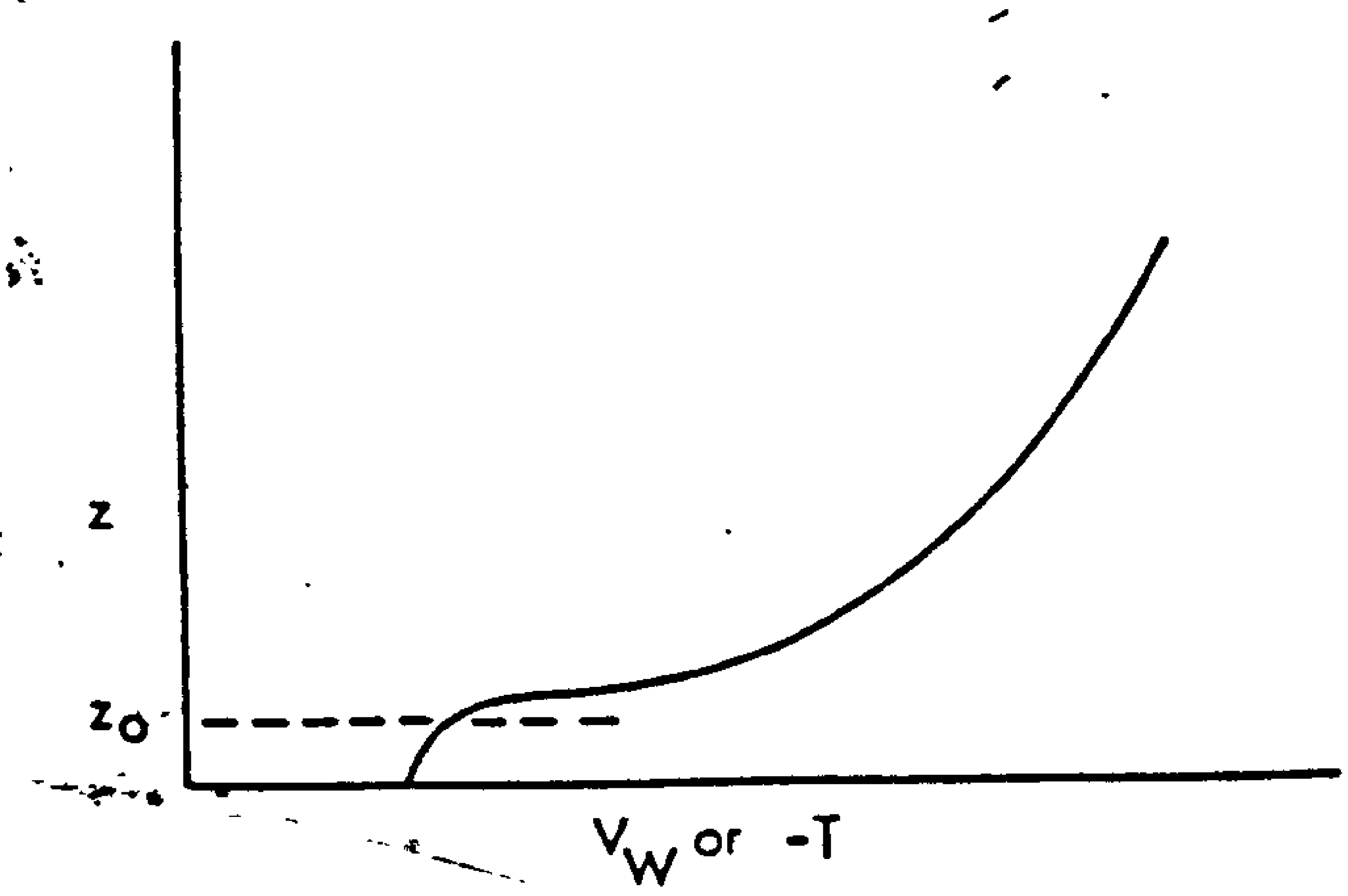

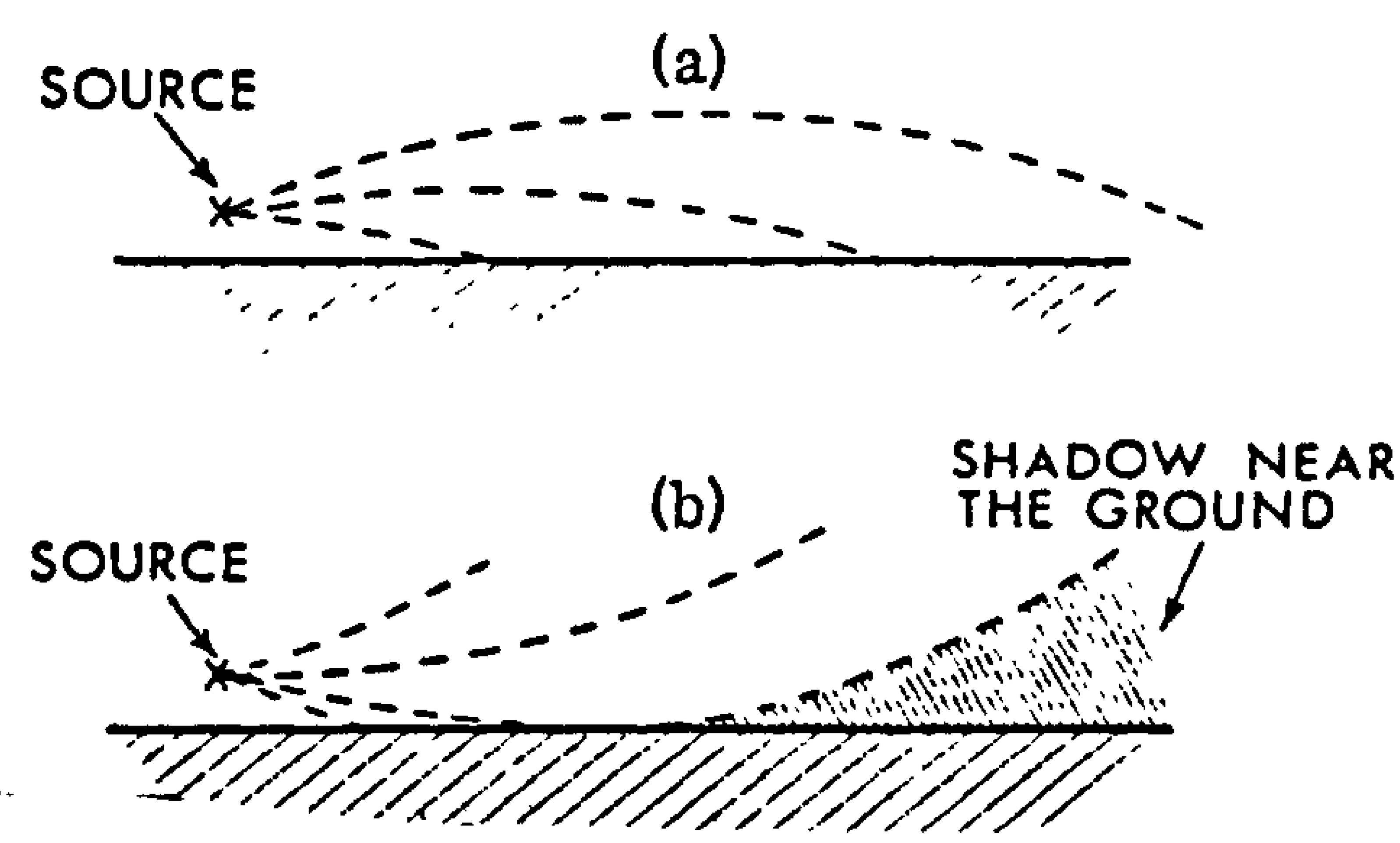

Fig. 3.2 (a) Refraction downward-inversion or downwind propagation. (b) Refraction upwards- lapse or upwind propagation.

3.3.2 The Effects of Vertical Wind Gradients on Barrier Performance

In the study by Dejong and Stusnick (32) a model barrier was constructed in a wind tunnel that was designed to simulate typical outdoor vertical wind profiles and degrees of wind turbulence as translated to the model scale. They primarily considered the refraction due to vertical wind velocity gradients causing measured barrier attenuations that differed from the wind-free condition, the effects of turbulent scattering being considered negligible.

They replaced the straight ray paths between source, barrier and receiver as they would appear in wind-free conditions with curved ray paths, the radius of curvature being given by $r = 2C_o Z/u$, where Co = speed of sound
and u = wind speed (see Fig. 3.3)

Drawing tangential rays to this curved path gives the locations of an image source and an image receiver allowing an equivalent Fresnel number to be derived for the wind-affected ray paths.

The derivation of wind corrected narrier attenuation requites that the Fresnel number be approximated by:

$$N \approx \frac{l_s \; l_r \; (M_s + M_r)^2}{\lambda (l_s + l_r)} \qquad (3.2)$$

where $m_s = (h_B - h_S)/l_s$ and $m_r = (h_b - h_r)/l_r$

If m_s and m_r are less than 0.5 then the above approximation for N is valid.

It was found that barrier attenuation is increased for upwind propagation and decreased for downwind propagation, an effect that is greater at higher wind velocities. The results of this model scale study and the ensuing theory that is developed, are in good agreement with the field measurements made by

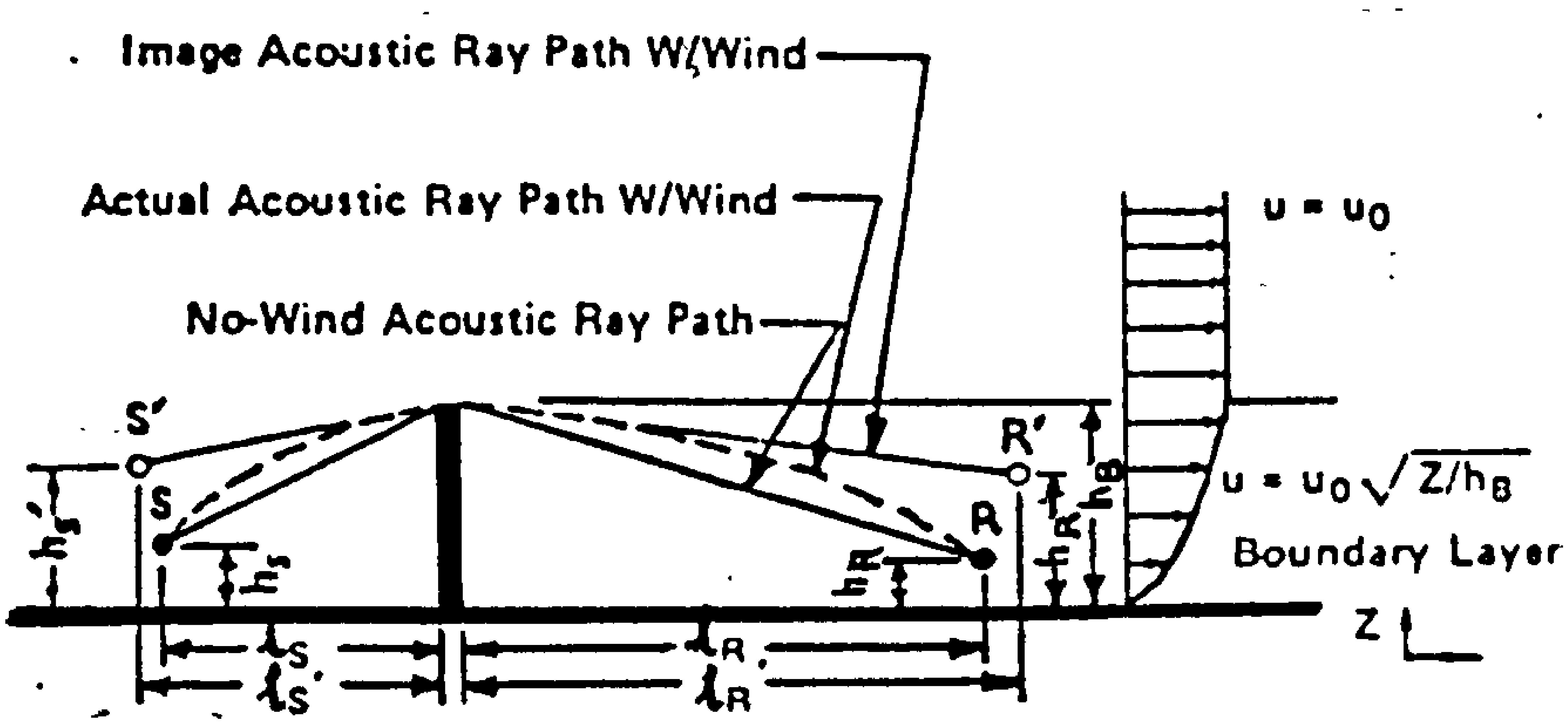

Fig. 3.3 DeJong-Stusnick wind effect model.

Scholes, Salvidge and Sargent (33, 34). A second conclusion of that work was that instantaneous measured levels of the barrier reduction with the wind blowing fluctuated widely from the mean value, with the deviations often reaching a value comparable with the mean.

3.4 Vertical Temperature Gradients

Under normal daytime conditions, temperature decreases with increasing altitude as a result of surface heating by the sun. Again from the review paper by Piercy, et al, (1), the temperature, T, at some height, Z, within the boundary layer under these conditions is given by: "Some [illegible]"

$$T = T_o - K_t \log \left(\frac{Z}{Z_o} \right)$$

where T_o = ground temperature

K_t is a constant characteristic of the surface, and Z_o is linear dimension representative of surface obstacles.

Since the velocity of sound is temperature-dependant, sound rays will be refracted upwards in a manner similar to upwind propagation as discussed in 3.3 above.

The situation when temperature increases with increasing altitude is known as temperature inversion and may typically occur at night when the surface radiates stored heat energy. This causes downward refraction similar to downwind propagation.

Note that the effects of temperature, a scalar quantity, are omnidirectional unlike the vertical wind gradient effects described in 3.3.

In a study of jet noise at an airport, Parkin and Scholes (35) concluded that the refractive effects of vertical wind and temperature gradients are both equivalent and additive.

As is the case for refraction caused by wind gradients, the radius of curvature of sound waves refracted by temperature gradients is large and focii or shadow zones will only be evident over large propagation distances.

3.5 Microstructure of the Wind

At all times wind is turbulent in nature due to instabilities in the thermal viscous surface boundary layer inducing the formation of eddies (29, 36). The eddies grow progressively smaller until they are about 1 mm in diameter when the energy is dissipated by viscosity and so the statistical distribution of eddy size is variable and characteristic of the wind conditions. Since the wind velocity on a microscopic scale is proportional to the eddy size turbulence can be represented by a spectrum, obtained from the output of a small, low-time constant anemometer.

3.5.1 Wind Turbulence Effects on Unobstructed Sound Propagation

The effect of atmospheric turbulence on light and microwave propagation has been extensively studied. However, some studies have considered sound waves (36). Vertical propagation has been of greatest interest since this permits the sounding of the atmosphere to indicate meteorological conditions. (37).

For near-horizontal propagation (a condition which is of interest to this study) the effect of atmospheric turbulence has been approached by considering turbulence to cause a loss of energy from an acoustical beam by a scattering process. (38).

This is caused by inhomogeneities in the atmosphere and scattering is mostly in the forward direction through a small solid angle. The superimposition of primary and scattered waves produce fluctuations in the phase and amplitude of a pure tone. Such fluctuations increase with distance until a point is reached ($\sim 70\ \lambda$) where the signal is uncorrelated with the source and amplitude fluctuations are limited to a $\pm$ 6dB standard deviation (1).

It is evident that the effect on phase fluctuations can cause the sound field in areas of interference maxima and minima to be unpredictable. Ingard and Malling (39) studied the effect of turbulence on the interference between direct and reflected waves for distances up to 75 m.

They assumed plane waves, uncorrelated between direct and reflected waves. Meteorolgical data was not measured but fitted to the acoustical data. Daigle, et al, (40), have developed this work by treating the direct ray and that reflected off the ground as being partially correlated. They produced a theory that is valid for spherical waves since they used a point source with sufficiently small receiver distances to consider the waves as spherical. Wind and temperature spectra were measured and used quantitatively when comparing predicted and measured sound levels.

The effects of meteorologically induced refraction are only noticeable over large distances. Turbulence, whether viewed as a scattering process or as a randomising process is likely to be of more importance in the study of outdoor barrier performance over moderate propagation distances.

3.5.2 The Effect of Wind Turbulence on Barrier Performance

The effect of atmospheric turbulence on barrier performance has been studied by Daigle (41). He reports that measurements of traffic noise behind a barrier and the results of a more idealised experiment using a point source and rigid thin screen, reveal discrepancies with diffraction theory, especially at higher frequencies. Energy arriving behind the barrier, in excess of that expected from diffraction alone, is calculated as being largely due to the forward scattering of energy from the atmosphere directly above the barrier.

3.6 The Microstructure of Air Temperature

Since wind turbulence is a consequence of viscous mechanisms it is reasonable to expect that temperature in a microscopic scale will vary temporally and spatially in a similar manner to that described above for wind turbulence. Consequently the work of Daigle et al (40) and Daigle (41) treat temperature fluctuations in a similar way to wind fluctuations, referring to the joint effect as atmospheric turbulence.

3.7 Résumé

From the evidence presented in the above sections only turbulence effects predicts a temporally fluctuating received sound level, bulk and refractive effects of wind and temperature being constant over extended periods.

The results of an investigatory experiment by the author revealed that the sound pressure level of octave-band noise propagated horizontally 1.4 m above open grassland fluctuates temporally in a manner that increases with propagation distance and frequency.

This indicated that atmospheric turbulence was influencing the received sound pressure level and may therefore be a contributory factor in the reduced predictability of outdoor noise barrier performance as mentioned in the introduction to this thesis. For this hypothesis to be examined further it was necessary to investigate the mechanism by which turbulence affects sonic propagation. Although several papers have been cited concerned with turbulence effects, the results published have dealt with long time-averaged measurements which do not reveal anything of the physical processes concerned.

It was therefore essential in this thesis to measure instantaneous meteorological and acoustical data for both open propagation and in the neighbourhood of a barrier. In Chapter 4 the design of experiments intended to collect relevant data is described.

CHAPTER 4

The Experimental Design

4.1 General Design Requirement

It was noted in comments on the references cited in Chapter 3 that little is known of the instantaneous effects of meteorological conditions on sound propagation in the open air, both in the case of unobstructed propagation and also with a barrier present. Such relevant previous works as exist relate instead to some form of averaged effects of wind as determined for example through the measurement of some form of time averaged received signal levels.

Precisely which meteorological parameters, or statistical derivatives of these parameters, would or might show any degree of correlation with fluctuation in propagation constants is thus a matter of speculation. It is not even possible, it is argued, to attempt an inspired guess at what might experimentally turn out to be significant. The overall experimental design, therefore, had to take this fully into account. This was done by arranging for the collection of data of a wide variety of types, both meteorological and acoustical. Thus, and bearing in mind the normally expected limits of feasibility in experimental techniques, arrangements were made to measure or record in a manner suitable for subsequent data handling and analysis, the following information:

Meteorological: (i) Instantaneous wind speed covering the time taken by the passage of a burst of sound between a source and the further of two microphone measurement positions.

(ii) Wind direction

(iii) Air temperature

Acoustical: The acoustical signal received at each of two spatially separated microphones following the release of an appropriate sound burst from the source.

It is in the essential nature of the work of this thesis that a pilot experiment to provide an initial investigation of the role of significance of various possible parameters was not feasible. Any measurement of worthwhile significance could only come through the full development of the complete experimental set-up. Effects sought were in any event likely to be slight and therefore only likely to show up as a result of rigorous experimentation anyway. The experimental design had to accommodate this fact and did so by building in a considerable degree of operational flexibility. Thus the nature of the acoustical signal used could be selected on demand from:

(i) Pure tones of a known frequency

(ii) Octave bands of noise

(iii) Pure tones of frequency arbitrarily chosen from within an octave band

It was appreciated that measurements would have to be made subject to a wide range of factors that are within experimental control. Examples of these are:

(i) Nature of acoustical signal, as stated above

(ii) Frequency of acoustical signal

(iii) Source/receiver geometries (with and without a barrier present) in respect of horizontal and vertical aspects.

The experimental design had also to allow for the whole range of the meteorological conditions which in the circumstances of the natural environment are, of course, beyond the control of the experiment and clearly a matter of the reality of the moment.

The major consideration to be derived from the above was that it pointed to the requirements for a system to reliably, accurately, flexibly and conveniently make a large number of measurements as an exercise, initially, of collecting experimental data.

Thus the logical requirement for an automatic, microcomputer-based measurement system in which appropriate variables could be selected under programme control became clear.

At the outset it was unclear whether open air sites that were satisfactorily free of vertical reflecting surfaces would be readily available. Such surfaces would naturally lead to acoustic reflections which could potentially modify any received signal. For instance, a reflected signal adding 10% in amplitude to the direct signal over half of the measurement period will give about 0.5 dB apparent increase in sound pressure level. Accordingly it was decided at an early stage to use time limited signals and to discriminate against unwanted reflections in the time domain.

The value of having additional information derived from a 16:1 laboratory based scale model situation to set against, and compare with, information obtained at full-scale became evident in the initial stages.

Scale model techniques originally developed for auditorium design (see Ref.(42) for instance) are increasingly used in barrier and free propagation experiments, (27, 28, 32, 43) due to the ease of testing theoretically feasible proposals or for experimentation on a trial and error basis at a design stage without the inconvenience in erecting full size structures that may be found to be unsuitable. It also permits a rigorous study of an existing situation, perhaps with a view to some remedial action, using artificial test conditions since measurements at the actual site may be inconvenient or even impossible, (e.g. motorways, airports, factories etc.).

The fact that the measurements were primarily directed at the open air situation pointed to the desirability of creating a mobile laboratory which could be conveniently moved on site when weather conditions made measurements possible.

Certain steps must be taken for a model to equate to the corresponding full size situation. Since linear dimensions are scaled, sonic wavelengths and pulse lengths must also be reduced to preserve diffraction and interference effects. Model materials must be carefully chosen to give absorption and reflection coefficients at the increased frequencies that are similar to the values of the actual material in the real situation. The absorption of acoustical energy by the atmosphere becomes increasingly significant as frequency increases and this must be either allowed for in the measurements or minimised by performing model experiments in low humidity air or in a less absorptive atmosphere, such as freon.

To permit scale-modelling, an additional constraint on the experimental design was the requirement, if it was instrumentally possible, to use the same developed equipment under 16:1 frequency enhanced conditions in the laboratory.

4.1.1 Summary

It was necessary for the selected experimental design to fulfill the following requirements:

(i) A source and two measurement microphones complete with associate electronics to create and measure sounds, in open air conditions and with selectable measurement geometry.

(ii) To provide a facility for the recording of these signals in such a way that quantative data could be extracted at the time or later.

(iii) To provide a means of measuring instantaneous wind speed, wind direction and, should it be subsequently be found of interest, air temperature. Again the requirement is esentially to record the values concerned for subsequent computation.

(iv) To allow for calibration of the above, preferably in a manner which may be carried out automatically into the computation process.

(v) To allow for the automatic operation of the above under, for example, micro-computer control.

(vi) To permit portability to site for open air work

(vii) To permit operation at a 16:1 reduced time scale so that direct transfer of the equipment to scale-model experimentation in the laboratory is possible.

(viii) To undertake and complete the above with the resources available for the experiment, in terms of both hardware and personnel.

The development, and the rationale underpinning it, of the various elements outlined above are separately discussed further in the sections that follow.

4.2 Realisation of the Measurement Requirements

This section forms a description of the general outline of the experimental set-up selected as suitable to implement the individual design requirements set down in section 4.1, in particular 4.1.1.

4.2.1 Geometrical Aspects

The requirements regarding the need to be able to handle a range of measurement geometries was satisfied by envisaging lay-out arrangements as indicated in Figs. 4.1 a - c and where all the spatial parameters indicated are considered open to variation over reasonable ranges without undue practical difficulty.

4.2.2 The Source Signal

The need to avoid the effects of interfering reflections, it has already been noted, is to be achieved using time-limited signals. It is a matter of further experimental detail (see Section 4.2.5) that a particularly convenient duration of acoustical signal is 28.7 ms which, for propagation in air at 20° and atmospheric pressure ($c = 344$ ms $^{-1}$) corresponds to a sonic path of 9.9 metres. Furthermore, this path corresponds to the following number of wavelengths at the frequencies subsequently chosen for investigation.

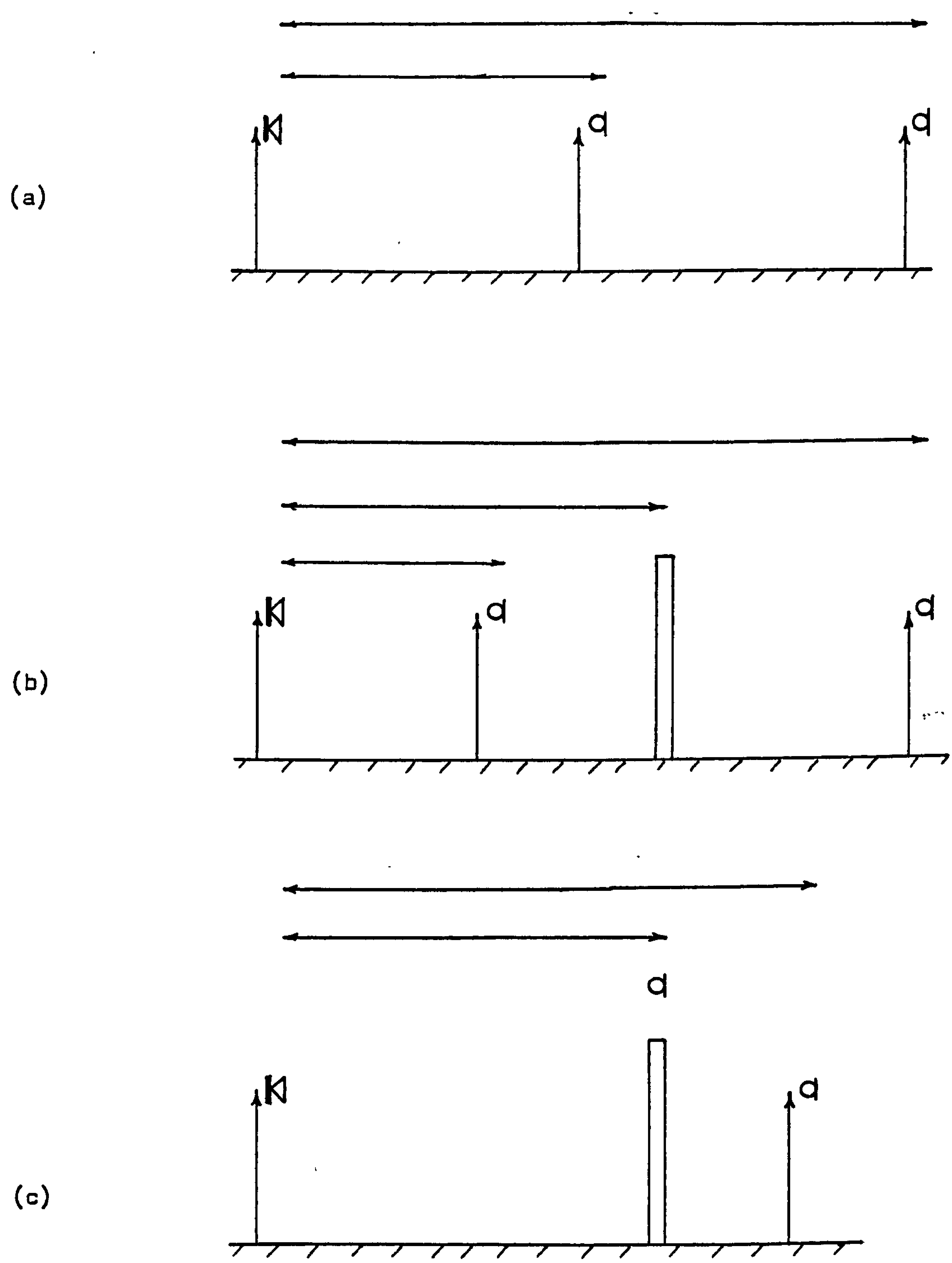

Fig. 4.1 Geometries used for Outdoor Experiments.

Frequency (Hz)	No. of Captured Wavelengths
250	7.2
500	14.4
1000	28.7
2000	57.4
4000	114.8

Fig. 4,2 Number of Captured Wavelengths

The role of interference caused by reflections from the ground plain was initially very much an unknown issue. Accordingly a conscious decision was taken at an early stage that the sound burst should be derived by time-wise gating of a variety of types of source signal. The first and most obvious choice was that of pure tone of fixed frequency. The second source signal was 1/1 octave-band limited white noise. (1/1 octaves were selected as the relevant frequency band primarily because of the availability of commercial precision filtering equipment. 1/3 octave bands were rejected at the outset because of known transient response problems when signals of the time duration of those envisaged here are being measured).

To provide potential information, should this subsequently become desirable, about the role of interference from ground plane reflections, the possibility of using a third kind of source signal was envisaged. These were again in the form of pure tones, but instead of being at fixed frequencies, were of variable frequency selected, for a particular sequence of tests, randomly from within an octave band.

In terms of actual frequencies chosen when using pure tones these were 250 Hz, 500 Hz, 1 kHz, 2 kHz and 4 kHz because these were the centre frequencies of the octave bands and their respective filters used with noise signals.

4.2.3 The Acoustic Source

The basic requirements here were for a source of adequate frequency response, efficiency, acoustic power output, stability and portability.

These properties were considered, after experimentation discussed in Section 5.2.1 to be optionally satisfied with a folded-horn loudspeaker. The cut-off frequency for the unit used in this work was known from prior experiments to be about 160 Hz but this was thought adequate for satisfactory implementation of the 250 Hz octave band. The frequency-dependant sensitivity of the instrument was such as to require the introduction of a frequency-selective compensation in the source signal path.

4.2.4 Microphone Measurement Systems

Proprietary ½" B & K condenser microphones were selected as having, by common experience, adequate sensitivity, stability and frequency range for the purpose.

Amplification was provided by instrumentation quality microphone amplifiers with some signal conditioning facilties available, and with adequate bandwidth (2-200,000 Hz) and gain stability.

PAGE

NUMBERING

AS ORIGINAL

allowed the onset of the capture phase for each channel to coincide with the arrival of the acoustic signal at each microphone.

This meant, in experiments where the barrier was to be used for example, the captured signal from the first microphone was separated from the signal reflected by this barrier providing that the microphone was no closer than 4.4 metres from the barrier.

4.2.6 Calibration of the Acoustic System

Arrangements were made to introduce standardised acoustic signals to each channel. These were handled in precisely the same way as the genuine signals to become internal references for all signals that follow.

4.2.7 Wind Velocity Measurements

The requirements for instantaneous wind velocity measurements relating to the time episode during which the acoustic signal is travelling the selected path was considered best satisfied by the use of a hot wire anemometer and associated circuitry. The circuitry maintains the hot wire at a constant temperature and the time-varying voltage that is required for this to happen is available as an output which is related through a known transfer characteristic to the instantaneous wind speed at the probe.

The device handles wind speeds on the range 0-10 ms^{-1} and over this range the output varies typically over the range one to two volts.

The overall bandwidth of the selected device (i.e. 0-10 kHz) was considered adequate to preserve information about particular local changes in wind speed. 8-bit digital conversion under system command using a separate proprietary

8-bit transient capture device made it possible to store wind velocity signal for subsequent analysis.

4.2.8 Wind Direction Determination

There was at the time of the original design no commercial wind direction meter available with output suitable for electrical recording. A device was, therefore, designed and constructed to perform this function producing a direct measurement of wind bearing in computer intelligible digital form with an angular resolution of 2^o.

4.2.9 Air Temperature Measurement

A particular ecperimental approach was adopted to harmonise with the rest of the equipment. A temperature dependant current source produced a signal which was converted to a frequency modulated signal for subsequent decoding.

4.2.10 Mobile Laboratory

A redundant motor caravan was converted for use as a mobile laboratory. All equipment was, or was modified to be, capable of being powered by either high capacity lead-acid storage cells, or else by these cells via a 240v inverter. Operation of sites distant from mains electric supplies was thus guaranteed.

4.3 Microcomputer Control

Complexity of the fully developed system, of which the component parts are described in outline above, together with the desirability of operating the system in a programmed manner highlighted the value of designing the entire experiment to be run under microcomputer control. It was clear from an early stage that such a system would also be particularly valuable for storage and intermediate processing of experimental data and also, potentially, for convenient transfer of partially processed data to a mainframe computer at a later stage.

At an early point in the investigation in this report it was clear that there was a choice between two basic methodologies. The first approach was to develop a comprehensive purpose-built system from readily available small scale electronic components. In this way, in principle, a system tailored to the precise requirements of the system would result, although it was acknowledged that the effort involved in such an action would be considerable.

The second approach was, clearly, to utilise as far as was practicable, the benefits offered through the incorporation of a developed system.

Considered opinion leant towards the view that the benefits in terms of convenience offered by the second approach outweighed any problems that were likely to arise from a lack of flexibility.

Accordingly, a control and computational system was developed around a Commodore PET microcomputer since at the time, admittedly one of extraordinarily rapid developments in the subject, that instrument was the most readily available and one which incorporated particularly attractive high level and machine code language facilities.

4.3.1 Microcomputer Interface Development

Comprehensive interface circuitry was designed, developed and evaluated to permit efficient communication between the microcomputer and its various peripherals. The overall system is shown in the block diagram of Fig. 4.3.

4.3.2 Software Development

Software was developed to permit the carrying out of the entire experiment on an automatic basis. For example, acoustic frequencies were selected, time-limited source signals were generated, auto-ranging received channel sensitivities adjusted the associated time-dependant acoustical and meteorological data captured.

In order to do this, and bearing in mind the importance of achieving the required speed in various elements of this process, a particularly convenient blend of high level and low level programming was used. Thus, the operating software comprised a number of segments of machine code programme set into a framework of a high level language programme. The high level language interpreted by the PET is BASIC.

In this way it was envisaged that a whole series of experiments could be undertaken for a particular measurement geometry with a minimum of human intervention.

The software developed also allowed initial calculation to be performed on the received data, the results of these calculations being stored in a way suitable for transfer to a larger, laboratory-based computer for further analysis.

4.4. Alternative Measurement Methods

Arrangements were built into the system, in the event that for practical reasons this became desirable, to substitute a method of on-site analogue

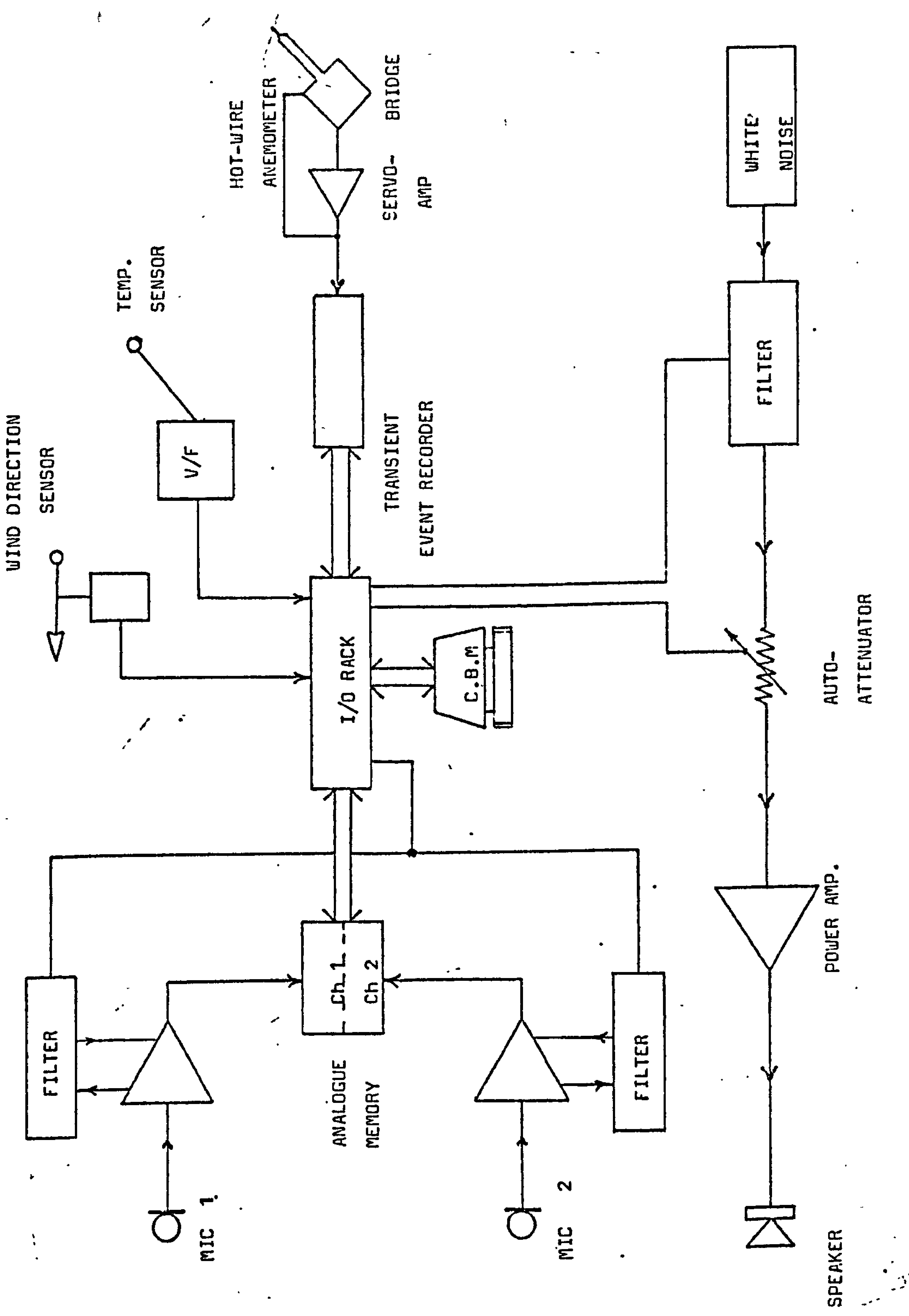

Fig. 4.3 The Automatic Measurement System Block Diagram.

recording using a Nagra IV SJ instrument quality tape recorder with two direct recoding channels being used to record the acoustic signals and the single FM channel for wind velocity data.

4.5 Implications of the above for Scale Model Work

Section 4.2 stated the desirability for designing a system with such flexibility that it could, with the minimum of modification (transducers are an obvious example), be used for parallel experiments at model scale (1:16) for example.

In the system of which the component parts are described in outline above, the analogue acoustic equipment possessed adequate bandwidth without modification. It was inherently impossible to reduce the temporal, and hence the spatial, extent of the acoustic signal as such. However, this was effectively achieved in part by using only the first quarter of the 4096 sampled points for each channel.

The signal source, and the circuitry driving it, together with two microphones, had to be changed to cover the increased frequency range.

CHAPTER 5

Details of the Measurement System

In this chapter the individual components of the measurement system, introduced in Section 4.2, are discussed in more detail. Where the inclusion of certain aspects of the description, programme listings for instance, would become cumbersome they are mentioned here but actually appear in Appendix A for reference.

5.1 Source Signal

As discussed in Section 4.1, the requirements were for a signal source capable of producing noise (to be filtered into octave bands), pure tones of a single frequency or pure tones of random frequencies within an octave band. A single signal generator capable of producing all three types was not available and so they were treated separately.

5.1.1 The Electronic Noise Generator

This was purpose built for this project and the circuit is shown in Fig. 5.1. It consisted of a back-biased diode (actually half of a transistor) producing the noise signal which was passed through two stages of amplification. An optional filter stage was included to shape the spectrum of the noise output to be attenuated by 3 dB per octave to give equal energy per octave band, known as "pink noise".

5.1.2 The Pure Tone Source

For reasons of stability, precision and purity of signal, the Beat Frequency Oscillator (BFO) of a heterodyne analyser, B & K type 2010, was used to produce pure tones.

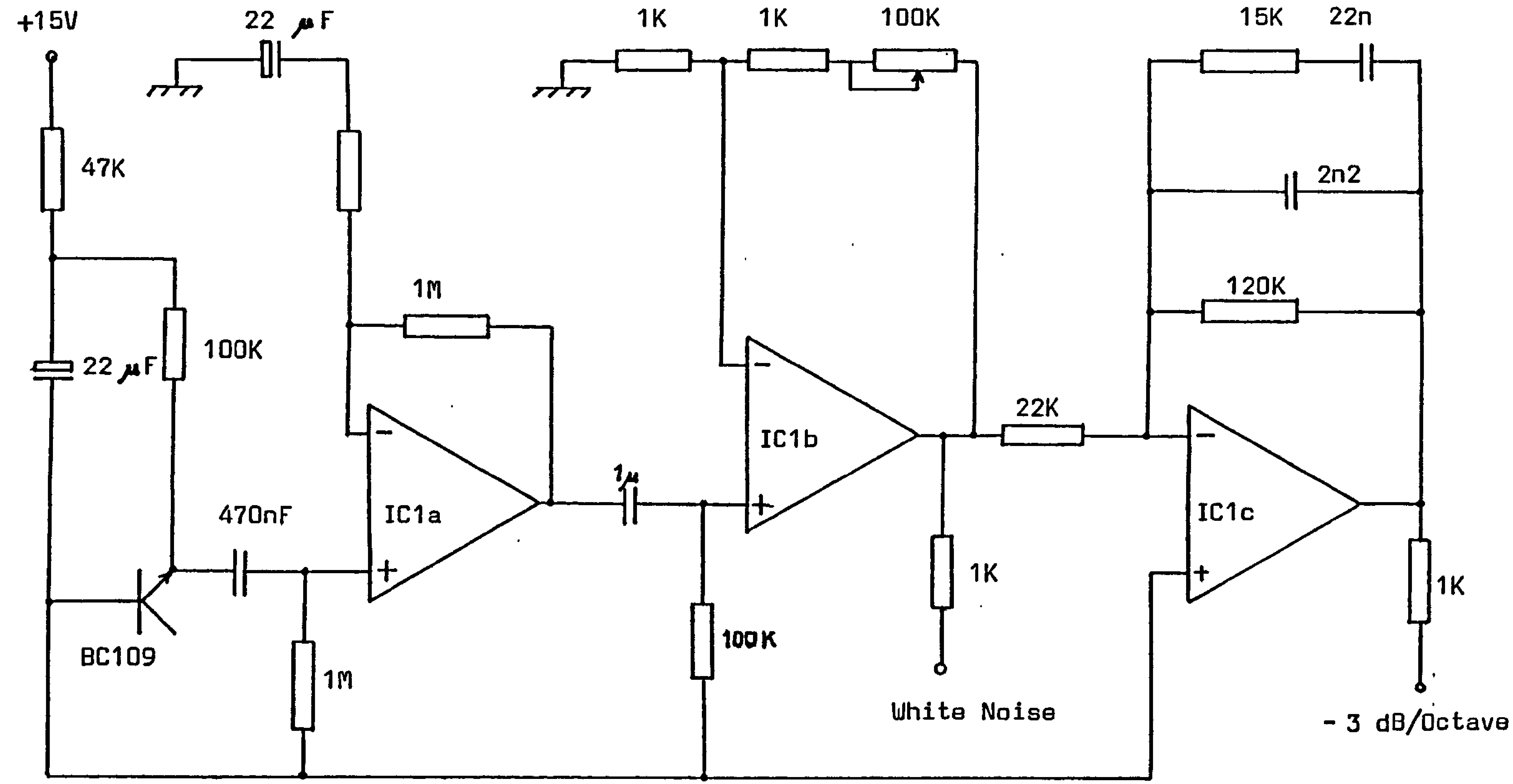

IC1: LM348 Quad Operational Amplifier

$\pm 15V$ supply regulated by 7815 regulating using

$\pm 27V$ from 6 x PP4 batteries

Fig. 5.1 Noise Generator Circuit Diagram.

5.1.3 The Random Pure Tone Source

This facility was provided by the BFO mentioned above. The signal frequency could be selected either by manipulating knobs on the front panel of the analyser or, as utilised in this case, by applying a DC voltage to a socket at the rear of the instrument.

The logarithm of the signal frequency is directly proportional to the applied voltage, 20 Hz to 20 kHz being covered by 0 to 10 volts. The voltage signal applied to the analyser consisted of two components:-

(i) a static voltage set to select the lower limit of an octave band

(ii) a linearly ramped voltage covering a range from 0 volts to a voltage such that the frequency of the BFO attains the upper limit of the octave band.

The static voltages were obtained by dividing the output of a DC power supply using a set of five potential divider networks (one for each frequency band used), housed in a box with a five position select switch for convenience of operation. The ramp voltage was provided by a proprietery signal generator, the extent and rate of the ramp being set by preliminary experiments. The ramp rate had to be such that the signal frequency was effectively constant during the 28 ms duration of a sound burst, yet was able to cover the octave range a number of times, perhaps 5, throughout the course of the measurement period for each frequency.

Note that, due to logarithmic dependancy of frequency on voltage, once the ramp characteristics are set for one octave band they then apply to octave bands centred on other frequencies.

5.2 The Sound Source

This is shown in block diagram form in Fig. 5.2. The source actually comprises the source signal which has already been discussed in Section 5.1 above. The remaining units are now described.

5.2.1 The Loudspeaker

The requirements stated in 4.2.3 pointed towards the need for a horn-loaded loudspeaker. However, it was known that a previous worker (44) had adapted a pressure unit to approximate a point source by adding a uniform cross-section tube with a length carefully chosen to minimise resonance peaks in the desired frequency range.

The choices available were, then:

(i) a point source, as described above

(ii) a folded exponential horn

(iii) a straight exponential horn

An example of each of the above was investigated under anechoic conditions for efficiency, extent of frequency range and flatness of frequency response.

Despite the usefulness of having a near-ideal point source, the pressure unit-plus-tube option was rejected since it was predicted on the basis of the anechoic measurements that the sound field would be indistinguishable from background at a distance of about 20 m from the source, even allowing for the maximum permissable applied voltage signal.

Although the straight horn was more efficient than the point source, the cut-off frequency was found to be at about 200 Hz. This was considered to be too high to provide a sufficient bandwidth in the 250 Hz octave.

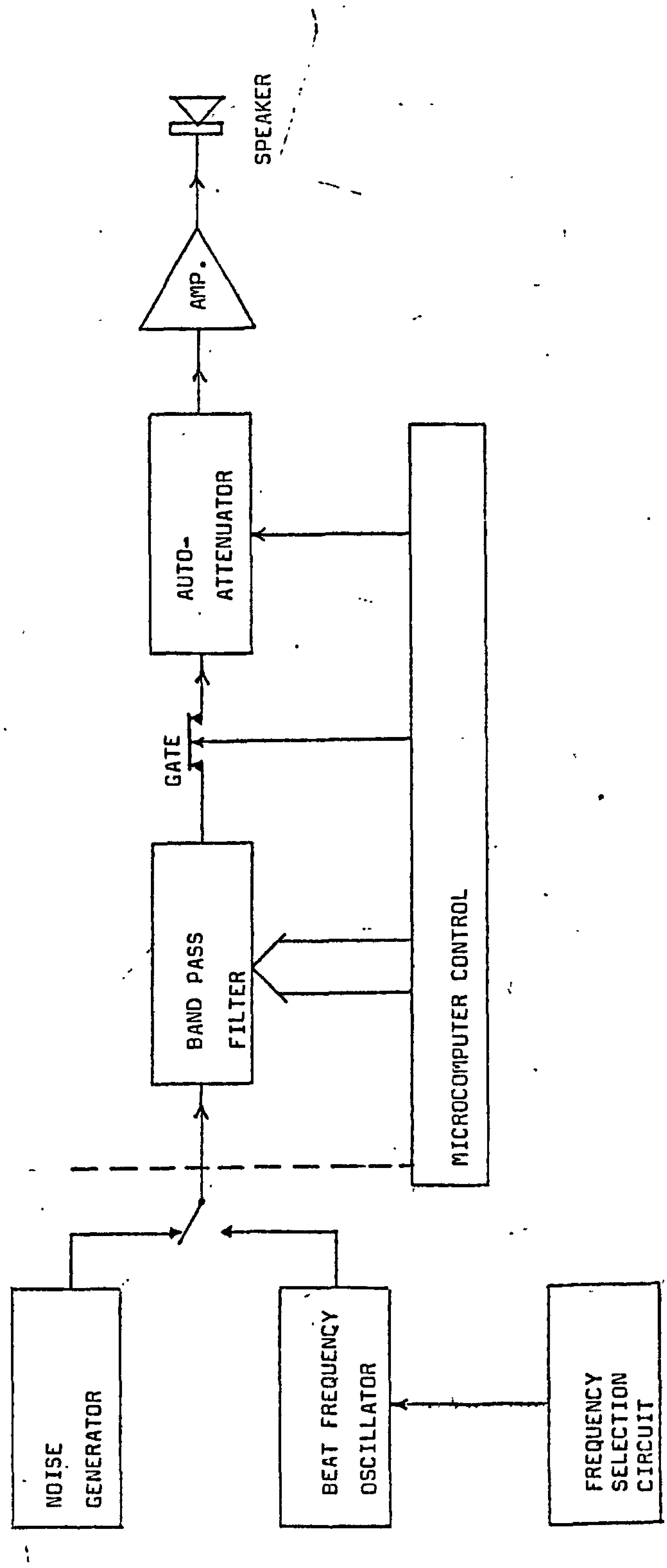

Fig. 5.2 SOUND SOURCE BLOCK DIAGRAM

The folded horn had an effective length of about 1.8 m and an experimentally determined cut-off frequency of 160 Hz. Due to the efficient radiation impedance matching characteristic of the horn, it was expected that the signal would be measurable at the maximum source/reciever distance envisaged in this work. For these reasons the folded-horn loudspeaker was used throughout this work.

5.2.2 Equaliser

The circuit was required to compensate for frequency dependant changes in the efficiency of the loudspeaker and is shown in Fig. 5.3.

The analogue signal is attenuated in non-linear proportion to the value of R_A. One of eight resistors can be selected under computer control by closing one of the eight analogue switches.

The resistors were in fact screwdriver adjustable multi-turn potentiometers which were set up in a preliminary experiment in the following manner for full-size experiments:

(i) the first switch is closed

(ii) continuous 250 Hz octave noise is emitted from the loudspeaker

(iii) the first potentiometer is adjusted until the signal received from the microphone occupies as much of the input range of the appropriate channel of the capture device without causing overloads. The overload LED's on the capture device are a useful indicator in this procedure.

(iv) the process is repeated for the second to fifth resistors corresponding to the 500 Hz to 4 kHz octave band.

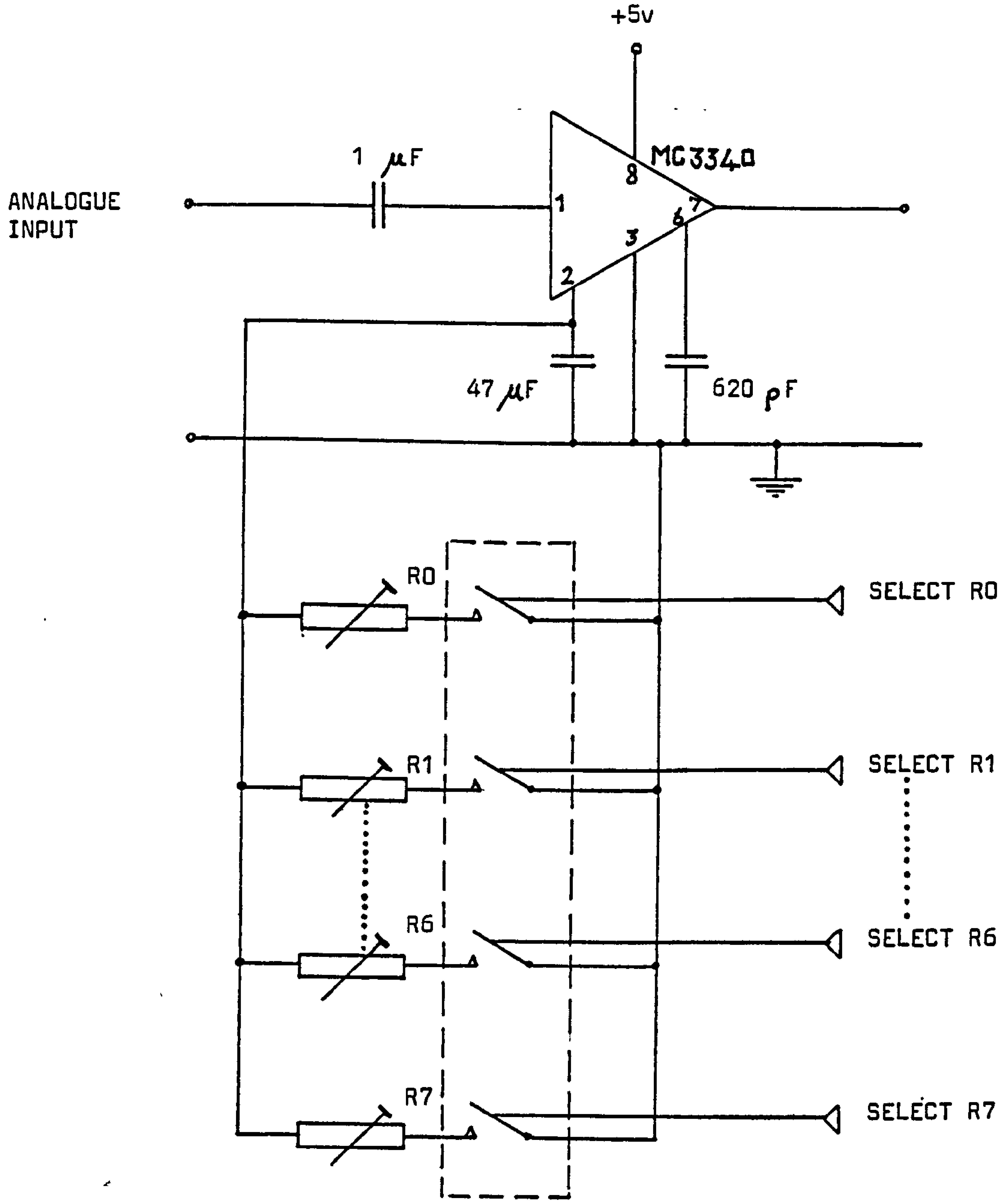

Fig. 5.3 THE EQUALISER CIRCUIT

A similar set-up procedure is used for model work, the frequency range being transposed to 4 kHz to 63 kHz.

5.2.3 The Signal Gate

A quad bilateral switch integrated circuit, type CD4016B was used to gate the source signal to provide the required noise burst facility. This device had the attraction of being digitally controlled whilst capable of passing analogue signals.

5.2.4 The Power Amplifier

It was necessary to amplify the small signals from the signal source to produce a voltage to excite the loudspeakers.

The loudspeaker had a low DC resistance (4 Ω) and so the requirements were for a high input impedance, so that the signal source and associated electronics was not unduly loaded, and a low input impedance. Additionally, it was important that the amplifier did not distort the signal or introduce noise.

A suitable device satisfying the above requirements was the Quad 33/303, a high quality audio amplifier. However, the many additional features on this device, such as stereophonic capability, and various signal processing features were unnecessary in this application and resulted in an undesirably high power consumption, considering the limited power available in the mobile laboratory.

It was, therefore, decided to construct a purpose-built amplifier from proprietary modules, and some associated electronic circuitry to provide a DC power supply.

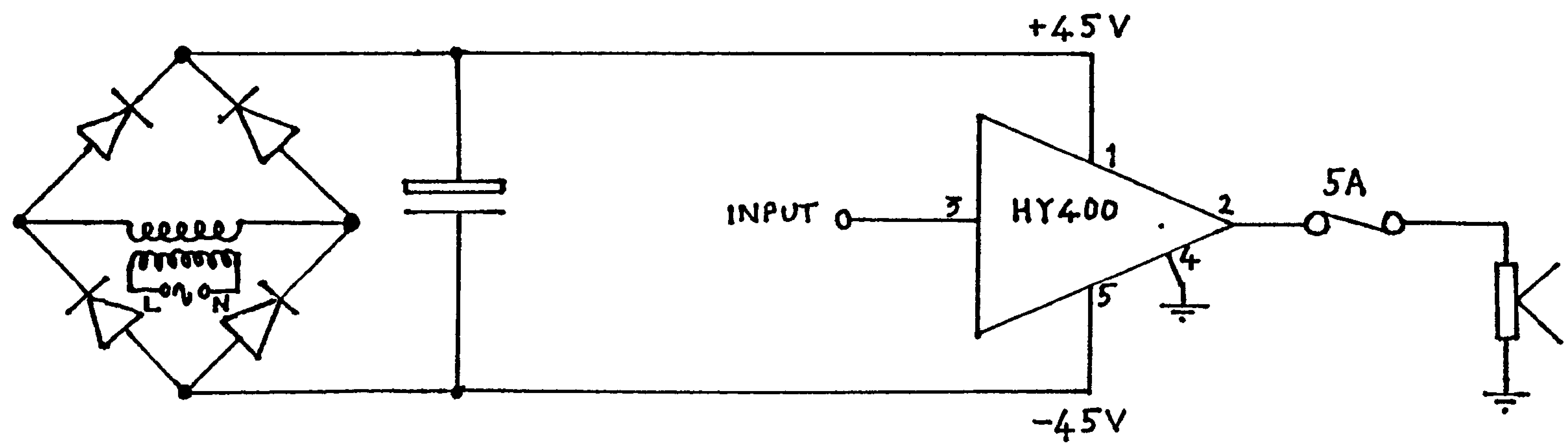

Fig. 5.4 Power Amplifier

The circuit diagram for this device is shown in Fig. 5.4. The performance of the amplifier was assessed by visual inspection of microphone signals as displayed on an oscilloscope.

5.2.5 The Band Pass Filter

Ideally, the requirements would be met by an octave band pass filter set with computer-selectable frequencies. Alternatively, a computer-controlled filter with a fast roll-off approximating that of a standard octave filter could be used if the cut-off frequency could be digitally controlled.

The chosen band pass filter consisted of two Kemo filters, type VBF 22, configured as a low-pass and high-pass in cascade to provide a band-pass characteristic. These were 6-pole elliptical filters which provided a characteristic as shown in Fig. 5.5. which was considered to be a good approximation of a third octave filter when compared with a B & K filter. The cut-off frequency of each filter is set by three rotary knobs to specify two significant digits and a decade multiplier between .1 and 1000. It is also possible to set the cut-off frequency digitally via an interface at the rear of each filter. The two significant digits are required in a Binary Coded Decimal (BCD) format whilst the decade multiplier is specified by setting a logic high level on one out of five possible inputs. (See Appendix A).

5.3 Microphone Channels

As stated in Section 4.2.4 the microphones used in the full-sized experiments were ½" B & K microphones or ⅛" B & K microphones in model experiments. Associated with each microphone was a B & K 2606 measuring amplifier, including a B & K octave filter set.

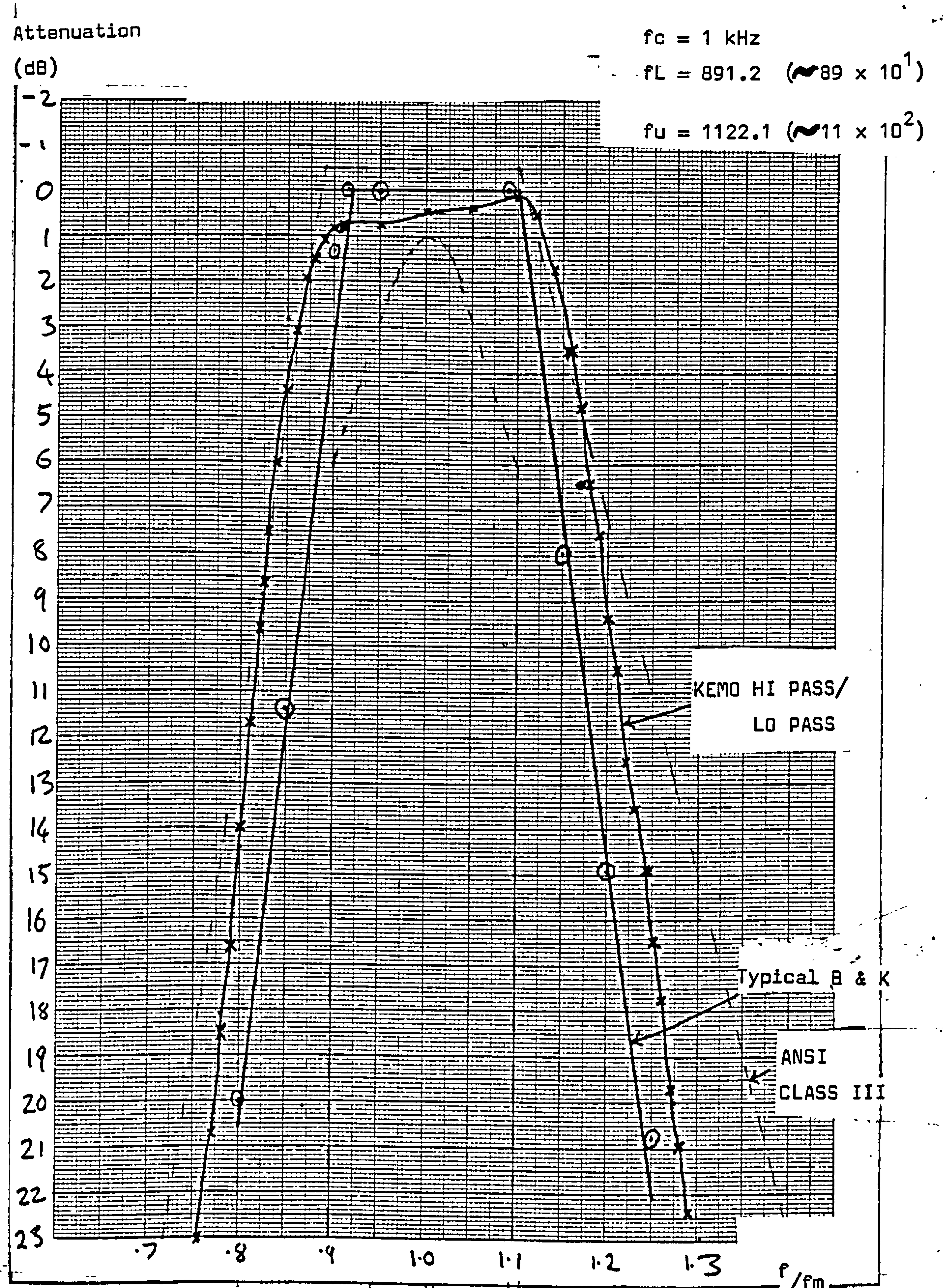

Fig 5.5 Comparison of two VBF 22/05 filters with B & K Third octave filter set and ANSI Class III standard.

5.3.1 The Autoranging Device

An autoranging device was included in the signal channel that serviced the microphone nearest to the sound source. In terms of construction and operation this device was the same as the equaliser circuit discussed in Section 5.2.3 and shown in Fig. 5.3.

The purpose of the device was to prevent the received signal from the microphone from overloading the input range of the twin channel capture device (See Section 5.4 below).

The eight resistors were pre-set in the laboratory to produce a constant attenuation, either 1 or 2 dB, between adjacent resistor settings. The attenuation was automatically set by the microcomputer when a series of measurements at a new frequency was to begin. The sequence of events is as below:

(i) The final measurement at a particular frequency is made. (Clearly this step is omitted for the first frequency).

(ii) All filters and the equaliser are set for the next frequency

(iii) The autorange device is set to minimum attenuation.

(iv) A continuous sound of the new frequency is emitted by the loudspeaker.

(v) The output of the near microphone channel of the capture device is inspected by the microcomputer for an overload condition (that is a 0 or 255).

(vi) If an overload occurs then the attenuation of the autoranger is increased by one attenuation step and the process repeated from step (v).

(vii) If no overload condition occurs while the memory is filled ten times over then the autoranger is considered to be set.

The final setting of the autoranger was stored with the measured data in order to calculate the received level.

The autoranger and equaliser together should provide good-sized signals at both microphones. However, if an overload does occur during the course of the measurements, this is flagged by storing the measured RMS level as a negative number.

5.3.2 Automatic Operation of the Microphone Filters

Although these filters, B & K Type 1615, could not be set digitally in the same way as the source filter, it was possible to energise an internal solenoid that produced the mechanical equivalent of manually operating the front panel knob that selects centre frequencies.

The circuit used to achieve this is shown in Fig. 5.6. On receiving a pulse from the microcomputer the solenoid will be moved once which will advance the filter by one third octave. Clearly, to advance by one octave requires three consecutive pulses.

The opto-isolation device was used to prevent electrical interference caused by the energising of the solenoid from affecting the microcomputer.

5.4 The Twin Channel Capture Device

The digitisation of the microphone signals was performed by a Kemo twin

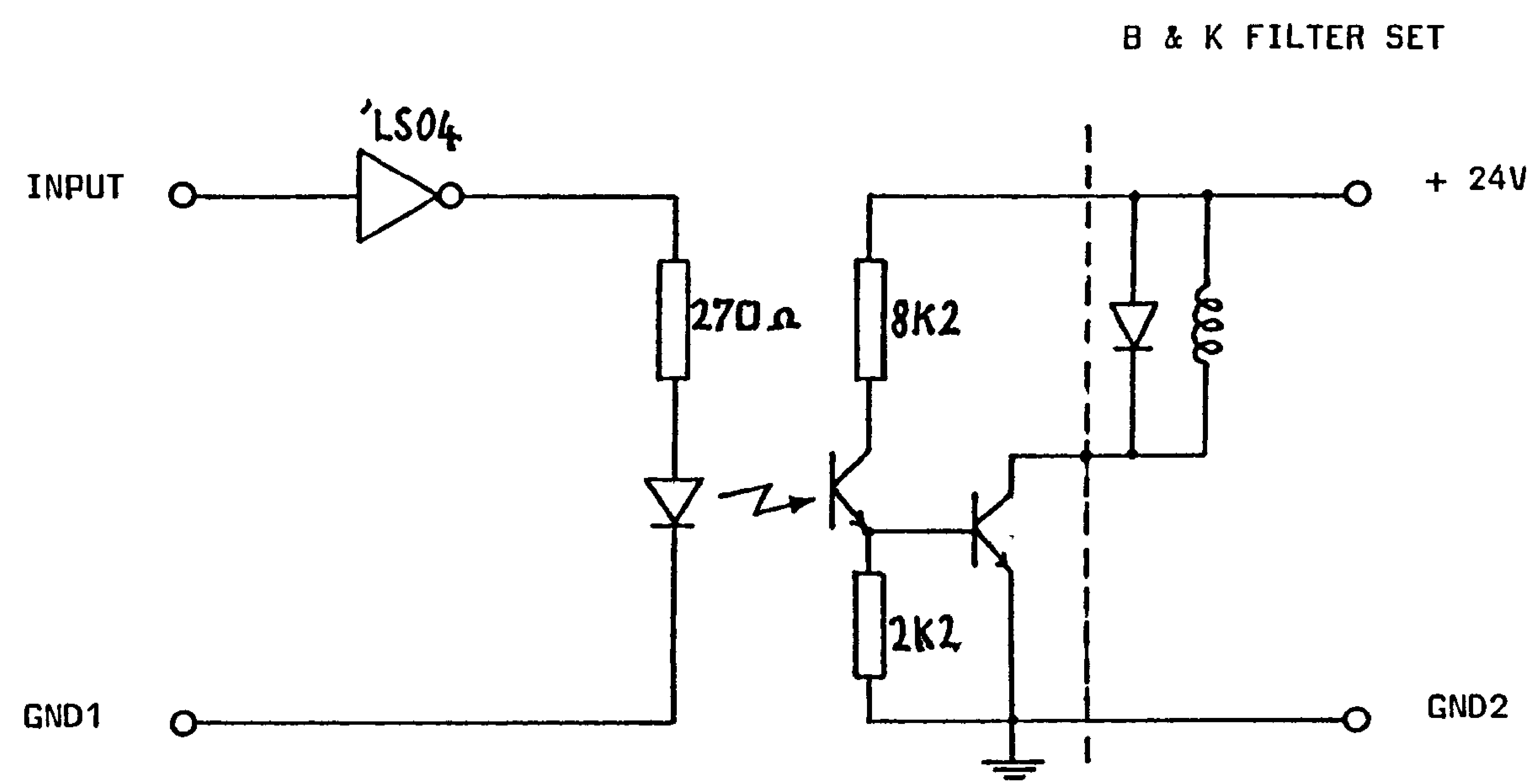

Fig. 5.6 FILTER SET SOLENOID CIRCUIT DIAGRAM

channel capture device known as an analogue memory. This device performs the analogue to digital conversion (ADC) and stores the information in a semiconductor memory, from which it can be transferred on demand to the microcomputer.

This operation could alternatively be performed by straight forward analogue to digital conversion and either storing the data in the microcomputer random access memory (RAM) or performing the necessary calculations on the data in real time. However, to store the data could occupy a major part of the available RAM and impose a restraint on the software (the Kemo device has 2 x 4096 bytes of memory). Also the management of memory allocation would be a relatively time consuming operation. Real-time processing would also be time consuming bearing in mind that the various conditions should be measured as near instantaneously as possible in order to have confidence in any correlations uncovered when the data is analysed.

The use of the capture device permits the servicing of other transducers immediately after the microphone signal is recorded. The calculations on the captured signals can then take place some time later. It also facilitated overload indication, used in setting the equaliser (section 5.2.3) and routine background sampling. (Section 5.8).

5.5 Anemometer

The hot wire system used was a DISA battery operated constant temperature anemometer (CTA) type 55D05.

The system used a probe consisting of 0.5μ diameter wire, about 1 cm in length, suspended across two supporting metal conductors of a streamlined shape to minimise induced turbulence. The probe is connected by a coaxil cable to a remote box containing a Wheatstone bridge circuit in which the probe forms one resistive element.

An imbalance in the bridge is detected by a servoamplifier which automatically adjusts the voltage at the top of the bridge to redress the balance. The probe therefore remains at a constant temperature. In no-flow conditions an equilibrium voltage will be attained. If the probe is now subject to a flow of fluid the probe will be cooled causing its resistance to drop and the servoamplifier to inject a higher voltage to keep the bridge balanced, (i.e. to keep a constant probe temperature). Consequently, the servoamplifier output is representative of the fluid flow rate.

The relationship between fluid velocity and output voltage is given by King's Law:-

$$V = V_o + Bu^n$$

where V = output voltage

V_o = no flow voltage

u = fluid velocity

The coefficients B and n are specific to a particular probe and so a probe requires calibration as shown in Appendix C.

5.5.1 Digitisation of the Anemometer Signal

This was achieved using a single channel capture device, the Datalab DL 901 Transient Event Recorder. It is similar in principle to the Kemo capture device used in the microphone channel (section 4.2.5 and 5.4). The capture phase was triggered by the same microcomputer signal that initiated the sound burst, and so acoustical and wind speed data were recorded simultaneously.

Since the no-flow voltage of the anemometer was a finite DC voltage the offset gain controls of the capture device were adjusted to optimise the 8-bit dynamic range. Typically, the voltage range covered was from 1 to 2 volts.

The use of a capture device for the anemometer was consistant with the technique adapted for the microphone signals and served to optimise the correlation between the two forms of measurements.

5.6 Wind Direction Indicator

This device consisted of a conventional wind-vane mounted on an electromechanical assembly designed to sense the direction of the wind-vane and convey the information to the PET in a suitable digital form, this being achieved as follows:- A drum, a few inches in diameter and length, is rotated about a common axis with the wind-vane by a battery-driven motor. On its curved surface are alternate black and silver stripes spaced at 1^{o} intervals. When these pass a reflective optoelectronic sensor it emits a train of pulses with a periodicity equivalent to 2^{o} of drum rotation. If the microcomputer counts these pulses between a reference direction and the direction of the wind-vane then the wind direction can be obtained to within $\pm 1^{o}$. The reference direction is flagged to the PET by the interruption of the infra-red beam in a fixed opto-electronic switch by a radial projection fixed to the drum. Directly above this projection is an optical fibre which carries an infra-red beam from an LED housed on the drum. The open end of the fibre points upwards towards the wind-vane. A second optical fibre is mounted below the wind-vane and rotated with it. When the two ends of the fibres align, the infra-red beam passes along the second fibre and is detected by a phototransistor which signals to the PET to stop counting pulses.

For field experiments the equipment was mounted in plastic weather-proof shielding at the top of a stand some 9 feet off the ground.

Fig. 5.7 illustrates the equipment with the shielding removed. Details of the computer interfacing and processing appear in Appendix A.

5.7 The Electronic Thermometer

A temperature-dependant current source was the basis of this device. It was housed in a transistor-type metal casing and had an output of 1 μV per °K. It was incorporated in an amplifier circuit such that an output of 0.1 V per ^{o}c was obtained and this was fed to a voltage to frequency converter integrated circuit which, since the microcomputer with its added interfacing could count pulses in a given time, allowed the temperature to be read.(Fig.5.8)

5.8 Overall Control of the Automatic Measurement System

This section describes how the measurement techniques, so far discussed individually, are combined to make the complete automatic measurement system for any single geometry of source and receivers.

The machine code program used to service the individual devices are linked by means of a BASIC program which controlled the sequence of events as described below.

1. The first frequency, 250 Hz, is chosen and the sound source filter set for the octave band centred on the frequency and the attenuator set to the first setting.

2. The attenuator associated with the near microphone is set by closing the electronic switch in the sound source to produce continuous sound. The signal from the microphone is sampled, and if an overload is detected, the attenuation is increased. The overload is detected if a part of the signal is digitised

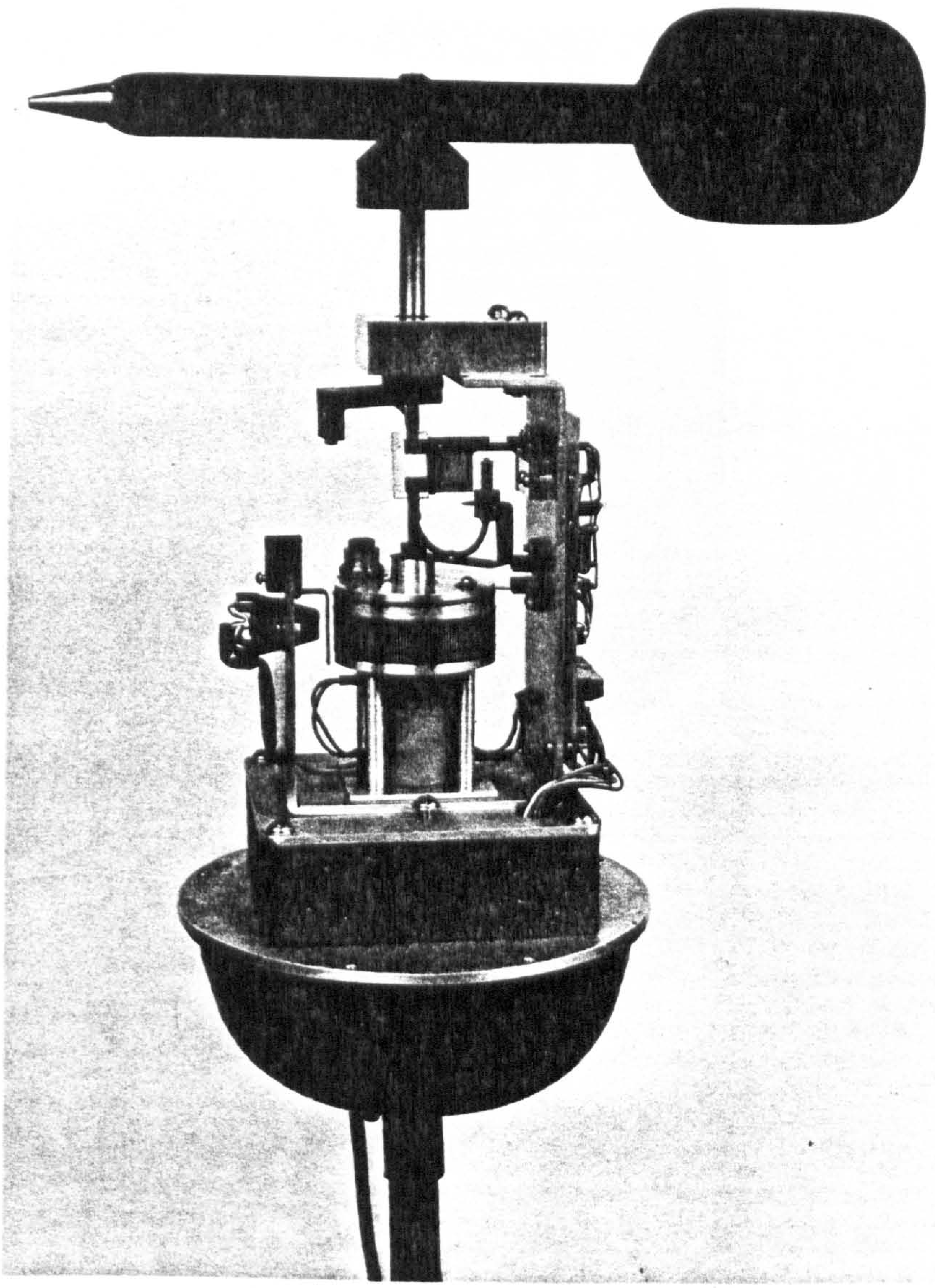

Wind Direction Sensor - Internal View

Fig. 5.7 (a)

Wind Direction Sensor - Showing Protective Cover and Battery Box

Fig. 5.7 (b)

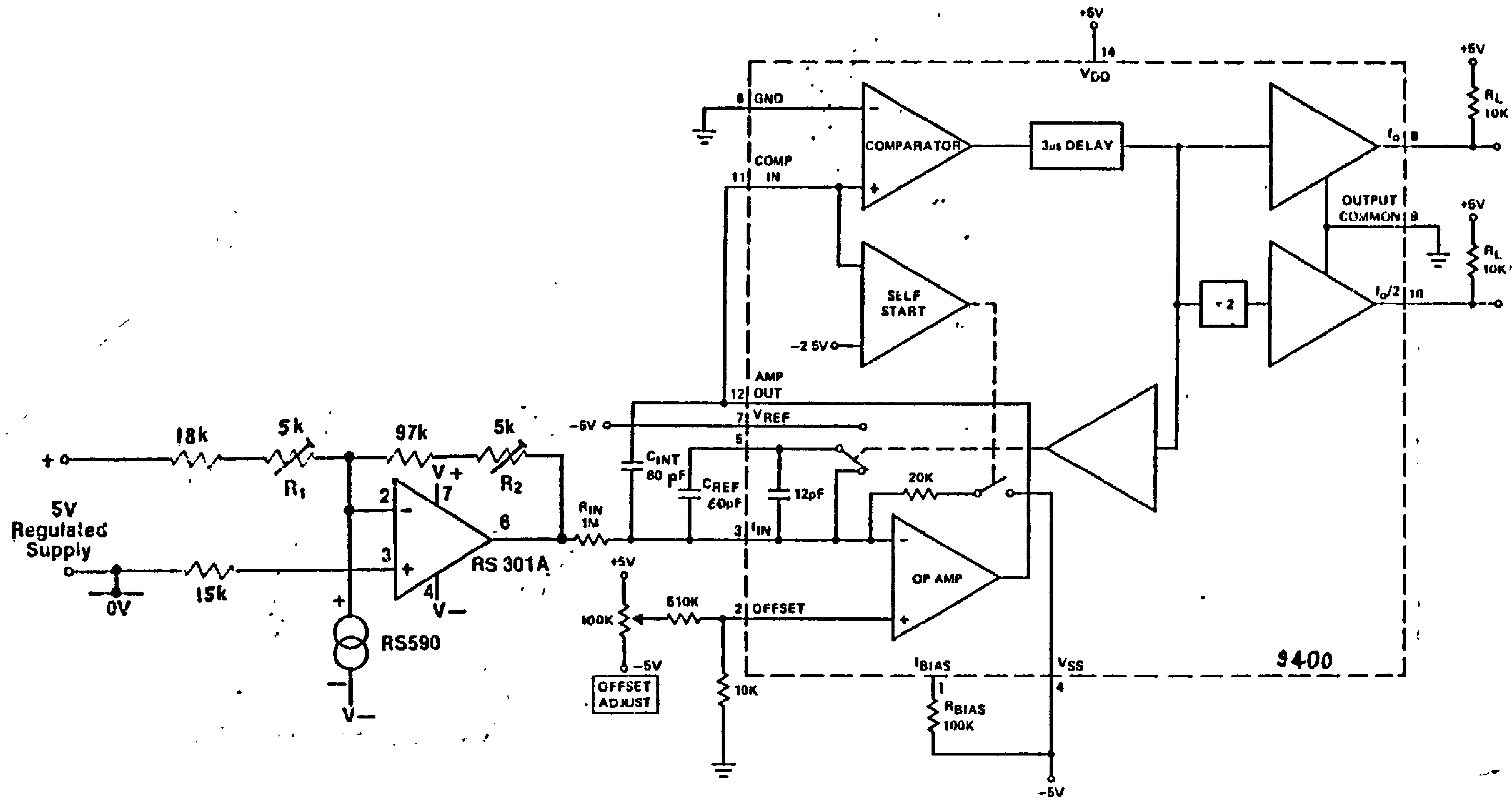

Fig. 5.8 Temperature Sensor Circuit Diagram.

as 0 or 255, that is either extreme of the 8-bit range of the ADC in the event recorder. The attenuation is considered to be sufficient if no overloads are detected when the event recorder fills ten times over at which point the sound burst is terminated by closing the electronic switch in the sound source.

3. The microphone's event recorder is armed with no sound issuing from the loudspeaker. If the recorder subsequently triggered it must be due to an excessive background level. If no trigger occurred for at least one second it was assumed that the background noise level was sufficiently low to make a meaningful acoustic measurement. This method proved to be efficient on numerous ocassions when overflying aircraft or approaching machinery temporarily inhibited the measurements until the noise had diminished.

4. Immediately after this background sampling the electronic switch in the sound source is opened and the ensuing microphone signals are sampled via the event recorder. The same pulse that initiates the sound burst also triggers the event recorder associated with the anemometer in order that the acoustical and wind speed measurements are as nearly simultaneous as possible. At this point, the data is left in the event recorder memories whilst the other devices in the system are serviced.

5. The wind direction sensor is serviced and the angular difference between the reference and the wind-vane direction is stored.

6. Pulses from the electronic thermometer are counted for one second and the result stored.

7. Acoustical data is transferred to the microcomputer which subsequently calculates the RMS level for each channel and stores the results.

8. Wind speed data are transferred to the microcomputer and the mean and the standard deviation of the signal is calculated and stored.

9. The process is repeated from step 3 for a chosen number of passes. Twenty was a usual compromise between statistical validity and excessive experiment duration.

10. The above sequence is repeated for frequencies up to 4 kHz.

11. The data accrued in the microcomputer's memory during the course of the measurements is transferred on to a floppy disc in order to make a permanent record for future analysis in the laboratory. The experimenter is prompted by the PET to enter a unique identifier for the data file for classification purposes.

5.9 Calculations

This section describes the calculations performed by the microcomputer at the time of the experiment to obtain RMS levels, standard deviations, etc., and in the laboratory to obtain sound pressure level, wind turbulence factors etc.

5.9.1 Sound Pressure Levels

The RMS levels of each microphone signal were to be calculated so that the sound pressure level could be found by referencing the individual RMS levels to that of the calibration tone. At the time of the experiment the 4096 digits representing a captured signal were treated in the following way to obtain the mean square value (see the flowchart of Fig. 5.9).

Knowing the zero volts level to be equivalent to a digital representation of 127, the signal was full-wave rectified in software by finding the modulus of the numerical value of every point minus 127.

The results were squared and accumulated in a floating point accumulator.

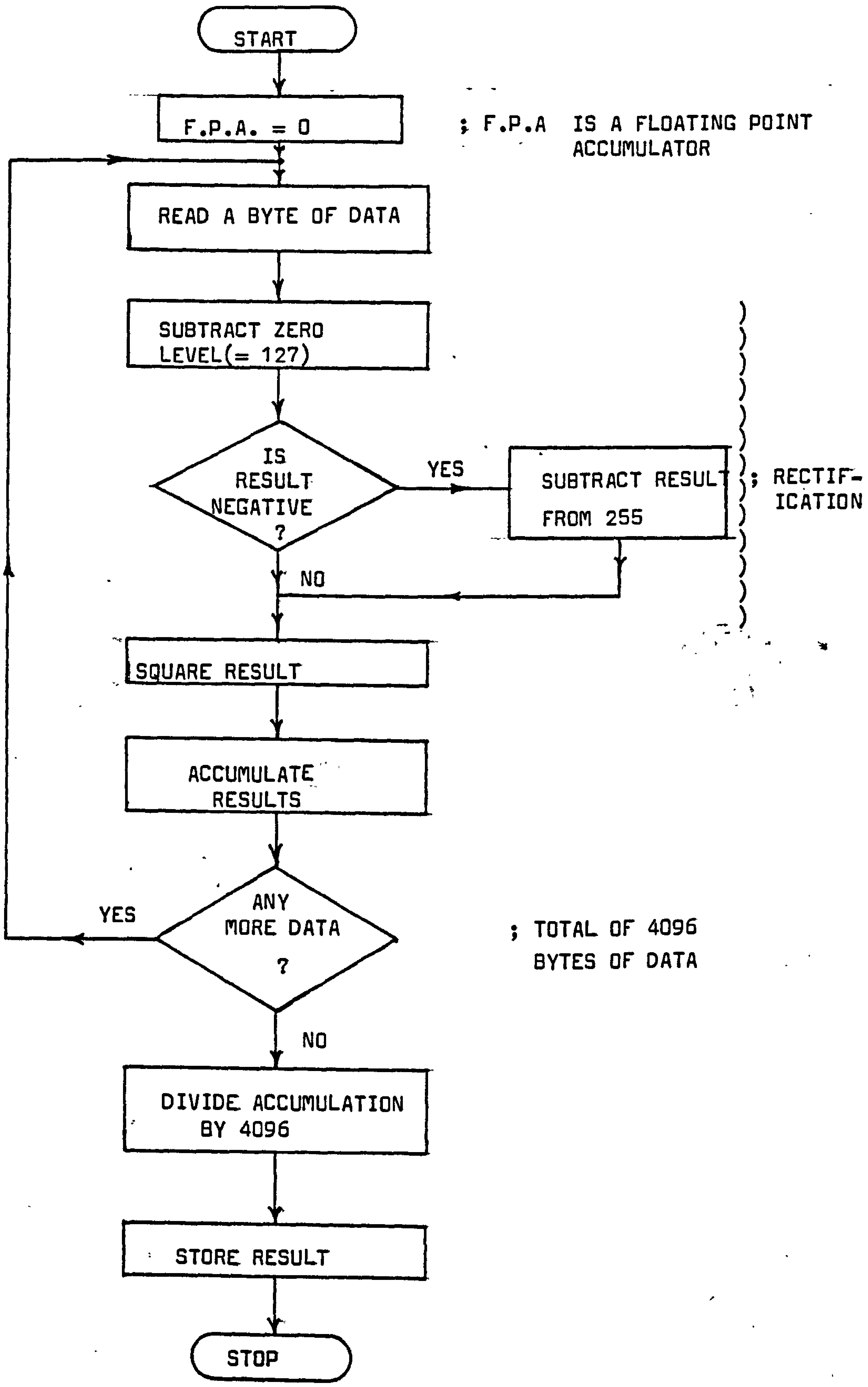

Fig. 5.9 FLOWCHART FOR THE RMS ROUTINE

After all points had been processed the contents of the floating point accumulator were divided by 4096 to give the mean square value which was then stored.

In the laboratory these mean sqaure levels were compared with the mean square level from a 94 dB microphone calibration tone. The sound pressure level can be calculated by:

$$\text{SPL (dB)} = 20 \log \frac{R}{R\ cal} + 94 + L \qquad (5.2)$$

Where R = root mean square of a measurement

R_{cal} = root mean square of the calibration tone

L = the attenuation introduced by the autoranger (zero for the far channel).

The standard deviation of the RMS measurements could be calculated from:

$$\sigma = \sqrt{\overline{x^2} - \bar{x}^2} \qquad (5.3)$$

If x is RMS level then

$$\sigma = \sqrt{\frac{\Sigma R^2}{N} - \left(\frac{\Sigma R}{N}\right)^2} \qquad (5.4)$$

where N is the number of measurements at a particular frequency, usually 20. The standard deviation was usually quoted in dB units.

5.9.2 Wind Speeds

Wind speed was determined from the mean value of the output of the anemometer as recorded by the transient capture device. The calibration of the probe relates the output voltage of the anemometer to the wind speed and so the calculation involved two stages: To recover the voltage from the digitised data and then to use King's Law with the calibration parameters in order to obtain the wind speed (see Section 5.5,). The digitised numbers were related to the voltage at the input of the capture device by a linear trnsfer function:

$$N = GV - O \tag{5.5}$$

where G is the gain and O is the offset. The device was set up to digitise signals in the range 1 to 2 volts as 0 to 255, therefore, G = O = 255.

If the digitised numbers are averaged we obtain:

$$\frac{1}{1024}\sum_{i=1}^{1024}\left(GV_i - O\right) = G\bar{V} - O \tag{5.6}$$

from which the required $\bar{V}$ can be obtained. It should be noted, that for reasons to be discussed in 5.9.3 below, the offset is eliminated by adding to every digit before summation.

5.9.3 Wind Turbulence

Wind turbulence was represented by the quantity known as Turbulent Intensity defined as the ratio of the standard deviation of the wind speed over the time average of the wind speed expressed as a percentage:

$$TI = \frac{du}{\bar{u}} \times 100 \tag{5.7}$$

It can be shown (46) that this can be approximated by:

$$TI = \frac{4\bar{V}v}{\bar{V}^2 - V_o^2} \tag{5.8}$$

where $\bar{V}$ = average anemometer

v = standard deviation of anemometer voltage

V_o = no flow voltage .

This approximation is valid for turbulent intensities up to 10%.

$\bar{V}$ is obtained from (5.4) above and so it only remains to determine v. As a first step the standard deviation of the numbers about zero can be found.

$$\sigma^2 = \frac{1}{1024}\sum_{i=1}^{1024}\left(gV_i - O\right)^2 \qquad (5.9)$$

Clearly the product term makes the recovery if Vi^2 difficult, and so the offset value is added to every digit before squaring and adding. The result of this procedure then gives:

$$\sigma = g^2\overline{V_i^2} \qquad (5.10)$$

The standard deviation about the mean is then found:

$$V = g\sqrt{\left(\overline{V^2} - \overline{V}^2\right.} \qquad (5.11)$$

Turbulent intensity could also be computed from the definition (5.7). In this case the digitised values were linearised using a "look-up" table which was produced from a knowledge of the transfer characteristic of the probe used.

The inverse transfer function was computed as a series of equivalent digits stored in a "look-up" table in microcomputer RAM. In this way the anemometer signal was linearised on entry to the microcomputer and the conventional mean and standard deviation formulae were then available.

5.9.4 Wind Direction

In a particular mode of operation of peripheral interface adaptor type MCS 6522 it is possible to allow pulses applied to a control line to decrement the number stored in a register within the device (See Appendix B). One of the MCS 6522 circuits added to the microcomputer was used to count the pulses emitted by the wind direction sensor starting from the detection of the reference pulse, when the register is loaded, to the detection of the coincidence pulse, when the value in the register is subtracted from the original value.

This gives the angular displacement from the reference direction to the wind direction in units of 2^{o}. That number is stored, but doubled when recalled in the laboratory.

5.9.5 Air Temperature

An MCS 6522 in pulse counting mode (see Appendix B) was used to count pulses from the electronic thermometer for one second, this being timed using the microcomputer's internal clock. The value of the count was stored. On recall in the laboratory the air temperature was calculated by:

$$T = n/2500 \quad {}^{o}C \tag{5.12}$$

where n is the number of counts in one second, since 100 kHz is the maximum frequency from the V/F converter and corresponds to a temperature of 40^{o} C.

5.10 Data Storage

This covers two stages: firstly in RAM and then on floppy disc.

Random access memory in the Commodore microcomputer used in this work is contiguous between memory locations 0000_{16} to 4000_{16} (the 16 suffix indicates hexadecimal notation). The top 1k of this (i.e. from $3C00_{16}$ upwards) was used for the anemometer data. The results of the data collection described in this chapter were stored immediately below $3C00_{16}$ downwards. (See Fig. 5.10)

The BASIC program was located by the operating system from address 0400_{16} upwards and the machine-code program above this at 1000_{16} upwards. Although the data could ultimately corrupt the top of the machine-code program, the amount of data collected at any one time was insufficient for this problem to occur.

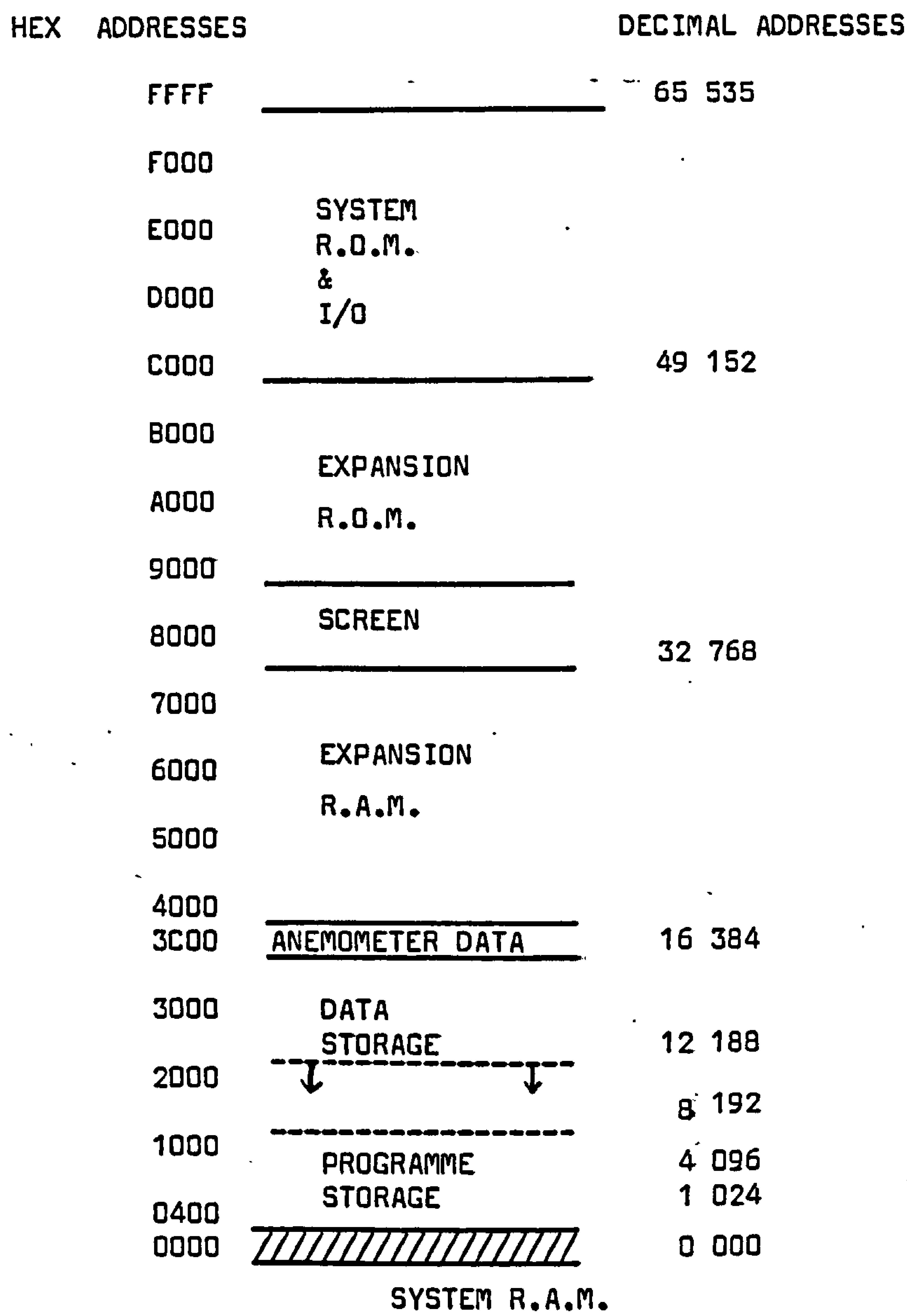

Fig. 5.10 MEMORY MAP OF THE COMMODORE SYSTEM (BY BLOCKS)

Throughout the execution of an experiment two memory locations were used to point to the current address to which data should be sent. This pointer was originally set to $3C00_{16}$ and was successively decreased as data was added to the stack throughout the course of an experiment.

At the completion of the experiment, a permanent record of the data was made by saving all memory locations from that in the current address pointer up to $3C00_{16}$ on floppy disc.

The experimenter was prompted by the microcomputer to enter a unique indentifier for the data file in order that it could be recalled in the laboratory. It was usual for such an identifier to comprise a page number in a log book and some simple numerical index to indicate the geometry used.

CHAPTER 6

Validation of Measurement System

Due to the unconventional nature of the automatic measurement system described in Chapters 4 and 5 it was essential to prove that the data collected was consistently accurate and precise in order to have faith in the conclusions drawn from the analyses, as discussed in Chapter 11.

This chapter describes the validation of the automatic measurement system by direct comparisons with either established measurement techniques or theoretical predictions.

6.1 Acoustical Measurements

The acoustical measurement system was validated by checking the proposed calculation software against theoretical values, using precisely defined electrical test signals throughout the various stages of development and finally by using acoustical signals under test-cell conditions in the fully-developed system.

6.1.1 Calculation Software

The accuracy of the root mean square calculation was essential to the dependability of the acoustical measurements. Another calculation performed was the standard deviation of a set of RMS measurements. This was used to test the hypothesis that the summation of many short segments of a truly random noise signal was statistically equivalent to a single long segment. That is, the mean and standard deviation of a set of short-time constant measurements could be as representative as the mean and standard deviation of one long time constant measurement.

Root Mean Square Calculations

This was tested by using various DC levels captured in the KEMO analogue memory and transferred to the microcomputer and by producing programmed signals stored in the microcomputer's internal RAM.

The DC levels were created by short circuiting the input to the analogue memory and adjusting the offset using a graduated potentiometer numbered from 0 to 5 in steps of 0.01. The offset could be selected either positive or negative such that the full scale input sensitivity was covered by -5.00 to +5.00. The following results were obtained:

Offset	Digitised Value	Calculated RMS	Expected RMS	Error %
+ 5.00	255	127.98	128.00	.02
+ 2.50	191	63.99	64.00	.02
+ 1.25	159	32.01	32.00	.03
- 1.25	96	30.99	31.00	.03
- 2.50	65	61.99	62.00	.02

∴ Calculated RMS of DC signals

The digitised values were rectified about a zero level of 127 and so the negative offset RMS values are one less than the corresponding positive offsets.

The error between calculated and expected RMS levels is small compared with the precision of the offset potentiometer. Indeed, the error appears to be systematic and probably attributable to the potentiometer.

The RMS calculation procedure was further verified by creating "signals" in software and storing the digital values in a 4K segment of the microcomputer's internal RAM, so forming a mimic of the capture device. Square waves and sine waves of an integral number of period and of various amplitudes were used. Since the waveforms were ideal, exact agreement between calculated and expected RMS was achieved.

Standard Deviation Calculations

The next experiment was an investigation into the effects of using very short time constant measurements by finding the standard deviation of a set of such measurements, and comparing them with theoretical standard deviations as described below.

Consider the RMS level of a sine wave measured for a duration very much less than its periodicity. The RMS of a sine wave is given by:

$$(\mathrm{RMS})^2 = \frac{1}{P}\int_Q^{Q+P} \sin^2 x \, dx \qquad \text{(see Fig 6.1)} \qquad (6.1)$$

$$(\mathrm{RMS})^2 = \frac{1}{P}\left\{\frac{P}{2} - \frac{1}{4}\Big(\sin(2Q+2P) - \sin(2Q)\Big)\right\}$$

$$\mathrm{RMS} = \sqrt{\frac{1}{2} - \frac{\cos\left(\cdot 02\pi\left(P' + 2Q'\right)\right)\sin \cdot 02\pi P'}{\cdot 04 P'}}$$

$$\text{where} \quad P = \frac{2\pi P'}{100} \quad \text{and} \quad Q = \frac{2\pi Q'}{100}$$

With $P' = 1$, Q' is changed from 1 to 100 in steps of 1 and the standard deviation of the results is determined. This is representative of measuring a signal with a very short time constant meter. In this case, the time constant is 1/100th the periodicity of the signal and we would expect the standard deviation of the measurements to be large. However, if the measurements period was equal to half a wave period (i.e. $P' = 50n$, $n = 1, 2, \ldots\ldots$ etc) then the

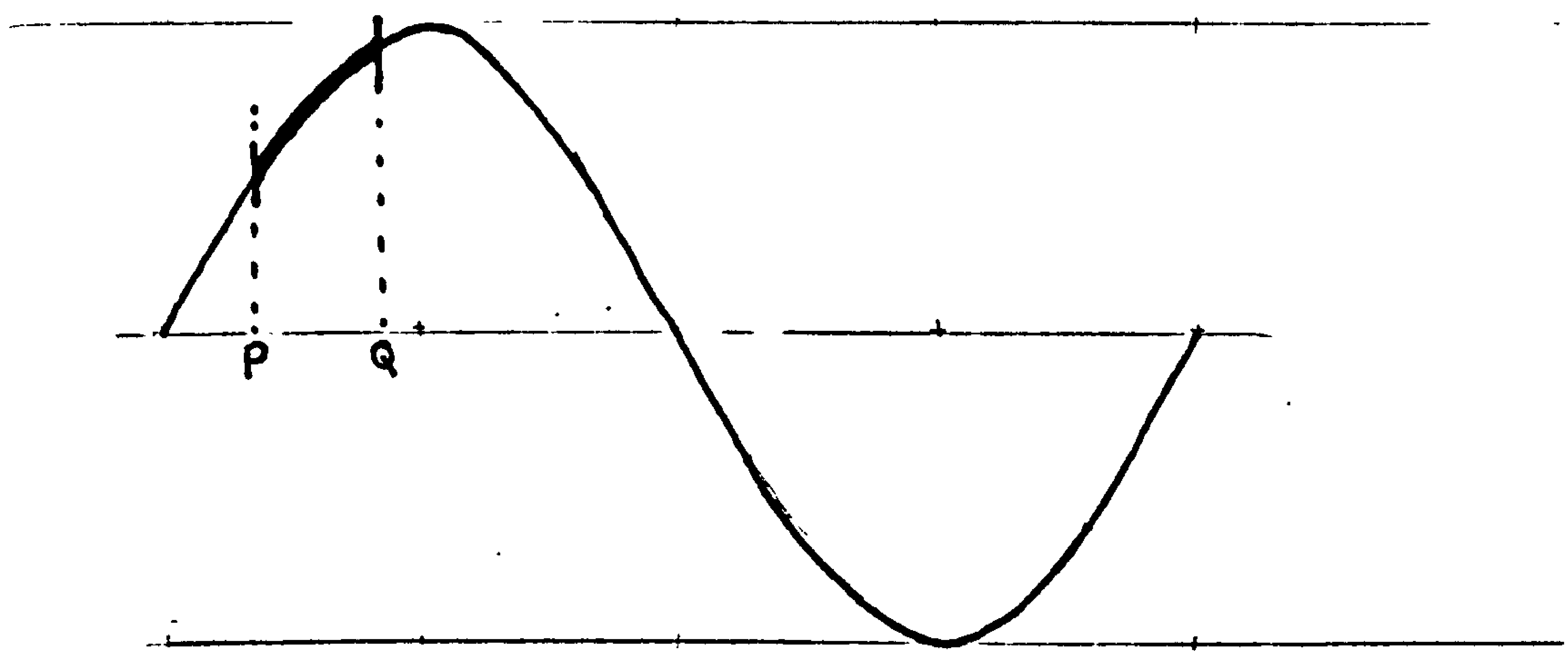

Fig. 6.1 Integration Limits for standard deviation calculations.

area under the wave should be the same for each period irrespective of the starting point, Q', and so the standard deviation will be zero. This effect is seen when the results of the above calculations are plotted as in Fig. 6.2.

As the measurement period increases past one half wavelength the standard deviation will increase again since the additional area under the curve will be dependant on the starting point of the measurement period. The sequence of maxima and minima continues, although the maxima become increasingly small since the proportional addition of the area under the curve beyond an integral number of half wavelengths decreases.

Note that the theoretical intercept of the graph at P' = 0 is the standard deviation of a sine wave measured over half a wavelength, calculated as follows:

$$\mu_0 = \frac{2}{T}\int_0^{\frac{T}{2}}\left(\sin \omega t - \frac{2}{\pi}\right)^2 dt$$

$$\therefore \sigma_0 = 0.308$$

This value fits in well with the graph and provides confidence that the theoretically derived equation (6.1) is correct.

The theoretical behaviour can now be used to verify actual measurements of electrical sine waves. By varying the capture rate and the signal frequency it is possible to cover the range of measurement periods used in Fig. 6.2.

For each point the standard deviation of 256 measurements was made ($256 = 2^8$, a convenient count limit for machine code programmes on 8-bit computers).

When the results are plotted with the theoretical values a good agreement is achieved, (see Fig. 6.2). Note that whereas standard deviation for

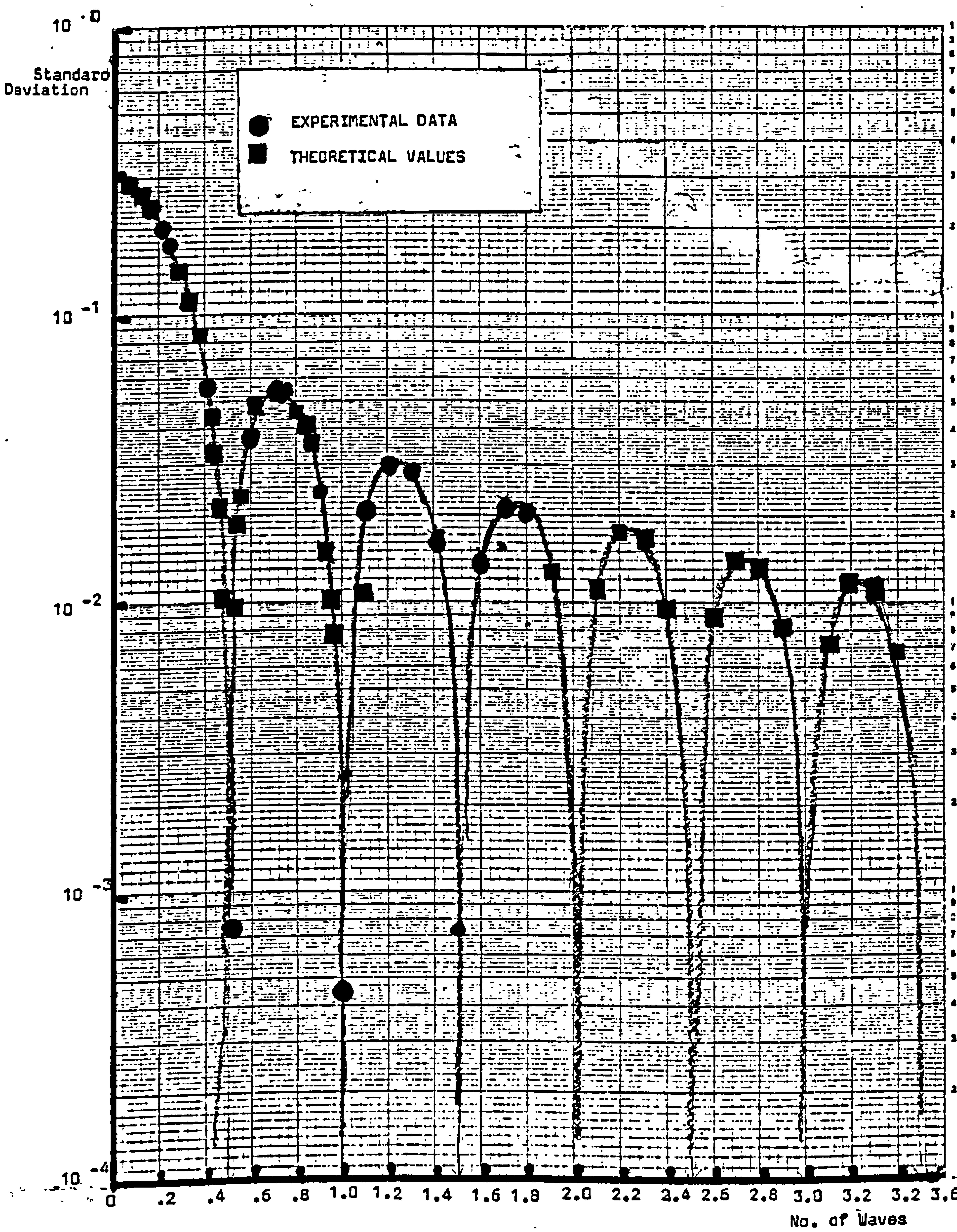

Fig. 6.2 Standard deviation of pure tones with random phases.

integral numbers of half wavelengths is expected to approach zero, in reality the value is limited by the electrical noise and the quantisation noise.

6.1.2 Electrical Test Signals

The envisaged acoustical measurement system involved the interaction of several devices and so it was necessary to test the system at various stages of complexity. In the early stages of development, before the inclusion of acoustical transducers, electrical signals were used as pseudo-acoustical signals.

The electrical signals were used in the series of system configurations shown in Fig. 6.3.

The system in Fig. 6.3.(c) becomes the eventual acoustical measurement system when a loudspeaker and microphone is inserted in the signal path between the auto-attenuator and the measuring amplifier.

In the first instance electrical signals were applied directly to the micro-computer via one channel of the capture device. It was envisaged that such an arrangement would be equivalent to a measurement amplifier or voltmeter (see Fig. 6.3 (a)).

The use of sine waves has been covered in testing the standard deviation calculation software. Octave bands of noise were also used in which case the signal generator comprised a noise generator, B & K 1024, a measurement amplifier, B & K 2607, and an octave filter set, B & K 1615.

The measurement amplifier, B & K 2606, was used to provide a comparison with the RMS levels computed by the microcomputer. The latter could be converted

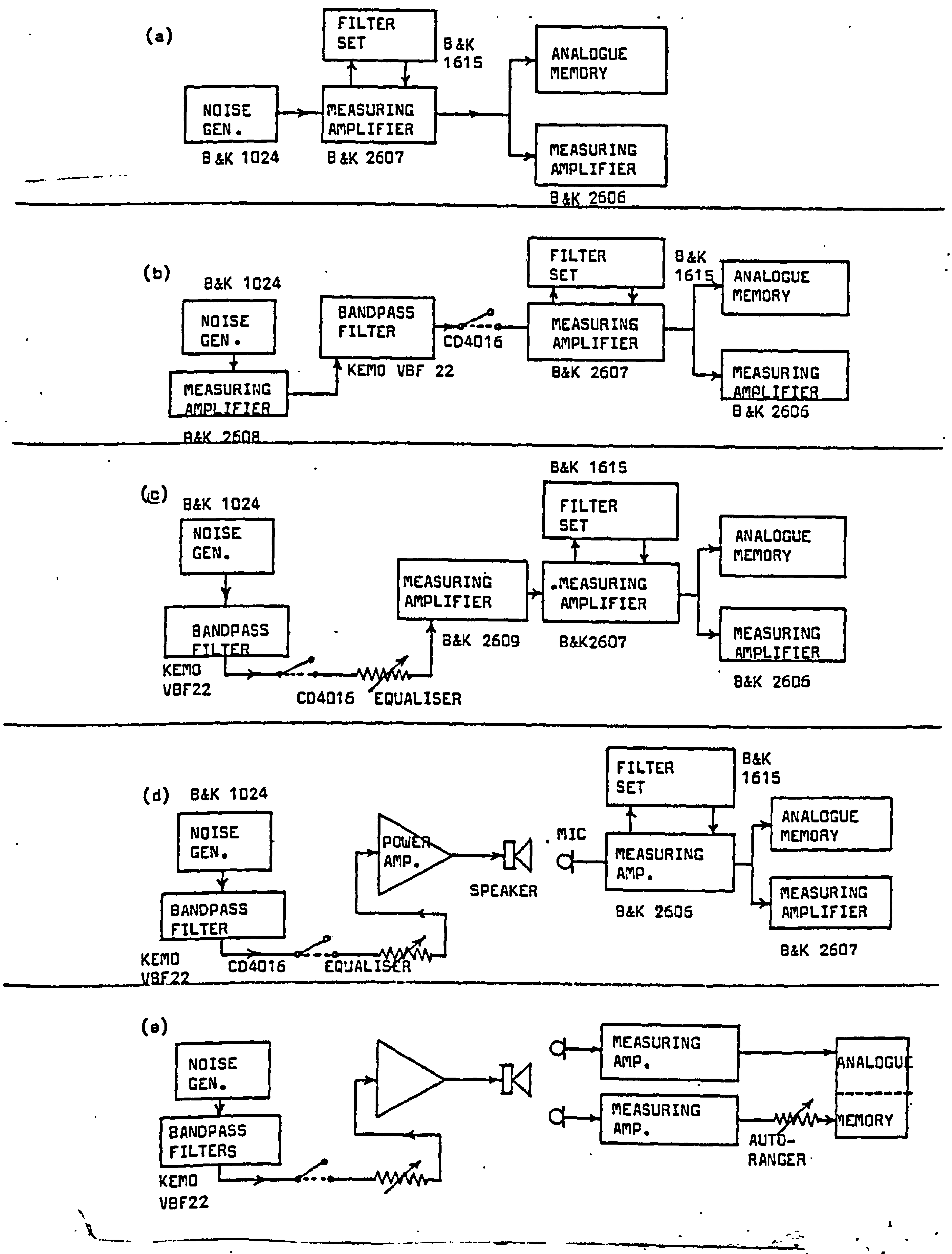

FIG. 6.3 Sequence of Development of Automatic Acoustical Measurement System.

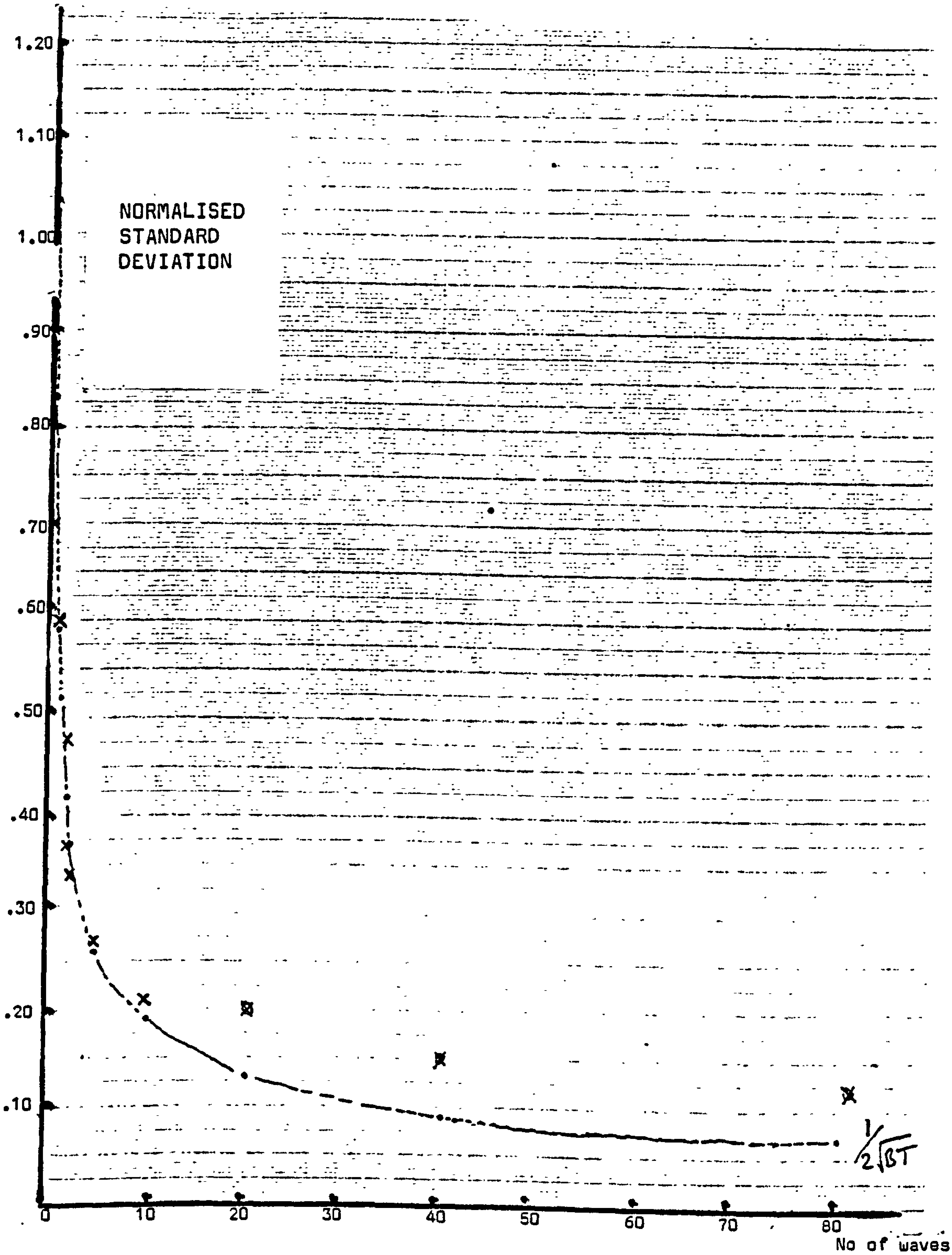

STD. DEV. of 256 RMS levels vs No. of waves measured.

FOR CONTINUOUS OCTAVE BANDS OF NOISE (ELECTRICAL)

Fig. 6.4

from ADC digits to an equivalent voltage knowing that, in the setting used, the 8-bit range of the ADC was covered by 20 volts.

For each of the several signal amplitudes the mean and standard deviation of 256 measurements was reported. The mean was compared with the 2606 reading and the standard deviation compared with the theoretical error in noise measurements. This is given by:

$$E = \frac{1}{2\sqrt{BT}} \tag{6.2}$$

where B is the bandwidth, and T is the measurement time constant.

The results are plotted in Fig. 6.4 and can be seen to agree with theoretical predictions for the most part with a slight departure from predicted at fractional waves per capture where assumptions in the deviations of the formula are contravened.

The system used above is modified to include the gating switch and a "microphone" measurement amplifier and filter set. See Fig. 6.3 (b).

In this arrangement the transient response of the octave band filter is under investigation. It is known that the output of the filter, a 6-pole Butterworth, reaches a steady state after about seven cycles of pure tone within the relevant octave band. From the table of Fig. 4.2 in Section 4.2.2. it can be seen that probably all of the captured 250 Hz signal will be within the transient response. If one assumes an exponential rise in output amplitude to steady state, this means that the calculated mean will be about 37% down on the true value at 250 Hz or 37 x 7/112 ≅ 2% down at 4 kHz. However, it is conceivable that the standard deviation of a set of measurements is unaffected by the transient response.

To investigate these predictions measurements were taken with all permutations of:-

- pure tone or octave noise generated signal
- "microphone" filter in or out
- gated or continuous signal

The signal frequency was 1 kHz.

For each permutation a set of 256 measurements was made and the mean and standard deviation calculated.

The results are as follows:

Signal		Filter	Standard Deviation dB
Pure Tone	continuous	Out	.023
	gated	Out	.017
	continuous	In	.016
	gated	In	.026
Noise Band	continuous	Out	.72
	gated	Out	.76
	continuous	In	.92
	gated	In	.98

Fig. 6.5

The standard deviation for pure tones is predictably small and is the same, within statistical variation, for continuous or gated signals, with or without the filter in circuit.

For the band limited noise it can be seen that the introduction of the filter increases the spread of the measurements. However, the spread does not differ between the transient and continuous case.

The evidence of this experiment is that the standard deviation of a set of measurements is independent of whether the transient response of an octave filter is evoked or not.

As a further verification of this conclusion, the standard deviation of gated octave bands of noise at centre frequencies from 250 Hz to 4 kHz were calculated from measured data aad plotted in Fig. 6.6 with $1/2\sqrt{BT}$ for comparison. The two curves can be seen to be in good agreement although the calculated values appear to be significantly higher than the formula at 4 kHz.

The system was further developed to include the equaliser as described in Section 5.2.3 see Fig 6.3 (c).

The B & K 2608 measuring amplifier is used to boost the signal which is limited to 0.5 volts RMS input to the equaliser. When the loudspeaker/microphone link is used this will be repleced by a power amplifier. See fig. 6.3 (d).

The band pass filter at the signal generator is now the Kemo filter described in Section 5.2.6.

For comparison purposes steady-state signals were measured with B & K 2606 measuring amplifier placed in parallel with the capture device.

Octave bands of noise between 250 Hz and 4 kHz were generated and the micro-computer used to calculate the mean and standard deviation of 256 measurements at each frequency.

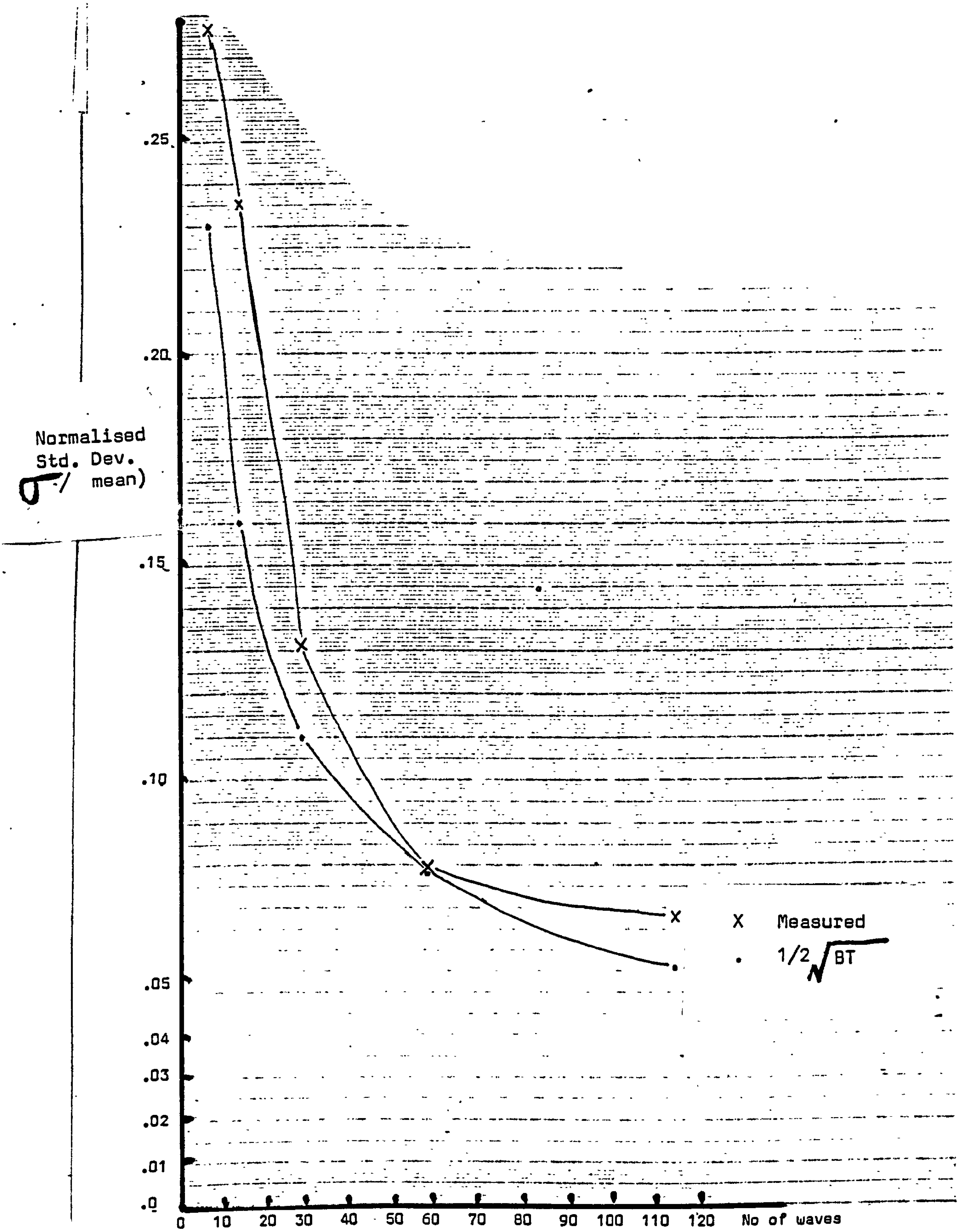

Fig. 6.6 Standard deviation of 256 RMS levels vs No of waves measured for Gated Octave noise bands (Electrical).

The results are shown below with standard deviation normalised to the mean level.

Centre Frequency (Hz)	Normalised Std. Dev.	Computed RMS	Computed RMS volts	2606 Reading
250	0.251	13.43	1.05	1.5
500	0.233	24.76	1.93	2.0
1000	0.207	24.31	1.90	2.0
2000	0.125	22.71	1.77	1.8
4000	0.086	21.88	1.71	1.70

Fig. 6.7

The standard deviation against number of capture waves is plotted in Fig. 6.8 and can be seen to reassert the trend found in the previous test in that a significant departure from the formula is seen at 4 kHz.

As expected, the computed voltage levels for transient signals are lower than the measured voltage for stationery signals at low frequency. At 250 Hz the discrepancy is 30% and at 1 kHz it has reduced to 5% which is consistent with the assumption that the rise in amplitude of the filter output is broadly exponential, as stated earlier.

Since the acoustical measurements proposed in this thesis were concerned with level difference between two microphones the discrepancy shown above should have no detrimental effect since the symmetry of the reception channels makes it equally applicable to both microphone signals.

6.1.3 Acoustical Signals

Having calculated the mesurement system using electrical test signals it was then necessary to ensure that the introduction of an acoustical link in

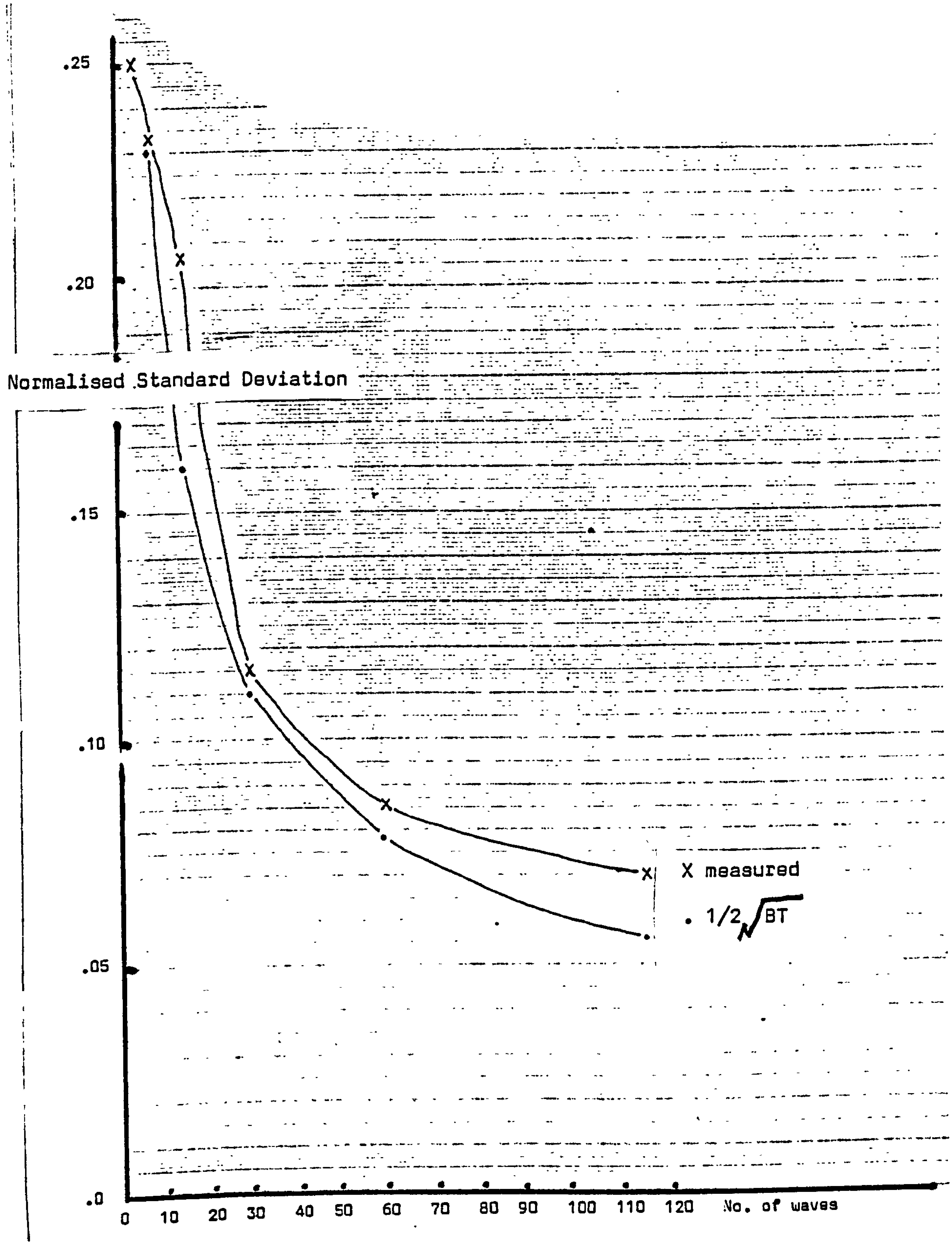

Fig. 6.8 Standard Deviations vs. No. of waves captured for Continuous Octave Bands of Electrical Noise with Equaliser in Circuit.

in the signal path produced no anomolies.

Pure Tones

The apparatus as in Fig. 6.3 (e) was used. The loudspeaker and the two microphones were erected in a small anechoic chamber, used to prevent interference effects from occluding the interpretation of the results of this test. The microphones were placed as close to each other as possible. The Autoranger circuit, described in Section 5.3.1 was included in one of the reception signal paths and set to a minimum attenuation. The signal gate was permanently closed to produce a continuous signal, which was a 1 kHz pure tone.

The system was calibrated by capturing a 1 kHz test tone from a microphone calibrator.

The mean sound pressure level of 256 measurements at the microphones was reported to be 90.32 dB and 90.35 dB. The B & K 2606 measuring amplifiers each gave a reading of 90.3 dB.

The experiment proved that the inclusion of the acoustical link did not cause any loss of precision and that the inclusion of the autoranger in one reception channel did not result in a difference between the two channels.

Octave Bands of Noise

This experiment invoked the fully developed acoustical measuring system with attendant software. It was considered as a "dry-run" test, taking place in the semi-anechoic chamber at the British Leyland Test Facility, Leyland, Lancashire.

The signal processing arrangements are shown in Fig. 6.9. Two different source/receiver geometry were used as shown in Fig. 6.10.

RESULTS

	250	500	1K	2K	4K
Geometry 1					
Level diff.	3.3	8.8	3.9	3.9	2.1
Standard Deviation (dB)					
Near mic.	1.9	1.3	0.9	0.9	0.6
Far mic.	1.6	1.4	0.9	1.0	0.7
Geometry 2					
Level diff. (dB)	1.4	3.1	3.2	2.7	5.5
Standard deviation (dB)					
Near mic.	2.5	1.3	0.9	0.7	0.6
Far mic.	1.5	1.1	0.8	0.8	0.6

When standard deviation is plotted against the number of captured waves of the centre frequency of each band as in Fig, 6.11 close agreement with the theoretical $1/2\sqrt{BT}$ is observed. As was the case with the earlier tests involving electrical signals, at higher frequencies the standard deviation is above $1/2\sqrt{BT}$. It should be noted that within statistical fluctuations, the same value for standard deviation is obtained for near and far microphones, independantly of which of the two geometries is used. This indicates that, as expected, the percentage dispersion from the mean is independant of the mean itself.

6.2 Meteorological Measurements

6.2.1 The Anemometer

The determination of wind turbulence by the computer was compared with measurements

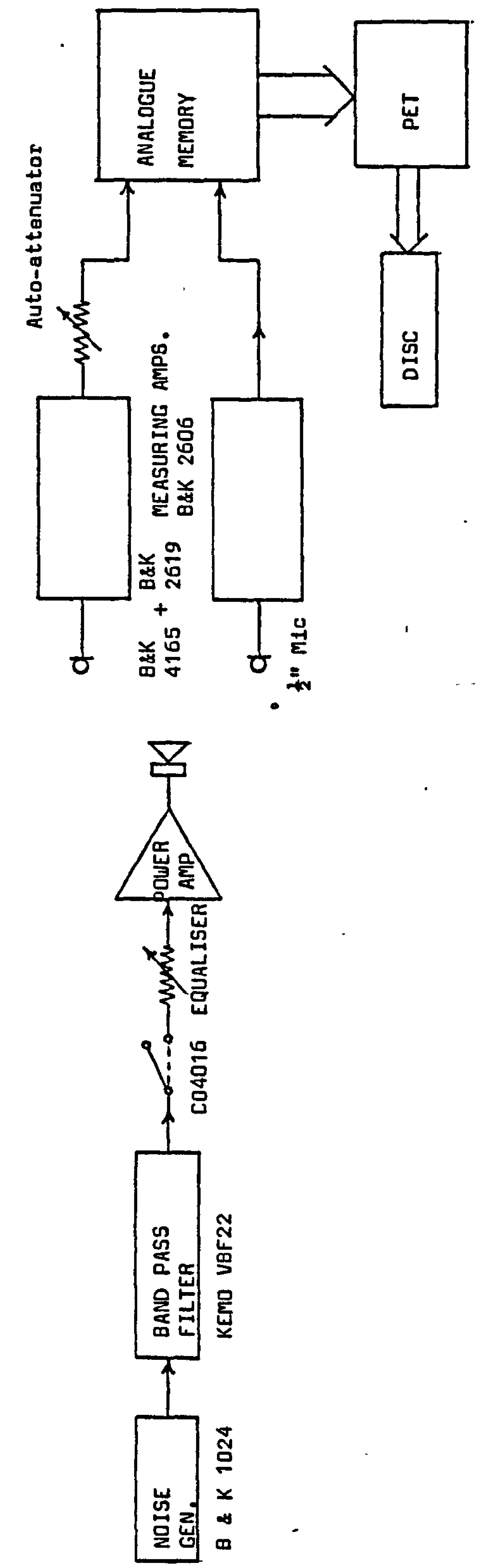

Fig. 6.9 Instrumentation for Acoustic Tests at Leyland.

(a)

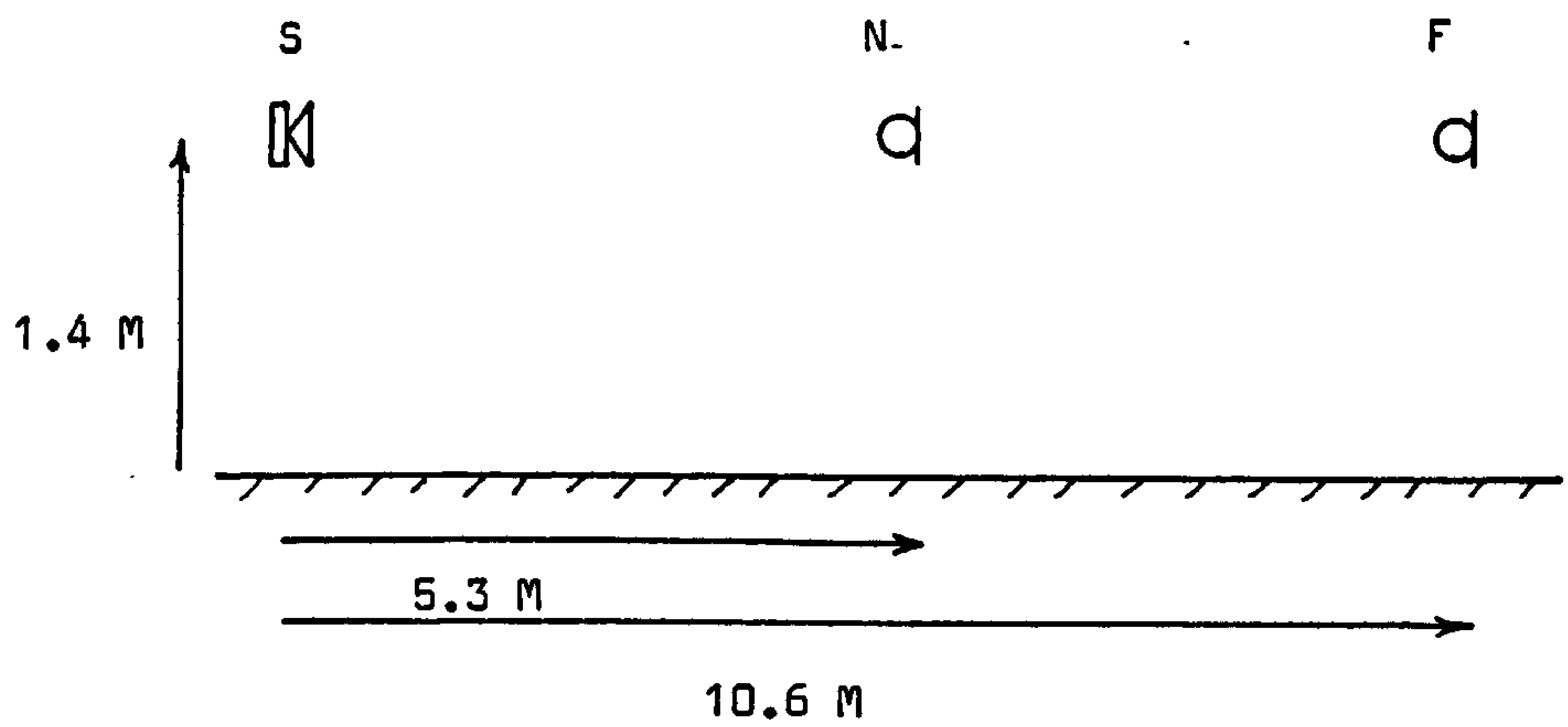

(b)

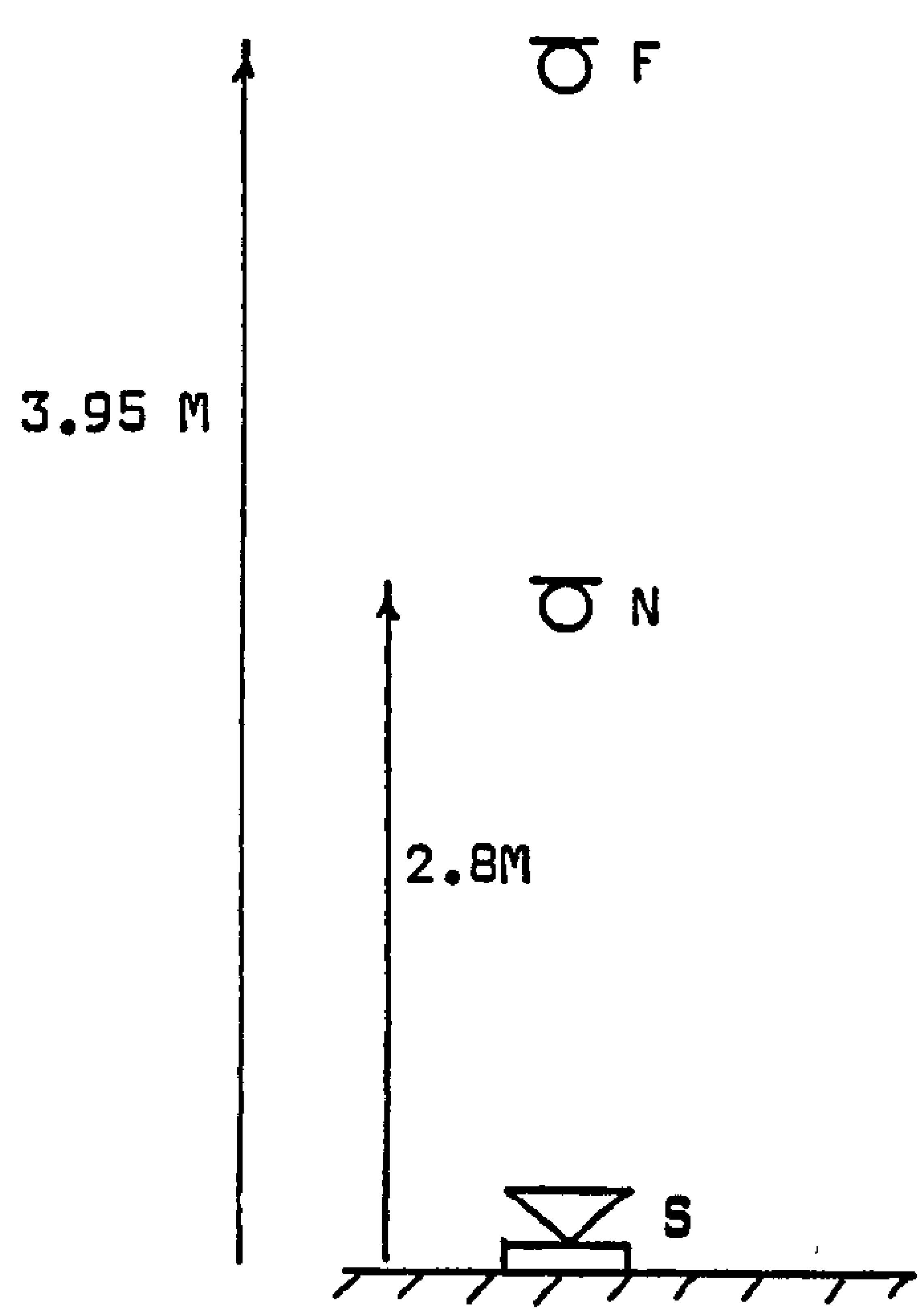

Fig. 6.10 Geometries for Acoustic tests at Leyland.

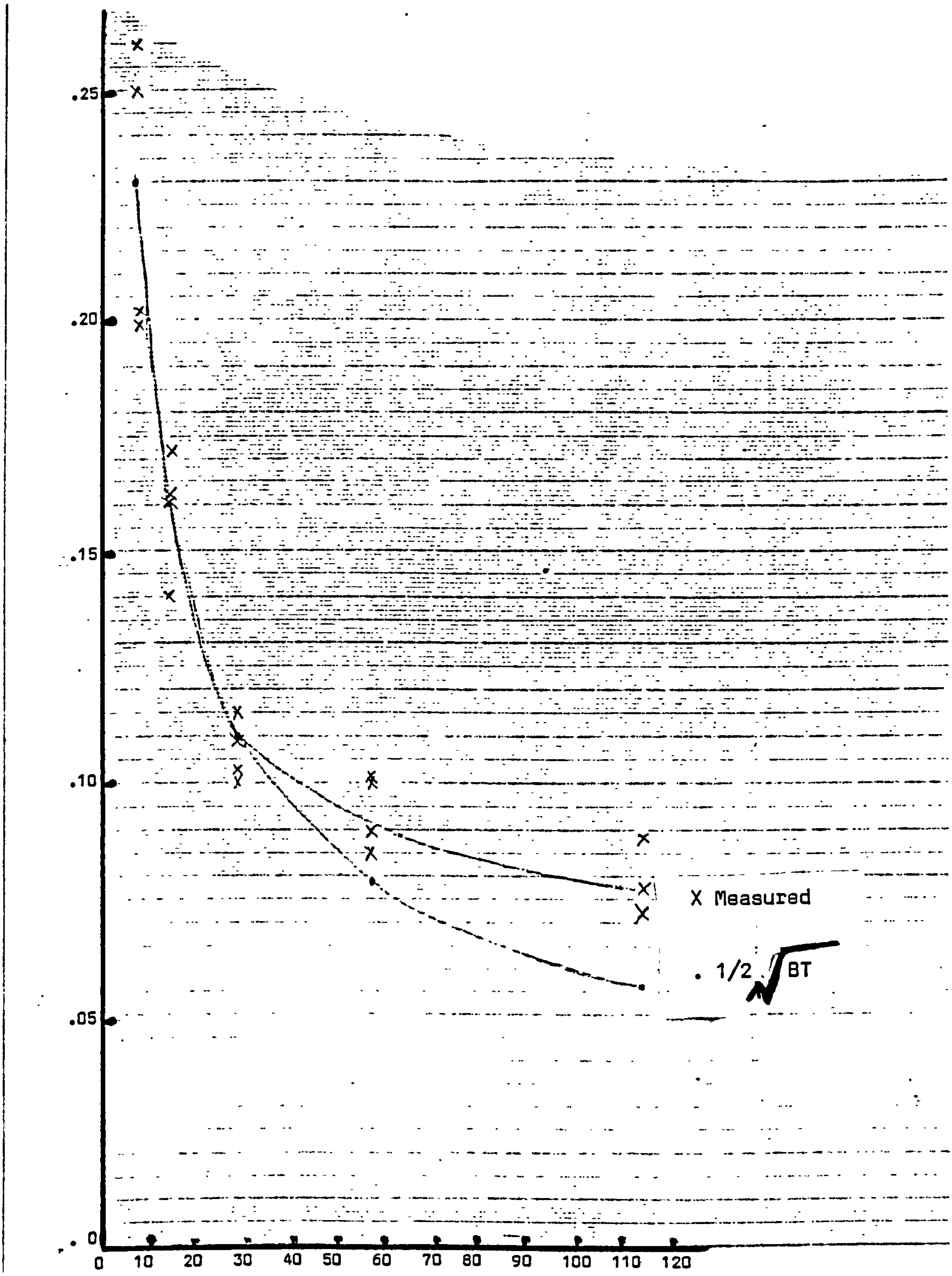

Fig. 6.11 Standard deviation of 256 RMS levels vs. No of waves for Gated octave noise bands (Acoustical).

made by a Laser-Doppler Anemometer (LDA).

In essence this technique involves intersecting two laser beams, split from a single beam, at a point of interest in a fluid flow.

An interference pattern will be in evidence at a receiver. This pattern will shift depending on the vector addition of the velocity of light and the fluid. Dedicated microelectronics associated with the receiver uses this information to determine fluid velocity. After sampling for an appropriate time the mean and standard deviation of the fluid velocity and the turbulent intensity (defined as the ratio of these two) is printed.

Air flow in a perspex tube was measured with the LDA and the hot-wire probe was placed at the end of the tube and connected to its associated electronics and the microcomputer. The hot-wire anemometer was also output to either an RMS meter (supplied with the hot-wire anemometer) or a DC voltmeter. With these it was possible to read the average voltage and the standard deviation of the voltage. This was used in verifying the approximate formula (45):

$$TI\ (\%) = \frac{4\ V\ v}{V^2 - V_o^{\ 2}} \times 100$$

where V is the average output voltage

v is the standard deviation of the output voltage

V_o is the no flow voltage

Note that this formula does not require the hot-wire probe to be calibrated. It is claimed to be a good approximation for turbulent intensities up to about 10%.

The table overleaf (Fig. 6.12) shows the results of the three measurements

WIND SPEED $(m.s^{-1})$			STD.DEV $(m.s^{-1})$			TURBULENT INTENSITY %						
LDA	PET	ERR%	LDA	PET	ERR%	LDA	PET	ERR%	MANU.	ERR%	FORM.	ERR%
3.18	2.71	-14.77	.19	.16	-16.40	5.97	5.86	-1.92	6.68	11.78	6.11	2.30
3.24	3.15	-2.77	.19	.17	-9.76	5.86	5.44	-7.19	6.68	13.89	5.68	-3.11
3.83	4.25	11.06	.20	.23	11.89	5.35	5.39	.75	5.99	11.86	5.63	5.17
4.92	5.48	11.45	.24	.29	22.30	4.86	5.33	9.73	5.72	17.82	5.56	14.53
5.89	6.68	13.55	.30	.32	7.40	5.04	4.77	-5.41	5.48	8.66	4.98	-1.13
8.16	8.63	5.86	.39	.43	10.86	4.78	5.01	4.72	5.27	10.23	5.23	9.36
10.47	9.72	-7.21	.52	.49	-5.89	4.97	5.04	1.42	5.21	4.83	5.26	5.90

Fig 6.12 Anemometer Comparisons

used averaged over similar time scales. The microcomputer calculated turbulent intensity using both the approximate formula and by the true definition, which required knowledge of the calibration parameters. The results table shows the mean wind speed in ms^{-1}, the standard deviation of the wind speed in ms^{-1} and the percentage turbulent intensity for both the laser Dopler anemometer (LDA) and the hot wire anemometer interfaced to the microcomputer (PET). For each of these three headings the percentage deviation of the PET result from the LDA result is shown (ERR%). Under Turbulent Intensity the results obtained from manually reading the output of the hot wire anemometer with the DC Voltmeter and RMS meter, and the results using the PET results in the approximate formula are also quoted (MANV. and FORM.) together with the percentage error of each from the LDA result.

It can be seen that the PET system underestimates low and high wind speeds and overestimates within these extremes. This is most likely to be due to some inaccuracy in the calibration procedure for the hot wire probe. The standard deviations also exhibit this pattern.

Despite these apparent inaccuracies the turbulent intensity measured by the PET system is always within 10% of that obtained using the more sophisticated LDA system. With the exception of one high result in the middle of the wind speed range, the same can also be said of the turbulent intensity derived from the approximate formula.

The manual results appear to be systematically too high, which is likely to be due to the fact that the mean and the standard deviation of the hot wire anemometer output were measured on two different instruments whose characteristics (e.g. sensitivity, input impedance, etc.,) may be poorly matched.

It was concluded that the PET system gave acceptable results in view of the attractiveness of the high degree of portability and the low cost of the battery operated hot wire anemometer.

6.2.2 Wind Direction Sensor

This was evaluated simply be adjusting the position of the wind-vane manually in the laboratory.

The sensor was repeatedly interrogated by the microcomputer and "wind direction" displayed on the microcomputer screen. This was compared with the known direction. Directions of 0^{o}, 90^{o}, 180^{o} and 270^{o} were used.

6.2.3 Electronic Thermometer

The thermometer was evaluated by direct comparison with good quality mercury-in-glass thermometer.

The bulb of the mercury thermometer and the current source of the electronic thermometer were placed together in a beaker of melting ice. The beaker was gradually heated on a hot plate to $40^{o}C$. The electronic sensor was constantly interrogated by the microcomputer and the temperature displayed on the screen.

The gain and offset were adjusted until the two thermometers agreed to within 1^{o}C throughout the range 0^{o} to 40^{o} C.

This exercise was repeated at intervals of about two weeks for maintenance purposes.

CHAPTER 7

Modification of the Measurement System for Model Work

This chapter describes the changes to the measurement system for scale modelling brought about by the decrease in linear dimensions, with a corresponding increase in acoustical frequency, and by the move to a more controlled atmosphere.

A 16:1 scale was used for the model since this implied a model barrier of a manageable 6" height whilst the transposed acoustical frequencies would remain within the capability of the filters, measuring amplifiers etc. (250 Hz to 4 kHz range becomes 4 kHz to 64 kHz). Wind was simulated using a wind cabinet fitted with a honeycomb flow-straightener.

7.1 Modifications to the Acoustical System

Smaller loudspeakers and microphones were required to cope with the higher frequencies used in the model. The half-inch microphones of the field experiment were replaced with eighth-inch versions. At normal incidence these microphones have an increased sensitivity in a narrow band around 60 kHz. However, if the angle of the incidence is 90^{0} a flat frequency is obtained over the required frequency range.

A single loudspeaker to cover the frequency range 4 kHz to 64 kHz could not be found. Instead a piezo-electric tweeter was used up to 16 kHz and a solid dielectric capacitance transducer beyond that frequency. It was also necessary to replace the power amplifier, designed for audio-frequency work, with the amplifier section of a wide frequency range signal generator in conjunction with a B & K measuring amplifier used as a pre-amplifier. Conveniently, the signal generator had a 5 ohm and a 600 ohm output which could be used for the tweeter and the ultrasonic transducer respectively. In operation this required a pause to be inserted in the microcomputer's programme at the appropriate point so that the experimenter could unplug the leads to the tweeter and plug in the other leads before allowing the programme to continue.

A further modification to the measurement system was that only the first 1K of the full 4 K of data stored in the event recorder was used for each channel. This was equivalent to a duration of sound burst of 7 ms, or about 2.4 m in length. Therefore reflected sound which travels from source to receiver over a greater distance than this can be ignored, allowing the laboratory, treated in certain areas with proprietary rockwool absorbers, to have anechoic characteristics, similarly to the open grassland site in the field experiments.

7.2 Modifications to the Meteorological System

In determining the atmospheric conditions it was only necessary to use the hot-wire anemometer since the wind direction was set for any one geometry and the ambient temperature showed negligible drift over a period of time similar to the duration of a typical experiment. Wind direction and temperature were entered into the programme by the experimenter.

7.3 Additional Tests Required for Model Work

The use of two loudspeakers essentially acting as one required that the equivalent point source position and the polar response for each loudspeaker should be known in order that , if necessary, corrections could be made to levels measured at different frequencies.

7.3.1 Measuring the Point Source Origin of a Loudspeaker

For this exercise, an optical bench, of the type used for experiments involving lenses, diffraction gratings etc., was erected in an anechoic chamber and covered with foam rubber to minimise acoustical reflections. This allowed microphone and speaker to be placed at various separations but always in a plane parallel to the floor.

A pure tone of a certain frequency was played through the loudspeaker and the microphone response noted for various source-receiver separations up to 1 m.

A graph of sound pressure level at the microphone against the logarithm of the separation was plotted. It can be expected that this will give a curve that has three separate regions. Since the source is of finite size and the effects from separate elements can produce complex interference patterns at close quarters, sound levels near to the speaker are difficult to predict, although the general trend is a decreasing level with increasing separation. This region is known as the near field. If separation is increased further the far field region is reached where the source appears to act as a single unit, increasingly similar to a point source emitting spherical waves. Attenuation, due to beam spreading, is proportional to the square of the separation giving a straight line on a log. separation plot-6 dB per doubling of distance. The third region occurs at large separations when the sound pressure level is indistinguishable from background.

The points plotted on the graph should be corrected for air absorption (47) which produces an attenuation directly proportional to distance, giving the log. separation plot a curve of increasing negative gradient. For the distances up to 1m used in this experiment, air absorption is only significant above 16 KHz.

The results of the experiment for the electrostatic transducer and the piezo-

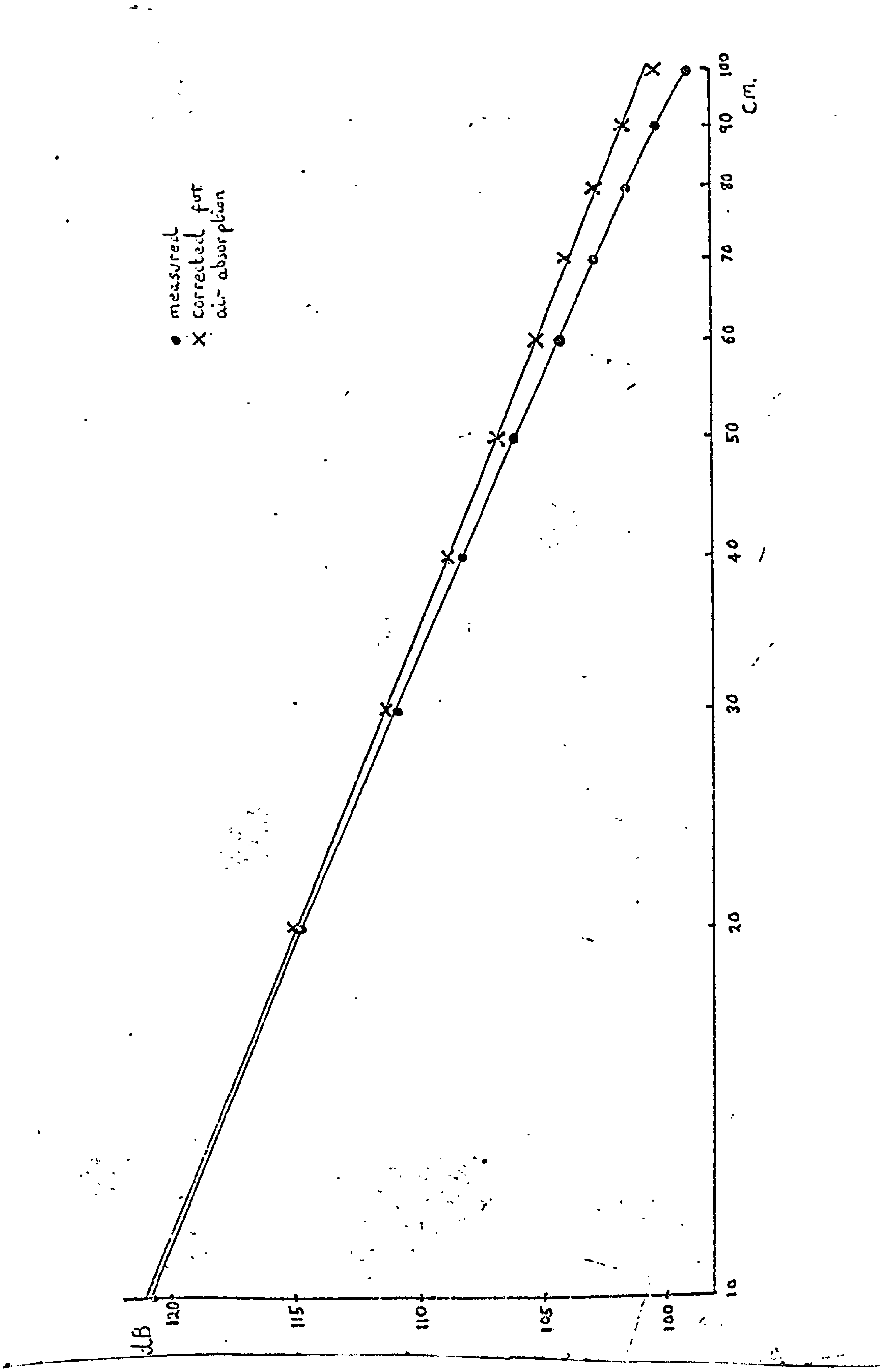

Fig. 7.1 On-axis response of electrostatic transducer

S.P.L. vs Source/Receiver separation.

electric device are shown in graph 7.1 and 7.2 respectively.

The Electrostatic Transducer

After correction for air absorption (using figures published by Bazley (47)) all the points can be seen to lie on a line of gradient - 6 dB per doubling of distance.

This indicates that the near field is not shown, although the interpolated level for 5 cm separation does not agree with measured values, indicating that the near field/far field boundary lies between 5 - 10 cm from the source.

The separations were measured from the face of the electrostatic transducer which, it can be concluded, appears to be the source of the waves when received in the far field.

The Piezo-electric Tweeter

Even after correction for air absorption the points lie on a straight line of a steeper gradient than expected. It was assumed, therefore, that the separation was not measured from the apparent point-source position, so there would be greater fractional error at close microphone positions, giving a curve of incorrect gradient. To decrease the gradient as required would indicate that the measured separations are too small. They were taken as being from the microphone grid to the tip of the horn on the tweeter. If the origin was, not unreasonably, at the junction of the pressure unit and the horn, a correction of 6 cm would be required.

Such a correction is shown on the graph of Fig. 7.2 and can be seen to bring the points considerably nearer to the required line. The fact that they

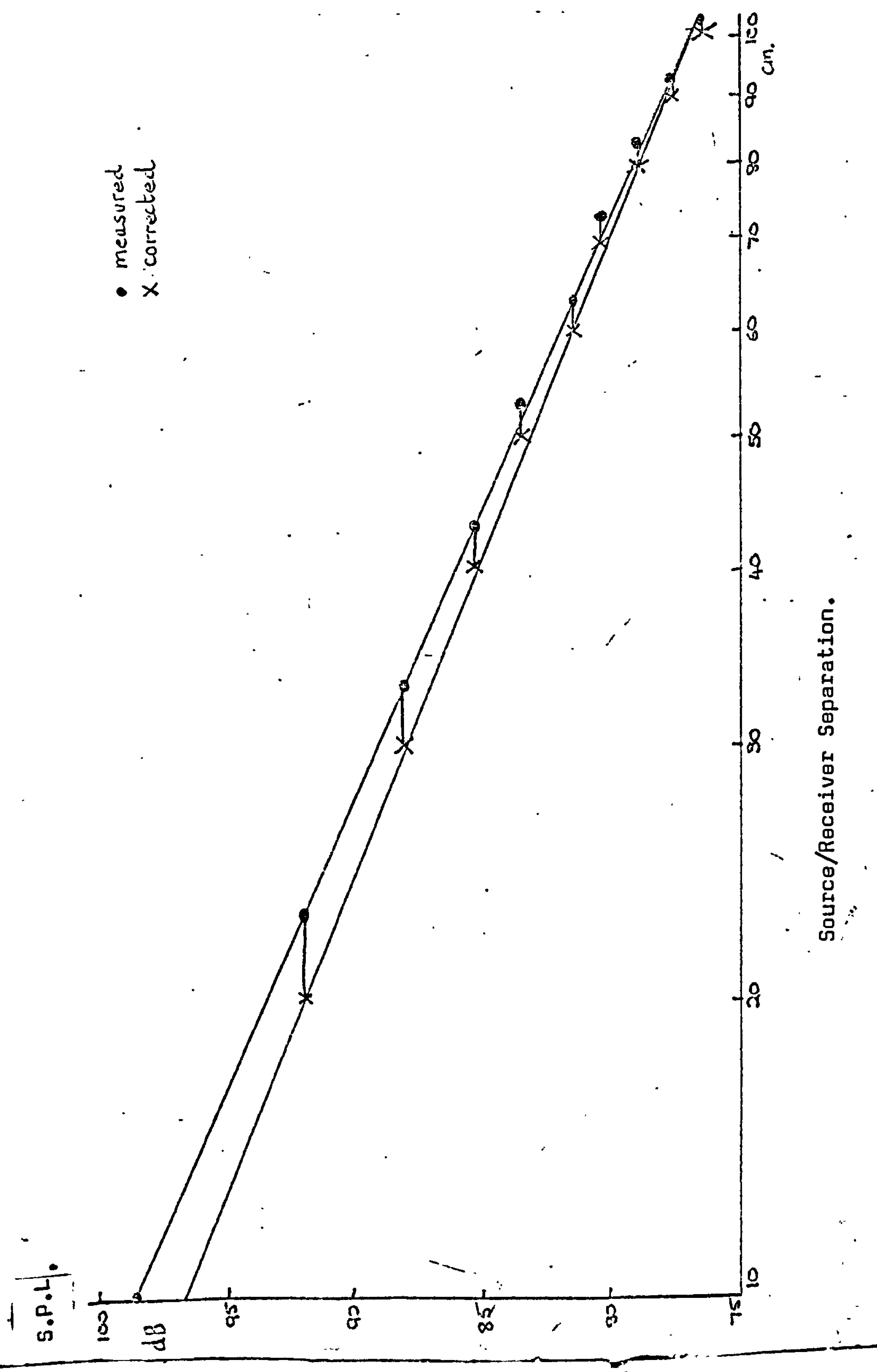

Fig 7.2   On-axis response of piezo-electric tweeter

do not all fall on the line within experimental error implies that the wave does not simplify to a spherical wave over the range of distances investigated.

7.3.2 Polar Diagrams

A microphone was placed 30 cm from the loudspeaker under test. The received sound pressure level for a pure tone emitted from the speaker was measured for a range of source-receiver angles.

To produce the different angles the loudspeaker was rotated. The angle was measured using a protractor rigidly mounted on the stand that holds the speaker, with the 90^{0} line pointing away from the speaker but parallel to a line drawn through the axis of symmetry of the speaker. The origin of the protractor was vertically above the speaker origin as determined in the previous test. (See Fig. 7.3).

The source-receiver angle was read off the protractor according to a pointer suspended by a thread from the ceiling of the anechoic chamber.

The results of this experiment indicate that the polar diagram of the electrostatic speaker is narrower than that of the piezo-electric device.

This is to be expected since the directivity factor (48) is dependant on the ratio of the emitted wavelength to the dimensions of the source, and the elctrostatic speaker has the bigger cross-sectional areas of the two devices but is emitting the higher frequency sounds.

Assembling the Speakers for Model Work

The most convenient geometry for the mounting of the two speakers for scale model experiments was with the electrostatic device clamped to the periphery

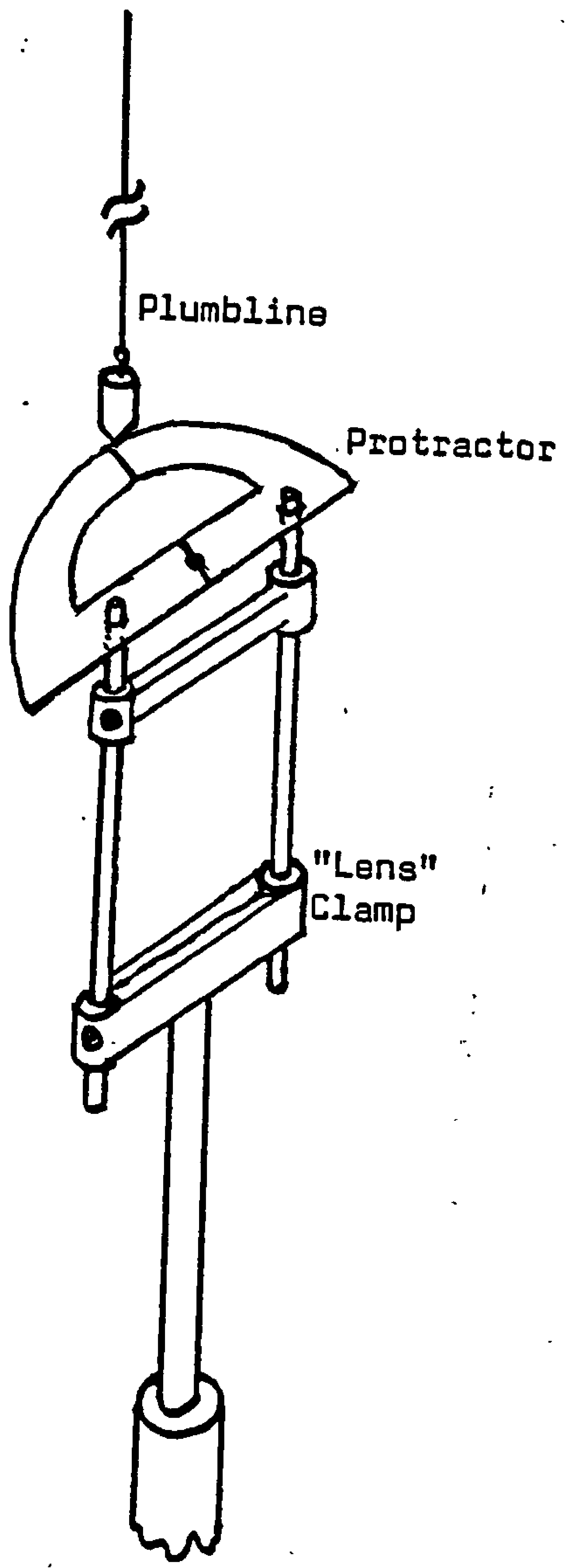

Fig. 7.3. Arrangement used to determine Polar Response of loudspeakers

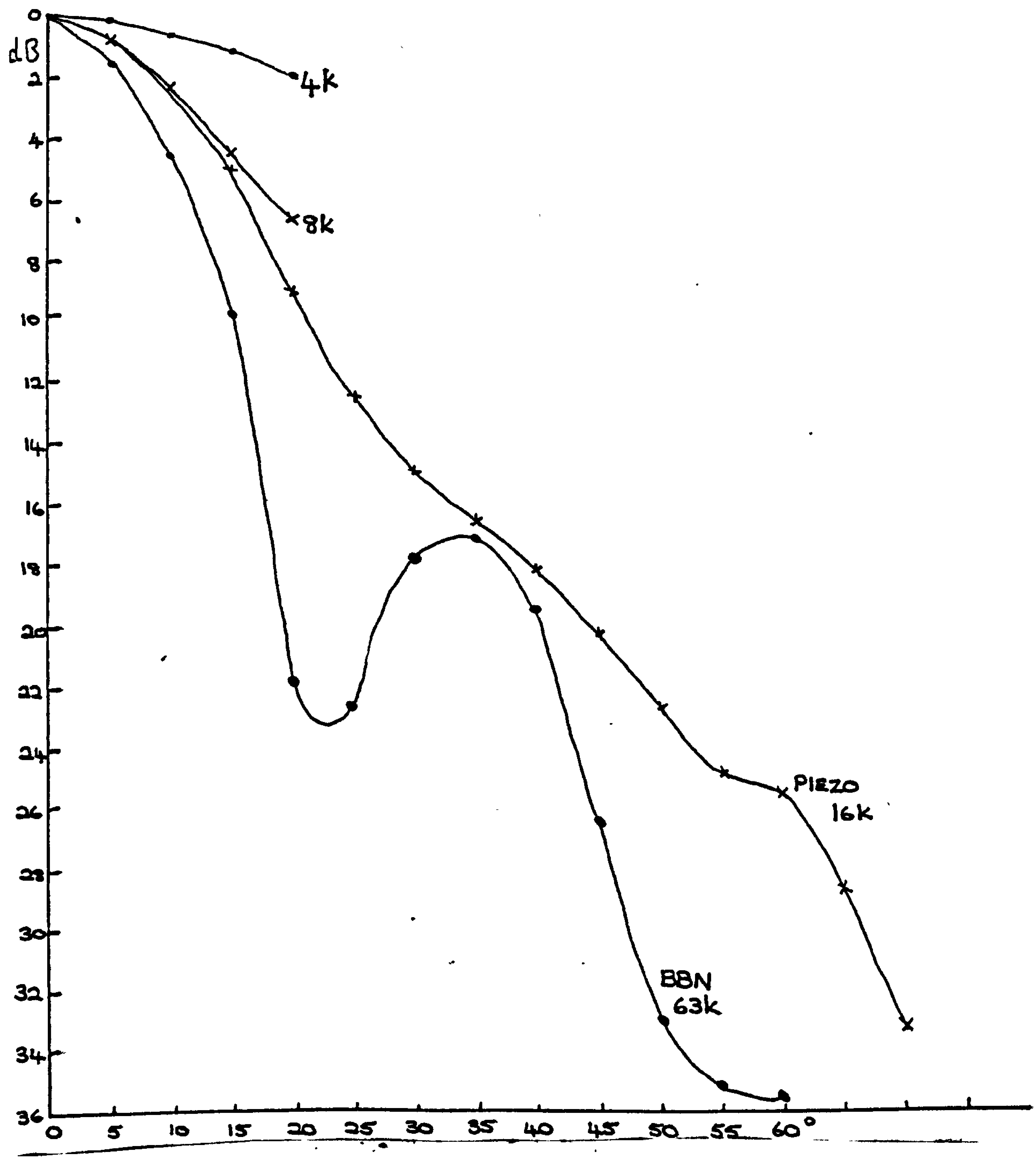

Fig 7.3 (b) Polar Response of Loudspeakers

Attenuation re axial response vs Angular deviation.

of the horn of the piezo-electric tweeter using one of the four holes intended for screws to mount the tweeter on a baffle (See Fig. 7.4).

The assembly was so positioned that the electrostatic transducer and the axis of symmetry of the tweeter lay on a plane parallel to the floor.

Because the directivity of the electrostatic device is narrower than that of the tweeter the microphone should be placed opposite the face of the former when measurements are to be taken.

The two speakers were assembled as described above and placed on the optical bench with a $\frac{1}{8}$" microphone initially at 30 cm from the diaphragm of the electrstatic unit and directly opposite it. Sound pressure level at the microphone was measured for a 16 kHz tone from the piezo-electric tweeter and 50 kHz for the electrostatic device at several microphone distances between 30 cm and 100 cm. The result can be seen in Fig. 7.5, including corrections for air absorption (at 50 kHz) and angle of incidence for the 16 kHz tone.

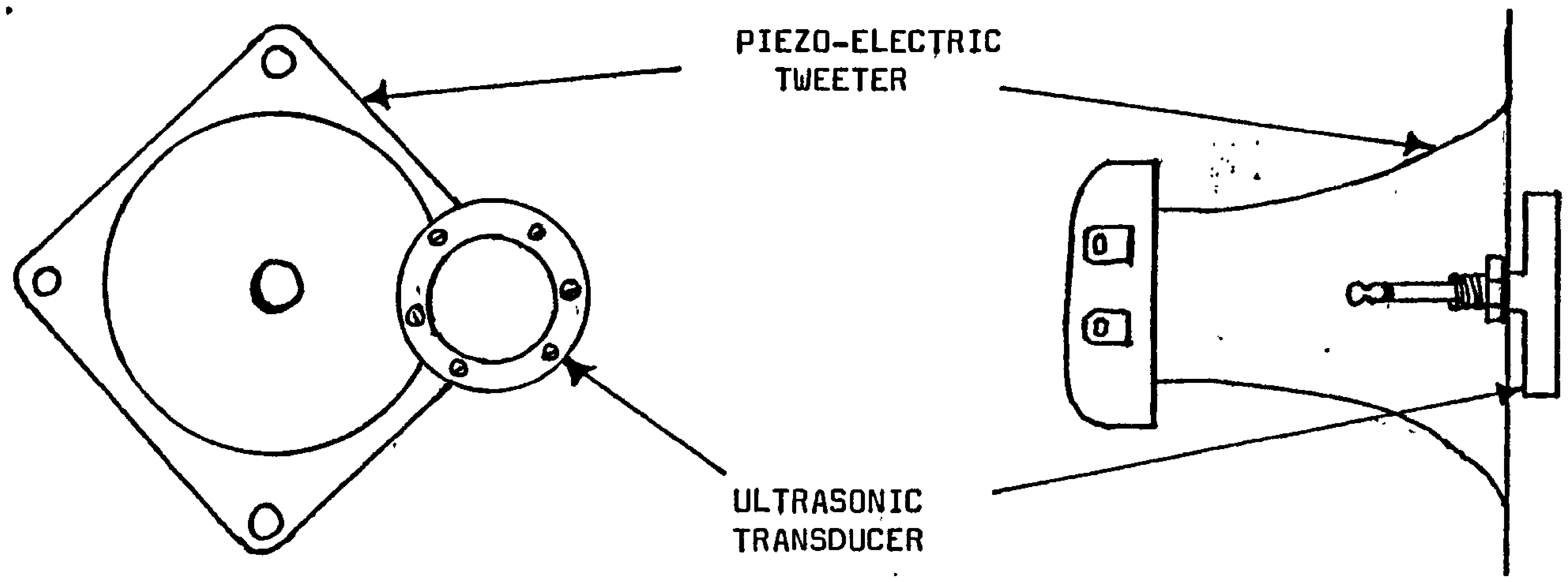

Fig. 7.4. Method of mounting loudspeakers for model work

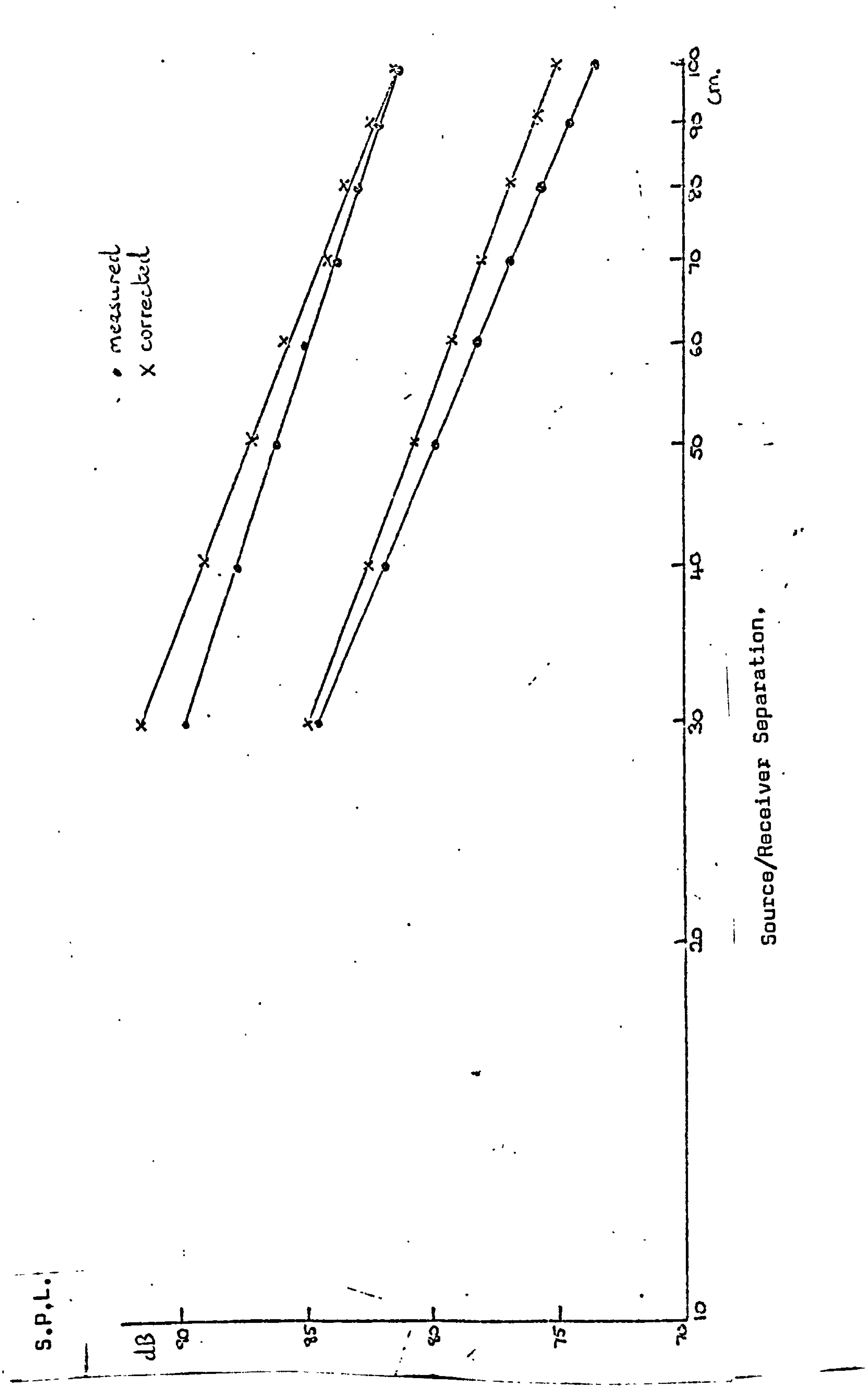

Fig 7.5 Response of Combined Loudspeaker Assembly.

7.4 Validation of Automatic Acoustical Measurements at Model Scale

The model experiments were to take place in a somewhat enclosed laboratory area since the only available anechoic chamber was prohibitively small. However, wave trains on only about 3 m in length were to be used (as described previously in this chapter) and in view of the high frequencies required it was reasonable to expect that the judicious placing of rockwool absorbers could produce quasi-anechoic conditions. The abosorbers were placed around the proposed model site to prevent reflections from objects less than 1.5 m away from the line of propagation from the speaker to the microphones. The automatic measurement system was used with the speaker assembly at a certain position with the near microphone at a distance of 30 cm away and the far microphone at a series of distances ranging from 1 to 6 times the above. The results are shown in Fig. 7.6.

The results show that, after correction for atomic absorption and origin position as determined in the previous tests, the response at all frequencies of interest approximate to the -6 dB/doubling line achieved in the anechoic chamber. This was taken as evidence that the measurement system was still valid at model scale and that the model surroundings had been adequately treated to produce an essentially anechoic environment as far as the automatic measurements were concerned.

7.5 Choice of Covering for the Model Floor

Preliminary experiments showed that reflections from the model floor had a significant effect on acoustical measurements and so the material for the floor had to have similar properties as the grassland used in the full-sized experiments. That is to say, the amplitude reflection coefficients and phase change on reflection had to be similar at the transposed frequency region as the grass

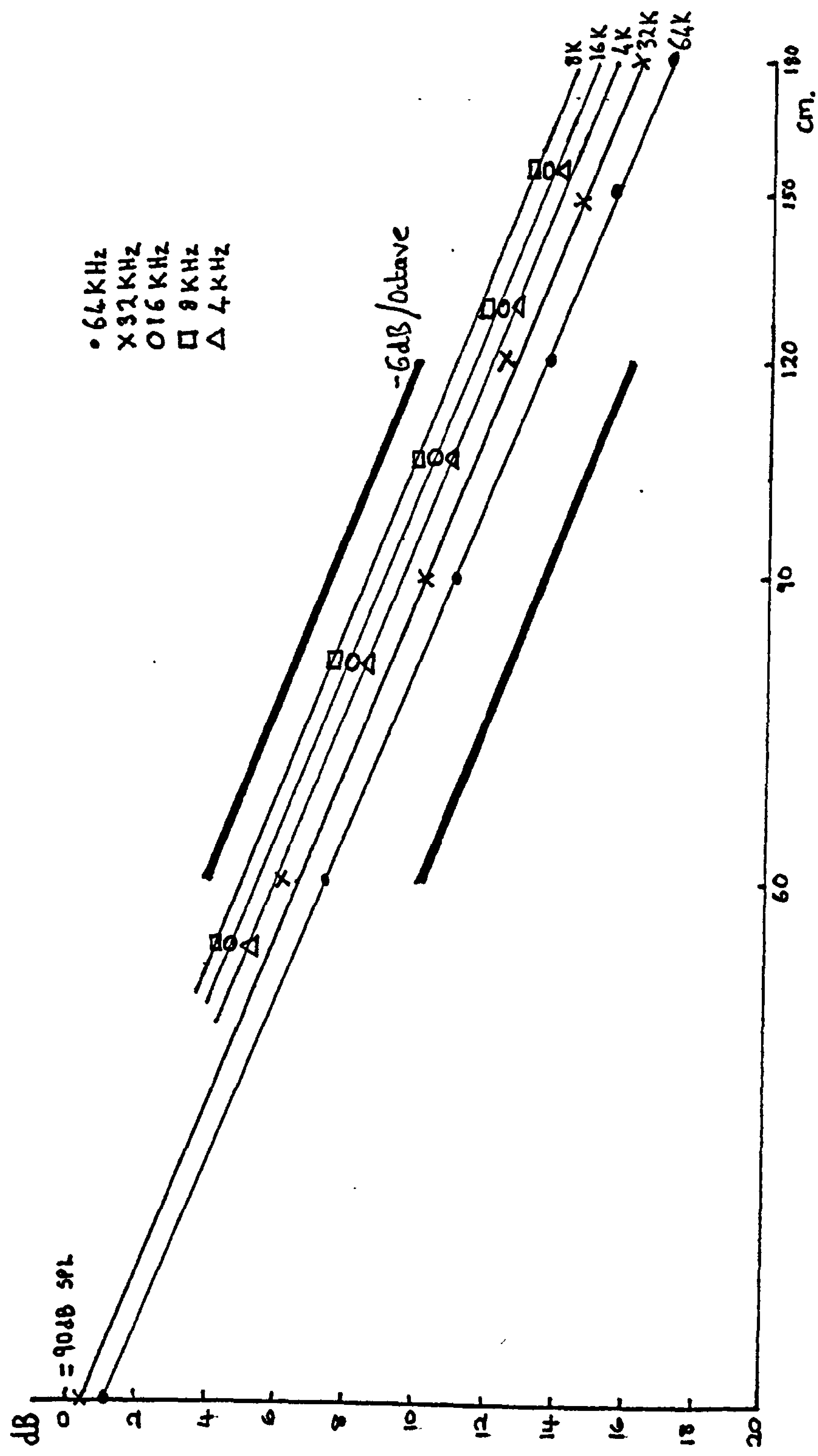

Fig. 7.6 Response of Loudspeaker Assembly in Quasi-anechoic Laboratory.

S.P.L. vs Source/Receiver Separation.

surface has at the original frequency region.

7.5.1 Determination of Amplitude and Phase Changes on Reflection

The procedure was basically one of comparison of pure tone microphone signals with and without the model floor in position, the speaker to microphone separation remaining constant. A number of ways of achieving this were tried.

A convenient method of comparing two signals taken under the two different conditions was as follows: capture the signals in the analogue memory (Section 5.4) one in each channel, so that they can be displayed on a double-beam oscilloscope. The relative amplitudes can be read from the oscilloscope graticule and the relative phases can be determined using the following facility of the event recorder. By activating a spring-loaded switch the digitised signal in the associated channel is rotated by one memory location. The signal is shifted a number of times until the two traces on the oscilloscope appear to have the same phase. Knowing the sampling frequency of the event recorder, the signal frequency and the number of memory locations shifted, the phase difference between the signals is calculated.

The data from such measurements can be used to determine the amplitude and phase changes on reflection by considering the vector diagram of waves reaching the microphone. Fig. 7.7 shows the vector addition of a direct wave and the wave reflected from the model floor.

$$B \cos(\omega t - \emptyset) = A \cos \omega t + \frac{r}{r + \Delta} K A \cos(\omega t - (kr + \emptyset))$$

where Δ = path length difference between direct and reflected waves

r = direct path length

k = wavenumber

ϕ = phase change on reflection

The measurement sequence described above yields the ratio B/A and the angle ϕ. The Δ term is small enough compared with r that $r/(r + \Delta) \approx 1$.

The triangle SRX can be solved using the cosine rule to find K:

$$K^2 A^2 = A^2 + B^2 - 2AB \cos\theta$$

$$K^2 = 1 + \frac{B^2}{A^2} - \frac{2B}{A} \cos\theta$$

or to find ϕ:

$$B^2 = A^2 + K^2 A^2 - 2KA^2 \cos(\pi - (k\Delta + \phi))$$

$$\cos(k\Delta + \phi) = \frac{1}{2K}\left(\frac{B^2}{A^2} - 1 - K^2\right)$$

$$\phi = \cos^{-1}\left\{\frac{1}{2K}\left(\frac{B^2}{A^2} - 1 - K^2\right)\right\} - k\Delta$$

The first attempt to produce the measurements involved positioning the loudspeaker assembly and the microphone 9 cm above the model floor in a horizontal plane and then reproducing the loudspeaker-microphone geometry in a vertical plane to make the direct-only measurement.

This proved impractical since it was impossible to reposition the loudspeaker and microphone whilst still maintaining the original separation of the required accuracy (wavelengths are of the order of millimetres).

It was then decided to leave the geometry, once arranged, and remove the floor of the model from in between the loudspeaker and microphone. This was possible by arranging for the floor to be made up of strips of wood suspended across

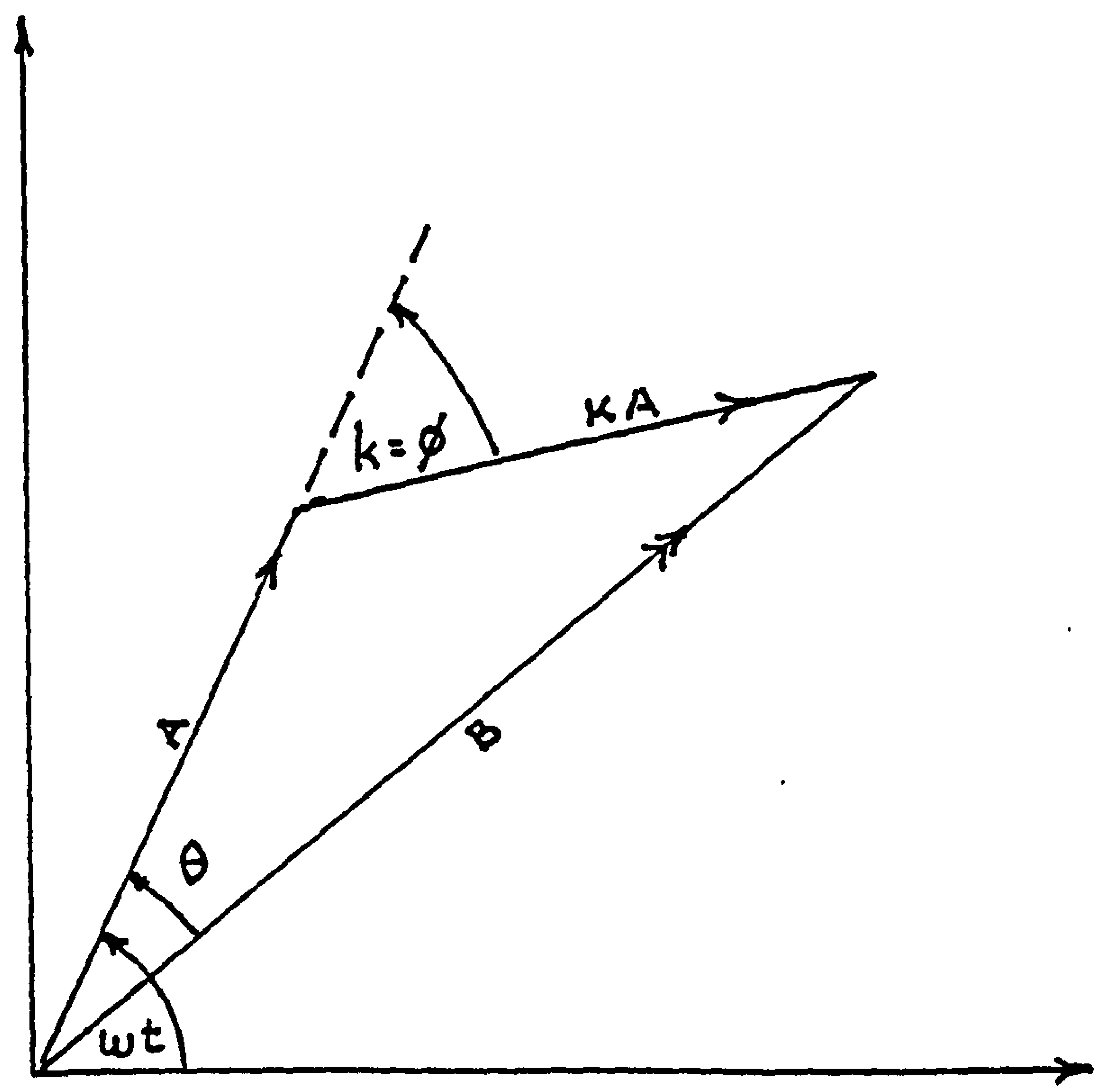

Fig 7.7 Vector Diagram of Direct and Reflected Wave over a plane reflective surface.

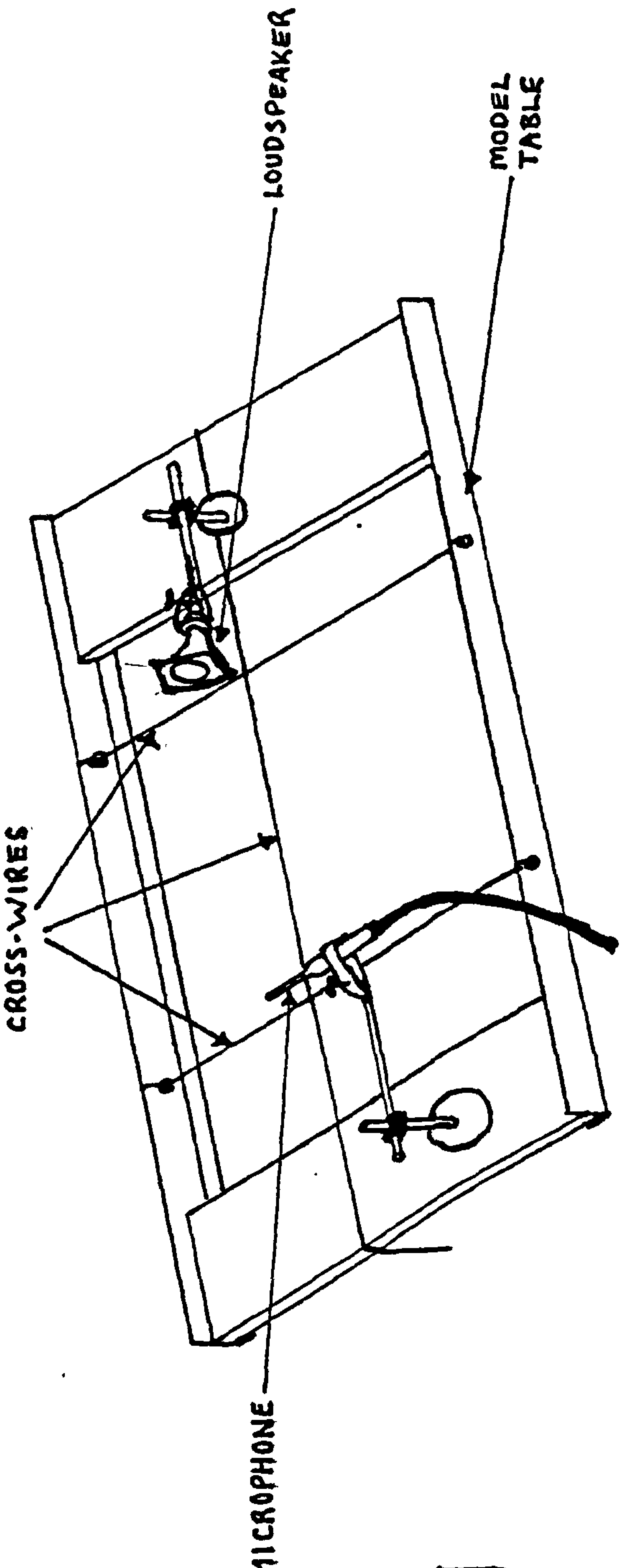

Fig 7.8 Arrangement of Model Table for Reflection Coefficient Determinations.

brackets running the length of the model site and mounted between two trestles, as in Fig. 7.8.

The only problem with this technique was that removing the strips of wood often caused the microphone or loudspeaker to be moved accidentally.

The eventual solution is now described in some detail.

To avoid moving the microphone when lifting the boards on and off it was decided to capture the sine bursts in the event recorder without the boards for a whole series of frequencies and separations, each time transferring the full 4K of data to a floppy disc via the microcomputer. When the boards are replaced the relevant set of data can be returned to the event recorder for comparison, as described previously. The same data can be re-used for investigations of several floor coverings.

A requisite of this technique was that the microphone and loudspeaker should be placed in the same position for each set of measurements to within a very small tolerance.

This was arranged by marking the correct positions by three taut lengths of string, one running centrally along the length of the model and the other two crossing the model, suspended across the brackets that support the boards.

The two points at which the strings crossed were to mark the position of the loudspeaker and the microphone.

The loudspeaker was positioned by lining up the face of the loudspeaker opening with one crossing point. In order to position the microphone, two pointers were made. These were pointed straight lengths of thin metal rods with an eye at one end. One fits over the grill of the microphone and the other over the pre-amplifier. The microphone grill is positioned over the second crossing point as indicated by one pointer, the second being used to ensure orthogonality. The pointer on the grill is removed during measurements whilst the other is slipped back over the cable, taking care not to move the microphone.

Both transducers are mounted on small laboratory stands positioned on boards suspended across the model. Extended metal rods are used to hold the transducers away from these boards. The floor underneath the model is covered with rockwool absorber.

In total five source-receiver separations were used and the appropriate positions on the brackets were marked.

Initially data was captured when the microphone signal level rose above the trigger level set on the event recorder. This proved unsatisfactory since the starting phase of successively captured signals could vary. To overcome this an electronic circuit was made that produced a trigger pulse to the event recorder when the electrical signal fed to the loudspeaker passed through a certain voltage. The result was that successive captured signals had the same starting phase when inspected on the oscilloscope. The diagram of this circuit is shown in Fig. 7.9.

The experiment was carried out using foam and felt as floor materials as well as melamine (i.e. the uncovered boards). The foam and felt were attached to

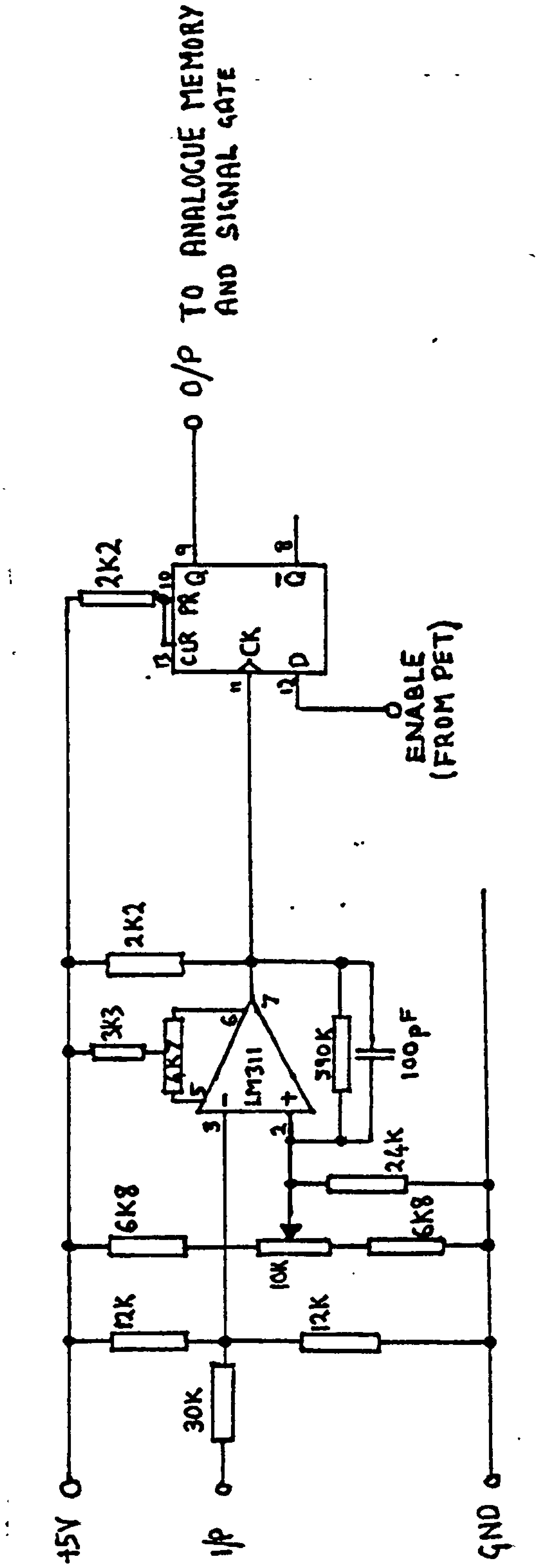

Fig 7.9 Constant phase triggering circuit for Kemo Analogue Memory

opposite sides of the boards using double-sided sticky tape. The choice of these materials was made because previous scale model studies (49) indicated that a soft and/or fibrous material was required.

The results are shown in Fig. 7.10 and graphs in Fig. 7.11 and 7.12., which show the phase change on reflection and amplitude reflection coefficient as a function of frequency for the five source-receiver separations used.

(a)

MATERIAL: FELT

SEPERATION (Metres): 1.66 GRAZING ANGLE: 6.2 degrees

Freq(KHz.)	Reflection coeff.	Phase change(Rad)
4.0	0.85 (+/-0.03)	1.39(+/-0.02)
5.0	0.88 (+/-0.03)	1.53(+/-0.01)
6.3	0.78 (+/-0.[illegible])	1.86(+/-0.01)
8.0	0.63 (+/-0.[illegible])	1.51(+/-0.03)
10.0	0.31 (+/-0.04)	.89(+/-0.15)
12.5	0.29 (+/-0.09)	-1.00(+/-0.23)
16.0	0.50 (+/-0.02)	-2.48(+/-0.16)

SEPERATION (Metres): 1.36 GRAZING ANGLE: 7.6 degrees

Freq(KHz.)	Reflection coeff.	Phase change(Rad)
4.0	0.94 (+/-0.03)	1.05(+/-0.02)
5.0	0.95 (+/-0.03)	1.36(+/-0.01)
6.[illegible]	0.73 (+/-0.01)	1.61(+/-0.02)
8.0	0.72 (+/-0.02)	1.07(+/-0.02)
10.0	0.55 (+/-0.06)	-0.00(+/-0.02)
12.5	0.38 (+/-0.08)	-1.82(+/-0.26)
16.0	0.53 (+/-0.02)	-3.11(+/-0.15)

SEPERATION (Metres): 1.05 GRAZING ANGLE: 9.7 degrees

Freq(KHz.)	Reflection coeff.	Phase change(Rad)
4.0	0.82 (+/-0.03)	.87(+/-0.02)
5.0	0.82 (+/-0.02)	1.10(+/-0.01)
6.3	0.[illegible]9 (+/-0.00)	1.27(+/-0.01)
8.0	0.59 (+/-0.04)	.18(+/-0.02)
10.0	0.57 (+/-0.08)	-.94(+/-0.04)
12.5	0.47 (+/-0.07)	-2.72(+/-0.24)
16.0	0.45 (+/-0.02)	-4.05(+/-0.16)

SEPERATION (Metres): .82 GRAZING ANGLE: 12.4 degrees

Freq(KHz.)	Reflection coeff.	Phase change(Rad)
4.0	1.04 (+/-0.03)	.82(+/-0.02)
5.0	0.82 (+/-0.01)	1.00(+/-0.01)
6.3	0.64 (+/-0.02)	.54(+/-0.02)
8.0	0.58 (+/-0.05)	-.60(+/-0.02)
10.0	0.31 (+/-0.06)	-2.69(+/-0.24)
12.5	.59 (+/-0.06)	-3.75(+/-0.21)
16.0	0.37 (+/-0.12)	-4.42(+/-0.24)

SEPERATION (Metres): .52 GRAZING ANGLE: 19.2 degrees

Freq(KHz.)	Reflection coeff.	Phase change(Rad)
4.0	0.76 (+/-0.01)	.50(+/-0.01)
5.0	0.71 (+/-0.02)	-.05(+/-0.01)
6.3	0.50 (+/-0.05)	-1.68(+/-0.03)
8.0	0.51 (+/-0.02)	-4.00(+/-0.03)
10.0	0.49 (+/-0.05)	-4.84(+/-0.17)
12.5	0.71 (+/-[illegible].09)	-4.91(+/-0.04)
16.0	0.33 (+/-[illegible])	-6.74(+/-0.11)

(b)

MATERIAL: FOAM

SEPERATION (Metres): 1.66 GRAZING ANGLE: 6.2 degrees

Freq(KHz.)	Reflection coeff.	Phase change(Rad)
4.0	0.83 (+/-0.01)	[illegible].15(+/-0.01)
5.0	0.87 (+/-0.02)	1.76(+/-0.01)
6.3	0.83 (+/-0.03)	1.30(+/-0.01)
8.0	0.77 (+/-0.06)	.45(+/-0.04)
10.0	0.69 (+/-0.08)	-.30(+/-0.09)
12.5	0.77 (+/-0.05)	-1.66(+/-0.20)
16.0	0.69 (+/-0.02)	-2.53(+/-0.12)

SEPERATION (Metres): 1.36 GRAZING ANGLE: 7.6 degrees

Freq(KHz.)	Reflection coeff.	Phase change(Rad)
4.0	0.86 (+/-0.01)	1.89(+/-0.01)
5.0	0.87 (+/-0.02)	1.43(+/-0.01)
6.3	0.80 (+/-0.04)	.70(+/-0.02)
8.0	0.67 (+/-0.06)	-.10(+/-0.06)
10.0	0.81 (+/-0.06)	-1.30(+/-0.14)
12.5	0.90 (+/-0.02)	-2.45(+/-0.06)
16.0	0.70 (+/-0.09)	-2.72(+/-0.25)

SEPERATION (Metres): 1.05 GRAZING ANGLE: 9.7 degrees

Freq(KHz.)	Reflection coeff.	Phase change(Rad)
4.0	0.85 (+/-0.02)	1.50(+/-0.01)
5.0	0.84 (+/-0.03)	.91(+/-0.01)
6.3	0.79 (+/-0.05)	-.04(+/-0.04)
8.0	0.76 (+/-0.06)	-1.14(+/-0.10)
10.0	0.73 (+/-0.04)	-2.29(+/-0.15)
12.5	1.04 (+/-0.08)	-2.54(+/-0.15)
16.0	0.67 (+/-0.13)	-2.81(+/-0.11)

SEPERATION (Metres): .82 GRAZING ANGLE: 12.4 degrees

Freq(KHz.)	Reflection coeff.	Phase change(Rad)
4.0	0.81 (+/-0.02)	1.08(+/-0.01)
5.0	0.65 (+/-0.04)	.20(+/-0.02)
6.3	0.65 (+/-0.05)	-.94(+/-0.07)
8.0	0.55 (+/-0.02)	-2.53(+/-0.04)
10.0	0.67 (+/-0.04)	-3.00(+/-0.16)
12.5	0.90 (+/-0.10)	-2.88(+/-0.10)
16.0	0.62 (+/-0.08)	-3.20(+/-0.04)

SEPERATION (Metres): .52 GRAZING ANGLE: 19.2 degrees

Freq(KHz.)	Reflection coeff.	Phase change(Rad)
4.0	0.68 (+/-0.03)	-.16(+/-0.02)
5.0	0.56 (+/-0.04)	-1.58(+/-0.07)
6.3	0.57 (+/-0.03)	-2.96(+/-0.08)
8.0	0.67 (+/-0.06)	-3.17(+/-0.09)
10.0	0.00 (+/-0.00)	0.00(+/-0.00)
12.5	0.41 (+/-0.04)	-4.30(+/-0.10)
16.0	0.40 (+/-0.12)	-7.66(+/-0.25)

Fig 7.10 Results of Reflection Coefficient Measurements for (a) Felt, (b) Foam

MATERIAL: MELAMINE

SEPERATION (Metres): 1.36 GRAZING ANGLE: 7.6 degrees

Freq(KHz.)	Reflection coeff.	Phase change(Rad)
4.0	1.04 (+/-0.03)	.33(+/-0.04)
5.0	0.71 (+/-0.04)	.64(+/-0.03)
6.3	0.31 (+/-0.05)	.17(+/-0.05)
8.0	0.86 (+/-0.05)	.36(+/-0.03)
10.0	0.83 (+/-0.05)	.26(+/-0.01)
12.5	1.00 (+/-0.03)	.17(+/-0.00)
16.0	0.30 (+/-0.08)	-1.05(+/-0.01)

SEPERATION (Metres): 1.05 GRAZING ANGLE: 9.7 degrees

Freq(KHz.)	Reflection coeff.	Phase change(Rad)
4.0	1.04 (+/-0.03)	.09(+/-0.04)
5.0	0.90 (+/-0.04)	.25(+/-0.04)
6.3	0.68 (+/-0.04)	.33(+/-0.02)
8.0	0.97 (+/-0.04)	.33(+/-0.01)
[illegible]	0.75 (+/-0.01)	.18(+/-0.02)
[illegible]	0.57 (+/-0.06)	-1.02(+/-0.02)
16.0	0.58 (+/-0.10)	-3.61(+/-0.26)

SEPERATION (Metres): .82 GRAZING ANGLE: 12.4 degrees

Freq(KHz.)	Reflection coeff.	Phase change(Rad)
4.0	0.98 (+/-0.03)	.15(+/-0.03)
5.0	1.05 (+/-0.04)	.28(+/-0.02)
6.3	0.77 (+/-0.03)	.35(+/-0.01)
8.0	0.84 (+/-0.00)	.20(+/-0.00)
10.0	0.60 (+/-0.04)	-1.02(+/-0.03)
12.5	0.71 (+/-0.09)	-3.24(+/-0.15)
16.0	0.79 (+/-0.08)	-4.94(+/-0.23)

SEPERATION (Metres): .52 GRAZING ANGLE: 19.2 degrees

Freq(KHz.)	Reflection coeff.	Phase change(Rad)
4.0	0.88 (+/-0.02)	.30(+/-0.01)
5.0	0.74 (+/-0.00)	.17(+/-0.01)
6.3	0.57 (+/-0.03)	-.95(+/-0.03)
8.0	0.49 (+/-0.06)	-3.39(+/-0.13)
10.0	0.62 (+/-0.04)	-4.89(+/-0.14)
12.5	1.04 (+/-0.10)	-5.46(+/-0.11)
16.0	0.54 (+/-0.04)	-6.16(+/-0.08)

Fig 7.10 (continued) Results of Reflection Coefficient Measurements for (c) Melamine

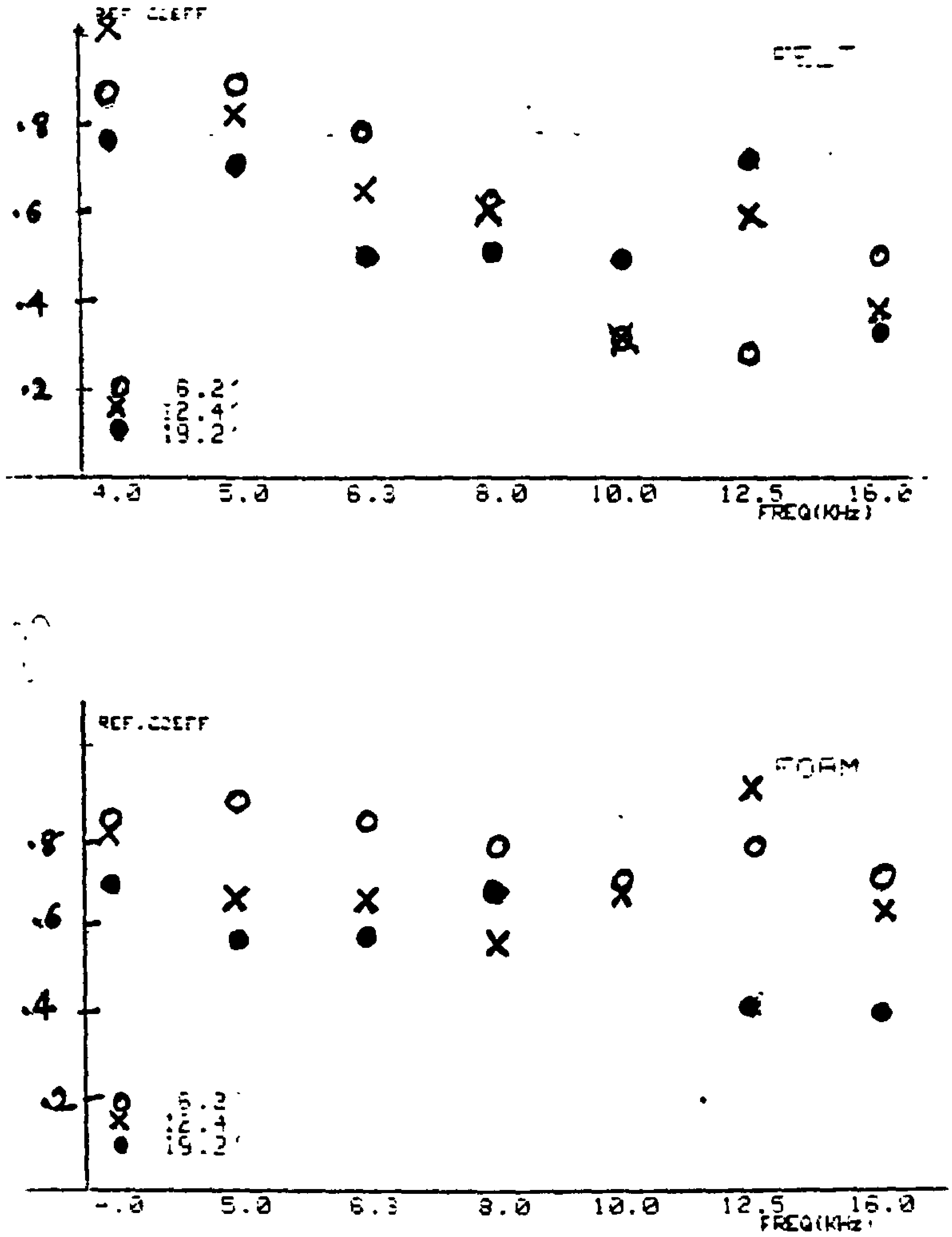

Fig 7.11 Amptitude Reflection Coefficient vs. Frequency for (a) Felt, (b) Foam

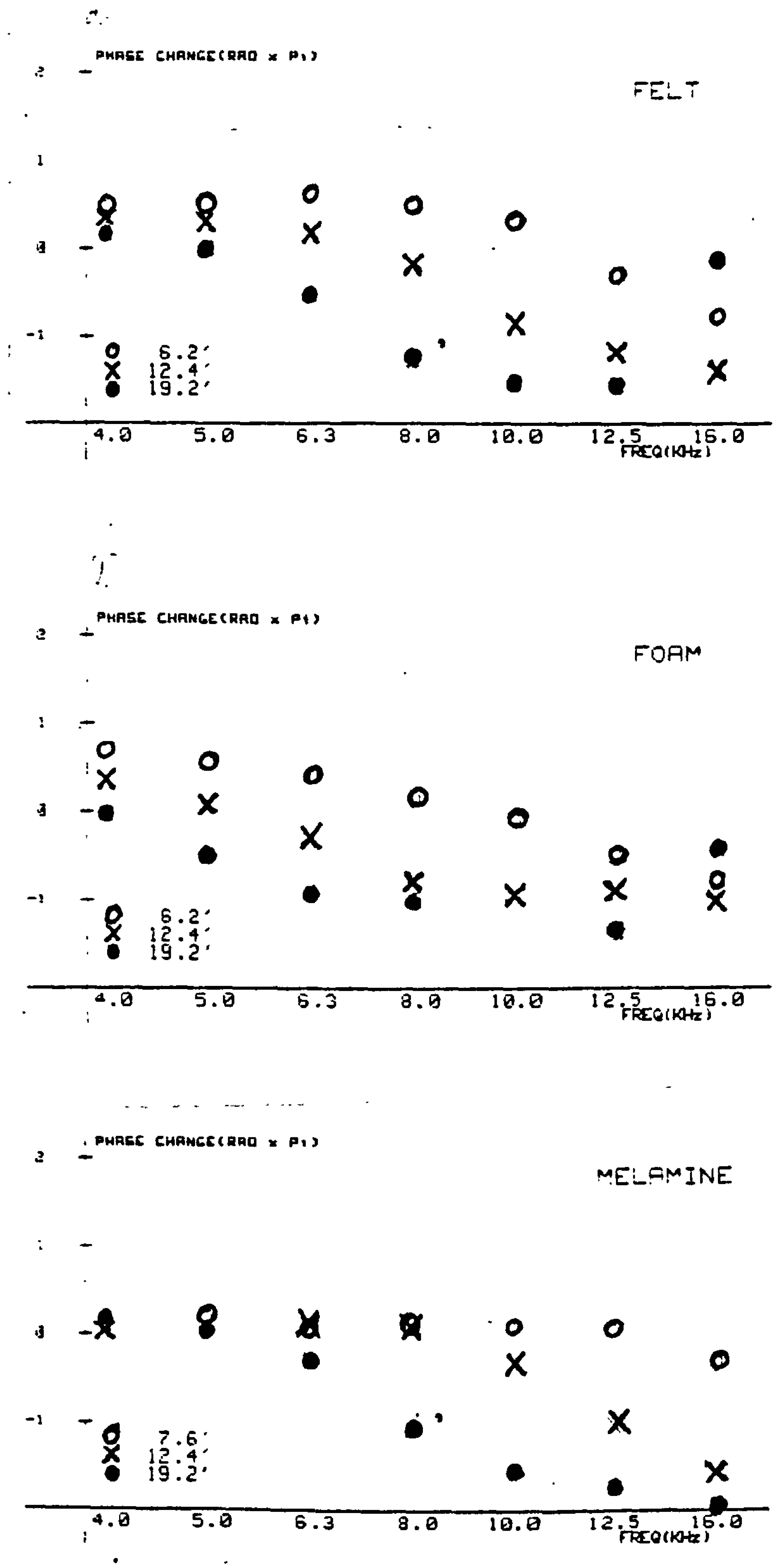

Fig 7.12 Phase Change on Reflection vs. Frequency for (a) Felt, (b) Foam, (c) Melamine

CHAPTER 8

Experiments

The field experiment initially involved a fact-gathering exercise on the effect of various meteorological parameters on unobstructed acoustical propagation, leading to a study of how any observed effects modify barrier performance.

The variables between experiments were the signal type and the geometry of the transducers and, if present, the barrier. The desirability of using different signal types has been discussed in Section 4.1 . Model experiments used a 16:1 scaled-down version of the experiments in the outdoors.

This chapter discusses the choice of outdoor location and documents details of the geometries and source signals used in each experiment, as already introduced in general form is Section 4.2.1.

The analyses of the results are discussed in Chapter 11.

8.1 Field Experiments

8.1.1. Location

The location for the field experiments was dictated by several factors:

(i) Avoidance of high background noise levels, such as main roads, factories, etc.

(ii) Accessibility for the mobile laboratory

(iii) Regular availability over prolonged periods.

(iv) Ease of barrier erection

(v) Level ground with a uniform covering

The following alternatives were considered:

Site 1 was an unused field attached to F L Calder College, an annexe of Liverpool Polytechnic. The field was on a steep slope and drainage was poor. This meant that the field often became water-logged and therefore inaccessible to the mobile laboratory.

Site 2 was the sports field of I M Marsh College, another annexe of the Polytechnic. This site was remote from the college buildings and was on firm, level ground. Additional advantages were the possibility of mains power from an outbuilding using long extension cables and the possibility of storage for the barrier materials.

Site 3 was a small piece of waste land belonging to Lancashire County Council and was the site of a disused railway. The ground ranged from being hard and barren to being covered in long uncultivated grass.

Site 4 was part of the disused Air Force Base at Burtonwood, near Warrington Cheshire. The ground was made up of concrete slabs and storage facilities were readily available.

A hard surface was acceptable from an acoustical viewpoint since its reflective characteristics are well documented in the literature. However, the erection of a barrier on a temporary basis would entail scaffolding which would be time-consuming, especially if the barrier had to be dismantled after each day's experiments, and would require a certain amount of skill.

A further handicap was that the site was within 1 Km of a motorway which might produce a high background noise level of an irregular nature.

After consideration of all the alternatives, Site 2, I M Marsh College sports field, emerged as a clear choice.

8.1.2 Open Propagation

The initial acquaintance with horizontal propagation through the atmosphere was made by monitoring the loudspeaker output with a microphone at a distance of 4.8 m and a second microphone at one of the series of distances, each of which was an integer multiple of 4.8 m. The loudspeaker and two microphones, referred to as the near and far microphone, were all at a height of 1.4 m. Octave bands of noise were used exclusively in these experiments.

The anemometer was placed near to the loudspeaker mouth (without obstructing the line of sight between source and receivers) since it has been postulated that turbulence at the start of an acoustical path has the greatest influence on a received signal (38).

The wind direction indicator was placed a few metres behind the loudspeaker with the reference direction pointing along a line joining the source and receivers, so that a direction of 180° is downwind propagation, 0° is upwind propagation and 90° or 270° represents a cross-wind.
The temperature probe of the electronic thermometer was suspended in the air near the mobile laboratory shaded from direct sunlight.

A summary of the source/receiver geometries is given in Fig. 8.1.

8.1.3 Barrier Experiments

Initially the geometries used with a barrier in place were chosen to provide a direct comparison with the open propagation experiments descriebd in 8.1.2.
The near microphone was at 4.8 m and the barrier at 9.6 m from the loudspeaker. The far microphone was placed beyond the barrier at one of a series of distances each of which was an integer multiple of 4.8 from the barrier. The loudspeaker and microphone were all at 1.4 m high. See Fig 8.2 and Fig 8.2(a)

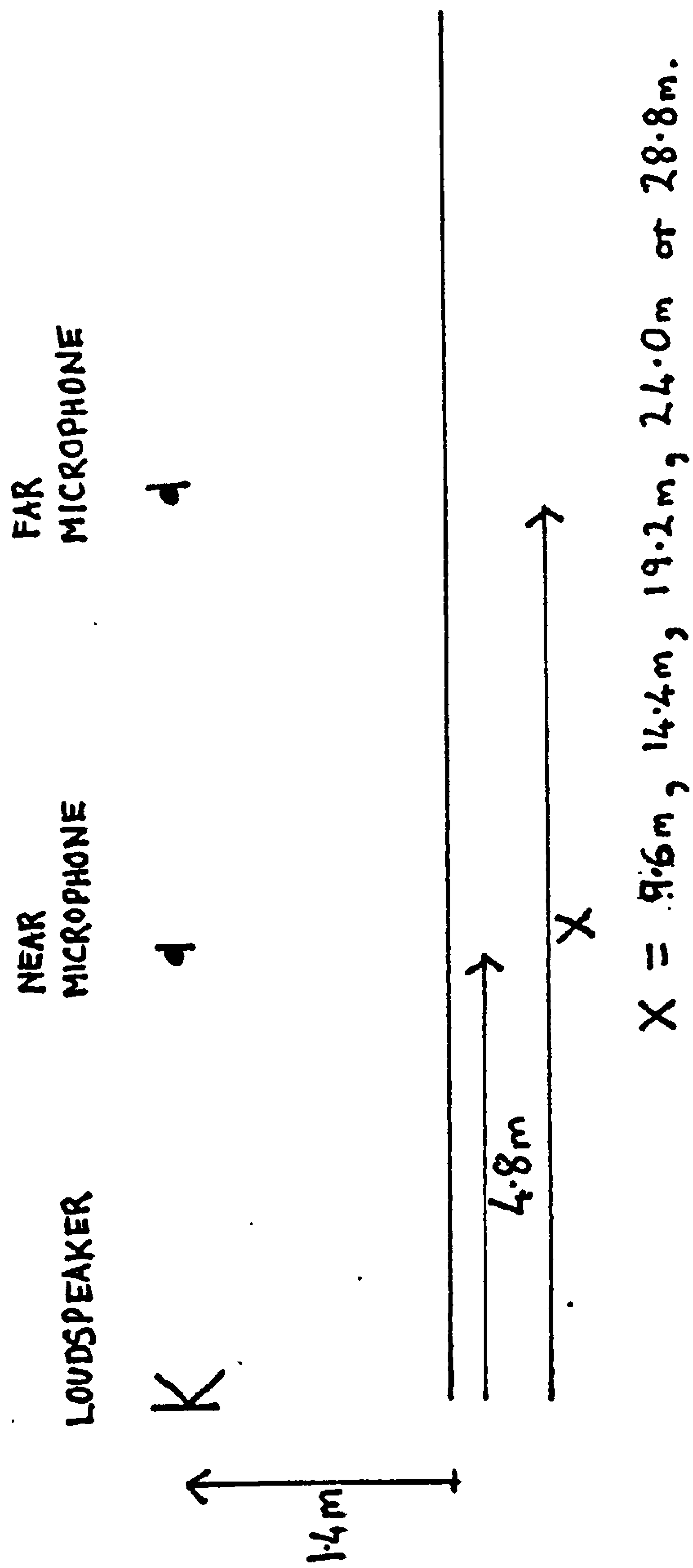

Fig 8.1 Summary of Open Propagation Geometries

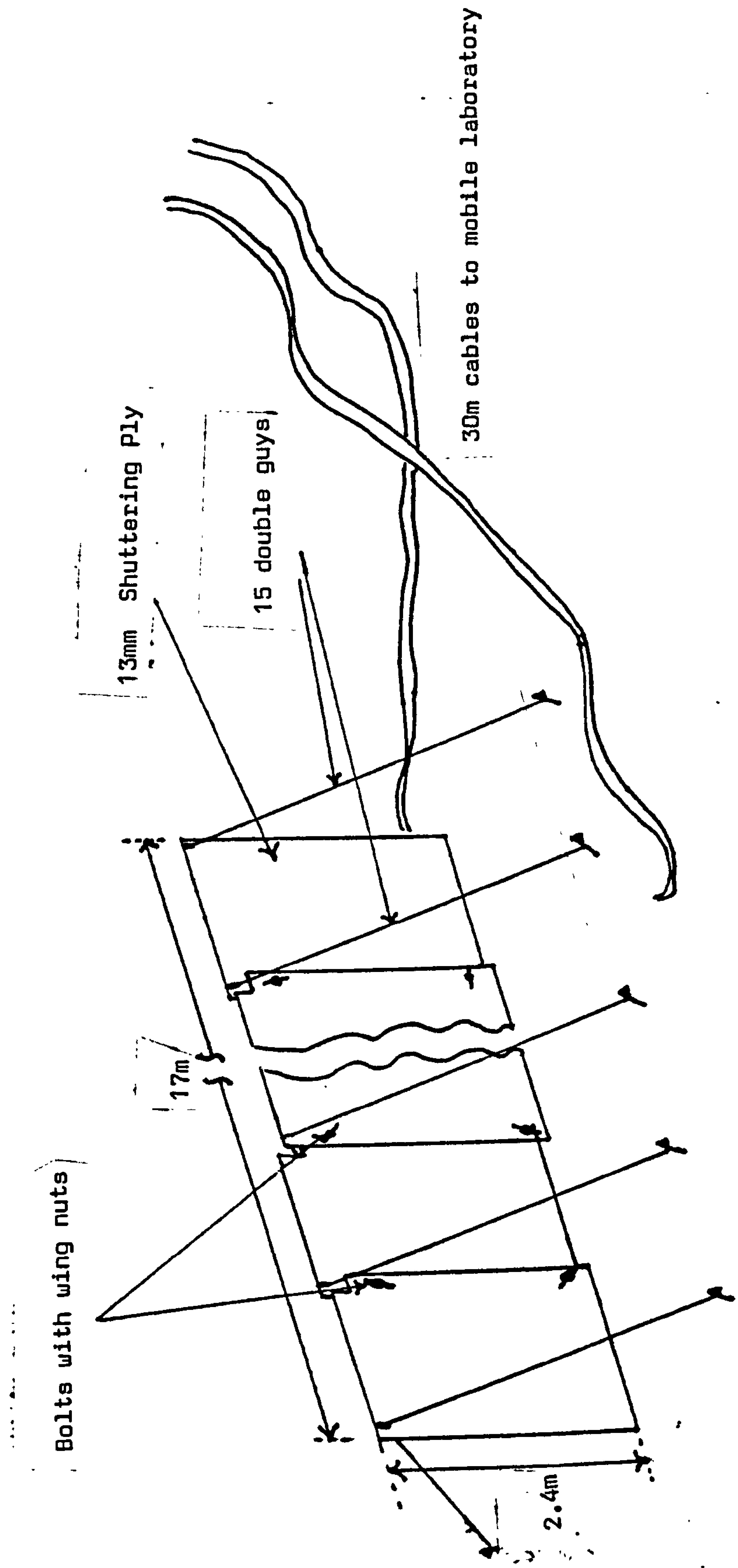

Fig 8.2 Barrier Construction

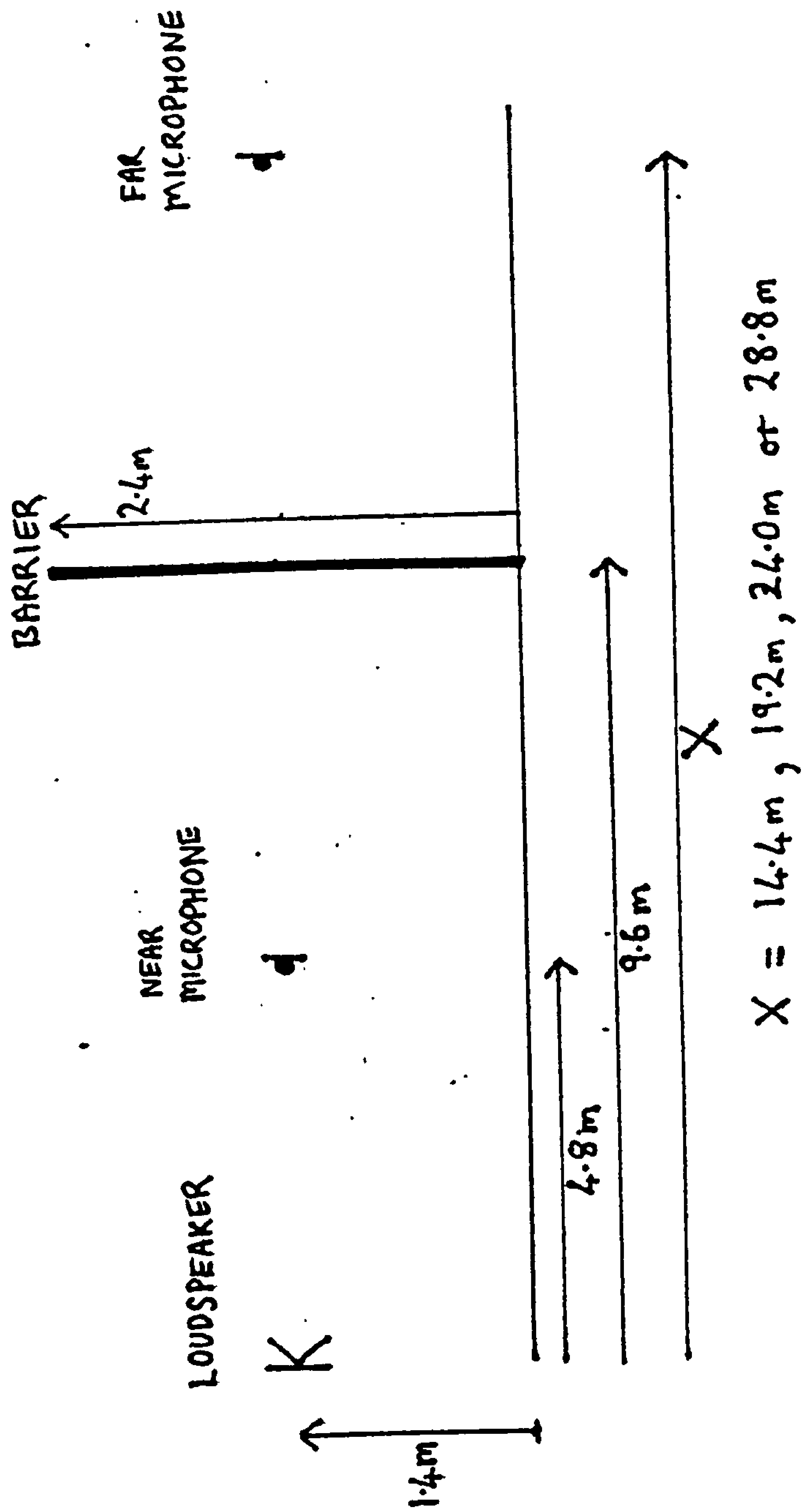

Fig 8.2 Summary of Barrier Geometries; Octave Bands of Noise.

(a) Source and Receivers above ground

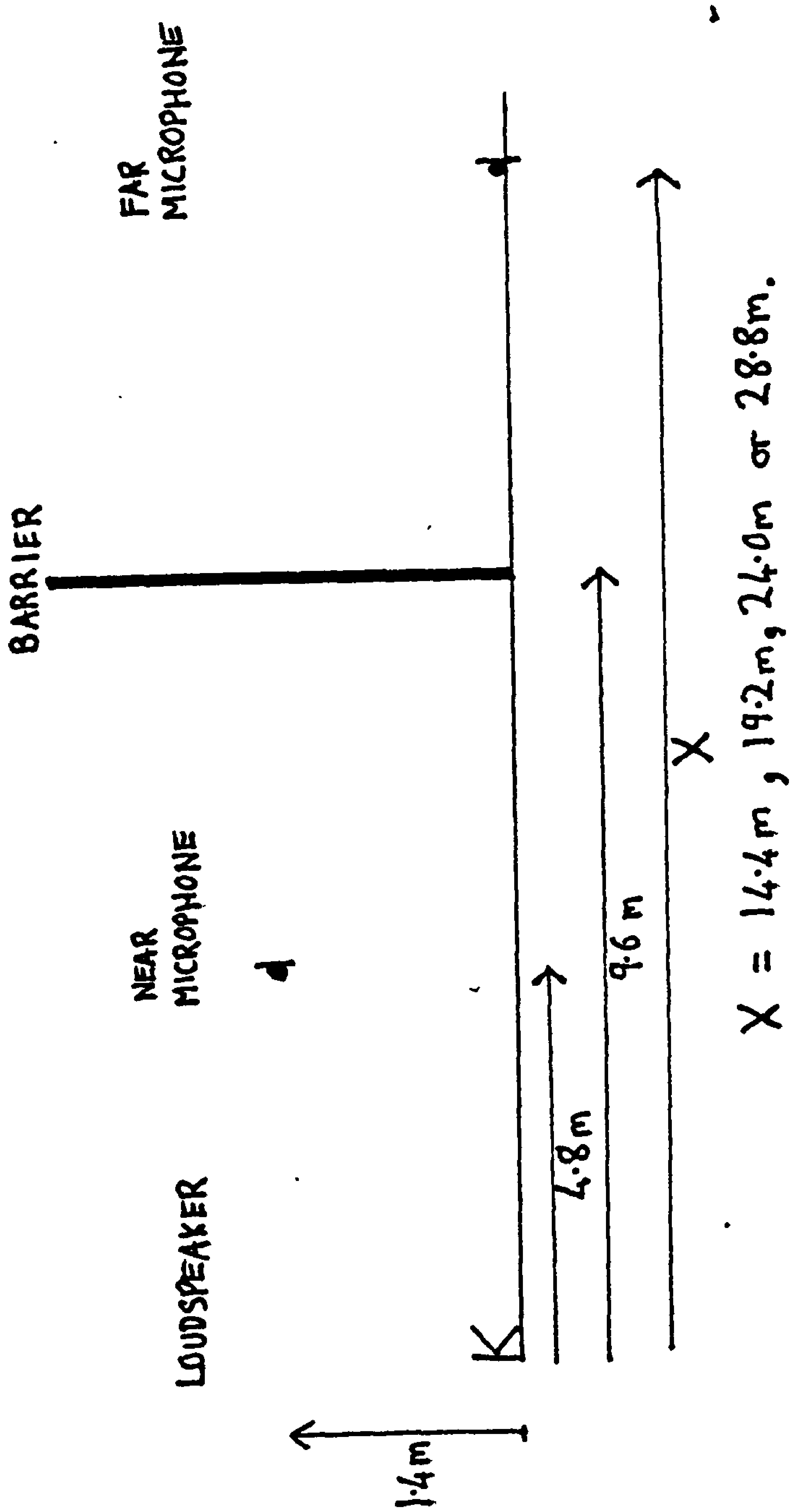

(b) Source and Far Receiver at Ground Level.

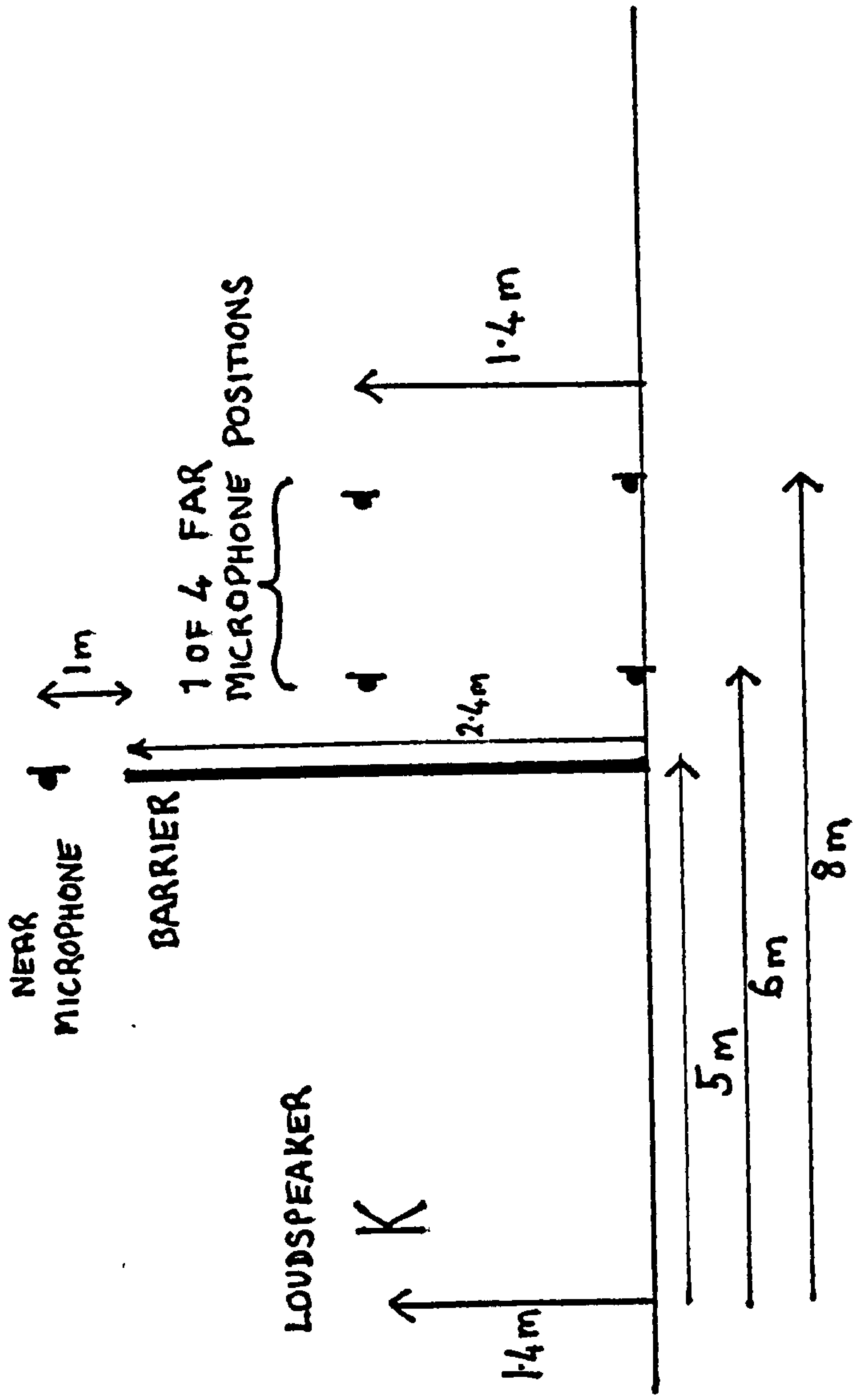

Fig 8.3 Summary of Barrier Geometries; Pure Tones and Random Pure Tones.

+ missing (wB)

For these two series of geometries the anemometer and temperature probes and the wind direction sensor were positioned as described in 8.1.2. Octave bands of noise were used.

In a development of this system the near microphone and anemometer were placed above the barrier which was at a distance of 5 m from the loudspeaker. The far microphone was beyond the barrier at a distance of 1 m or 3 m, and either 1.4 m high or at ground level. Fig. 8.3 summarizes these geometries.

For these experiments the source signal was pure tone, either of a fixed frequency or of random frequencies within an octave band, as described in Section 5.1.

8.1.4 Use of a Tape Recorder with the Automatic Measurement System

At one stage the throughput of data was increased by using a Nagra IV SJ tape recorder to monitor the signals from both microphones on direct recording channels and the anemometer on the frequency modulated channel. Of necessity, this technique neglected the air temperature sensor and the wind direction sensor.

Sound bursts could be measured in this manner at 1 second intervals instead of the approximately 8 seconds of the previous system. The recordings were taken to the laboratory and replayed through the original measurement system as if they were elements of data collected and analysed in real time. A calibration tone from each of the microphones was recorded before commencement of the experiment in order to relate the RMS levels measured from the recorded sound bursts to S.P.L. This is a similar procedure to the calibration performed in the real-time situation.

Once a recorded sound burst was captured in the event recorder the micro-computer processing time was about eight seconds, which includes the transfer of individual elements of the data to the mainframe computer (see Section 12.1.2). Since the sound bursts were recorded every second, the programme on the microcomputer only used every tenth recording. To process all the data the tape was re-run ten times with a different "offset" each time. That is, on the first pass every tenth burst starting with the first burst was used; on the second pass the process started on the second burst etc.

Recording the Anemometer Signal

It was necessary to ascertain the DC transfer characteristic of the FM channel of the tape recorder in order to calculate the true output voltage of the anemometer at the time of recording.

The output of stabilised DC power supply was applied to the parallel combination of a digital voltmeter and the FM channel of the tape recorder. The output was varied between 1 and 2 volts, which covers the range of a typical anemometer output. Each voltage setting was recorded for approximately ten seconds at 15 inches per second. Between settings the tape was stopped.

After the range of input voltages was recorded, the DVM was placed on the output of the FM channel and the recording replayed. A steady voltage was reached about 2 seconds after the start of each voltage setting.

The results showed a linear transfer characteristic with 1 volt recorded becoming -3.35 volts on play-back and 2 volts recorded becoming -2.42 volts on play-back. To counteract this voltage shift the FM channel output was replayed across a 3.35 DC voltage obtained from a stabilised power supply and then into the event recorder which had an offset control adjusted to allow the 1 to 2 volt range to occupy its dynamic range. A low pass filter with a cut-off of 1500 Hz was included in the signal path before the event recorder to remove some of the high frequency tape hiss. See Fig. 8.4.

The validity of this process was checked by recording a sine wave which varied between 1 and 2 volts obtained from a function generator. As required, this sine wave was digitised in the event recorder between the values 0 and 255 with no overload at either maximum or minimum.

The overall transfer function of the above system was incorporated in the algorithm for converting anemometer voltage to equivalent wind speed.

8.2 Model Experiments

To a large extent the experiments performed in the laboratory were a scaled-down version of those performed outdoors and described in Section 8.1. This Section details the model experiments and discusses the similarity, or otherwise, between the model and full-size situations.

8.2.1 Modelling Wind Conditions

Two conflicting criteria could be used to model typical wind conditions. Since linear dimensions are reduced in the model then an equivalent wind speed would be achieved if the model air flow equalled the outdoor wind speed divided by the scaling factor. It would then remain to produce similar degrees of turbulence in the model as existed in the outdoor situation. This is the approach adopted by Stusnick and Dejong. (32). However, this does not take into account barrier-induced wind turbulence. Fluid dynamics considerations indicate that, if similar degrees of fluid turbul-

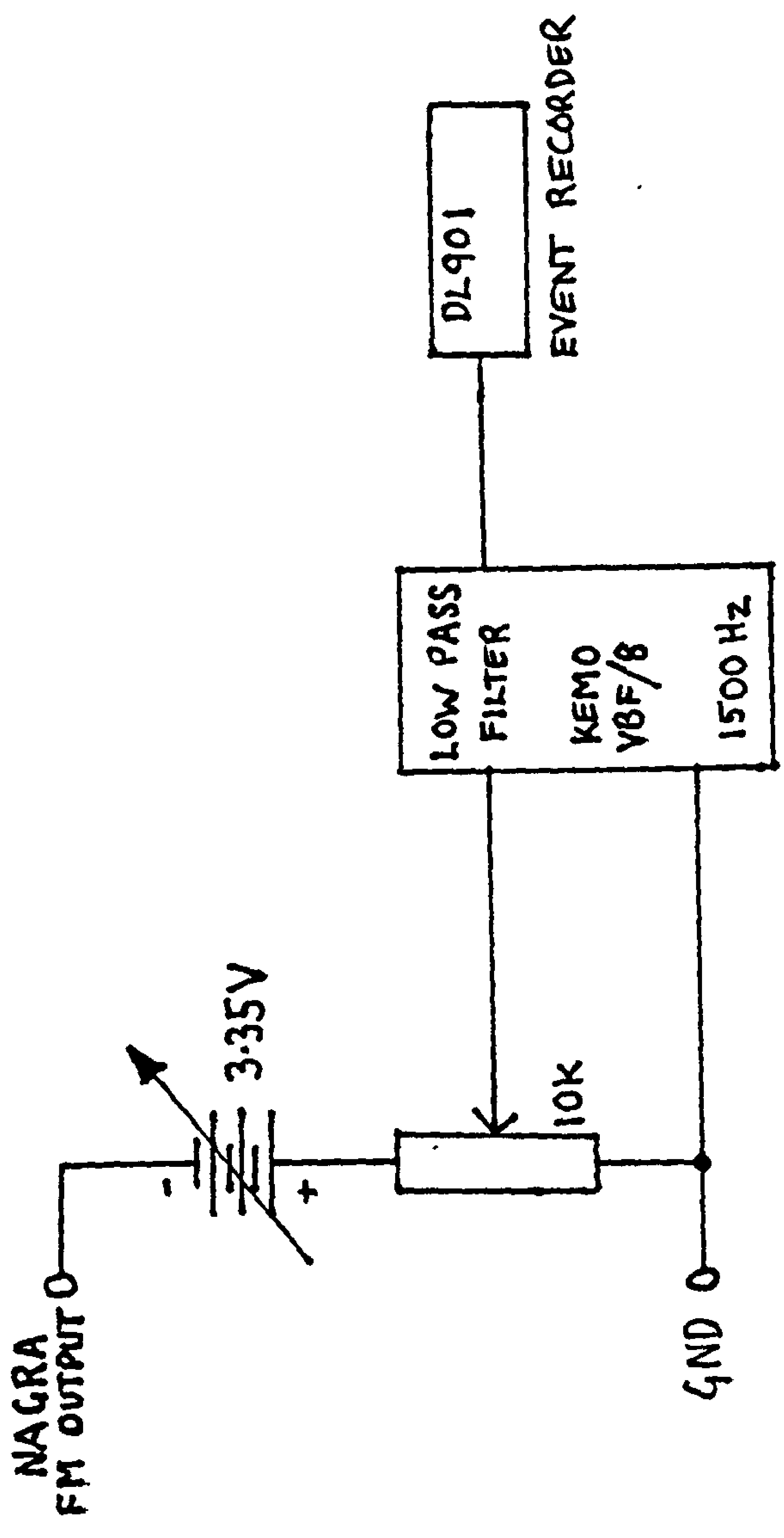

Fig 8.4 Nagra Playback circuit.

ence are to be produced in different systems, then a dimensionless quantity known as the Reynolds Nymber (Re) must have similar values in each system. (50).

The Reynolds number is given by:

$$Re = \frac{\rho U L}{\mu}$$

where ρ = fluid density

U = a representative velocity scale

L = a representative length scale

μ = fluid viscosity

If the model is in air, then ρ and μ are constant in each system, so decreasing linear dimensions would paradoxically indicate that air flow rate in the model system should be increased by a factor equal to the scaling factor. A 16 : 1 scale, as dictated by acoustical considerations, would mean such high air flow rates that a wind tunnel would be required. The size of wind tunnel needed to produce high flow rates over a floor area of the size required to mount an acoustic model generally have high acoustic emission which could produce a poor signal to noise ratios. Such a structure was not readily available and the designing and building of one specifically was beyond the intended scope of this project.

It was reasonable, therefore, to investigate the case in which ambient wind conditions are modelled, leaving the modelling of barrier-induced turbulence as a possible development.

To produce the required slow air flow above the model surface a so-called wind chest was used.

This apparatus composed a variable speed electric fan in a chipboard box of dimensions approximately 1.5 m x 1.5 m x 0.3 m.

One of the large area surfaces contained two square intakes near the bottom of the box, each about 0.3 m square, and covered with a square grid. Occupying the top half of the same surface was the opening that acted as the exhaust. It was filled with a honey-comb shaped structure constructed from thin metal foil which aided the production of laminar flow from the wind-chest.

With the fan rotating at its fastest an air flow of about 1 ms^{-1} is produced with a turbulent intensity of about 10%, which is representative of a wind speed of 16 ms^{-1} (i.e. 36 miles per hour) the turbulent intensity figure being the same in model and full-size conditions. It was concluded that the wind chest could model a range of wind speeds adequately covering the range that could be expected in the field.

8.2.2 Construction

The base upon which the model experiments were carried out comprised six melamine-clad boards each of a length 60 cm and thickness 1.3 cm. The depths were 15 cm, 22 cm, or 30 cm; two boards of each depth. The material covering for the boards was the subject of investigation as reported in Sec 7.5

The boards were laid lengthways across two parallel right-angle section brackets and assembled to form one continuous surface. The brackets were supported at a height of about 1 m by two trestles. See Fig. 8.5.

The above construction was placed in front of the wind cabinet so that the air flow was parallel to the angle brackets.

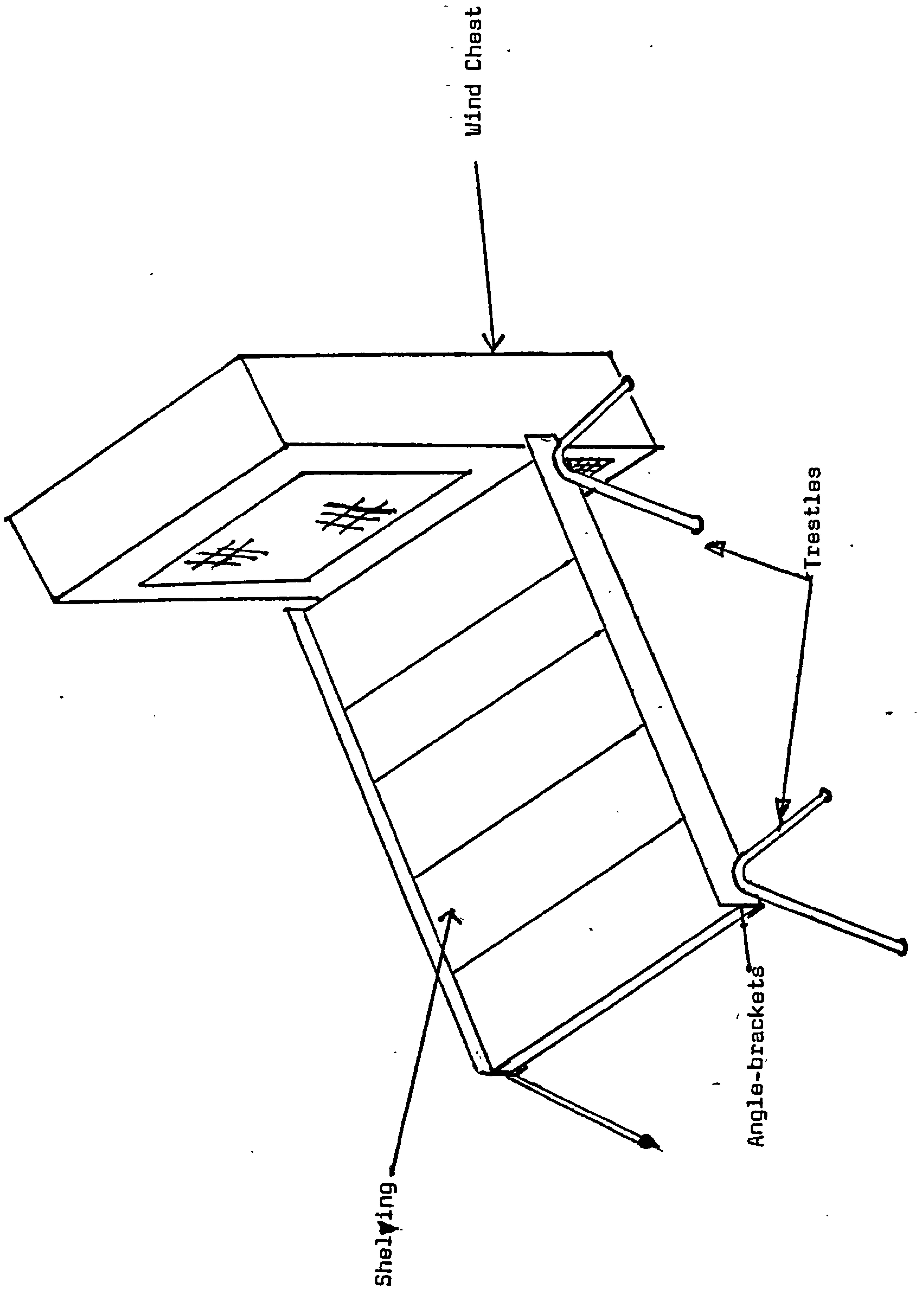

Fig. 8.5   Arrangement for Model Investigations.

The barrier was a thin sheet of aluminium measuring 60 cm by 15 cm.

8.2.3 Model Procedures

The series of geometries in the full-size experiments, see Sections 8.1.2 and 8.1.3 were reproduced in the model using a scaling factor of 1:16. The signal source emitted either a pure tone or octave band of noise.

In the outdoor experiments the meteorological conditions were beyond the control of the experimenter and so each procedure was repeated on a number of days to provide a range of conditions. In the model, however, conditions were not so variable. The ambient temperature remained constant throughout the course of one set of measurements to within 1^{o}C and the wind direction was set by the orientation of the transducers to the wind cabinet. These parameters were edited into the programme as data by the experimenter.

Model experiments involving air flow were limited to downwind propagation only.

CHAPTER 9

The Results of Full Scale Experiments

The results of the experiments of Chapter 8 are presented here in a series of graphs of level difference between near and far microphones in dB verses Turbulence Number, an index based upon the definition of turbulent intensity. Each point represents a measurement of a single sound burst.

Turbulence number was calculated from either a 50 ms or 500 ms capture of anemometer data and this is shown on the axis of the graphs as TN_{50} or TN_{500} respectively. This change was made since typical turbulence spectra (40) show a significant component below 20Hz (i.e. the lower frequency cut-off imposed by a 50 ms data capture). Additionally, TN_{50} used the approximate formula for turbulent intensity (equation 5.8) which is reported to be a reasonable approximation only for turbulent intensities up to about 10%. However, some of the data shows TN_{50} values of up to 18% and so the TN_{500} measurements were based on the definition of turbulent intensity (i.e. TN_{500}= $(du/\bar{u}) \times 100$).

Only turbulence is considered in the following graphs to the exclusion of such parameters as wind velocity, air temperature, wind direction, etc., since only when level difference was plotted against a TN value did the trends and tendencies to be discussed in Chapter 11 appear. In each of the figures that follow there are either four or, more usually, five graphs, a separate graph for each frequency used in a particular geometry. The figures are indexed as follows:

9.1a - 9.1e	Octave noise bands propagated over open grassland for five far microphone positions (See Fig 8.1)

9.2.1b - 9.2.1e	Octave noise bands propagated over barrier for four far microphone positions (speaker and microphones above ground). (See Fig 8.2(a))
9.2.2b - 9.2.2e	Octave noise bands propagated over barrier for four far microphone positions (speaker and far microphone at ground level). (See Fig 8.2(b))
9.3a - 9.3d	Pure tones propagated over barrier for four far microphone positions (See Fig 8.3)
9.4a - 9.4d	Random pure tones propagated over barrier for four far microphone positions. (See Fig 8.3)

Figs 9.2.1 and 9.2.2 start from letter b in order to ease cross-referencing to the geometrically similar arrangements of Figs 9.1b - c.

In the analysis discussion the above figures are referred to as representating a particular source/receiver geometry.

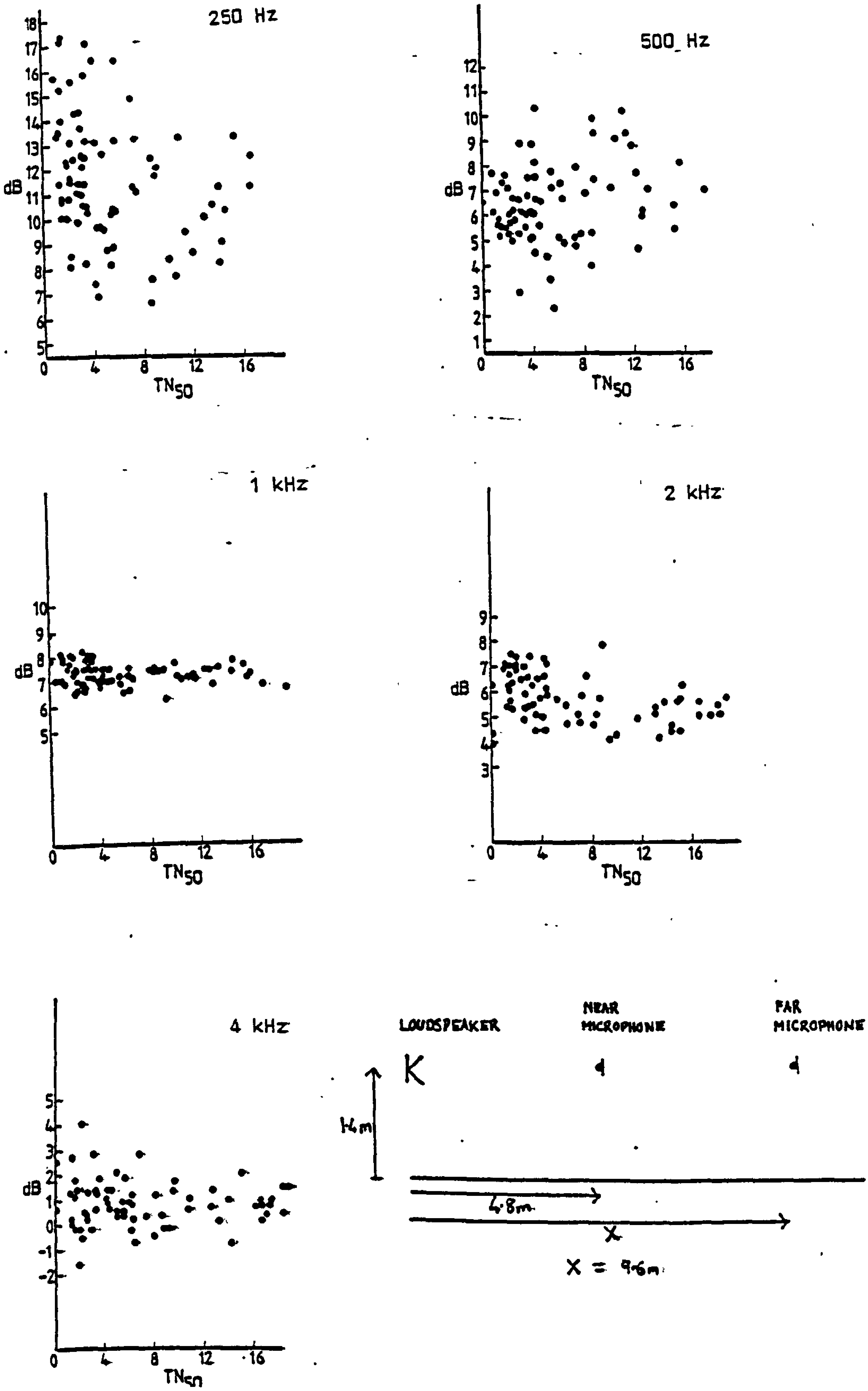

Fig 9.1a Full scale; Octave bands; unobstructed propagation.
Level difference vs TN_{50}; various frequencies.

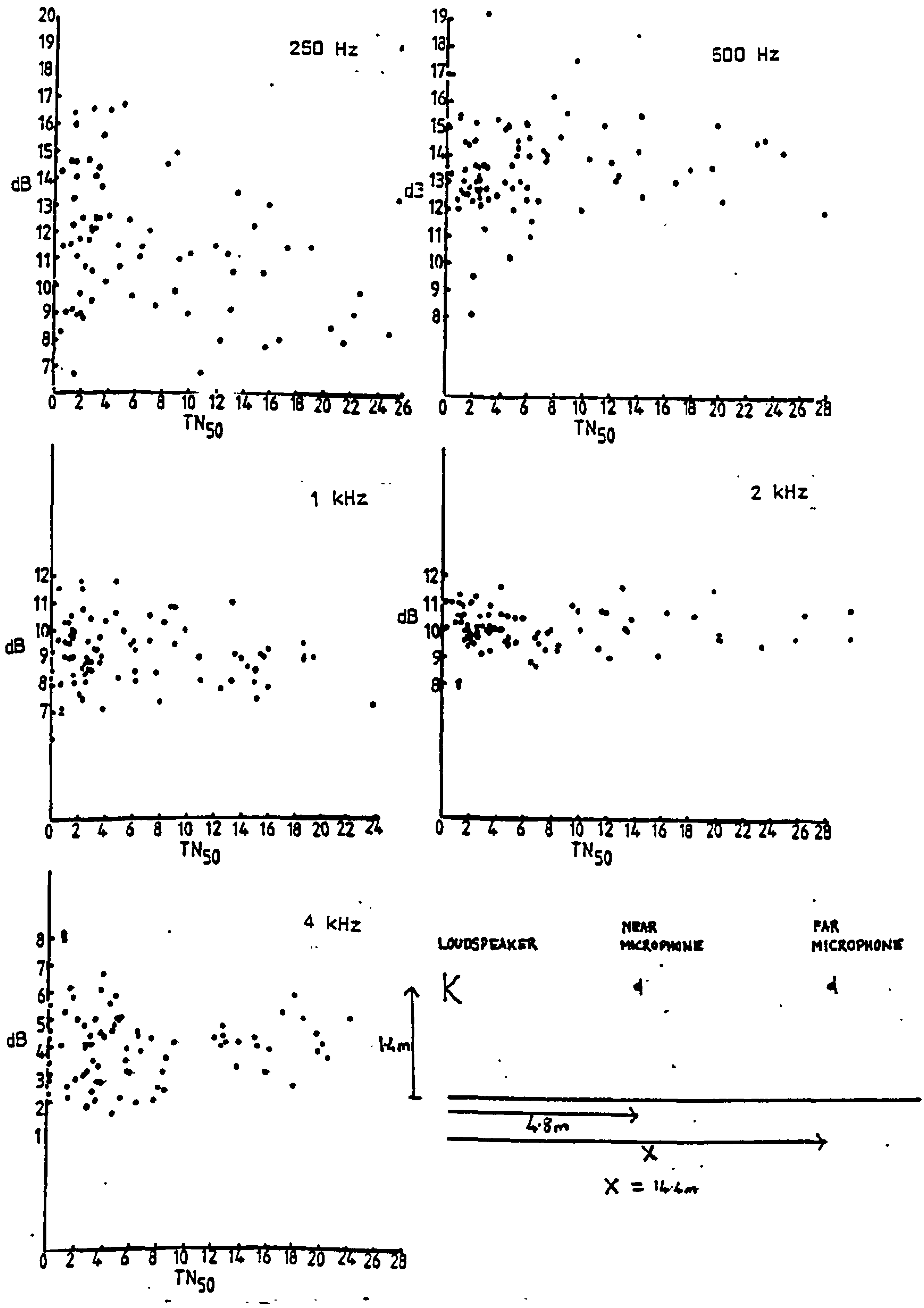

Fig 9.1b Full scale; Octave bands; unobstructed propagation.
Level difference vs TN_{50}; various frequencies.

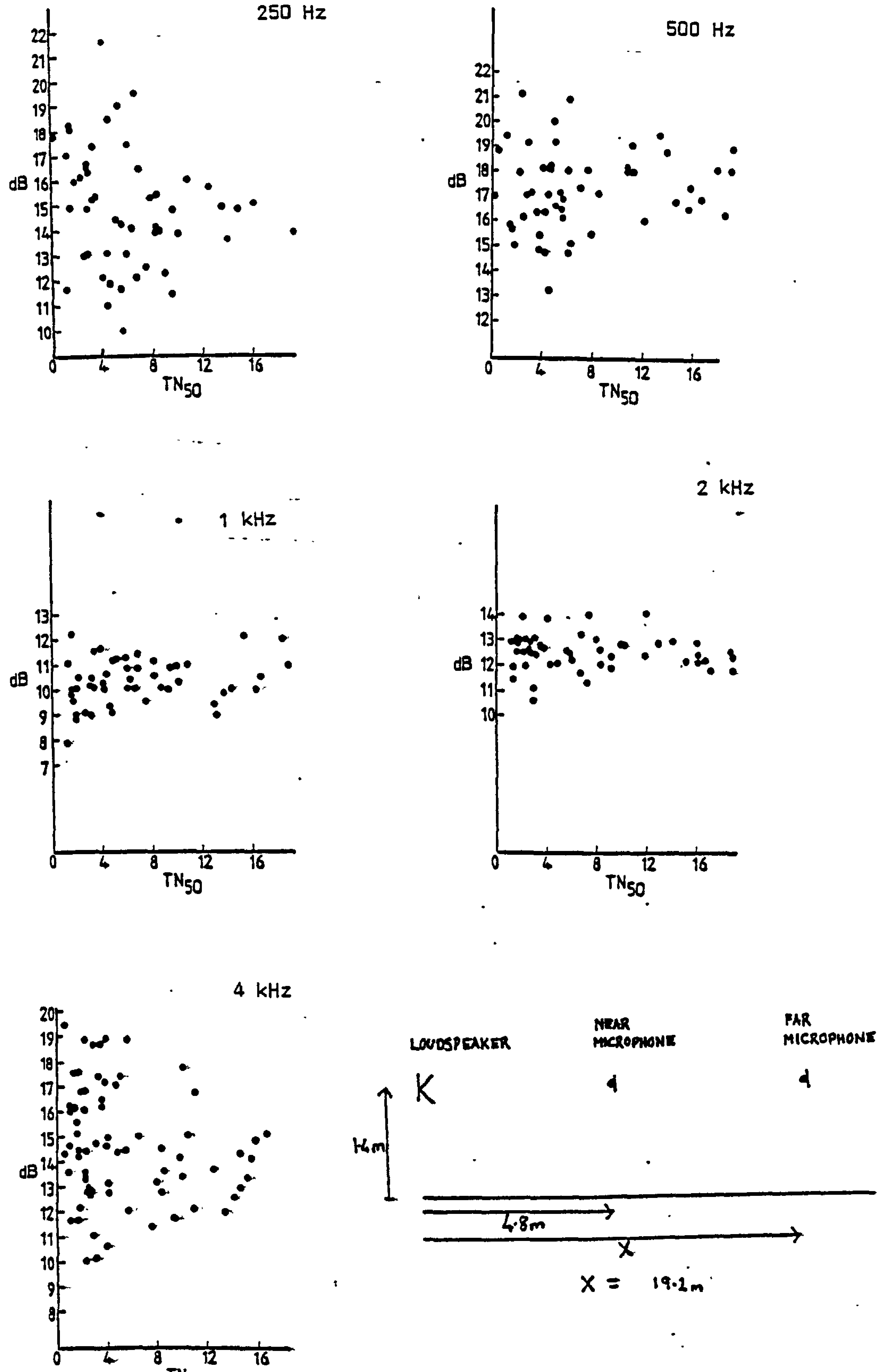

Fig 9.1c Full scale; Octave bands; unobstructed propagation.
Level difference vs TN_{50}; various frequencies.

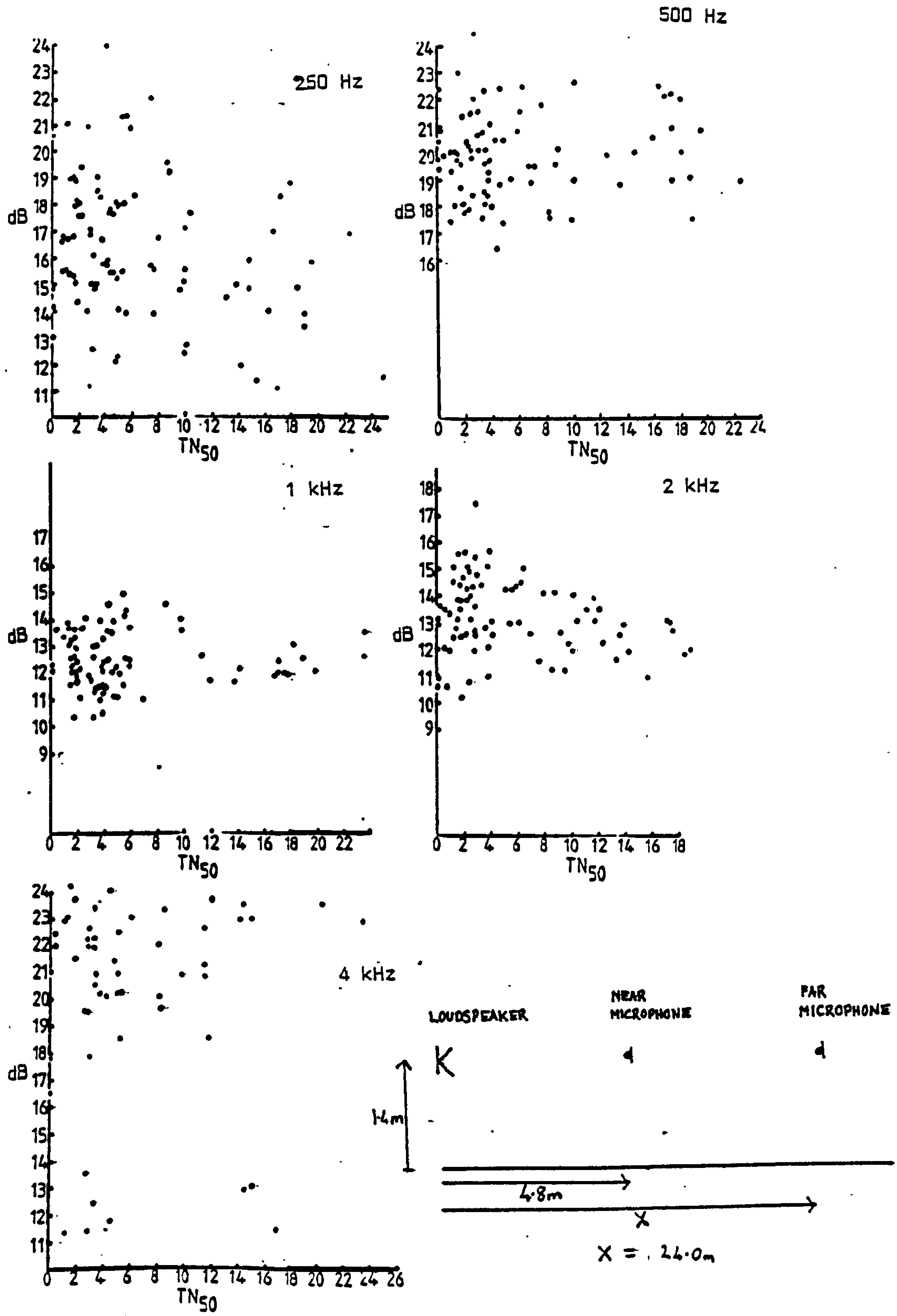

Fig 9.1d Full scale; Octave bands; unobstructed propagation. Level difference vs TN_{50}; various frequencies.

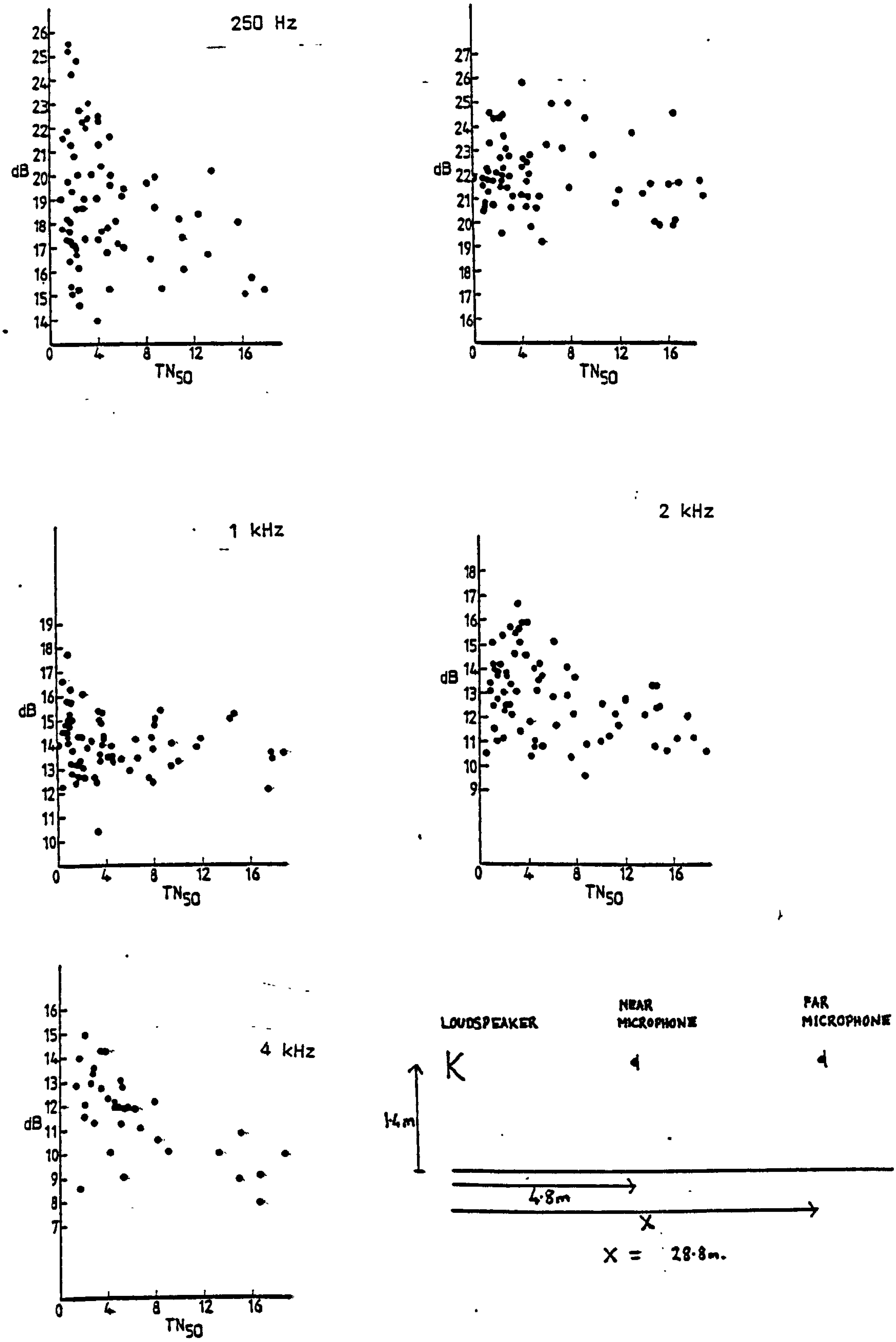

Fig 9.1e Full scale; Octave bands; unobstructed propagation.
Level difference vs TN_{50}; various frequencies.

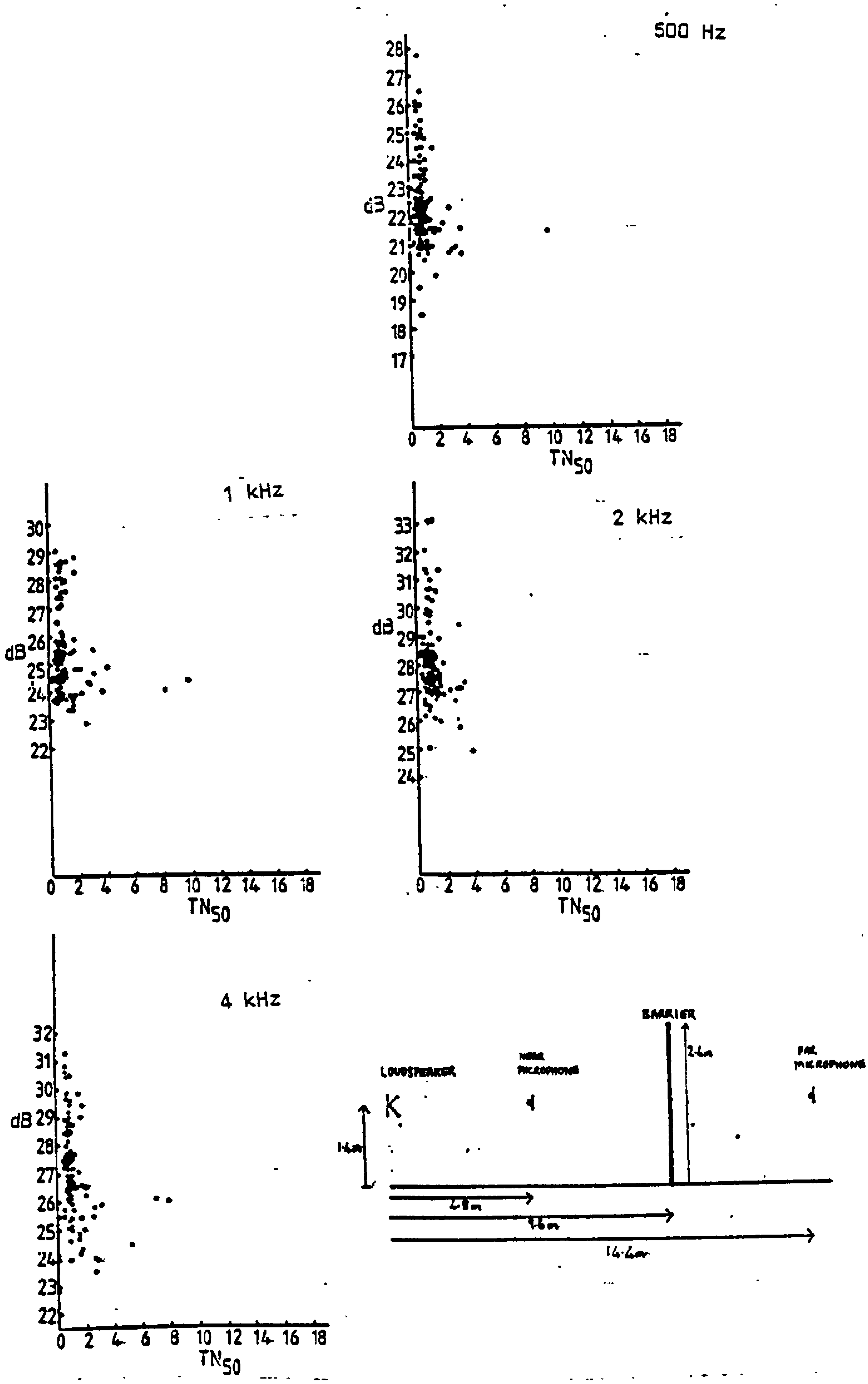

Fig 9.2.1b Full scale; Octave bands; barrier present (source and receivers all above ground).

Level difference vs TN_{50}; various frequencies.

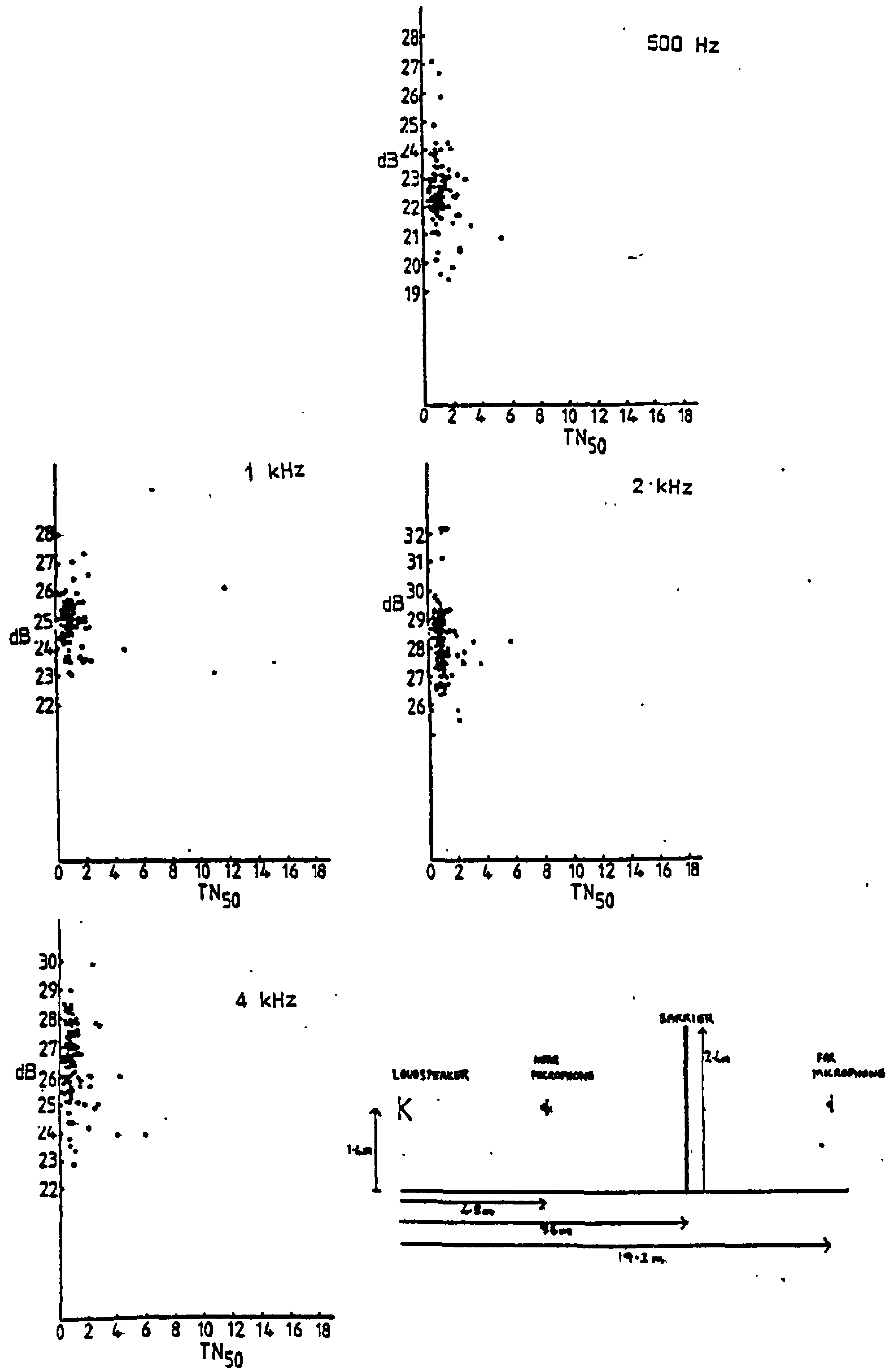

Fig 9.2.1c Full scale; Octave bands; barrier present (source and receivers all above ground).

Level difference vs TN_{50}; various frequencies.

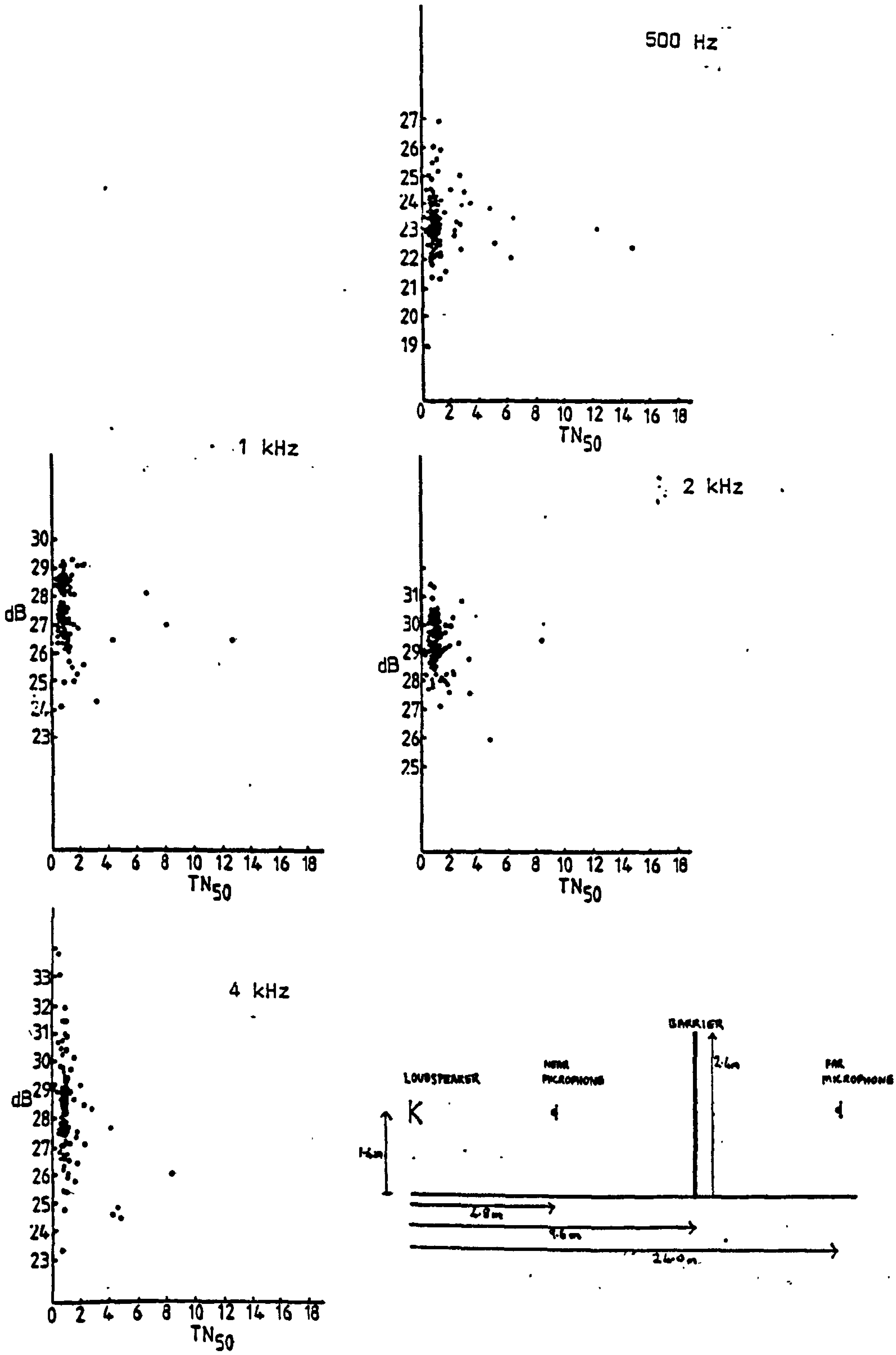

Fig 9.2.1d Full scale; Octave bands; barrier present (source and receivers all above ground).

Level difference vs TN_{50}; various frequencies.

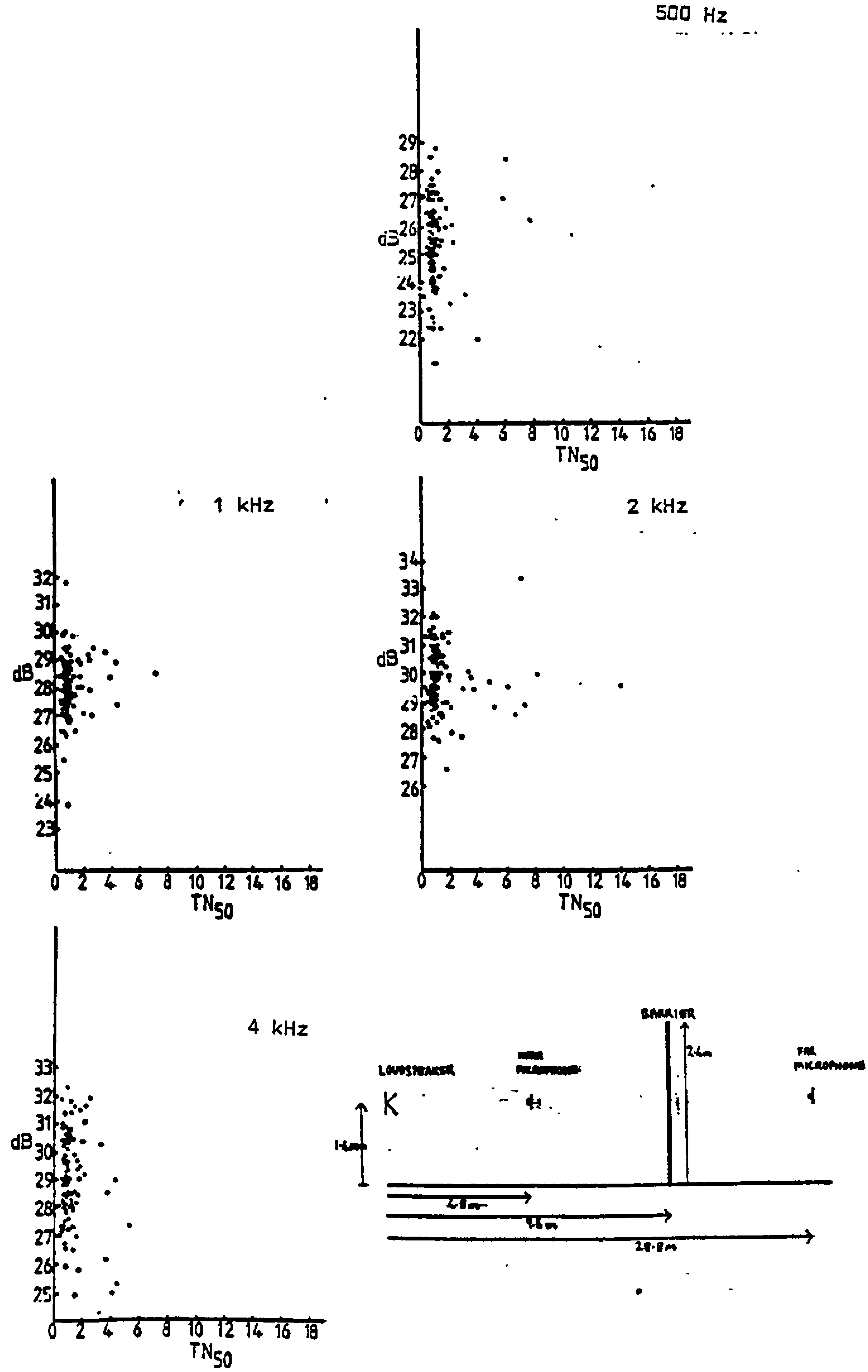

Fig 9.2.1e Full scale; Octave bands; barrier present (source and receivers all above ground).

Level difference vs TN_{50}; various frequencies.

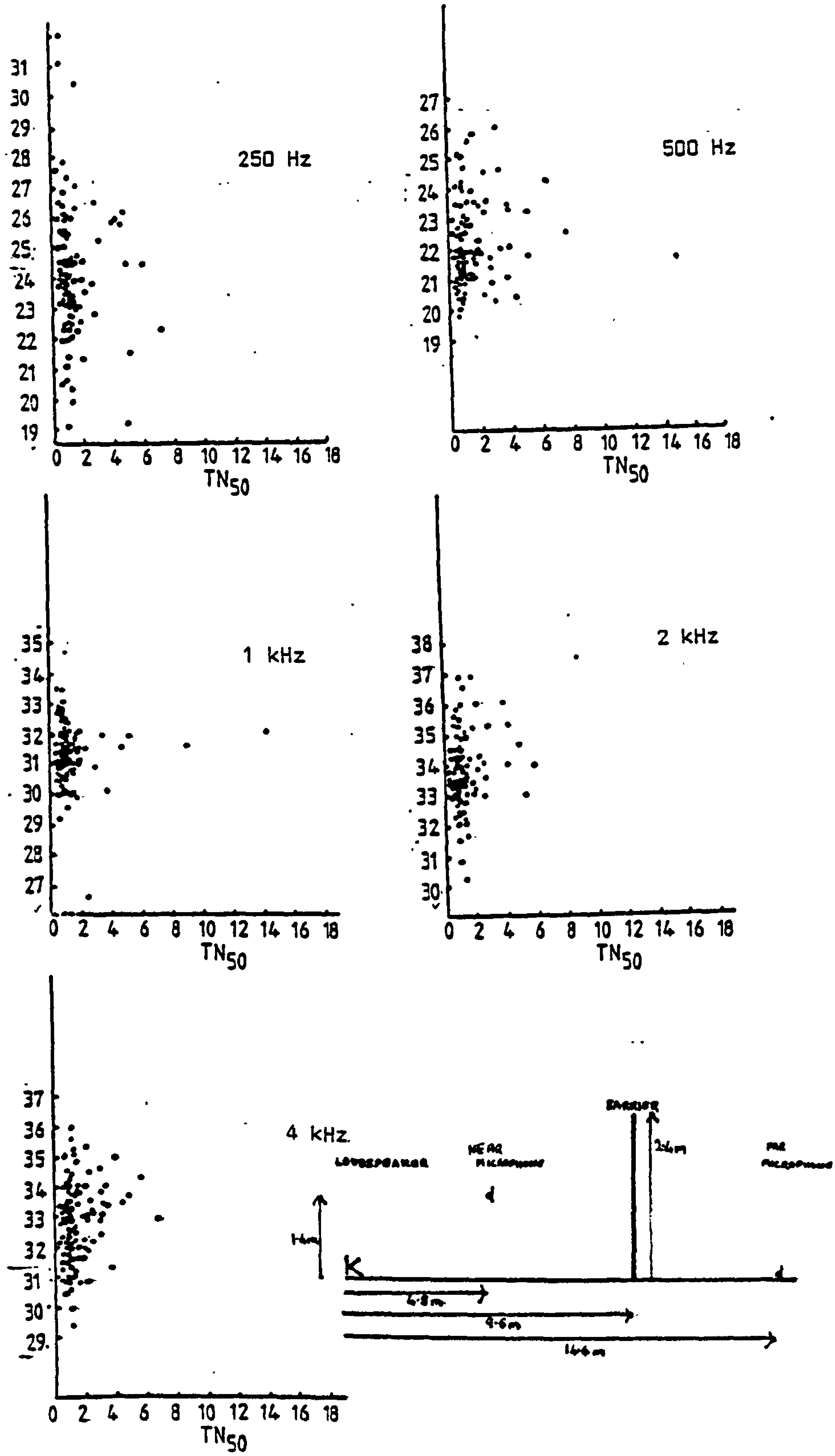

Fig 9.2.2b Full scale; Octave bands; barrier present (source and far receiver on the ground)

Level difference vs TN_{50}; various frequencies.

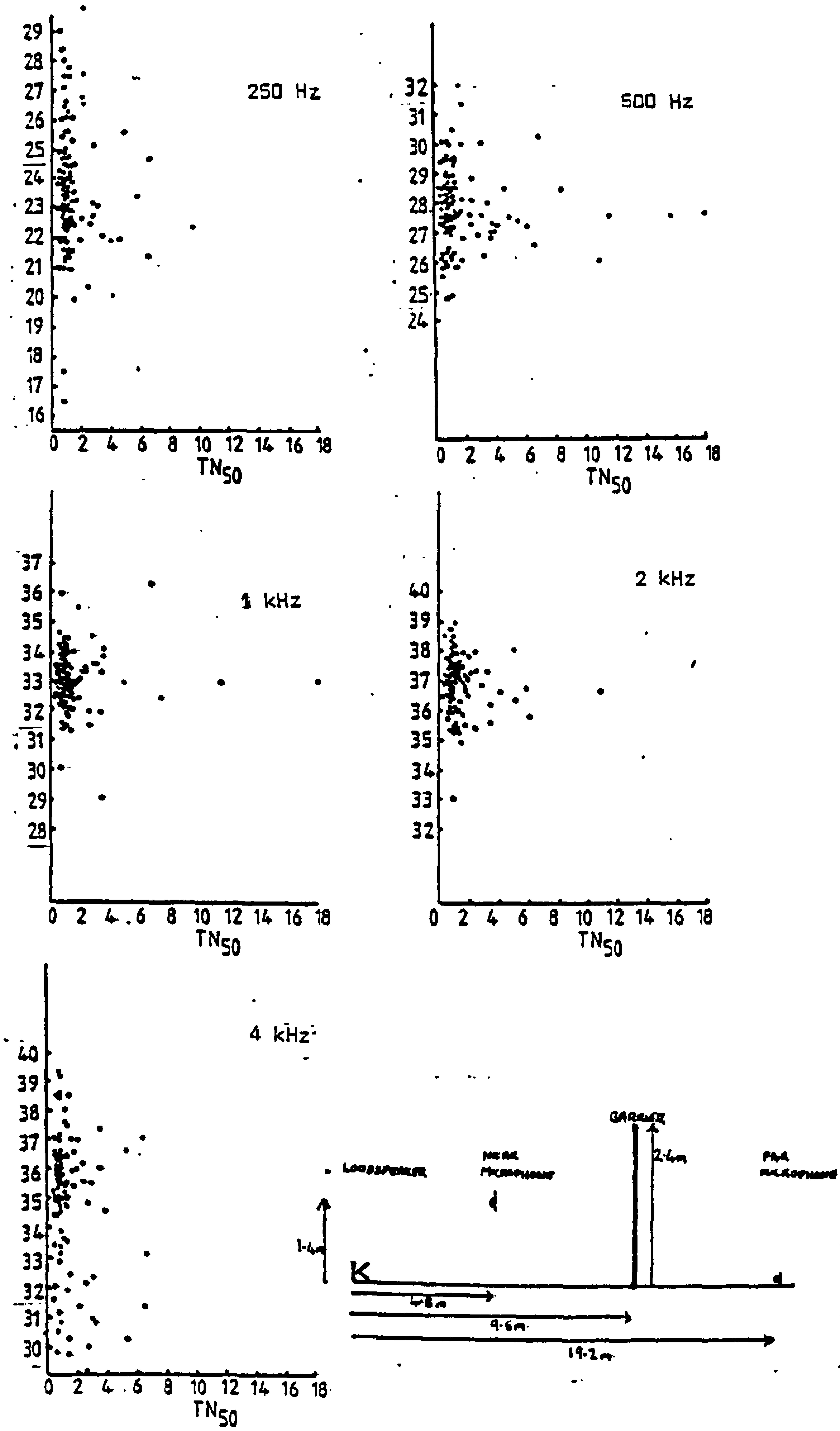

Fig 9.2.2c Full scale; Octave bands; Barrier present (source and far receiver on the ground).

Level difference vs TN_{50}; various frequencies.

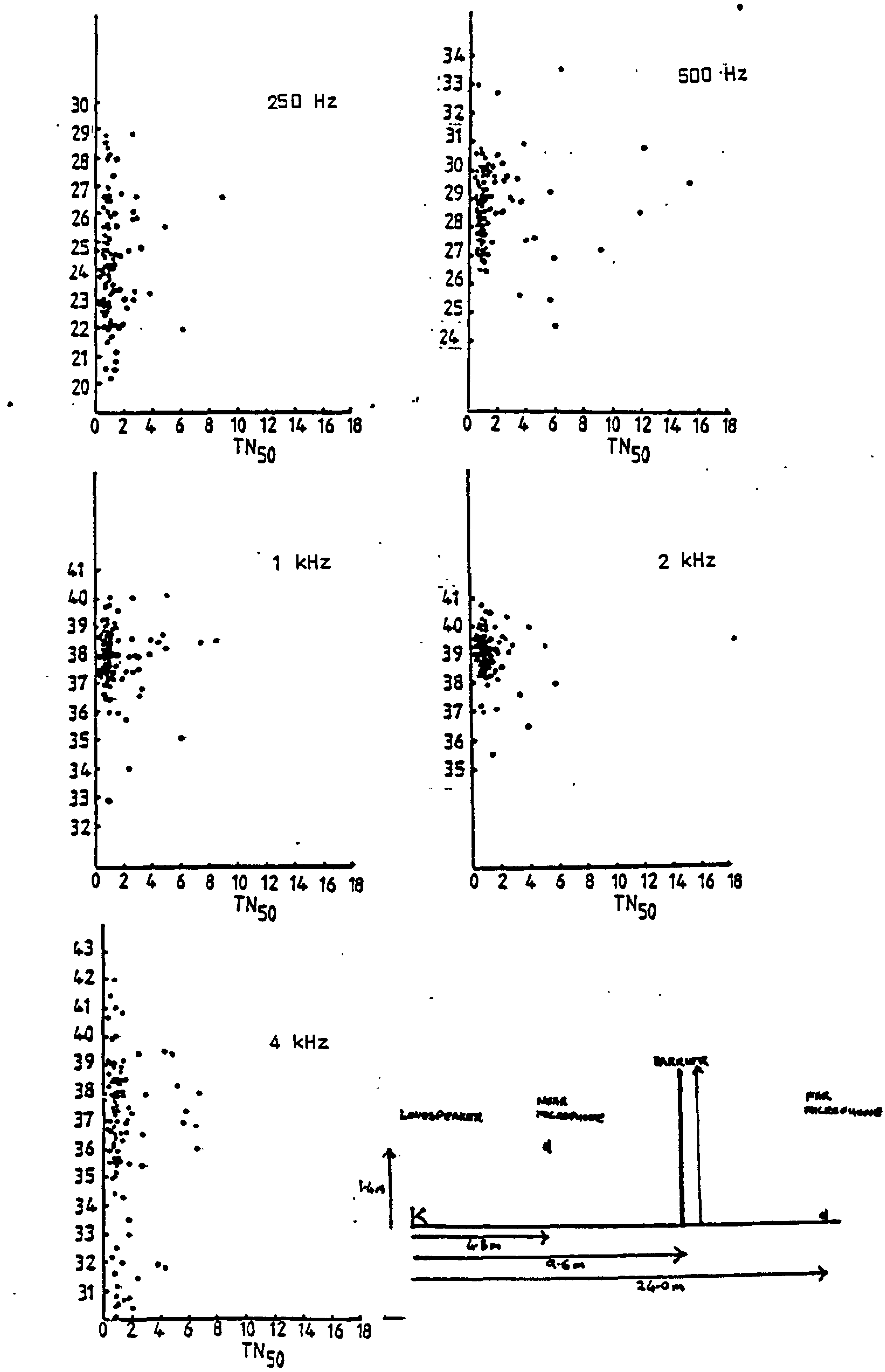

Fig 9.2.2d Full scale; Octave bands; barrier present (source and far receiver on the ground).

Level difference vs TN_{50}; various frequencies.

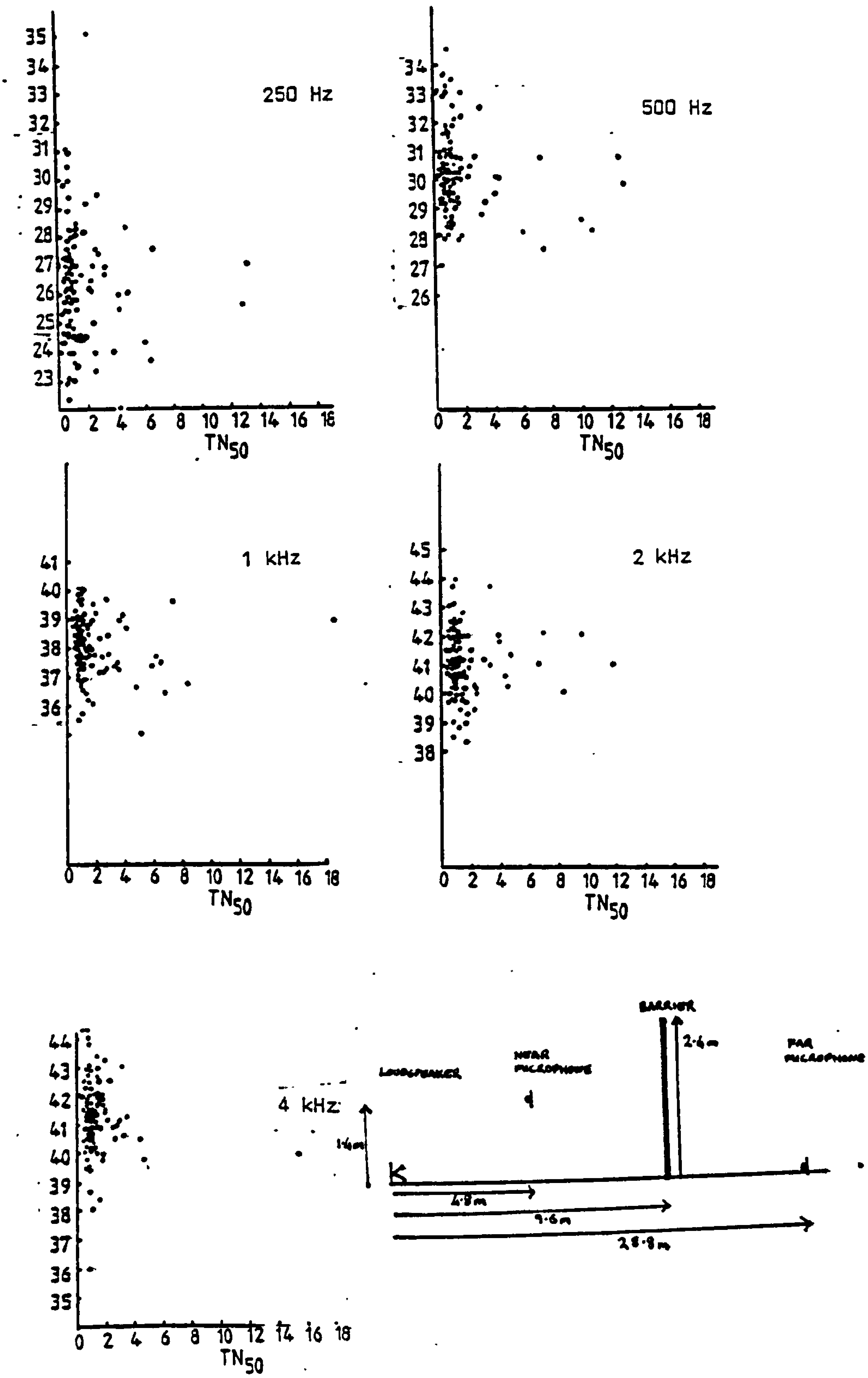

Fig 9.2.2e Full scale; Octave bands; barrier present (source and far receiver on the ground).

Level difference vs TN_{50}; various frequencies.

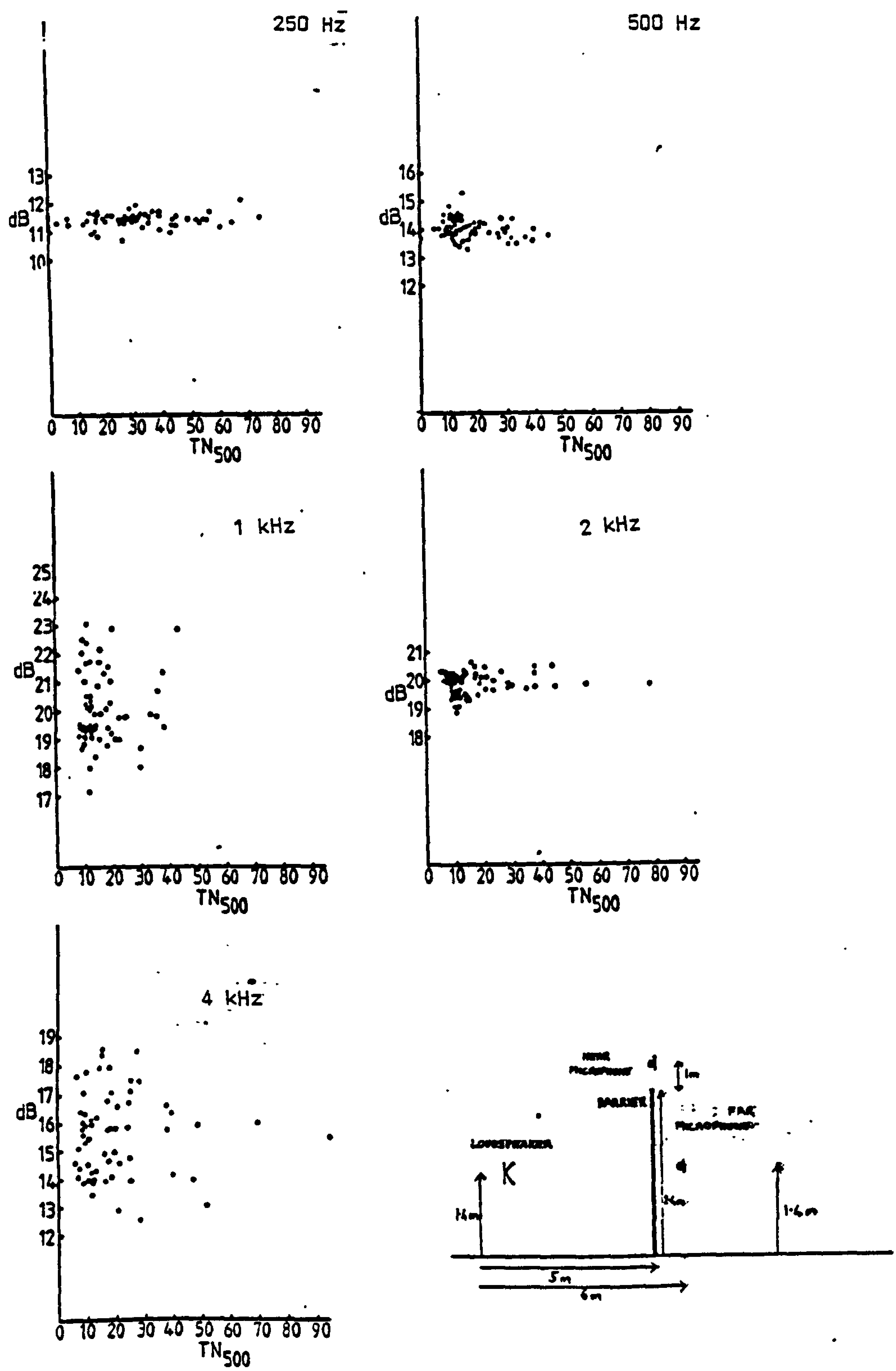

Fig 9.3.a Full scale; pure tones; barrier present;
Level difference vs TN_{500}; various frequencies.

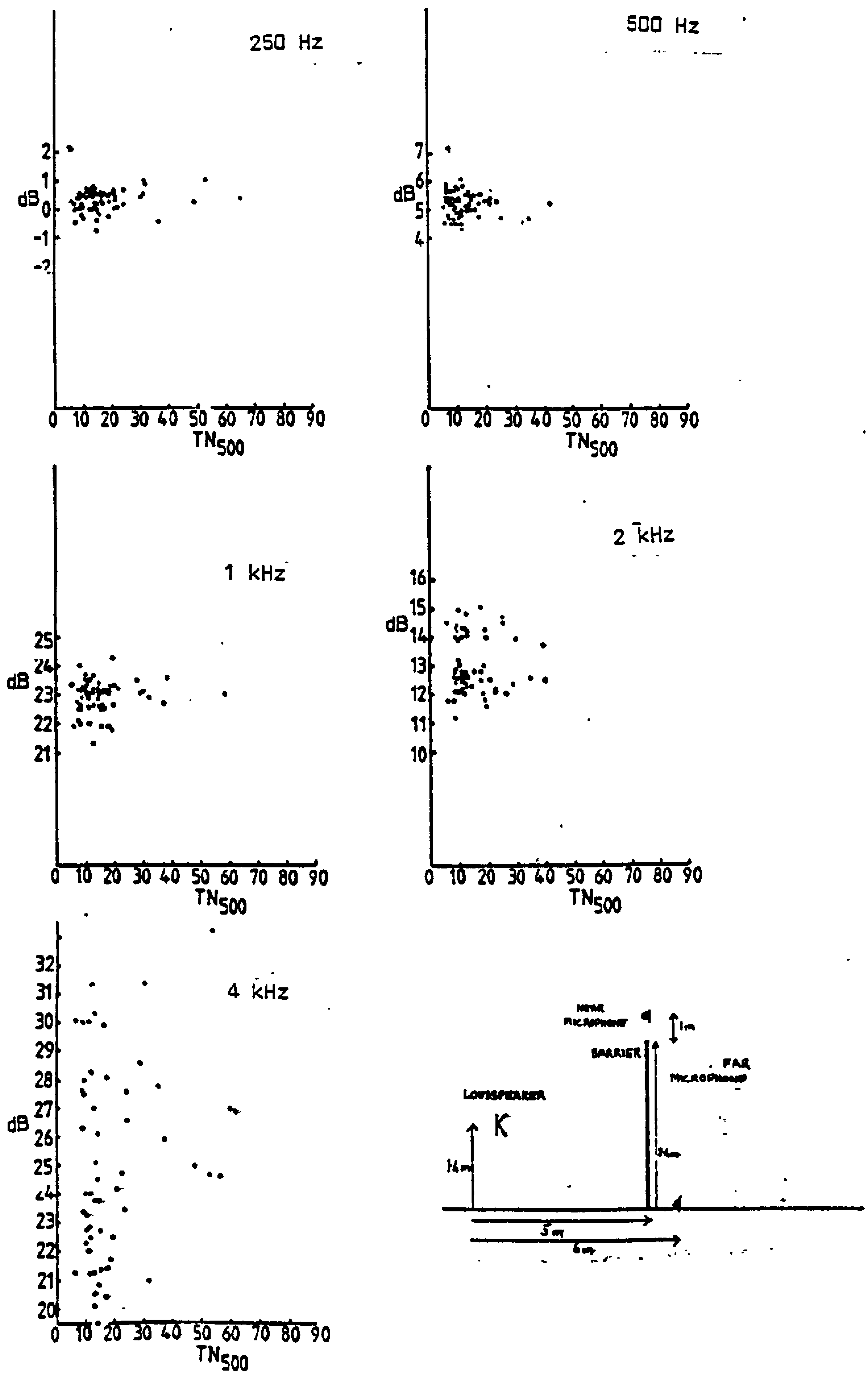

Fig 9.3 b Full scale; pure tones; barrier present;
Level difference vs TN_{500}; various frequencies.

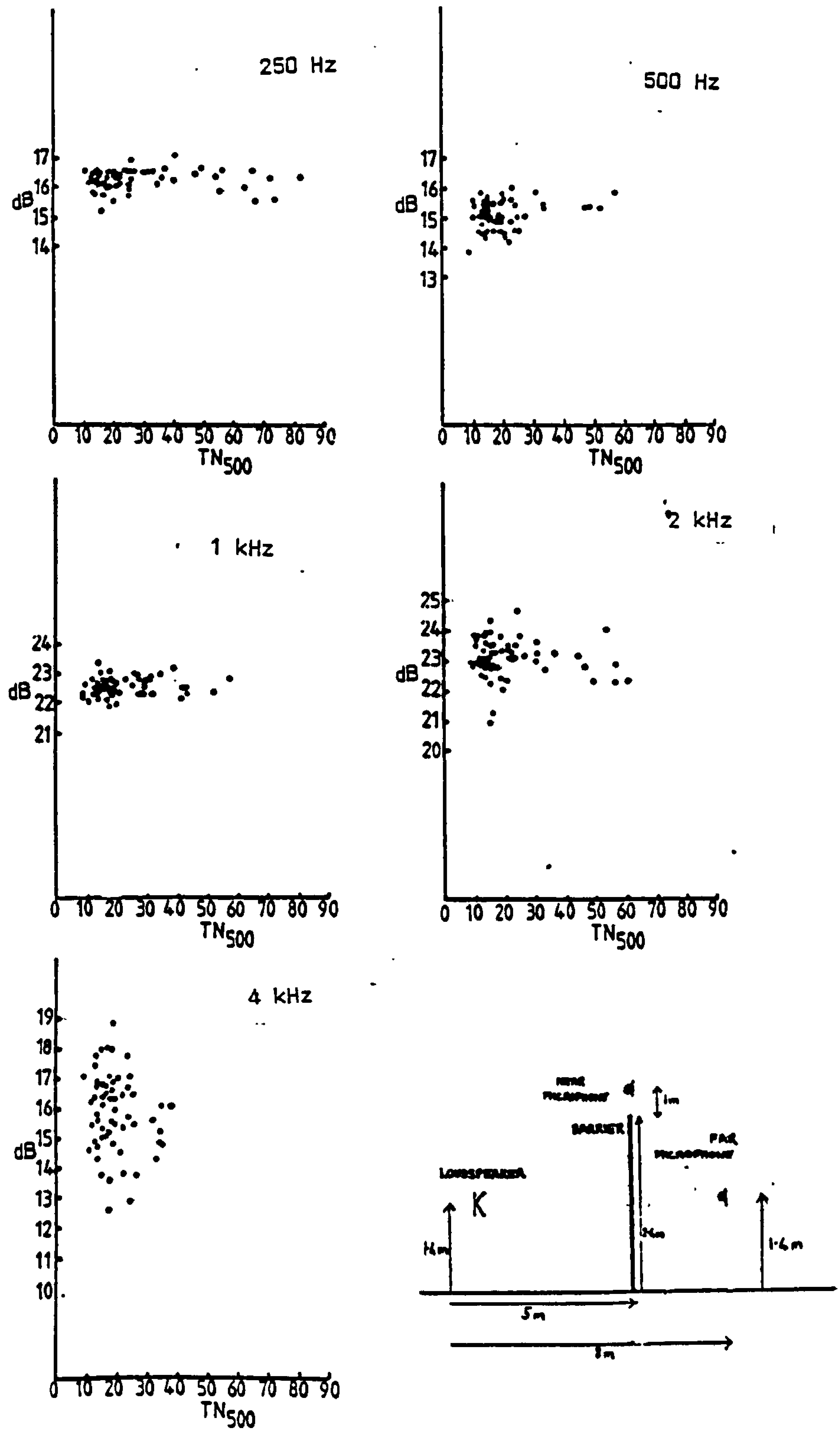

Fig 9.3 c Full scale; pure tones; barrier present;
Level difference vs TN_{500}; various frequencies.

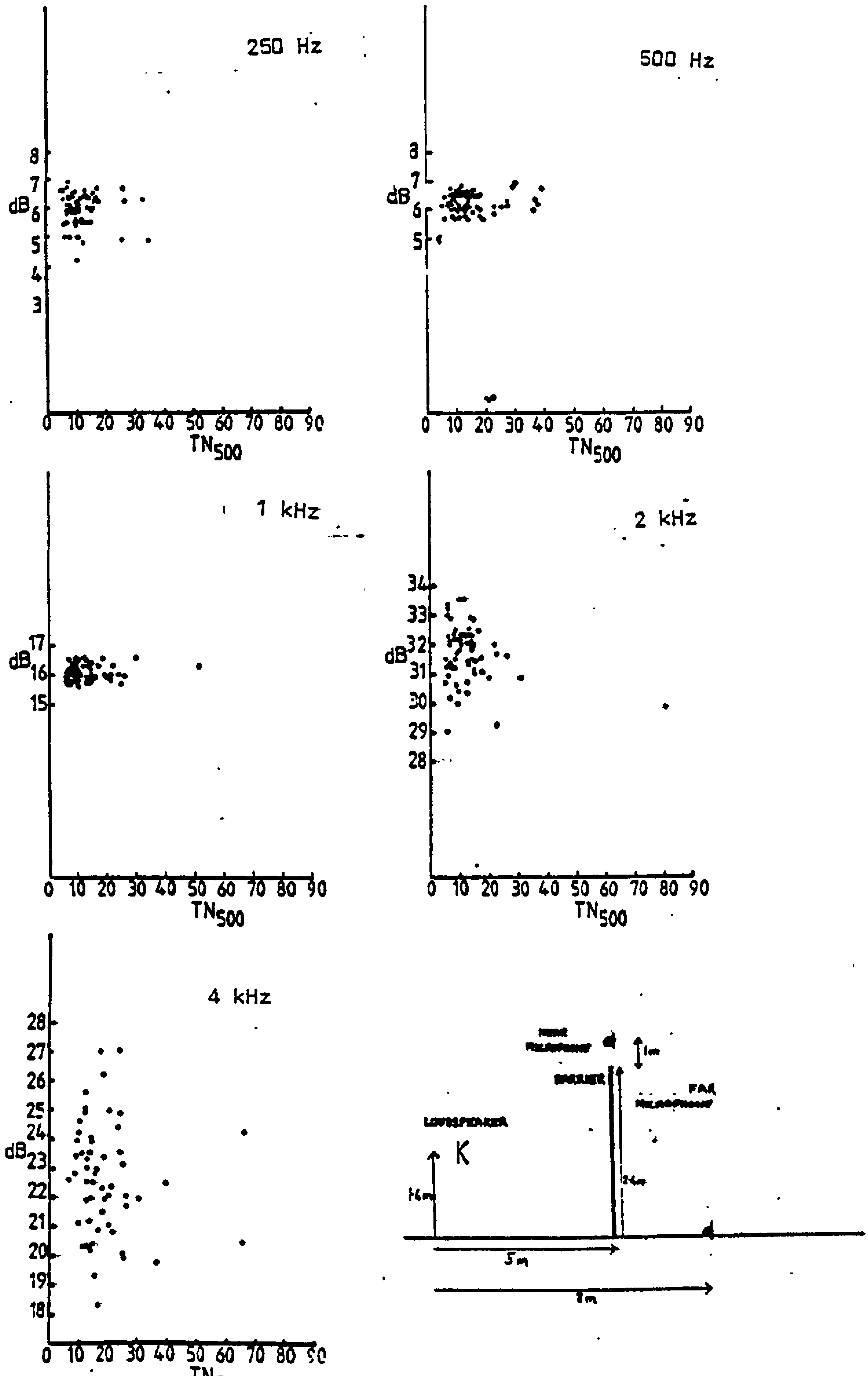

Fig 9.3 d Full scale; pure tones; barrier present;

Level difference vs TN_{500}; various frequencies.

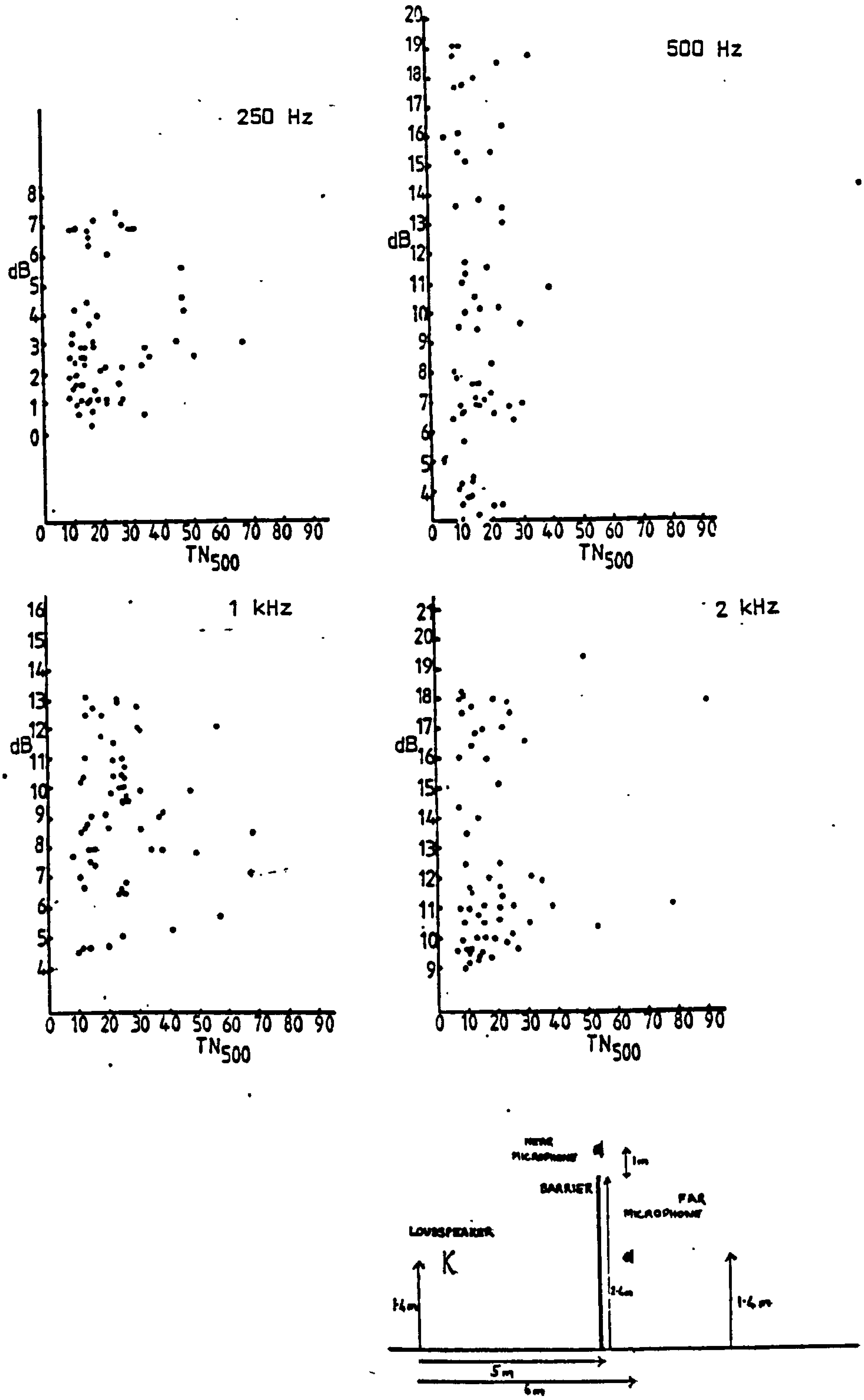

Fig 9.4 a Full scale; random pure tones; barrier present; Level difference vs TN_{500}; various frequencies.

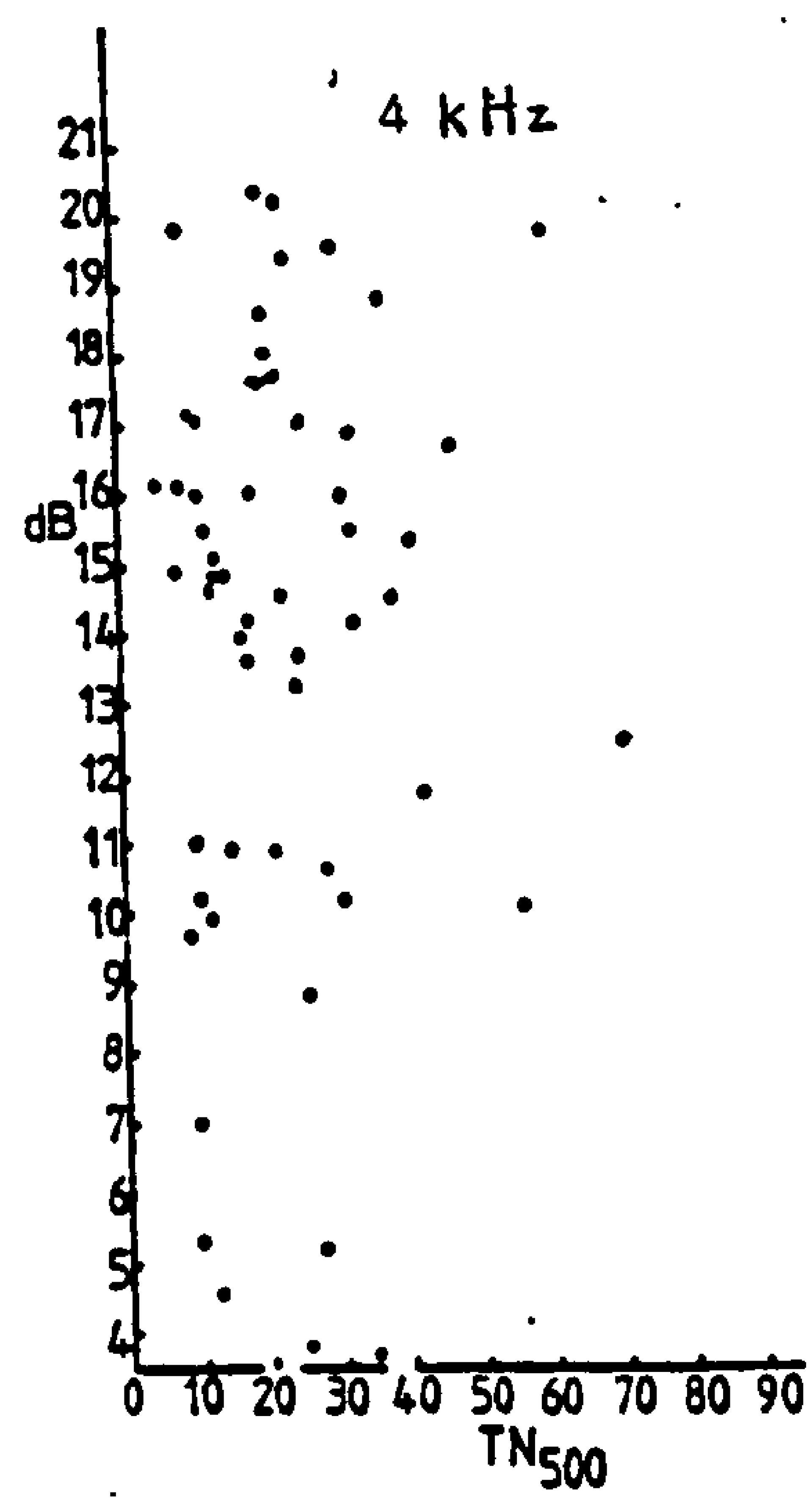

Fig 9.4 a Continued

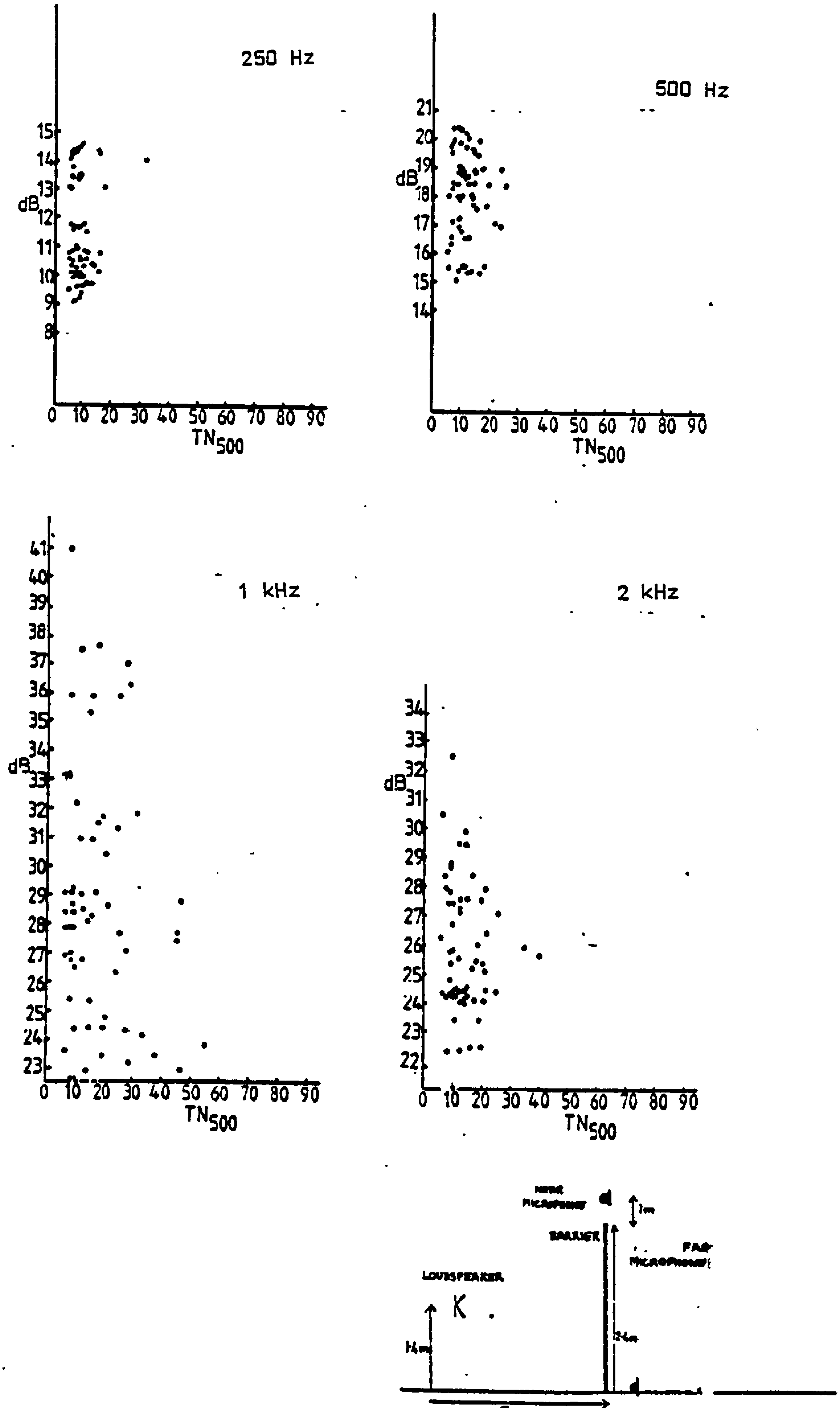

Fig 9.4 b Full scale; random pure tones; barrier present; Level difference vs TN_{500}; various frequencies.

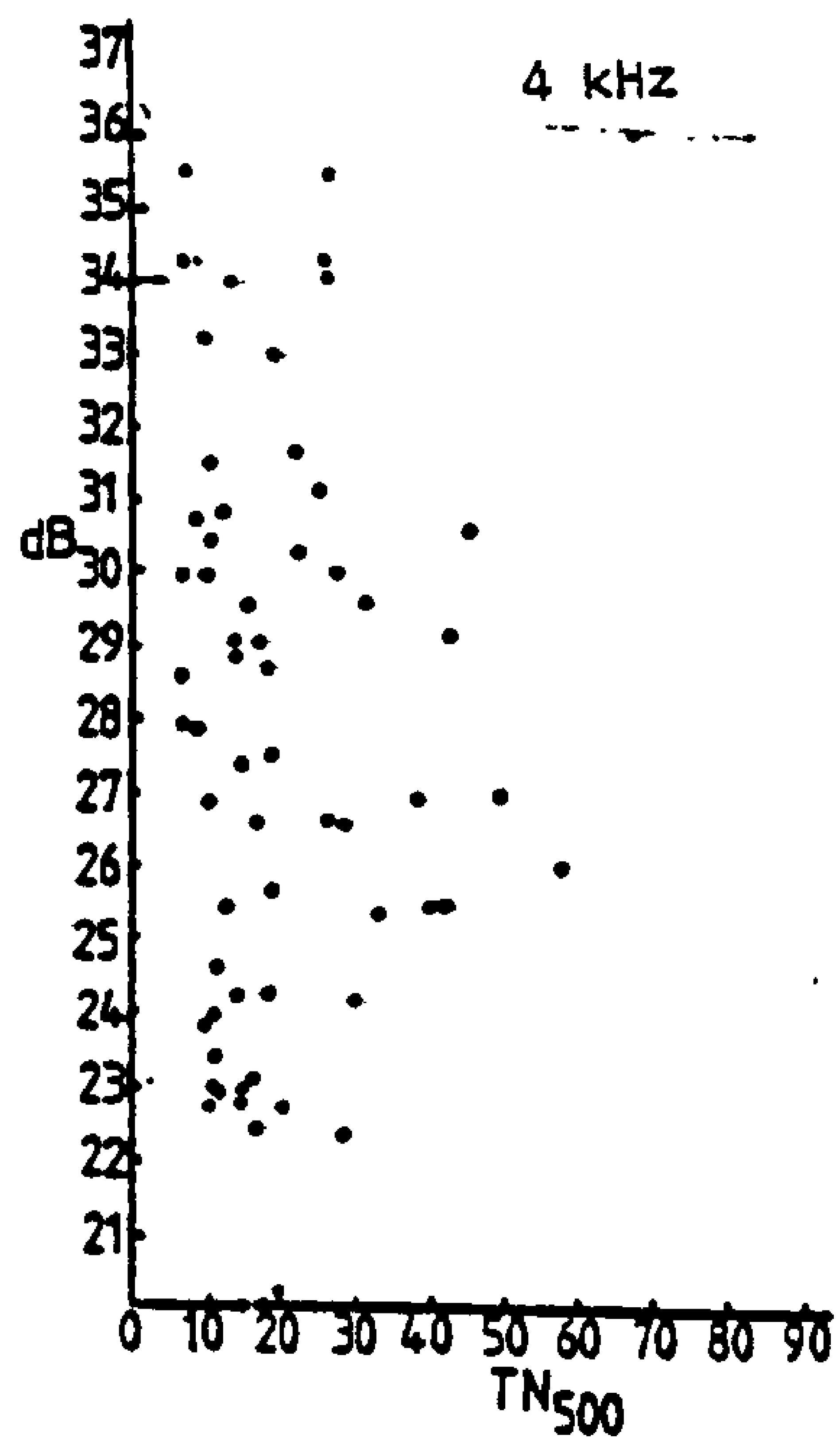

Fig 9.4 b Continued

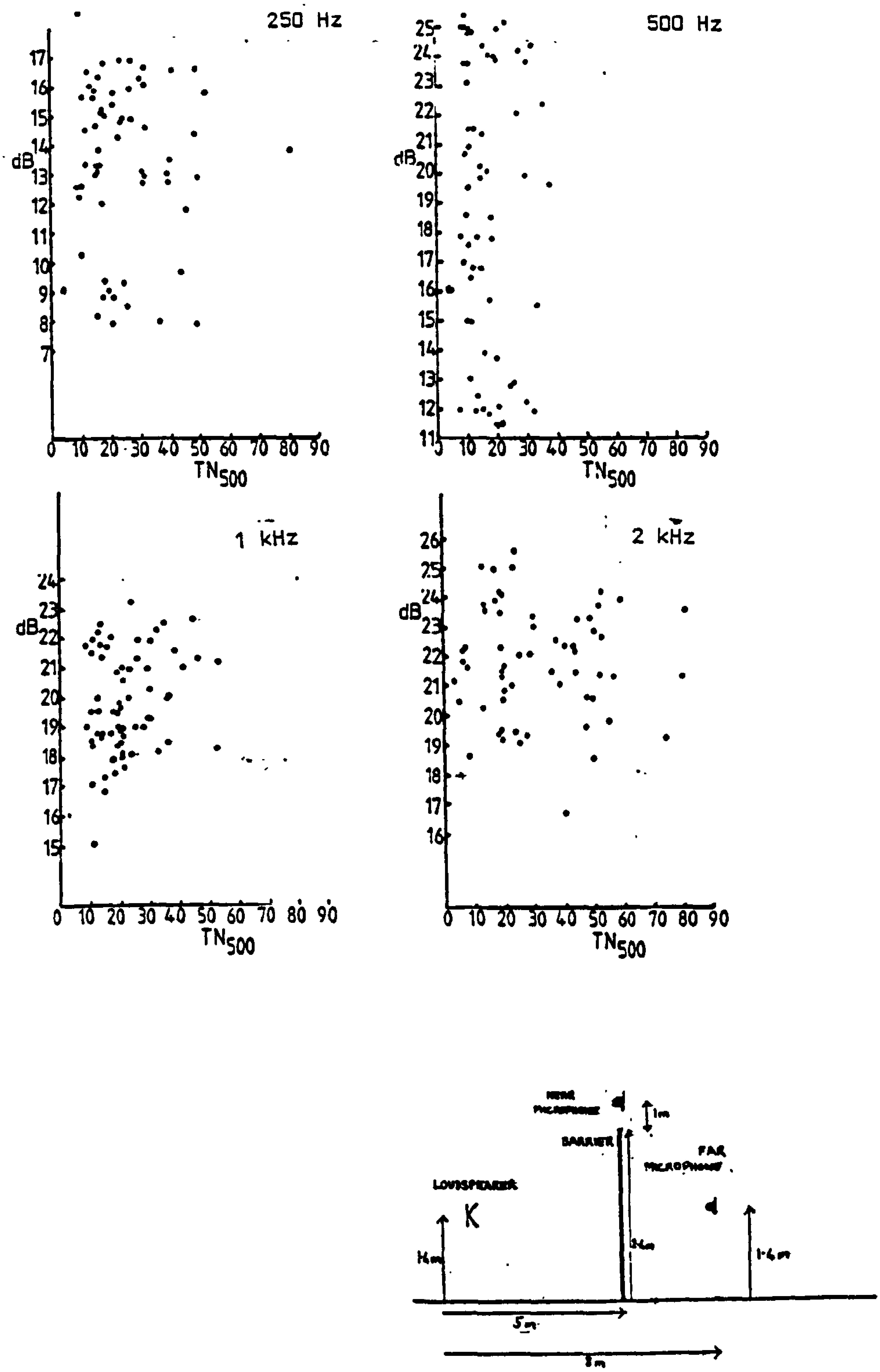

Fig 9.4 c Full scale; random pure tones; barrier present; . Level difference vs TN_{500}; various frequencies.

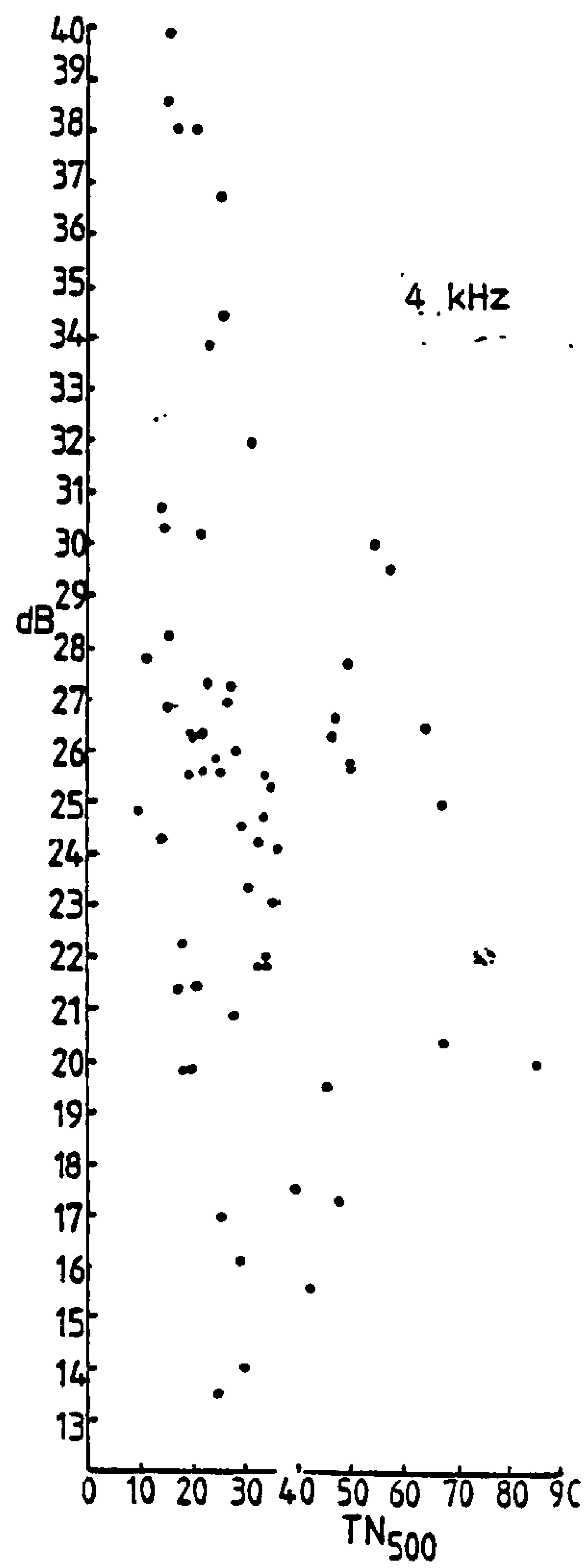

Fig 9.4 c Continued

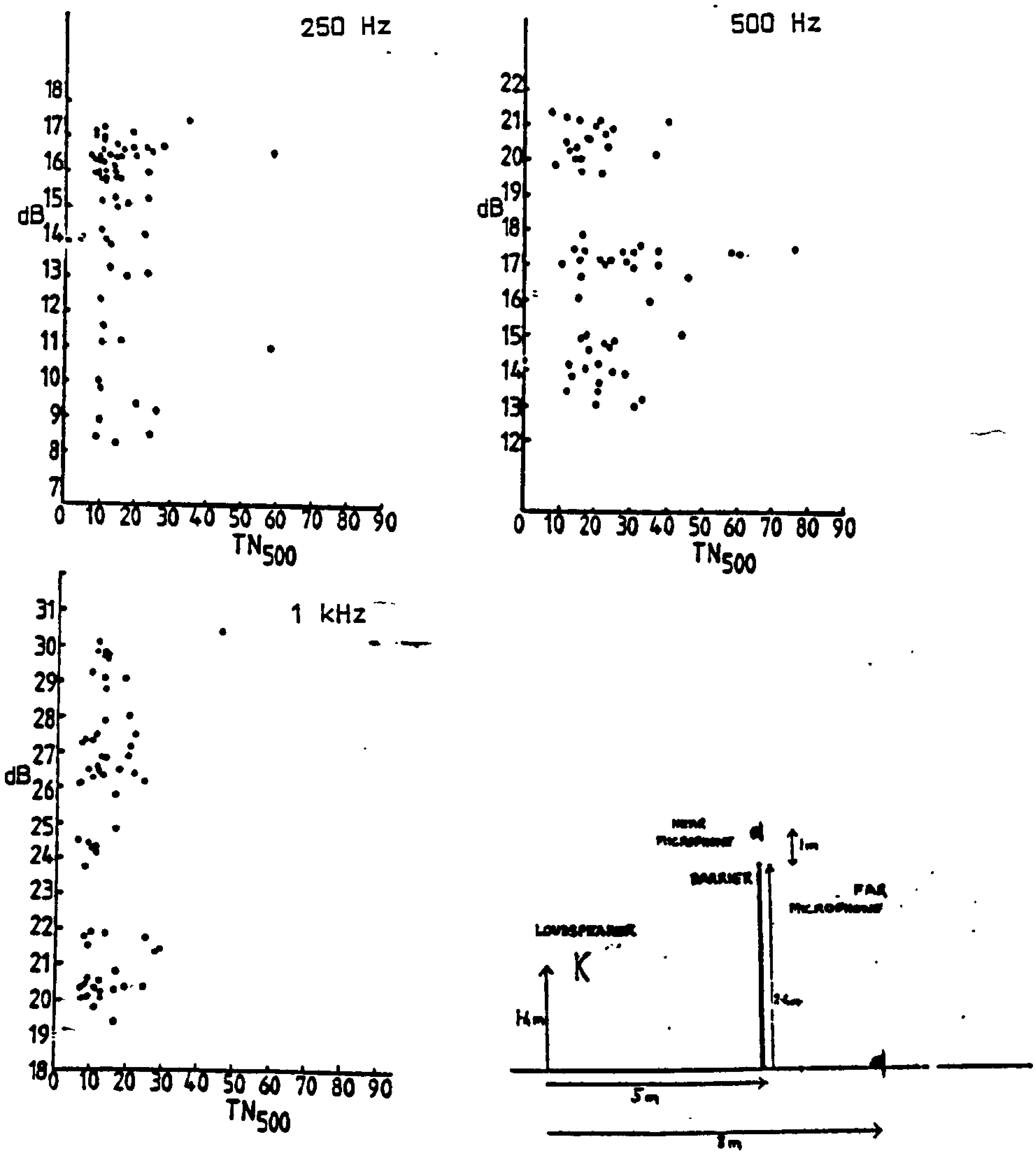

Fig 9.4 d Full scale; random pure tones; barrier present; Level difference vs TN_{500}; various frequencies.

CHAPTER 10

The Results of Model Scale Experiments

Because of similarities of source/receiver geometry and signal type the figures showing the results of model scale experiments are numbered 10.2a to 10.2d and 10.3a to 10.3d to ease cross-referencing.

It should be noted that the geometries of Figs 10.3a - d are 1/16 scaled versions of those in Figs 9.3a - d. Figs 10.2a - d are similar to 9.2.1a - d, however, the equivalence is not exact as in Figs 10.3 and 9.3.

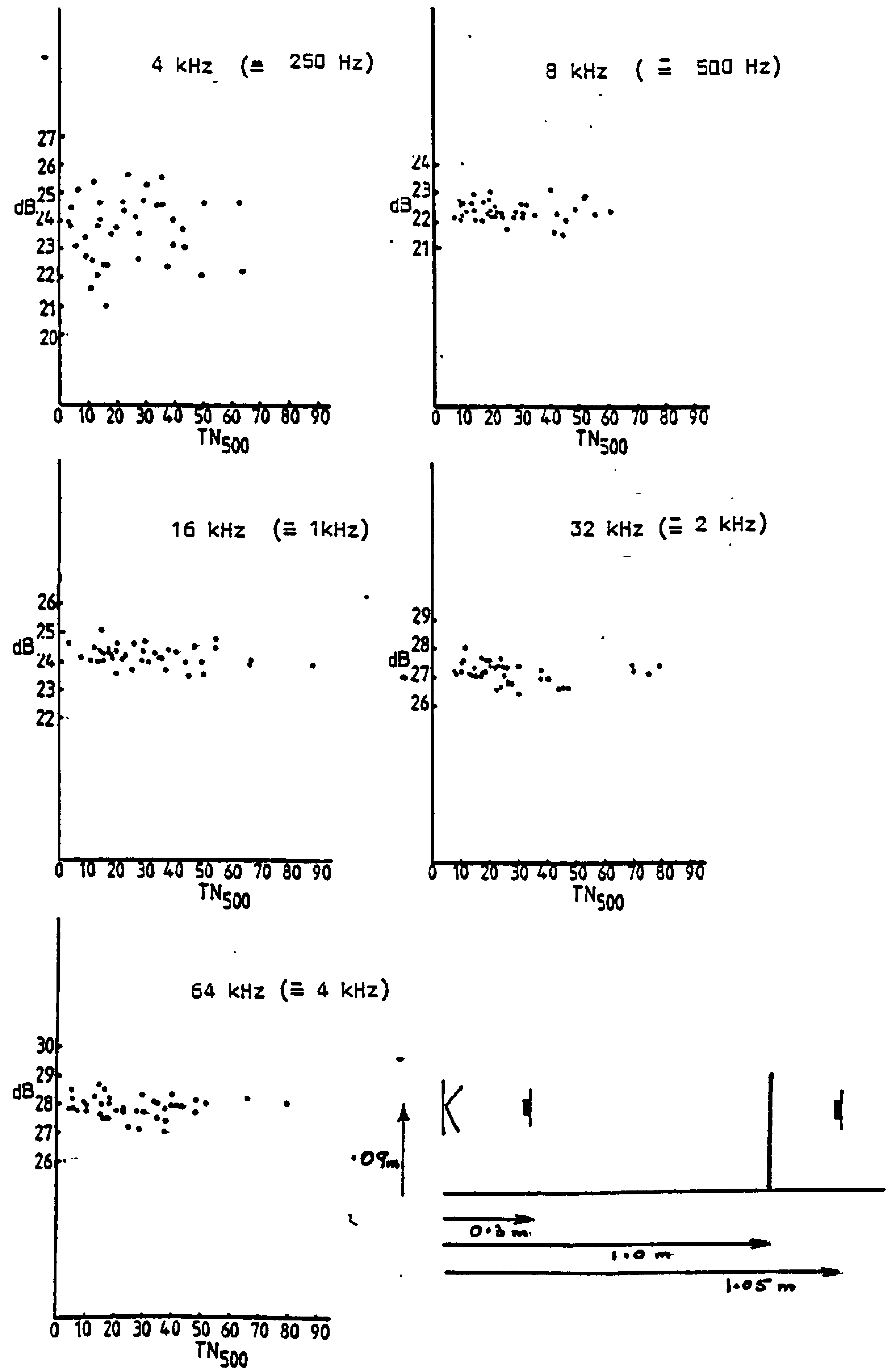

Fig 10.2 a Model scale; octave band noise; barrier present;

Level difference vs TN_{500}; various frequencies.

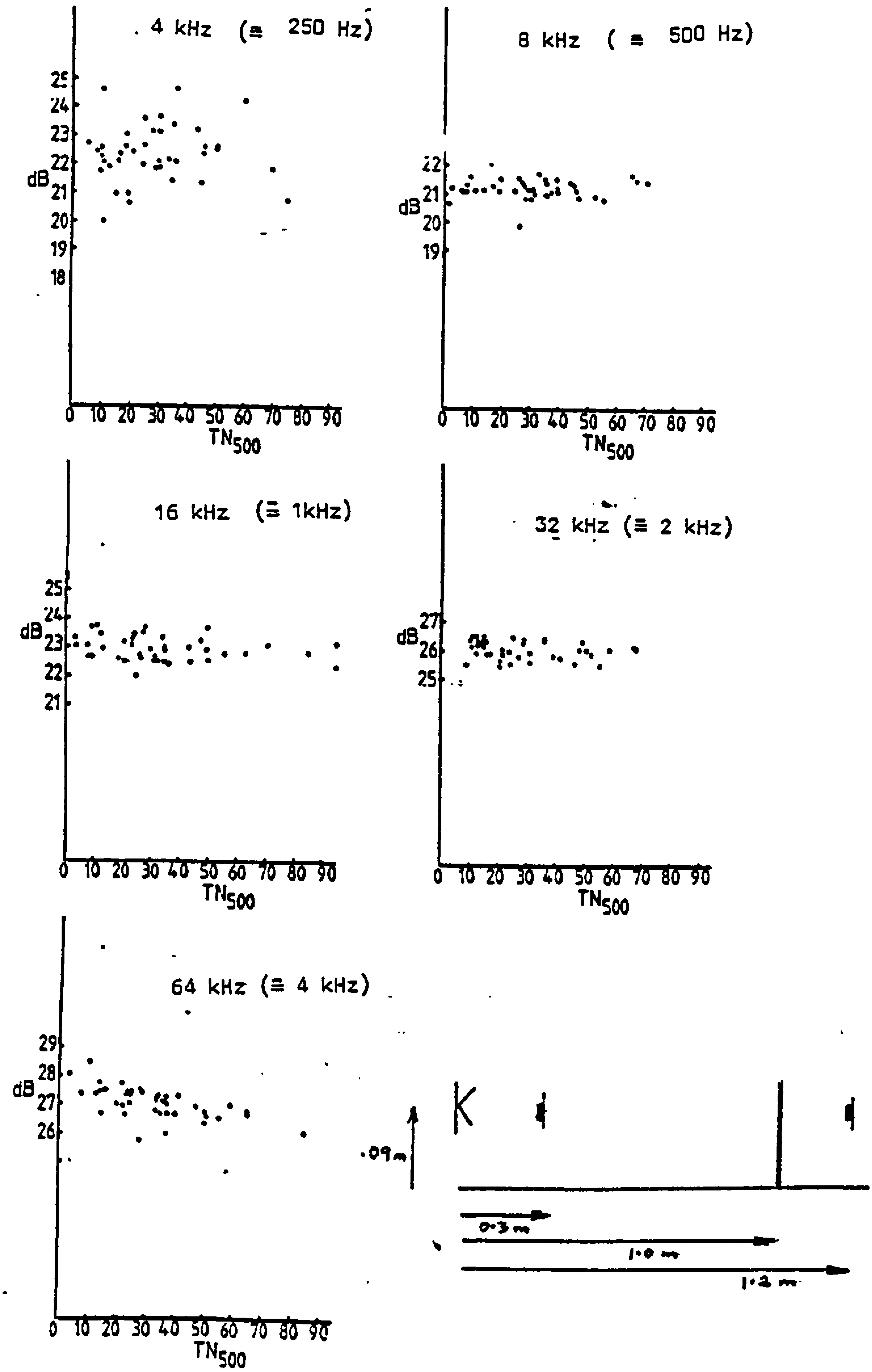

Fig 10.2 b Model scale; octave band noise; barrier present;
Level difference vs TN_{500}; various frequencies.

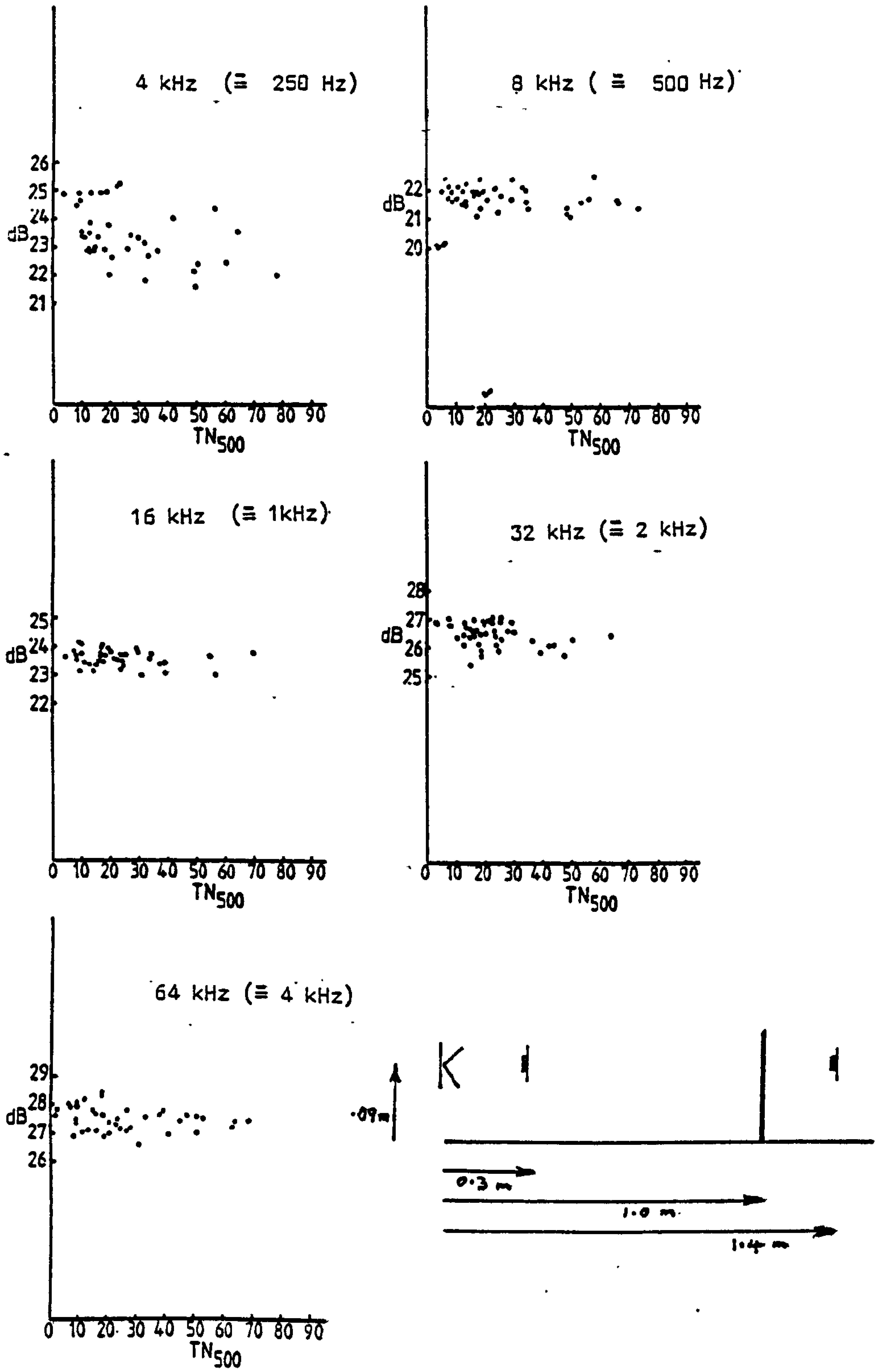

Fig 10.2.c Model scale; octave band noise; barrier present; Level difference vs TN_{500}; various frequencies

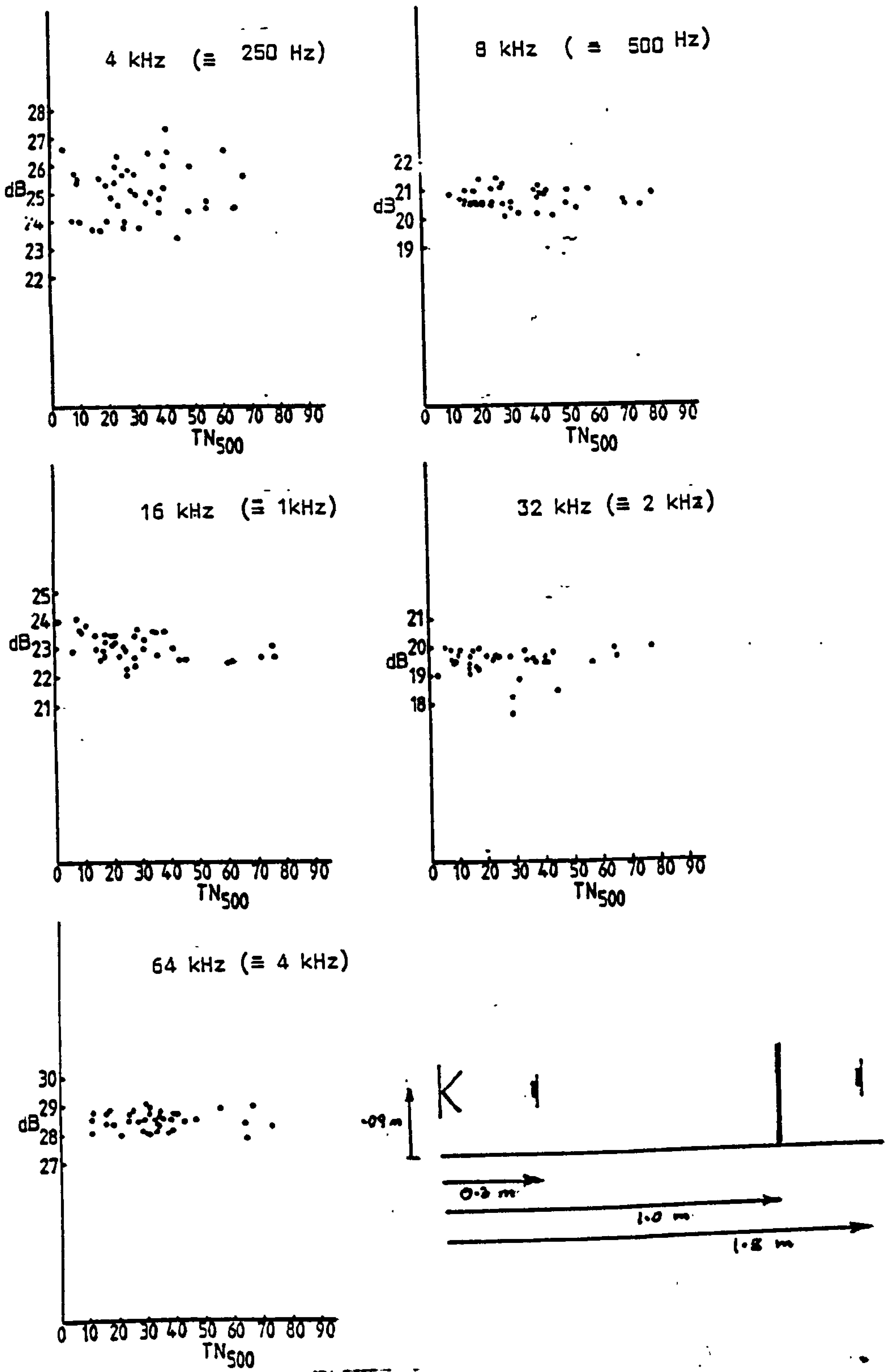

Fig 10.2 d Model scale; octave band noise; barrier present; Level difference vs TN_{500}; various frequencies.

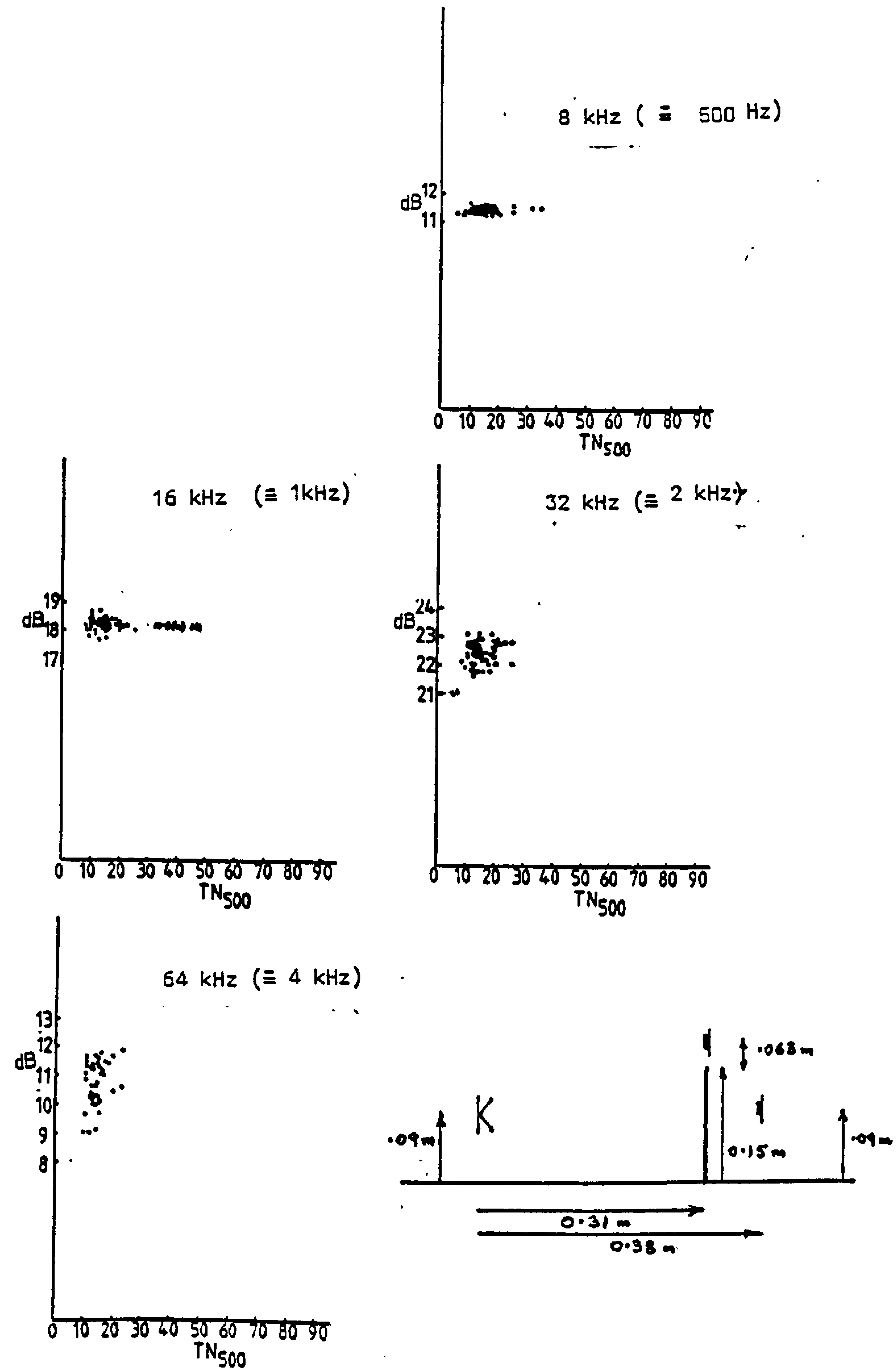

Fig. 10.3 a   Model scale; pure tones; barrier present;
Level difference vs TN_{500}; various frequencies.

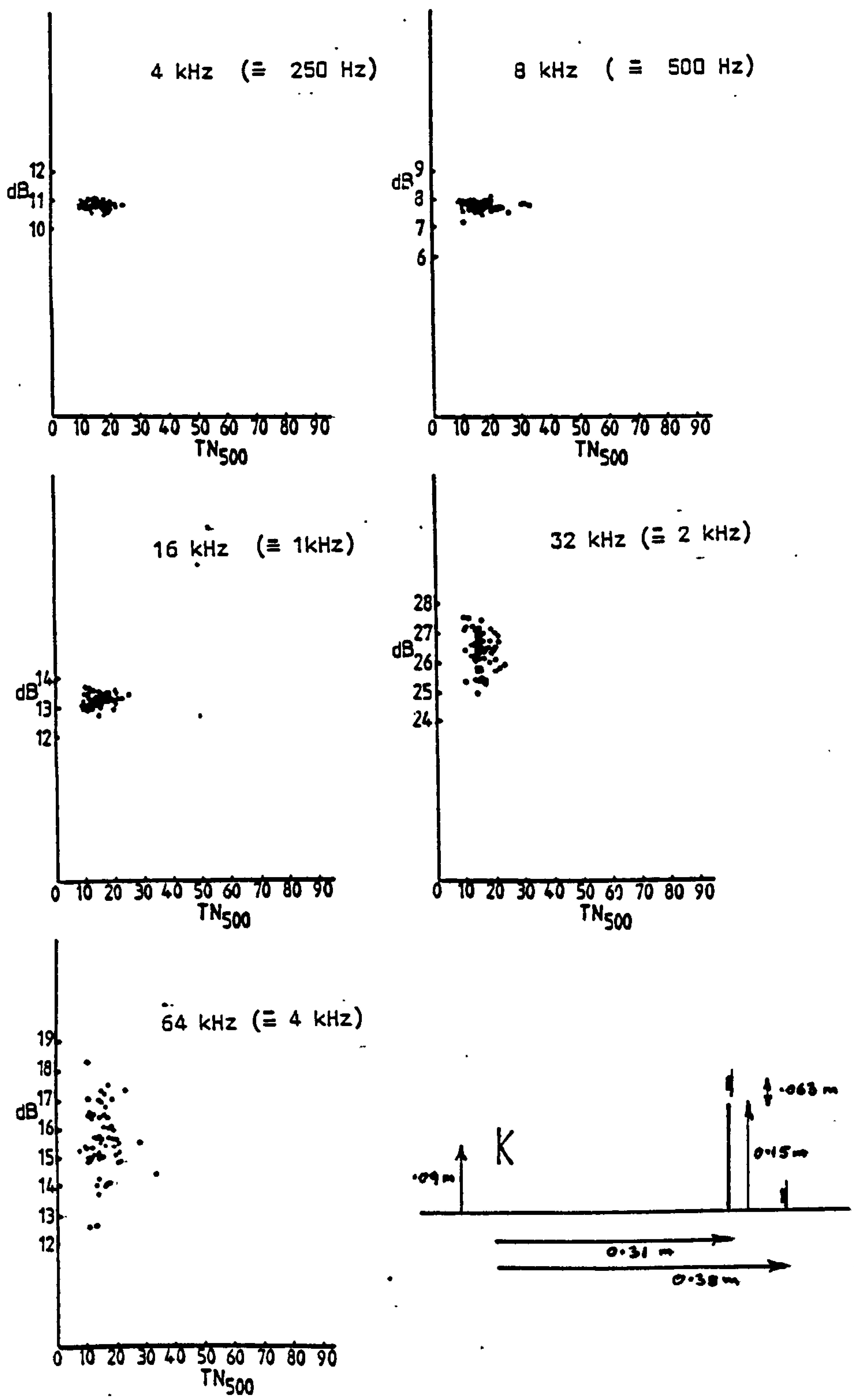

Fig 10.3 b Model scale; pure tones; barrier present;
Level difference vs TN_{500}; various frequencies.

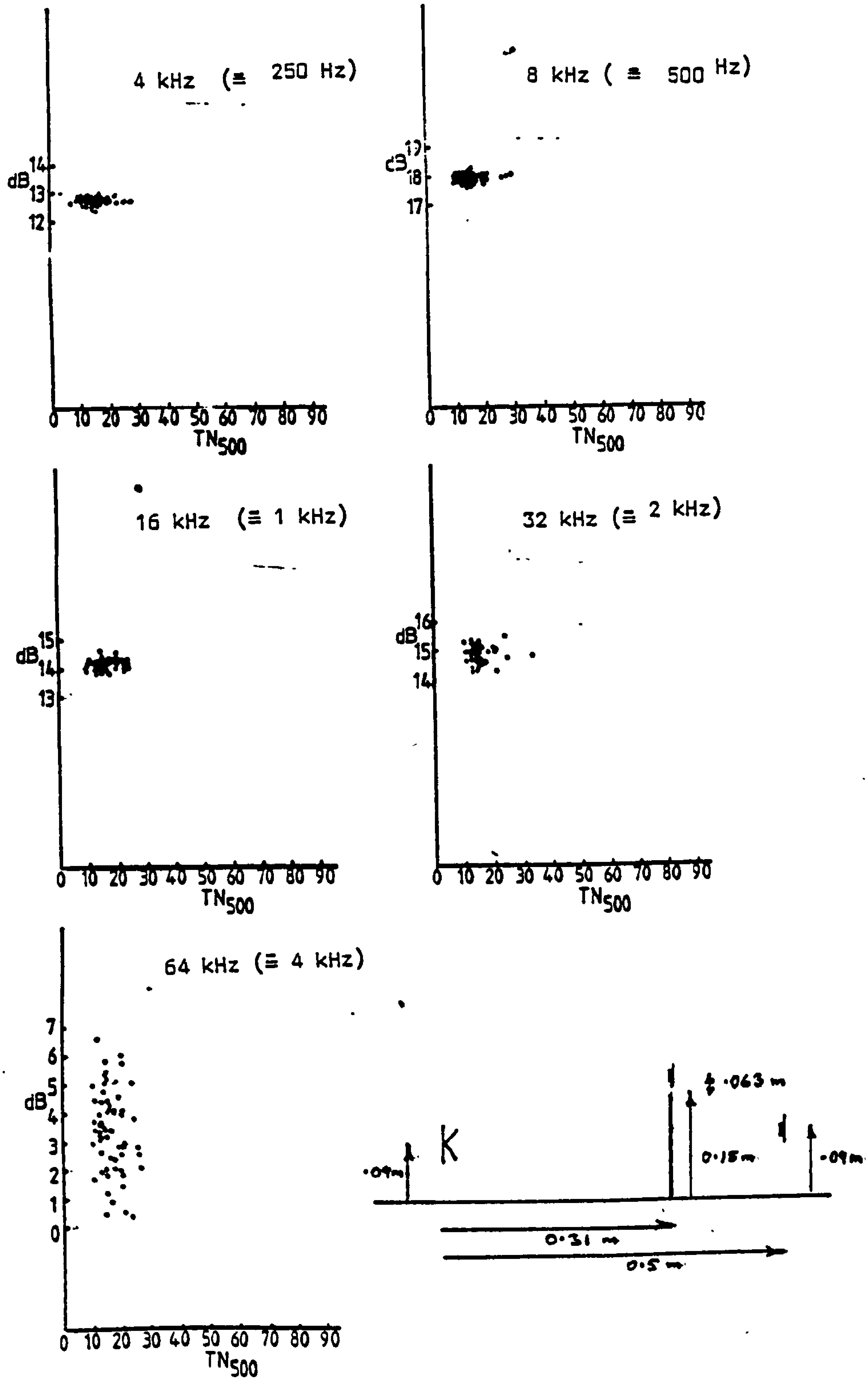

Fig 10.3 c Model scale; pure tones; barrier present;
Level difference vs TN_{500}; various frequencies.

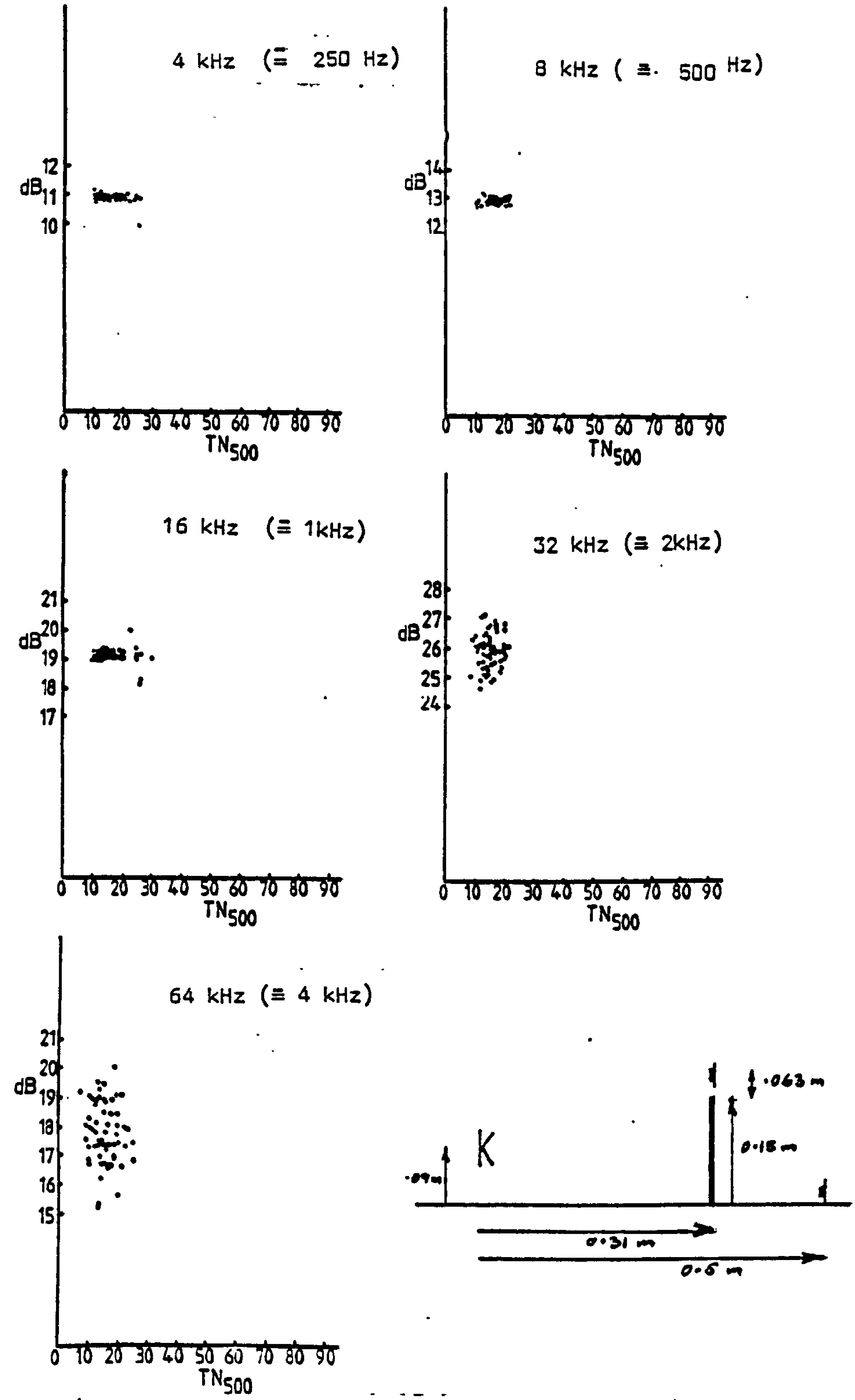

Fig 10.3 d Model scale; pure tones; barrier present;
Level difference vs TN_{500}; various frequencies.

CHAPTER 11

Analysis of Results

In this chapter the techniques used in analysing the data acquired in full-size and model experiments is described. The conclusions drawn from these results are then discussed.

11.1 Analysis Techniques

11.1.1 PET Printouts

Raw data collected by the automatic measurement system during experiments, model or full-sized, is stored on floppy disc to be re-accessed by a PET in the laboratory which then calculates more meaningful quantities such as sound pressure level, turbulent intensity, etc. In the first instance, data analysis was a simple inspection of the tabulated results from this procedure.

A typical table of results is shown in Fig. 11. It comprises the sound pressure level for the near and far microphones for each pass, together with a running average and a running standard deviation.

The wind turbulence wind direction and air temperature are also printed for each pass.

A separate table is produced for each frequency band measured. Before the first of these tables the name of the data file is printed and the calibration levels for each microphone, in terms of event recorder digits, corresponding to the 94dB calibration tones is also printed.

The facilities for formatting output data on the PET are somewhat limited

O:INM157/3
NEAR CHANNEL CALIBRATION= 79.2866558 FAR CHANNEL CALIBRATION= 84.8547832

CENTRE FRECUENCY= 4000 NO. OF PASSES = 20

NEAR CHANNEL			FAR CHANNEL			MET. DATA		
RMS (DB)	RUN.AVE (DB)	STD.DEV (DB)	RMS (DB)	RUN.AVE (DB)	STD.DEV (DB)	%TURBULENCE	TEMP(C)	W.DIR.(DEG)
82.235	82.235	0	72.096	72.096	0	5.382	17.131	298
81.973	82.105	.131	70.966	71.549	.583	26.496	17.092	244
80.678	81.655	.689	71.747	71.616	.479	18.524	17.597	226
82.754	81.943	.774	86.683	78.332	23.469	28.5	17.782	250
83.119	82.191	.849	70.919	77.273	33.034	9.602	17.828	254
82.361	82.22	.772	71.102	76.503	50.202	8.23	17.765	242
82.609	82.277	.723	88.219	79.473	29.349	20.372	18.221	272
83.419	82.428	.785	82.525	79.918	17.62	21.18	17.993	260
81.524	82.332	.802	83.661	80.423	13.511	19.199	16.972	286
82.17	82.42	.801	80.55	80.436	11.949	11.041	17.145	268
82.018	82.384	.775	72.301	79.942	13.019	19.711	17.441	272
81.844	82.34	.76	84.187	80.386	11.231	21.263	17.653	232
82.689	82.367	.734	86.797	81.087	10.367	10.035	18.666	240
81.91	82.336	.719	71.91	80.672	11.246	17.44	18.753	268
82.451	82.343	.694	72.002	80.299	12.057	24.654	18.036	258
83.186	82.398	.704	71.867	79.955	12.842	5.798	18.102	232
82.275	82.391	.683	64.833	80.332	11.6	0	17.834	220
82.218	82.382	.665	72.285	80.035	12.209	3.007	18.112	242
80.629	82.298	.756	71.569	79.746	12.881	6.68	17.863	224
81.775	82.2720001	.747	70.89	79.463	13.62	19.705	18.073	240

Fig 11 A typical PET printout of results.

and consequently the technique for producing the table is involved.

Inspection of these tables revealed no obvious trends in sets of measurements between, say, microphone level and wind turbulence etc. It was therefore desirable to extend the table to include other parameters, perhaps level difference, wind speed, etc., which would prove inconvenient as almost the full width of the paper was needed to produce the existing table. Additionally, the need for graphical representation and statistical testing of large amounts of data on a routine basis became increasingly obvious. The PET has no facility for printed graphics and to develop software for this purpose would have been time-consuming, as would the development of a comprehensive and versatile statistical package. The need to work with data acquired over perhaps many days would require the constant use of disc storage as virtual memory, since it was known that data from one geometry of one experiment would use nearly all the internal random access memory of the PET. The use of disc files on such a regular basis would produce unreasonably long execution times because of the relatively slow data transfer rate between disc and microcomputer.

It was decided to look to more powerful computers with ready-developed statistics packages to perform the data analysis in earnest.

11.1.2 The DEC - 20 Computer

The mainframe computer at Liverpool Polytechnic, a DEC - 20, has the ability to handle data files of such a size that data from many days worth of experiments could be stored at once. Also, developed statistics packages ideally suited to the analysis of scientific data were available.

The computer can be simultaneously accessed by many users throughout the Polytechnic by a time-sharing procedure using terminals connected to the computer via telephone cables. The data acquired during this study could be transferred to the computer using one of these terminals by manually typing in the results tabulated by the PET. This was unacceptable since it would still require the printing of results from the PET, typographical errors would be practically unavoidable and the process would be prohibitively time-consuming.

A solution would be for the PET to communicate directly with the mainframe computer sending results as they were calculated.

Data Communications

A system was devised by which the PET appeared as a conventional terminal to the mainframe computer and data was transferred between these devices on a hand-shaking basis. Use was made of a commercial electronic circuit board known as the "Netkit" designed to allow the PET to transmit and receive data according to the RS232 standard by which the mainframe computer communicates with all its terminals.

It was necessary to devise a means of running programmes simultaneously on the two computers by which a data file could be constructed on the mainframe computer.

11.1.3 The GENSTAT Package

The statistics software used to analyse the data was known as GENSTAT (a General Statistical language) (51). Other statistics packages were available but this choice offered the advantages that the construction was such that performing operations on sets of data involved simple instructions; it was developed specifically for scientific applications and the facilities available provided the degree of sophistication required to fully investigate the experimental data.

The following Section describes the statistical techniques used in the analysis of data.

(a) Analysis of Variance

This technique, often abbreviated to ANOVA, is used to determine to what degree variances in sets of data are related and can be classed as either a one-way or a two-way analysis. (51).

ONE-WAY analysis attempts to quantify the variance between groups of data compared to the variance within the groups. In this project such an analysis might relate the variance of sound level difference from day to day to the variance during each different day.

The technique measures the total variability and breaks this down into the two components mentioned above. A within-days and between-days mean square value is calculated and the ratio of these two is used as a test statistic to accept or reject the hypothesis that there is a significant long-term variation from one day to another by using the one-sided F table.

TWO-WAY analysis permits the introduction of a further variable. For instance, the level difference measurements could be classified by frequency as well as by days. In this way measurements are formed into "cells", each cell containing data from one day and one frequency only.

The between-cells variation is now made up of between-frequencies and between-days variation with an additional interaction variance. The sum of these three sources of variance is then subtracted from the total variance. The result is known as the residual and is actually the within-cells variation.

Covariates

The declared variate in the above analyses is level difference. It is possible to include other parameters known as covariates, such as wind turbulence, wind speed, temperature, etc. The analysis of covariance technique (ANCOVA) attempts explain the variation in the main variate by similar variation in one or more of the covariates. The effect of adjusting for covariates should be to reduce the within-cells variance if variate and covariate are related. In the analysis of variance table a covariance efficiency factor (labelled COV EF) is printed. Ideally this should be unity.

(b) Regression Analysis

In this technique an attempt is made to relate two stated parameters by a polynomial equation. The efficiency of the fit is indicated by a statistic called the correlation coefficient. This is formed from the sum of squares of the x and y variates and the sum of the cross products. Perfect correlation is indicated by an absolute value of unity, total uncorrelation being shown by a zero value. The sign of the value shows the gradient of the fitted line.

11.1.4 Inspection of Graphical Representations

In parallel with the formal statistical analysis described above, it was necessary to look for emerging trends by displaying the data in whatever graphical forms seemed appropriate. Typical examples are:

a) graphs of near or far level, or level difference, plotted against each of the calculated meteorological parameters drawn separately for each of the five frequencies used.

b) Mean levels of sets of measured attenuation plotted against frequency for a set of curves covering the geometries used in a set of experiments.

11.2. Analysis of Full Scale Results

The application of the GENSTAT techniques discussed above proved inconclusive in that no clear evidence of a statistical relationship between the acoustical parameters and the selected meteorological variables emerged.

11.2.1. Visible Trends and Tendencies in the Graphical Results of Chapter 9.

Notwithstanding the comments above, an inspection of the graphed results presented in Chapter 9 indicates patterns and consistencies which appear unmistakable and which would not have been identified by the GENSTAT procedures already referred to.

The patterns under discussion in this section were found in fact only to appear when level difference between the near and far microphones were plotted against one or other of the two selected turbulence numbers, TN_{50} or TN_{500} (By way of reminder TN_{50} and TN_{500} refer to a statistical representation of the fluctuation in instantaneous measured wind velocity, as defined in section 6.2, based upon a sample time of 50 and 500ms respectively.)

When considering the significance of the apparent trends being discussed here it is important to remember that the experimental points shown on the graphs of Chapter 9 represent the measured level difference and TN value for a single sound burst and that in each case measurements taken on five separate days have been aggregated on to each graph.

The patterns and trends referred to may be summarised as follows:

(i) The amplitude of scatter in level difference values at a given TN number is generally large at low TN values.

(ii) The scatter at the low TN limit varies with acoustic signal and measurement geometry.

(iii)There is a strong tendency, irrespective of acoustic signal and geometry, for the scatter to reduce, following a common pattern, to a very small value at high TN values.

(iv) The limiting value of level difference in (iii) above, the so-called asymptotic limit, also varies with signal and geometry.

(v) The frequently encountered triangular pattern of measurement points is not a consequence, as might initially be thought, of the reduced number of occurances in which high TN values were returned.

(vi) The above observations appear equally true of unobstructed propagation and when the barrier was present.

(vii)The total independance of the acoustical and meteorological measurement channels encourages the belief that the above are observations of real effects.

With the comments of this section in mind some of the data presented graphically in Chapter 9 have been extracted and presented in an alternative form for discussion below.

11.2.2. A Study of the high-turbulence level differences.

11.2.2.1. Open Propagation

In Figs 11.1 to 11.5 asymptotic (ie high turbulence limit) level differnces are plotted against frequency and for the various geometries including unobstructed propagation. Broken lines have been included as a guide to the eye in discerning trends rather than to imply any precise knowledge of the variations involved.

The behaviour shown in Fig 11.1 (unobstructed propagation) appears consistent with the results of Rasmussen (4) and Piercy etal (1) which relate to measurements of open propagation without consideration of turbulence. The reasons for this assertion are as follows:

(i) On four of the five curves (viz b,c,d,e) there is an increase in level difference which may be associated with the 500Hz dip characteristic of propagation over grassland and wide enough, in frequency terms, to be discernable even in the presence of the averaging effects expected from dealing with full octave noise bands.

(ii) A second local maximum appears on curves a,b and c which progresses to higher frequency with increasing propagation distance (i.e. decreasing path length difference) indicative of an additional interference effect. The parts of curves d and e available continue that trend. The maximum lies close to the frequency at which the path length difference is three half-wavelengths. This would suggest that the ground should still be considered acoustically hard at these frequencies. (The surface was indeed a grassed, hard packed top soil backed by a solid sandstone base).

(c) Additionally for the near microphone the same interference dip occurs at 680 Hz which is within the 500 Hz octave band producing a low near microphone level in that octave band. This may explain why the 500 Hz dip is not seen at a far microphone distance of 9.6m (curve b) where this dip is still moderately shallow when averaged over an octave band.

The above observations are considered to establish confidence in the overall measurement system and to characterise, acoustically, the ground at the experiment site. They also serve to emphasise that even unobstructed propagation over open grassland is a complicated matter.

11.2.2.2 Barrier Present (Octave Bands)

Fig 11.2 and 11.3 show the asymptotic level difference plotted against frequency for the two sets of geometries (9.2.1. and 9.2.2.) comparable with those used for open propagation discussed above. (For 9.2.2. the speaker and far microphone are at ground level).

In all cases the trend is an increase in level difference with increasing frequency and with increasing distance to the far microphone.
The indication is that the interference dips observed for open propagation have either become more frequency selective, due to the increased multiplicity of possible propagation paths, and so are smoothed out over an octave band, or have disappeared.

The fact that level difference is greater for far microphone distances where the microphone is on the ground could be attributable to one or a combination of the following:

(i) A plane wave shadow zone is being formed behind the barrier, although the propagation distances are rather short.

(ii) The diffraction angle is increased by a factor of about 2.3 when the speaker and far microphone are lowered from 1.4m above the ground down to ground level.

(iii) There are four ray paths above the barrier for the case of the far microphone and speaker above the ground but only one ray path for the speaker and far microphone on the ground.

The pronounced maximum of the curves in Fig 11.3 occurs at 2KHz irrespective of far microphone distance which tends to rule out a ground reflection type interference effect, which is reasonable since the far microphone is on the ground. However, 2KHz is approximately the critical frequency of the barrier and so the results of Fig 11.3 may be an indication of a cancellation effect between diffracted and transmitted sound. It is not clear why normally incident sound of the critical frequency should be so enhanced.

11.2.2.3 Barrier Present (Pure Tones and Random Pure Tones)

The experimental results for pure tones presented in Fig 9.3 a-d and summarised in Fig 11.4 and 11.5, exhibit clear similarities in cases a and c (Far microphone is on the ground) and in cases b and d (Far microphone is1.4m above ground). The 2kHz maximum noted above is again evident for three of the geometries; there is a suggestion of some fine structure among measurements taken at a fixed frequency, but as suggested above, is least within 2kHz octave band. (The one exception is for the microphone on the ground and 1m behind the barrier giving a diffraction angle of 83^{o}. In such a case there would be little diffracted sound, leaving only transmission through the barrier as significant)

The curves tend to reinforce the idea that special transmission conditions apply at 2kHz, possibly a partial cancellation of the diffracted and transmitted sound.

11.2.3. The Observed Scatter of level difference measurements

Variations in the overall magnitude of the scatter in measured level differences exhibited from graph to graph in Chapter 9 are clearly noticable.

It has been remarked above that the distribution of measurement points frequently follows a general pattern of a wedge shape indicating that the scatter reduces as the measured turbulence increases to yield the so called asymptotic level with the fall from high values being at a somewhat faster rate, in decibel terms, than the rise from below.

For further investigation an attempt has been made to quantify the magnitude of the scatter by extracting from the graphs of Chapter 9 a measure which might be called the low turbulence scatter which is the notional decibel range within which the level differences of some 90% of the measured points would fall at low TN values. These have been plotted in Figs 11.6 -11.10 with Fig 11.6 being for unobstructed propagation.

11.2.3.1. Low Turbulence scatter ranges(unobstructed propagation/octave bands of noise)

A pattern can be discerned in Fig 11.6. At low frequencies scatter rises in a manner that is not unexpected when time sampling a low frequency noise signal. Beyond a minimum at 1 to 2kHz,and depending on geometry, the scatter rises again as frequency increases towards 4kHz. The extent of that rise varies,in a broadly sensible manner,with increasing acoustic path - if it is assumed that the process giving rise to this increased scatter operates along the acoustic path rather than being associated,for example,with conditions at the ground surface.

11.2.3.2 Low Turbulence Scatter Range (Barrier Present/Octave Bands of Noise/Source and Receivers above Ground).

The data here is extracted from Figs 9.2.1b - e and presented in Fig 11.7. There is less variation of scatter range with frequency and geometry than the open propagation case as seen in Fig 11.6. However, with the exception of curve b which pertains to the far microphone close to the barrier, the trend is still a decreasing scatter range from 250Hz down to 1kHz and an increase again at the high frequency end.

It is unclear why the variation in scatter range should reduce overall compared with open propagation in this fashion.

11.2.3.3 Low Turbulence Scatter Range (Barrier Present/Octave Bands of Noise/Source and Far Microphone at Ground Level).

The graph of Fig 11.8 shows the scatter obtained from Figs 9.2.2b - e and can be compared with Fig 11.6 which shows the turbulent scatter for unobsturcted propagation of octave noise. Again the scatter level firstly decreases with frequency to a minimum at 1kHz to 2kHz in a manner that is similar for all geometries. The rise in scatter at 4kHz is greater than that of Figs 11.6 and 11.7. With the exception of curve e, the high frequency scatter can be seen to increase with increasing far microphone distance, as also observed in Figs 11.6 and 11.7.

The indication is that the obsence of interference phenomon due to the geometry chosen in this case limits the scatter at low frequencies to that expected of noise.

11.2.3.4 Low Turbulence Scatter Range (Barrier Present/Pure Tones).

The variation of scatter range with frequency and geometry is shown in Fig 11.9. The scatter is predictably lowerthan for octave bands, with a noticeable feature being the absence of the low frequency increase in scatter range. This indicates that where this increase has been seen in previous graphs (Figs 11.6 to 11.8) it was due entirely to the nature of the signal being octave bands of noise, the scatter being influenced by $1/2\sqrt{BT}$. consideration.

Additionally it indicates that the effect of turbulence on sound is frequency dependant with 250 Hz up to about 1kHz being relatively unaffected. There is support for this in the literature (41).

11.2.3.5 Low Turbulence Scatter Range (Barrier Present/Random Pure Tones)

The data here is presented in Fig 11.10.
Although this graph initially appears not to exhibit the previously noted structures, a closer inspection does reveal understandable behaviour.

With the exception of the 500 Hz points for curves a and c, and the 2kHz point for curve b, the underlying trend is again one of increased scatter at high frequency with the base line scatter of about 4dB being comparable with that obtained with octave bands of noise (compare with Fig 11.7, for instance). However, if the asymptotic level difference between near and far microphones varies within a particular octave band this will add to the base line scatter. In the case of the exceptional points noted above a change in asymptotic level difference of about 6dB is implied which, it isargued, is not unreasonable.

11.2.4 Résumé of the Observations Discussed in 11.2

The above findings may be drawn together as follows:

(i) The scatter in level difference between near and far microphones reduces as turbulence number increases.

It is not unreasonalbe that turbulence induced effects should be absent at large TN values if it is assumed that high turbulence infers a predominance of turbulent eddies of a size that is small compared with the wavelength of the sound. This idea is supported in the paper by Piercy (1) which states that the inherent instability of turbulent eddies will cause them to continuously break down into smaller eddies until a minimum diameter of ~1 mm is reached when the eddy disappears due to viscous losses. This size can be compared with a wavelength of 86mm for a 4kHz tone in air at 20°C ($c=344ms^{-1}$)

(ii) The low turbulence limit level difference scatter is a complicated function of wavelength and geometry. It is probably too difficult to suggest a model, at this stage, to fully account for the observed effects. It has been observed in results not presented here, houuever, that large scatter in level difference corresponds to large scatters in both the near and far received levels and that small scatter in level difference is a result of small scatter in near far received levels. Intermediate ranges of scatter could be a result of either a low scatter at the near receiver with large scatter at the far microphone, or vice versa.

Examples of this can be seen in the low scatter at 1kHz in Fig 9.1a (unobstructed propagation of octave bands) and in the large scatter at 4kHz in Fig 9.3b (pure tone propagated over a barrier). For the latter case a near scatter range of 9dB coupled with a far scatter range of 15dB produces a level difference scatter of about 9dB.

The low scatter at 1kHz in Fig 9.1a is worthy of closer inspection. It seems circumstancial that this particular geometry and frequency should result in a small degree of scatter of the instantaneous near microphone levels. That the same particular conditions should also apply at the far microphone may be linked, in a manner that is as yet unclear, to the fact that the path length difference between direct and ground-reflected rays changes from 0.76m for the near microphone to 0.4m for the far microphone, giving an additional path length difference for the near microphone over that for the far microphone of about the wavelength of a 1kHz tone ($\lambda = 0.34m$).

In section 11.2.3.4. it was proposed that only the high frequency scatter was a consequence of turbulence. There appears to be two possible explanations for this. Firstly, turbulence scatters energy out of the acoustical beam as it propagates through the atmosphere. This is evidenced by the general increase in low turbulence limit scatter as far microphone distance increases and is supported by the findings of Brown and Clifford (38) and Daigle, et al (40)
The effect that this scatter has on amplitude and phase of the acoustical beam can give rise to widely fluctuating levels at points where interference maxima or minima between direct and reflected pure tone sound occur since such conditions are highly phase dependant.

It is argued that for geometries were the far microphone is closest to the speaker (e.g. 9.1a, 9.2.1b, etc.) that the propagation path is too short to account for all the observed scatter. A second mechanism may be one that modifies the ground reflection conditions in a way that may in some cases decrease the correlation between direct and reflected waves and in other cases may cause little or no decrease in correlation.

Since it is stated elsewhere that the reflection coefficient of grassland is influenced by the pockets of air trapped within the grass and the top layer of soil that is broken up by the grass, (Ref (1), page 1408) it is possible that the wind turbulence affects these pockets causing theproposed change in reflection conditions.

(iii)There is no evidence to suggest that the observed effects of wind turbulence are significantly modified by the barrier chosen in this work.

11.2.5 Model Scale Results

11.2.5.1 Asymptotic Level Difference

Fig 11.12 summarises the results of Figs 10.2a - d which show the level differnce at two receivers when octave bands of noise propagate over a thin barrier.

With the exception of curve d the level difference vs. frequency curve is approximately the same for all geometries and exhitit a decrease of about 1dB from 250 Hz to 500 Hz and an increase of about 4dB as frequency rises to 4kHz. Curve d also shows this trend with the exception of the 32kHz (≡2kHz full scale) point. This may be due to interference between the direct sound and that reflected off the absorber placed behind the far microphone. Due to the time-limited source signal this will not be observed at the other geometries were the far microphone is closer to the speaker.

The data from Figs 10.3a - d is presented in Fig 11.13 which deals with pure tones propagated over the model barrier. This is directly equivalent to the full scale results shown in Fig 11.4.

All curves exhibit a maximum at 32kHz (≡2kHz full scale) as in the full scale equivalent. In section 11.2 it was proposed that this effect may be indicative of a cancellation of diffracted and transmitted sound since the critical frequency for the full scale barrier is about 2kHz. However, it seems unlikely that the model barrier, a thin aluminuim strip, should exhibit similar transmission irregularities at a transposed frequency. It is more likely that it is due instead to diffraction and interference effect since the relative linear of wavelength and geometry have been preserved.

11.2.5.2 Low Turbulence Limit of Level Difference Scatter

From Figs 10.2a - d it can be seen that for all geometries used with octave bands of noise propagated over the barrier the variation in the level difference between near and far receivers falls from about 3dB at 250 Hz equivalent to about 1dB for the remaining octave bands.

The implication is that the only scatter observed is due to the statistical nature of the acoustical signal and that the turbulence produced by the wind chest was not of the same nature as the turbulence in the atmosphere. It was found experimentally, in results not presented here, that outdoors low turbulent intensity occurs at low wind speed, implying that the fluctuating component of the wind is also low since turbulent intensity = du/u. However, a low turbulence was produced by the wind chest at high wind speeds, from which it is assumed that the air flow is more laminar at high flow rates. Without the use of surface obstructions to induce a more turbulent air flow, the wind chest does not produce model winds representative of typical outdoor situations.

For pure tones propagated over the barrier and a far microphone close to the barrier in its shadow (see Figs 10.3a - d and the summary in Fig 11.13) the scatter does become significant for all four geometries at 2kHz to 4kHz. One possible explanation is that a small degree of turbulence is produced in the wake of the barrier which could reasonably expected to affect the sound diffracted over the barrier. At low frequencies where there is little diffracted sound the effect is minimal.

There is no evidence to suggest that a similar phenomonon occurs with the full scale outdoor situation.

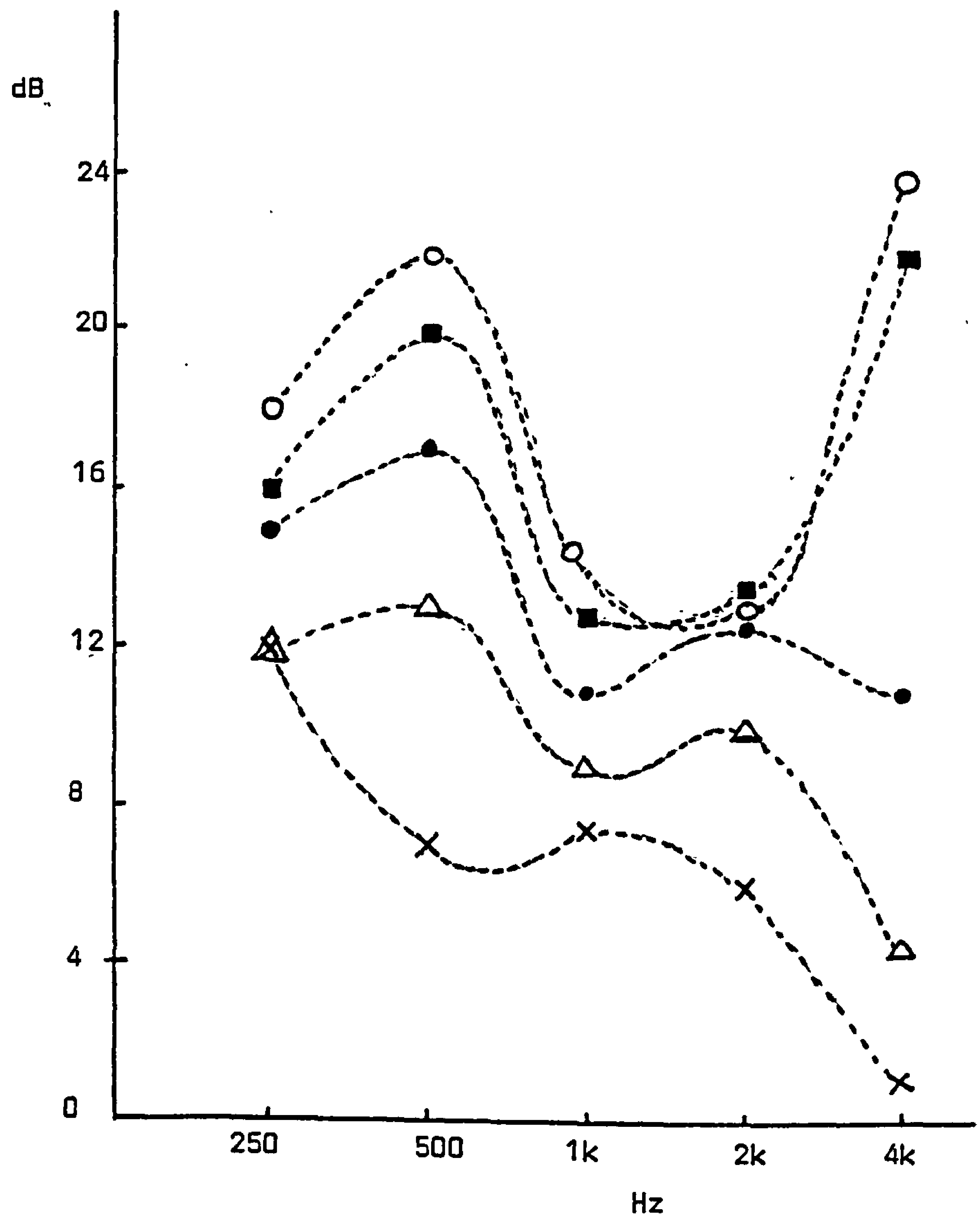

Fig 11.1 Level Difference*vs. Frequency for octave bands of noise propagated over unobstucted grassland. Geometry 9.1a (X), b(△), c(●), d(■), e(○).
* asymptotic (high turbulence) limit

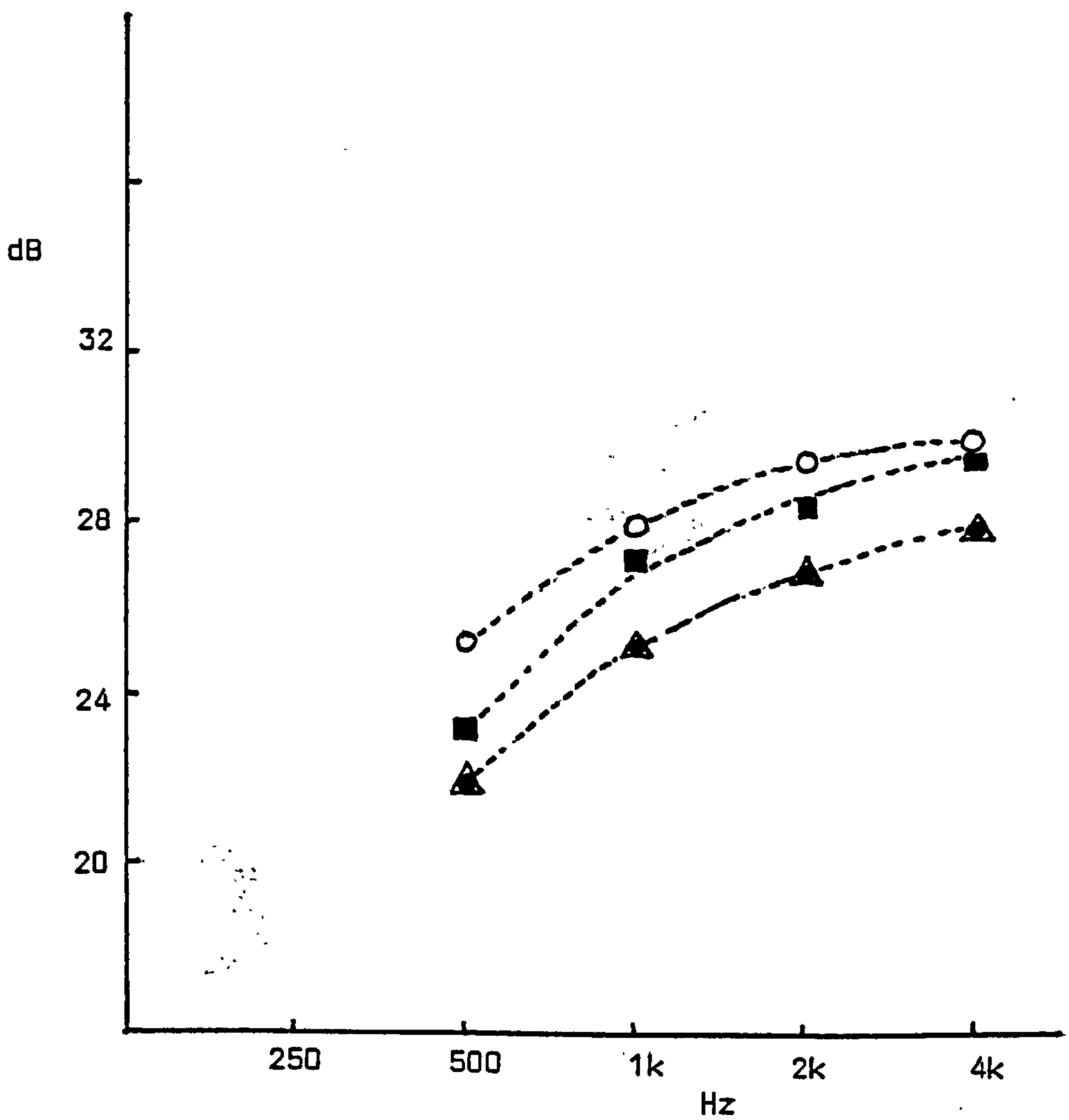

Fig 11.2 Level Difference * vs. Frequency for octave bands of noise propagated over a barrier.
Geometry 9.2.1 b(△), c(●), d(■), e(○).
*asymptotic (high turbulence) limit

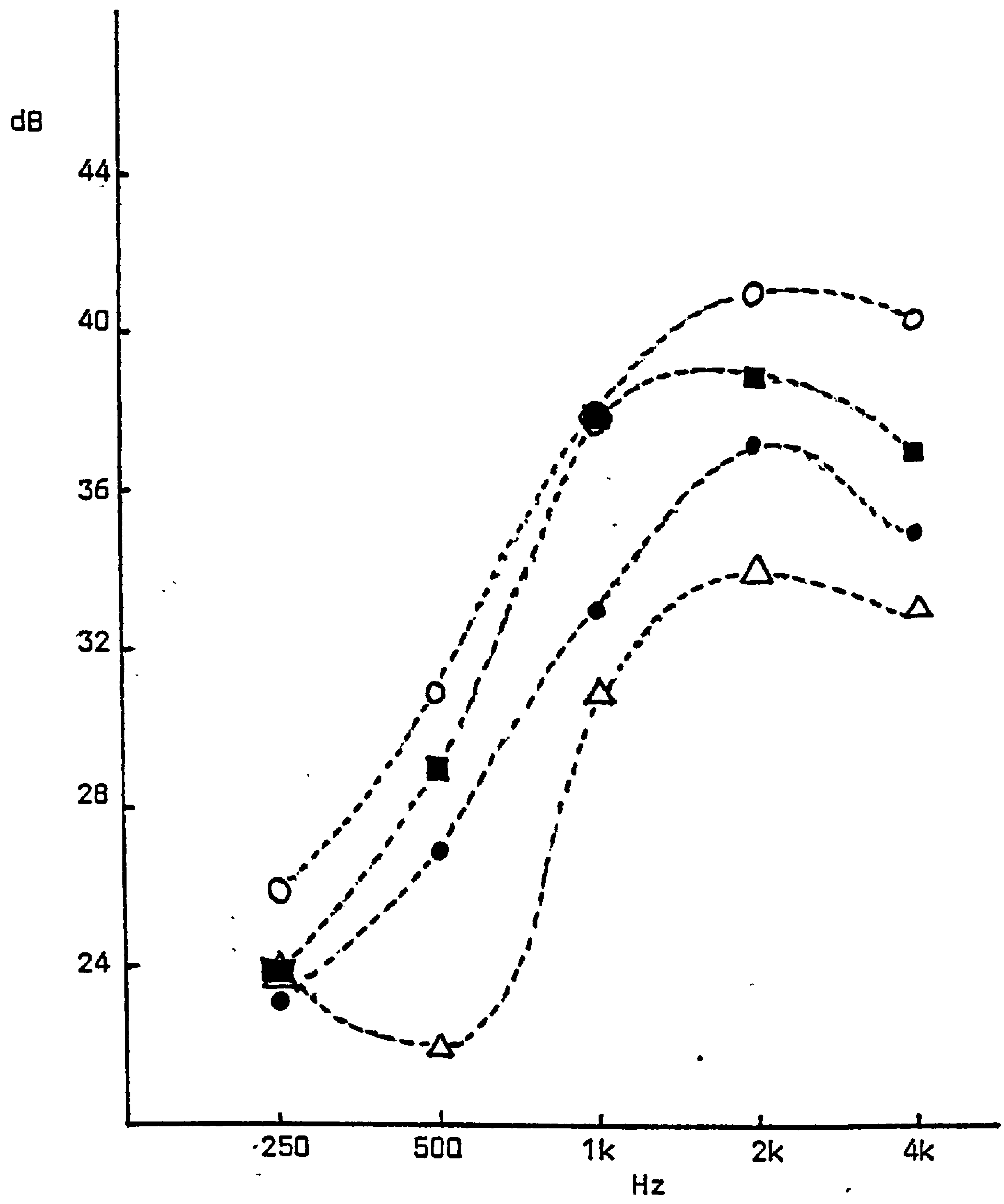

Fig 11.3 Level Difference * vs. Frequency for octave band of noise propagated over a barrier.
Geometry 9.2.2 b(△), c(●), d(■), e(o).
* asymptotic (high turbulence) limit

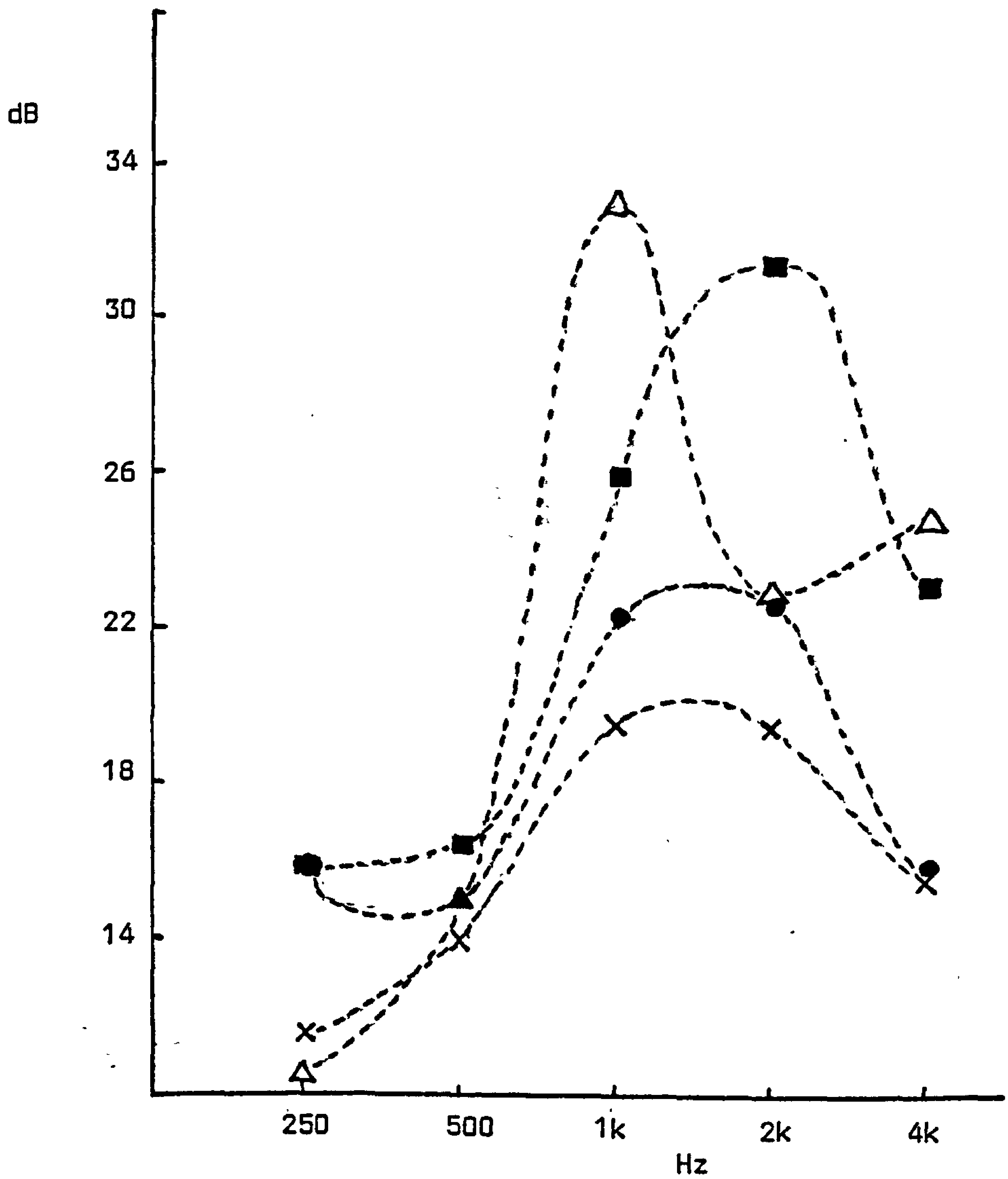

Fig 11.4 Level Difference *vs. Frequency for pure tones propagated over a barrier.
Geometry 9.3 a(X), b(Δ), c(●), d(■).
* asymptotic (high turbulence) limit

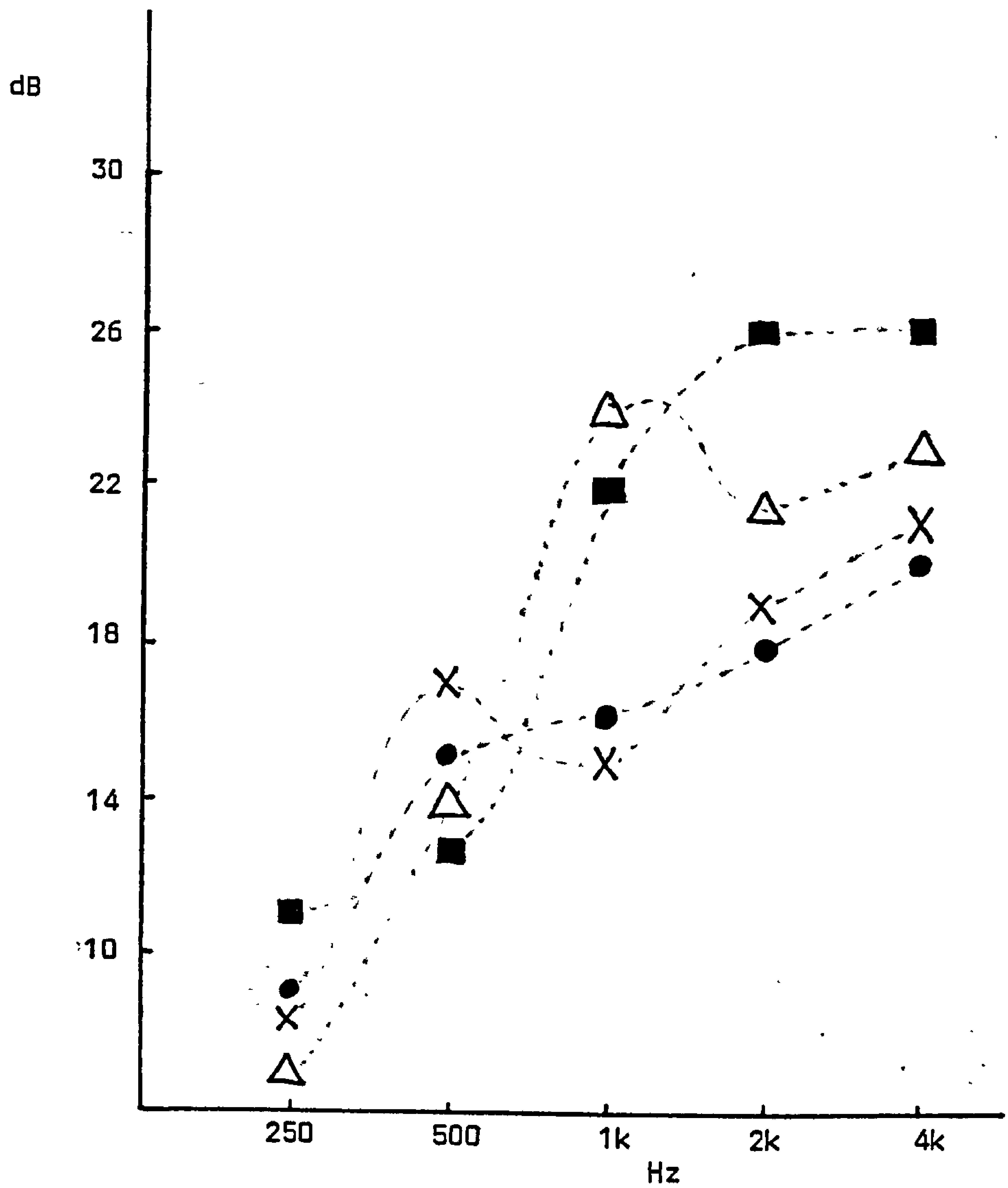

Fig 11.5 Level Difference *vs. Frequency for random pure tones propagated over a barrier.
Geometry 9.4 a(X), b(△), c(●), d(■).
* asymptotic (high turbulence) limit

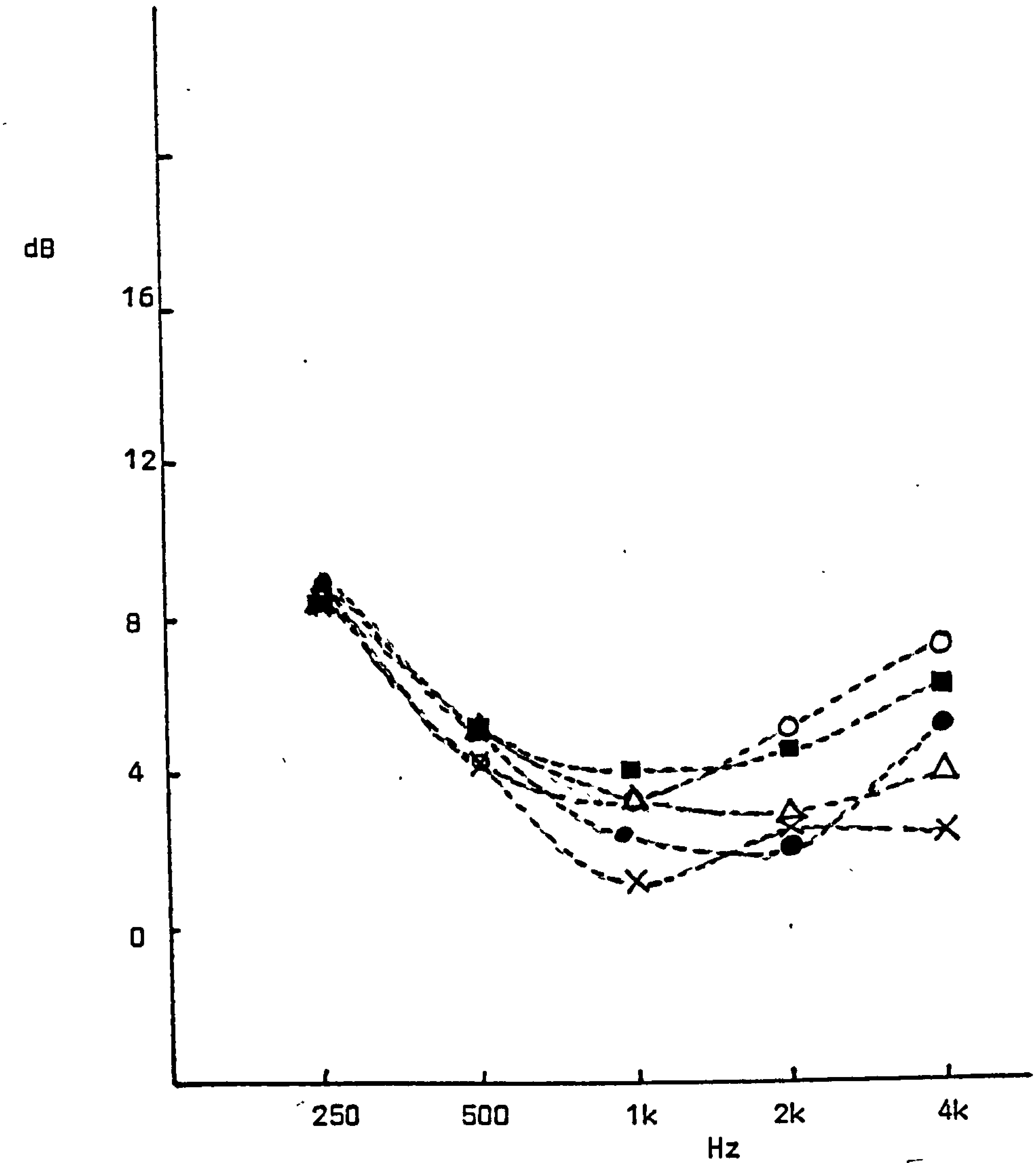

Fig 11.6 Low turbulence scatter range vs. Frequency for octave noise bands propagated over unobstructed grassland.
Geometry 9.1 a(X), b(△), c(●), d(■), e(o).

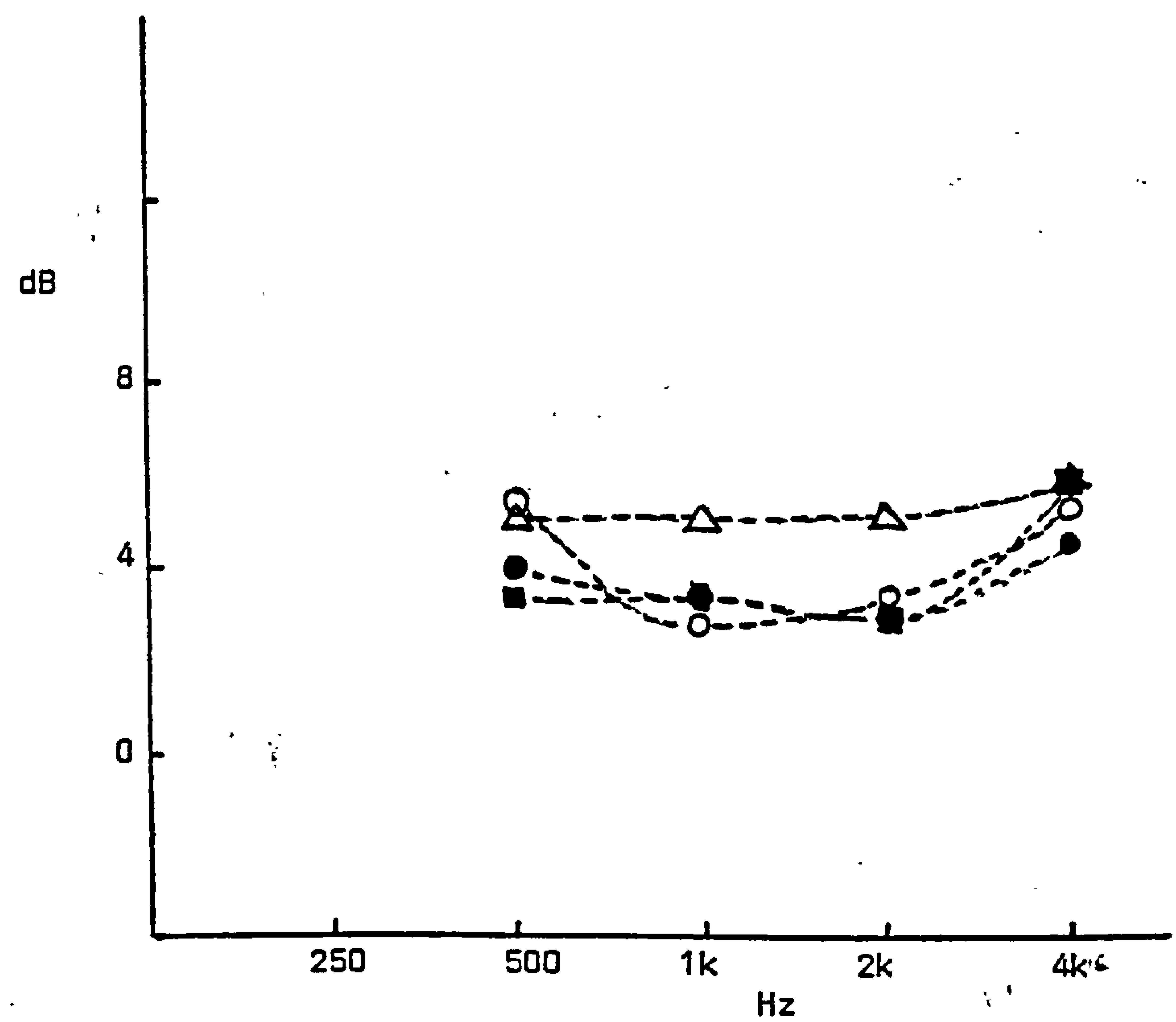

Fig 11.7 Low turbulence scatter range vs. Frequency for octave bands of noise propagated over a barrier.
Geometry 9.2.1 b(△), c(●), d(■), e(○).

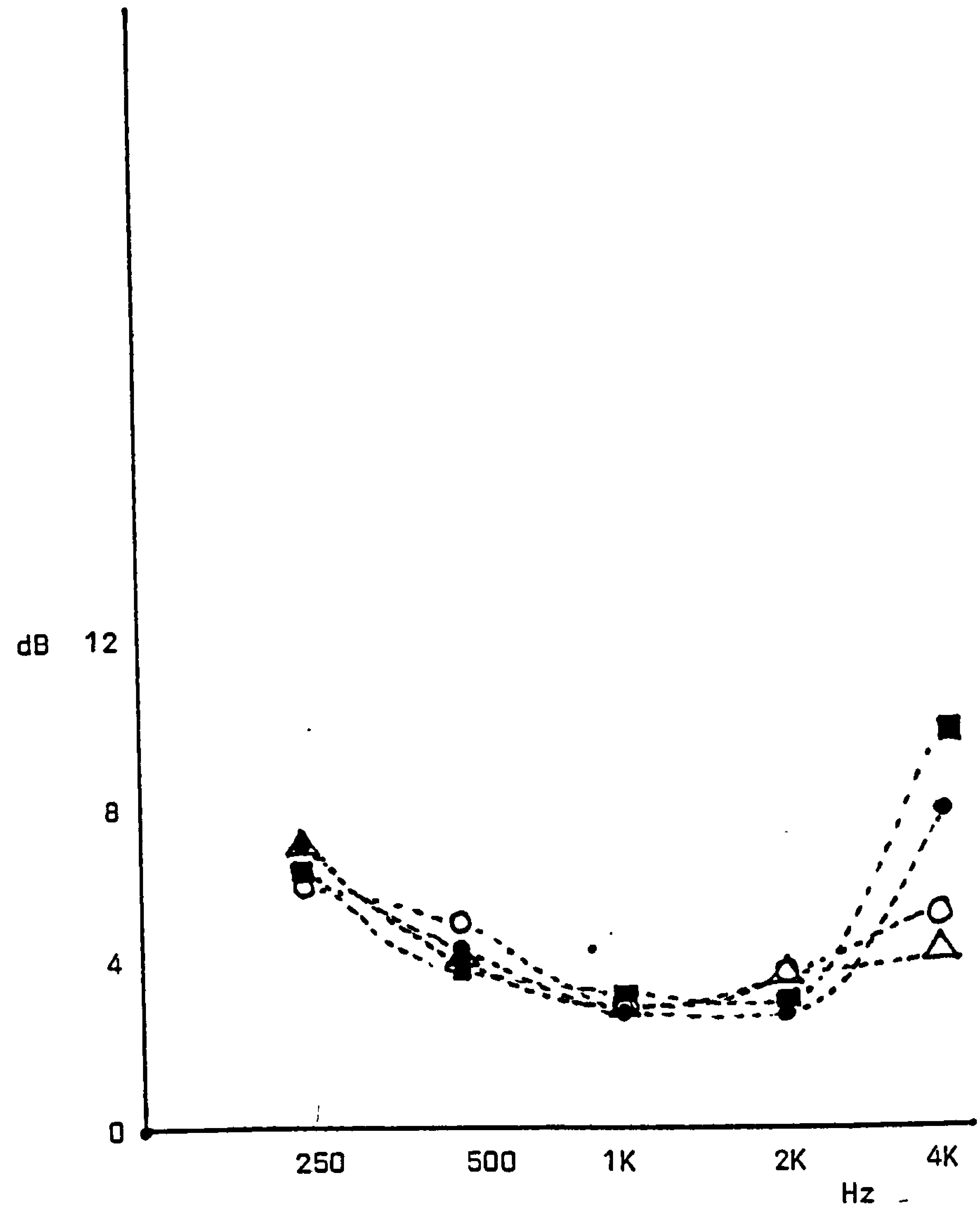

Fig 11.8 Low turbulence scatter range vs. Frequency for octave bands of noise propagated over a barrier.
Geometry 9.2.2 b(Δ), c(●), d(■), e(○).

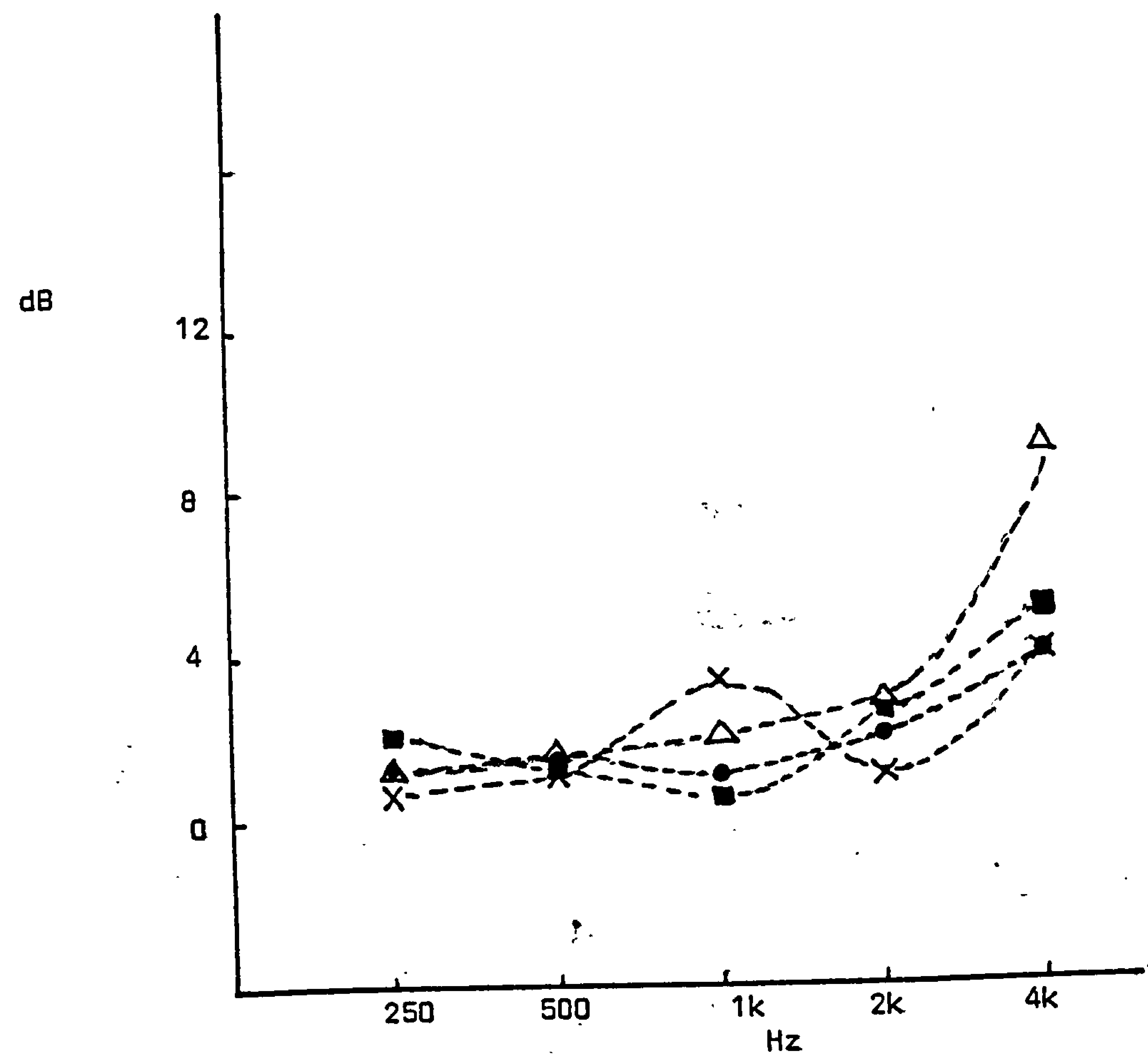

Fig 11.9 Low turbulence scatter range vs. Frequency for pure tones propagated over a barrier.
Geometry 9.3 a(X), b(△), c(●), d(■).

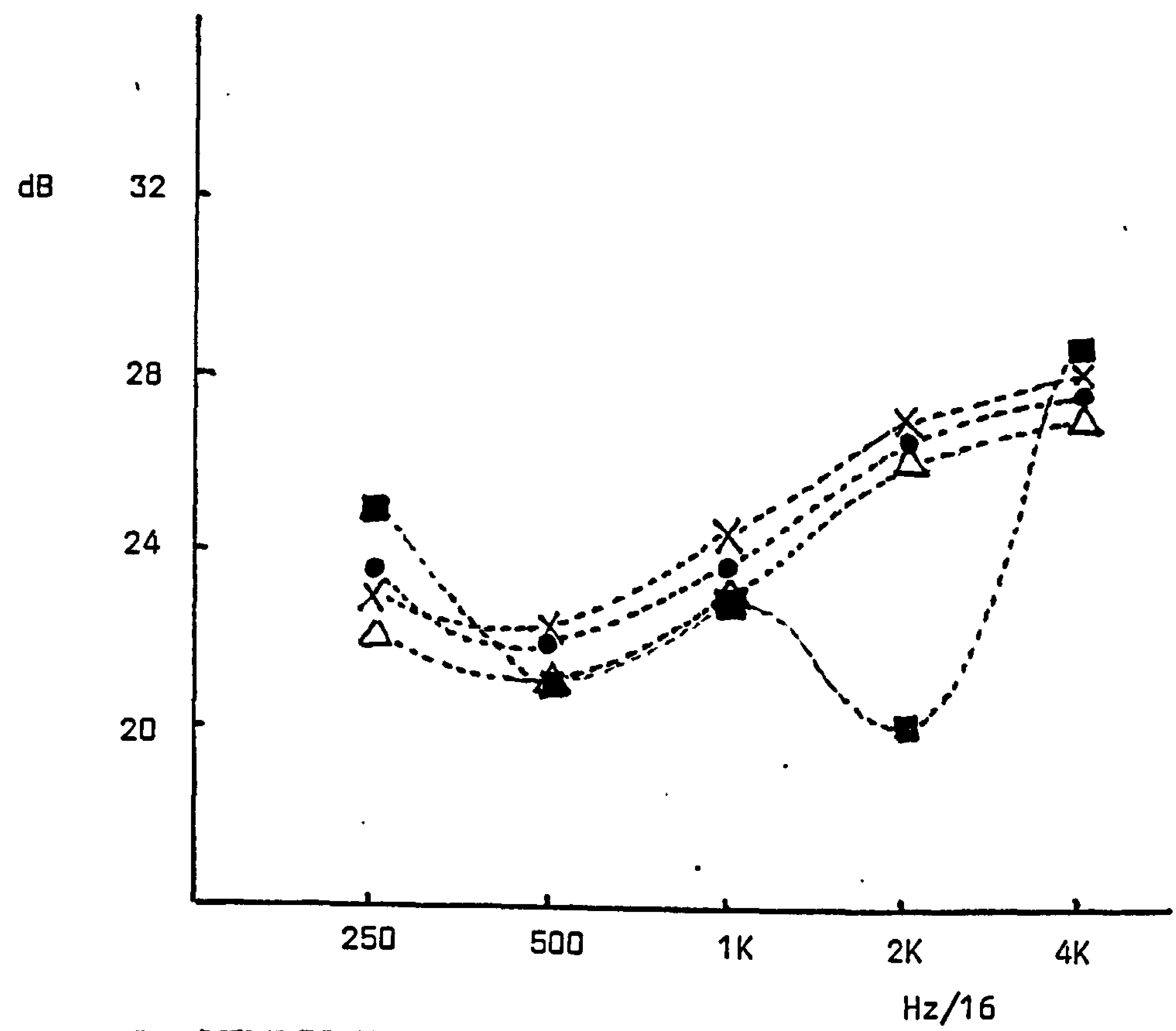

Fig 11.11 Model Scale: Level Difference* vs. Full Scale Equivalent Frequency for octave bands of noise propagated over a barrier.
Geometry 10.2 a(X), b(△), c(●), d(■).
*asymptotic (high turbulance) limit

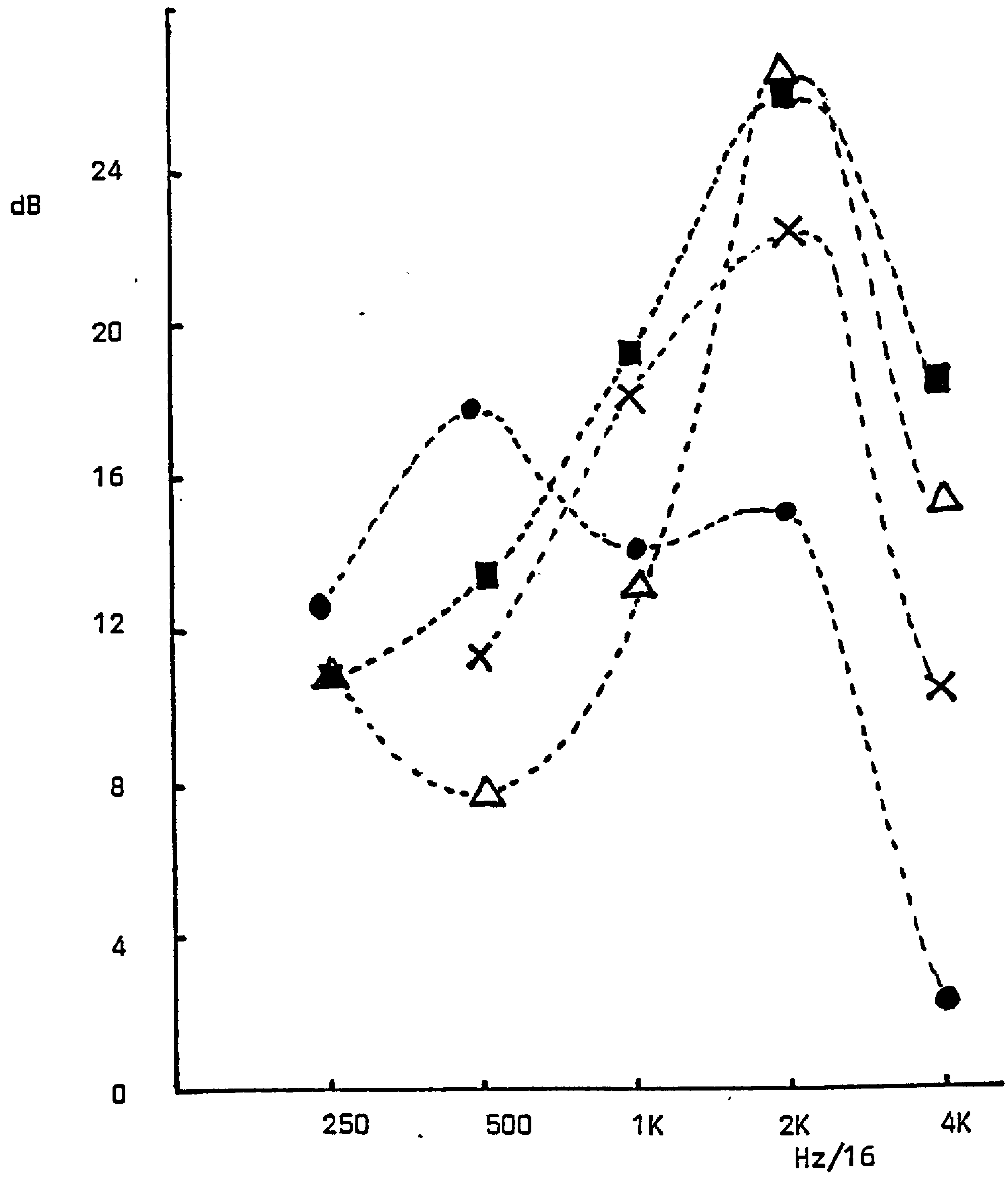

Fig 11.12 Model Scale: Level Difference* vs. Full scale equivalent Frequency for pure tones propagated over a barrier. Geometry 10.3 a(X), B(△), c(●), d(■).

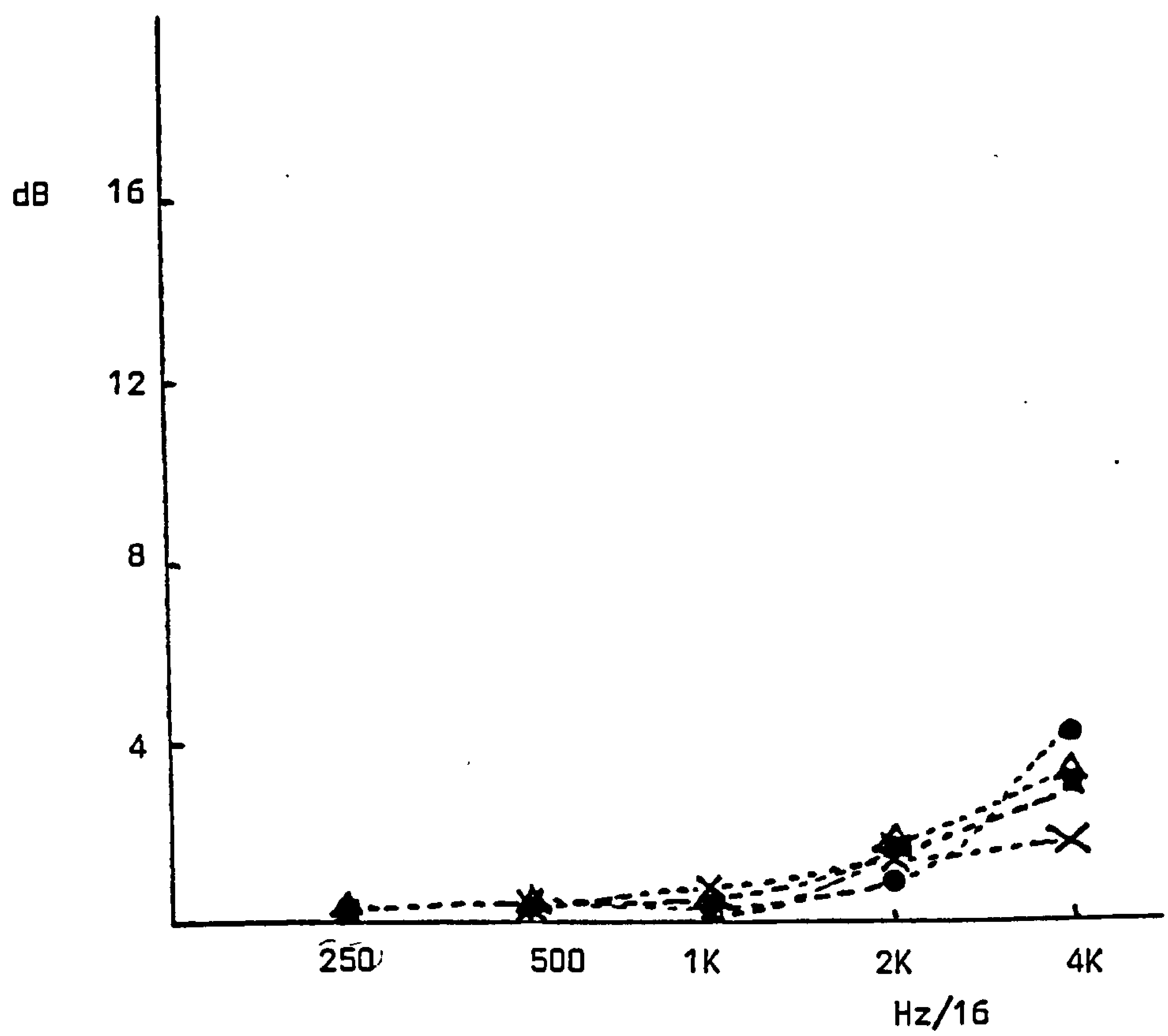

Fig 11.13 Model Scale: Low Turbulence Scatter Range vs. Full scale equivalent frequency for pure tones over a barrier. Geometry 10.3 a(X), b(Δ), c(●), d(■).

CHAPTER 12

Conclusions and Suggestions for Further Work

The conclusions of this thesis can be summarised as follows:

(i) Wind turbulence gives rise to a fluctuation in the instantaneous level difference between two receivers. The fluctuation reduces as turbulence increases.

(ii) The low turbulence limit of level difference is a complicated function of wavelength and geometry. It is probably too difficult to suggest a model to account for this.

(iii) There is no evidence to suggest that the effects of wind turbulence on received level are significantly modified by the presence of a barrier of the type used in this work.

The work of this thesis has highlighted the need for further investigation of the effect of turbulence on acoustic propagation, both for unobstructed atmospheric propagation and for propagation in the presence of a noise barrier.

The present study could be developed in the following ways:

12.1 Source/Receiver Geometries

It has been shown that the prediction of received sound pressure level at a point above open grassland is a complicated matter and the analysis of level difference between two microphones both above grassland is further complicated by the multiplicity of ray paths involved. It would, therefore, be beneficial to use one microphone only, the output of which could then be referenced to that expected from a standard acoustical condition such as for source and receiver above a perfectly reflective or a perfectly absorbent surface.

The loudspeaker output would need to be characterised for the appropriate range of frequency, propagation distance and input power for the chosen reference condition, since the horn loudspeaker is neither a point source nor could be guaranteed to give perfectly plane waves.

A second alternative would be to retain the use of a reference and a sample microphone but to perform the experiments above a perfectly hard surface such as ashphalt or concrete.

12.2 Development of the Anemometry

The results obtained in this work assumed that the output of one judiciously placed anemometer was representative of the wind turbulence conditions over the whole propagation path. It may prove to be more comprehensive to use an array of anemometers placed at various points on the propagation path and, possibly, at various heights (i.e. to yield the vertical turbulence profile above the ground). Clearly each additional anemometer requires a separater measurement channel, although time multiplexing units are readily available, and the amount of stored data would increase unless experimentation should indicate a suitable single descriptor to represent the combined outputs.

A further development may employ the "post trigger" facility of the DL901 event recorder in order to capture anemometer output before, during and immediately after the acoustical event.

With the recent advent of sophisticated signal processing instumentation it is now feasible to analyse anemometer output in the frequency domain in order to determine the turbulence spectrum and, therefore, allow a meaningful comparison with the results of other workers (40, 41). This may invlove the continued use of the Nagra tape recorder if the relevant instumentation is unable to work from the mobile laboratory.

12.3 Temperature Turbulence

This variable was excluded from consideration in this thesis, the emphasis being on wind turbulence. However, if a thermometric system of sufficiently short time constant is used its output could be treated in a similar manner to that of the anemometer to yield a more complete knowledge of atmospheric turbulence. The comments of 12.2 would also apply to the spatial sampling of temperature turbulence.

12.4 The Use of an Impulse Sound Source

A high energy, short duration impulse contains energy over a broad band of frequencies . An impulse sound source, such as a starting pistol, could be used in outdoor experiments to give the advantage of an increased throughput of data, especially if a multi-track tape recorder such as the Nagra IVSJ is used to record microphone responses for subsequent analysis in the laboratory.

The recorded impulses could then be studied in the time domain to identify the energy arriving directly from the source or from other reflective paths. This would allow the meteorological effects on sound following these various paths to be studied separately and so isolate the complication of a finite impedance ground plane.

In the model scale the impulse source may be conveniently provided by a spark produced by the discharge in air of a high potential which may be obtained from a car ignition coil or a charged high voltage capacitor (42).

12.5 Air Turbulence in the Model

No attempt was made in the work reported here to modify the turbulent structure of the air flow produced by the wind chest. However, it may be possible to represent typical outdoor day-to-day variations in wind turbulence by the use of various-shaped small scale obstuctions placed on the surface of the model table upwind of the measurement site.

12.6 Computer Prediction of Observed Effects

The review papers by Piercy, et al on noise propagation in the atmosphere (i) and by Kurze on noise reduction by barriers (12), amongst others, indicated that there are a number of algorithms designed to predict sound levels in situations relatable to some extent to the experimental situations of this work. It may be insturctive to implement some of these techniques on the mainframe computer. A model to explain the observed effects discussed in Chapter 11 may them be formulated by development and manipulation of particularly suitable algorithms to fit the data obtained.

REFERENCES

(1) J.E.Piercy, T.F.W. Embleton and L.C. Sutherland, "Review of Noise Propagation in the Atmosphere", J.Acoust. Soc.Am. 61(6), 1403-1418 (1977).

(2) T.F.W. Embleton, J.E. Piercy and N.Olsen, "Outdoor Propagation over Ground of Finite Impedance", J. Acoust. Soc. Am. 59, 267-277 (1976).

(3) K.V.Ingard, "On the Reflection of a Spherical Wave from an Infinite Plane", J. Acoust. Soc. Am. 23, 329-335 (1951).

(4) K.B.Rasmussen, "Sound Propagation over Grass Covered Ground", J. Sound Vib. 28(2), 247-255 (1981).

(5) M.E.Delany and E.N. Bazley, "Monopole Radiation in the Presence of an Absorbing Plane", J. Sound Vib. 13, 269-279, (1970).

(6) C.I. Chessel, "Propagation of Noise along a Finite Impedance Boundary", J. Acoust. Soc. A. 62, 825-836. (1977).

(7) S.I. Thomasson, "Sound Propagation above a layer with a Large Refractive Index", J. Acoust. Soc. Am. 61, 659-674, (1977).

(8) K. Attenborough, "Predicted Ground Effect for Highway Noise", J.Sound Vib. 81(3), 413-424 (1982).

(9) S.Simpson and D.C. Hathersall, "Sound Propagation over Surfaces Consisting of Hard and Soft Areas", Proc. Inst. Acoust. (Outdoor Sound Propagation), 5-8 (1981).

(10) S.N. Chandler-Wilde and D.C. Hathersall, "Diffraction at an Imhomogeneous Plane: The Boundary Integral Equation Method", Proc. Inst. Acoust. 6(4), 181-187 (1984).

(11) S.A. Petrusewicz and D.K. Longmore (Eds), "Noise and Vibration Control for Industrialists" (Elek Science, London, 1974), Chapter 5.

(12) V.J. Kurze, "Noise Reduction by Barriers", J. Acoust. Soc. Am., 55(3) 504-518 (1974).

(13) E. Skudrzyk, The Foundations of Acoustics, (Springer, New York, 1971), Chapter XXIV.

(14) J.B. Keller, "Geometrical Theory of Diffraction" J. Opt. Soc. Am., 52, 116-130 (1962).

(15) S. W. Redfearn, "Some Acoustical Source-Observer Problems", Phil. Mag. Ser. 7, No. 30, 223-236 (1940).

(16) Z. Makaewa, "Noise Reduction by Screens", Mem. Faculty of Eng. Kobe Univ. 11, 29-53 (1965).

(17) V.J. Kurze and G.A. Anderson, "Sound Attenuation by Barriers", Appl. Acoust. 4, 35-53 (1971).

(18) T.F.W. Embleton, "Line Integral Theory of Barrier Attenuation in the Presence of the Ground", J. Acoust. Soc. Am. 67(1) 42-45 (1980).

(19) T. Isei, T.F. W. Embleton and J.E. Piercy, "Noise Reduction by Barriers on Finite Impedance Ground", J. Acoust. Soc. Am., 46-58, 1980.

(20) W.C. Elmore and M.A. Heald, "Physics of Waves" (McGraw-Hill-Kogakusha, Tokyo, 1969).

(21) T.Kawai, K. Fujimoto and T. Itow, "Noise Propagation around a thin half plane", Acustica, 38, 313-323 (1978).

(22) S-I. Thomassen, "Diffraction by a screen above an Impedance Boundary", J. Acoust. Soc. Am. 63(6), 1768-1781 (1978).

(23) M.E. Delany and E.N. Bazley, "Acoustical Properties of Fibrous Absorbent Materials", Appl. Acoust. 3, 105-116 (1970).

(24) Z. Makaewa, "Noise Reduction by Screens", Appl. Acoust. 1, 157-173 (1968).

(25) A.D. Pierce, "Diffraction of Sound Around Corners and over Wide Barriers", J. Acoust. Soc. Am., 55(5), 941-955 (1974).

(26) H. G. Jonassen, "Diffraction by Wedges of Finite Acoustic Impedance with Application to Depressed Roads", J. Sound Vib. 25, 577-585 (1972).

(27) E.S. Ivey and G.A. Russell, "Acoustical Scale Model Study of the Attenuation of Sound by Wide Barriers", 62(3) 601-606 (1977).

(28) J.E. Masiak, "Model Studies of Acoustical Barriers", Master Thesis MIT, Cambridge, Mass., 1973.

(29) J.L. Lumley and H.A. Panofsky, "The Structure of Atmospheric Turbulence", (Wiley, New York, 1964).

(30) V. Ingard, "A Review of the Influence of Meteorological Conditions on Sound Propagation", J. Acoust. Soc. Am., 25, 405 (1953).

(31) A.R. Kriebel, "Refraction and Attenuation of Sound by Wind and Thermal Profiles over a Ground Plane", J. Acoust. Soc. Am., 51(1), 19-23 (1971).

(32) R. DeJong and E. Stusnick, "Scale Model Studies of the effects of Wind on Acoustic Barrier Performance" Noise Control Engineering 6(3) (1977).

(33) W.E. Scholes, A.C. Salvidge and J.W. Sargent, "Field Performance of a Noise Barrier", J. Sound Vib. 16, 627-642 (1971).

(34) W.E. Scholes, A.C. Salvidge and J.W.Sargent, "Barriers and Traffic Noise Peaks", Appl. Acoust. 5, 205-222 (1972).

(35) P.H. Parkin and W.E. Scholes, "The Horizontal Propagation of Sound from a Jet Engine Close to the Ground at Hatfield", J. Sound Vib. 2, 353-374 (1965).

(36) V.I. Tatarski, "The Effects of the Turbulent Atmosphere on Wave Propagation", (Ketor, Jerusalem, 1971).

(37) C.G. Little, "Acoustic Methods for the Remote Probing of the Lower Atmosphere", Proc. IEEE 57. 571-578, (1969).

(38) E.H. Brown and S.F. Clifford, "On the Attenuation of Sound by Turbulence," J. Acoust. Soc. Am., 60, 788-794 (1976).

(39) V. Ingard and G.C. Malling, Jr., "On the Effect of Atmospheric Turbulence on Sound Propagated over Ground", J. Acoust. Soc. Am. 35, 1056-1058 (1963).

(40) G.A. Daigle, J.E. Piercy and T.F.W. Embleton, "Effect of Atmospheric Turbulence on the Interference of Ground Waves near a Hard Boundary" J. Acoust. Soc. Am., 64, 622-630 (1978).

(41) G.A. Daigle, "Diffraction of Sound by a Noise Barrier in the Presence of Atmospheric Turbulence", J. Acoust. Soc. Am., 71, 847-854 (1982).

(42) M.Barron, "The Feasibility of Objective Acoustic Testing in 1:50 Scale Models of Auditoria", Acoustics Letters, 1, 44-48, (1977).

(43) N.W Heap, "Scale Modelling of Sound Propagation over Flat Unobstructed Absorbing Terrain".

(44) J.E. Piercy and T.F.W. Embleton, "Effect of Ground on Near-Horizontal Ground Propagation", Trans. Soc. Auto. Eng., Section I 83, 928-936 (1974).

(45) W.J. Weller, "Assembly Level Programming for Small Computers", (Heath, Massachusetts, 1975), Chapter 9.

(46) Course Notes, "Constant Temperature Anemometer", Hot Wire Anemometry, Cranfield Institute of Technology, 1980.

(47) E.N.Bazley, "Sound Absorption in Air at Frequencies up to 100 kHz", NPL Acoustics Report AC 74 (1976)

(48) M.L. Gayford, "Acoustical Techniques and Transducers" (Macdonald and Evans, London, 1961).

(49) H.Davies, "Modelling Materials for Acoustic Scale Models", MIT Dept., Mech. Eng. Report, (1974).

(50) D.J. Tritton, "Physical Fluid Dynamics", (Van Nostrand).

(51) Rothamstead Experimental Station "GENSTAT: A General Statistical Language", (REF, 1980)

(52) N. Hampshire, "The PET Revealed", (Nick Hampshire Publications, 1978)

ACKNOWLEDGMENTS

The author wishes to thank the Science and Engineering Research Council for the funding through a Research Studentship, of the work reported in this thesis, and Liverpool Polytechnic Physics Department for the use of equipment and facilities.

Appendix A. Control of Measurement Equipment

This appendix details the requirements for the control of the equipment used in data acquisition, how data is read into the PET and in what way the data is processed. Constructional details of specially made devices are also included here.

Each item is treated separately at first and an overall scheme discussed later.

Throughout this appendix reference is made to peripheral interface adaptors (PIA). These devices are discussed in Appendix B.

A.1 The Sound Source

The control of individual components of the sound source (see section 5.2) is detailed here.

A.1.2. The Band Pass Filter

This actually consists of a low pass and a high pass Kemo filter type VBF22, placed sequentially in the signal path. These devices can give a cut-off frequency in the range of 0.1Hz to 100KHz, which is either manually selectable, using front panel knobs, or computer selectable, using TTL gates accessed through a rear-panel connector.

Cut-off frequencies are specified in tens, units and the appropriate base ten exponent (from 10^{-1} to 10^{3}). The tens and units are in the form of

Binary Coded Decimal (BCD) words, whilst the multiplier is set by applying a logic law to one pin out of the choice of five.

The required cut-off frequencies are most efficiently calculated using BASIC. Firstly the centre frequency is determined as double the previous centre frequency, originally set to 250 Hz, and then the lower and upper cut-off frequencies are calculated from:

$$f_l = f_c . 2^{-\frac{1}{2}}$$

and $$f_u = f_c . 2^{\frac{1}{2}} = 2f_l$$

where f_c = centre frequency

f_l = Lower cut-off frequency

f_u = Upper cut-off frequency

The first two significant digits of these values are then found by repeated divisions by 10 until the number is less than 100.

Using the POKE instruction the BASIC interpreter of the PET places a specified decimal number in a memory cell in 8 bit hexidecimal form. However, it is required to produce two 4-bit BCD codes so the most significant digit of the decimal number is multiplied by sixteen then added to the second significant digit before being used in the POKE instruction.

The operation is illustrated here for the lower cut-off frequency corresponding to a centre frequency of 1KHz.

$$f_c = 1000$$

$$f_1 = 1000 \times 2^{-\frac{1}{2}} = 707.107$$

$$f_1/10 = 70.7107$$

Rounded integer of $f_1/10 = 71$

Required BCD codes are:

High order	0111
Low order	0001

Therefore the correct POKE instruction is

POKE memory, $7 \times 16 + 1$

where "memory" = the address of the register in an MCS 6535 peripheral interface adaptor, PIA (see Appendix B). The 16-bit binary word stored in the register will be 01110001.

The filter control input ENTER STROBE should be low for the data to be input to the filter. An output, ACKNOWLEDGE RESPONSE, reflects the state of the ENTER STROBE.

Each filter has a four-bit address selected by switches at the rear of the filter. Since only two filters were used the switches were set to all zero or all one and the address lines on each filter connected together. In this way only one line from the PIA was needed to address one filter or the other.

The PIA is configured so that the data Port A outputs the units and tens whilst data Port B outputs the range multiplier and controls the strobe and address line:

PAØ - PA3	Units
PA4 - PA7	Tens
PBØ	ENTER STROBE
PB1 - PB5	Range Multiplier
PB6	Address
PB7	ACKNOWLEDGE RESPONSE

A.1.3. The Electronic Gate

This integrated circuit, type AD7512, is capable of passing an analogue signal (i.e. one that may go above or below signal ground), but is switched using TTL levels of +5 volts or 0 volts. This makes it possible for a signal from the microcomputer to allow or inhibit the signal to the loudspeaker.

A.1.4 The Attenuator

The basis for this circuit was the Motorola electronic attenuator integrated circuit, type MC3340. It is possible to configure this device as an AC amplifier with gain controlled by an external resistor. Using integrated circuit analogue switches, different values of gain resistor can be incorporated into the circuit, therefore digital signals derived from the microcomputer can be used to control the attenuation of the noise signal. See Section (5.2.3). The eight analogue switches were controlled by the eight lines of a data port from a MCS 6532 PIA. The resistor to be included in the attenuator circuit could then be chosen by applying a high level from the data port to the appropriate switch.

It was normal practice to pre-set the eight resistors in such a way that moving from one resistor to the adjacent one increased the attenuation of the analogue signal by a constant number of decibels, either one or two, depending on requirements. Therefore, to increase attenuation a logic 1 was stepped through the register from bit 0 to bit 7(i.e. a decimal value of 1 to 128).

Note that it is possible to have more than one data line high at a time, causing two parallel reistors to be included in the attenuator circuit. However, due to the non-linear fashion in which parallel resistors combine, coupled with the non-linear attenuation/resistor characteristic of the attenuator circuit.this feature was not used.

A.2 The Digital Event Recorder

A.2.1 The Kemo Analogue Memory

This device is designed to digitise an electronic analogue signal over a set time and store the resulting eight bit binary numbers in a semi-conductor memory consisting of a fixed number of elements. This data can then be repeatedly re-converted to an analogue signal allowing for inspection of transient signals on an oscilloscope, X-Y plotter or chart-recorder. It is also possible to obtain the digital data in a bit-parallel, byte-serial mode.

The clock rate of the analogue to digital converter (ADC) is provided by either an internal clock, variable in fixed steps, or by an external clock. The initiation of the digitisation process can be triggered internally when the input signal exceeds a pre-set level, or by an external TTL pulse. The control signals available are listed below:

SIGNAL	INPUT OR OUTPUT	DESCRIPTION
RECORD	IN or OUT	Normally high. A low arms the device ready for data capture.
PLAYBACK	IN or OUT	Normally high. A low places the device in a mode to display the stored data on CRO OR X-Y plotter etc.
EXT TRIGGER	IN	If external trigger has been selected on the front panel a transition on this line will initiate the recording of data. The effective transition (positive or negative) is also front panel selectable.
EXT CLOCK	IN	If external clock has been selected, then the rate of pulses on this line dictates the analogue to digital conversion rate in record or the display rate in playback.
STATUS	OUT	High during record and low during playback.
DATA VALID	OUT	This line gives a low pulse after a byte of data has been placed on the data bus.
TRIGGER	OUT	Low when armed. High after a trigger.
SEL 1) SEL 2)	IN	A low determines which channel is output to the data bus.
PEN LIFT	OUT	High for duration of output sweep.
REFERENCE IN) REFERENCE OUT)	-	A single bit channel which passes through the 4K memory.

An MCS 6522 was used to interface the Analogue memory to the microcomputer, primarily for the ability to produce an automatic low pulse on the CA2 control line for one machine cycle after reading or writing the Input Register A. The CLOCK on the Analogue Memory was connected to the CA2 line and the data port to the peripheral Register A. Peripheral Register B was then used to manage the various control lines and to allow for override of the independent triggering modification (Section A.2.1), which will be necessary when setting the auto-attenuator (Section 5.3.1). Because the duration of the CA2 pulse was only one machine cycle (1μs.) a pulse stretcher circuit was added to the auxiliary board. The clock pulses were taken in through a spare pin on the rear 37-way connector and into the auxiliary board. It then formed the input to a 74121 integrated circuit, used as an astable multivibrator. Because of the shortage of spare positions on the auxiliary board edge connector, the output of the astable was connected to the vacant fourth channel output. This meant that the modified clock pulses were brought out to a front panel BNC connector. This was linked to the front panel external clock input.

It was essential that on recording data the clock rate should be as high as possible in order to comply with sampling theorem, i.e. that the Nyquist rate should be achieved for the maximum frequency in order to avoid signal aliasing. A programme loop is required to give clock pulses until the memory is full. If a software counter is updated on each pass through the loop, the counter can be repeatedly checked and a "jump out of loop" instruction given when 4096 pulses have been delivered. However, this technique has the problem that the counter must cross (1 page = 256 memory cells) producing a long pulse at each page boundary, in addition to which, updating and interrogating the counter reduces the clock frequency. The following alternative method was devised to overcome these problems.

A high to low transition on the status control line indicates the completion of a data capture. This was detected by the MCS 6522, through its CA1 line which then interrupts the microprocessor. The clock pulses can then be delivered by an uncontrolled loop which is halted by this interrupt, In this way a clock period of 7 μs (equivalent to 143 kHz) was attained. See the flowchart in Fig. A.1.

Independent Triggering of the Analogue Memory Channels

After placing the analogue memory in the RECORD mode the capture of data in each channel is initiated by an externally derived trigger pulse or by the input exceeding an operator-defined voltage level. In the original design a trigger level on either channel causes both to start recording data. Because of the time doscrepancy between the acoustical signal arriving at the two microphones in a typical geometry used in this work the channel associated with the far microphone would be part filled with background information. Independent triggering was arranged by adding the circuit of Fig. A.3 to the near microphone channel. It was located in the auxiliary board position of the equipment.

The output of the existing trigger level comparator is connected to a spare position on the rear edge connector (a22). It is then used to reset a counter which then counts 4096 clock pulses before applying a logic low to the clock control circuitry of the near channel. This is done by wiring to the switch at the top left side of the front panel at the side labelled "Hold on Playback". The channel will then be placed in PLAYBACK mode.

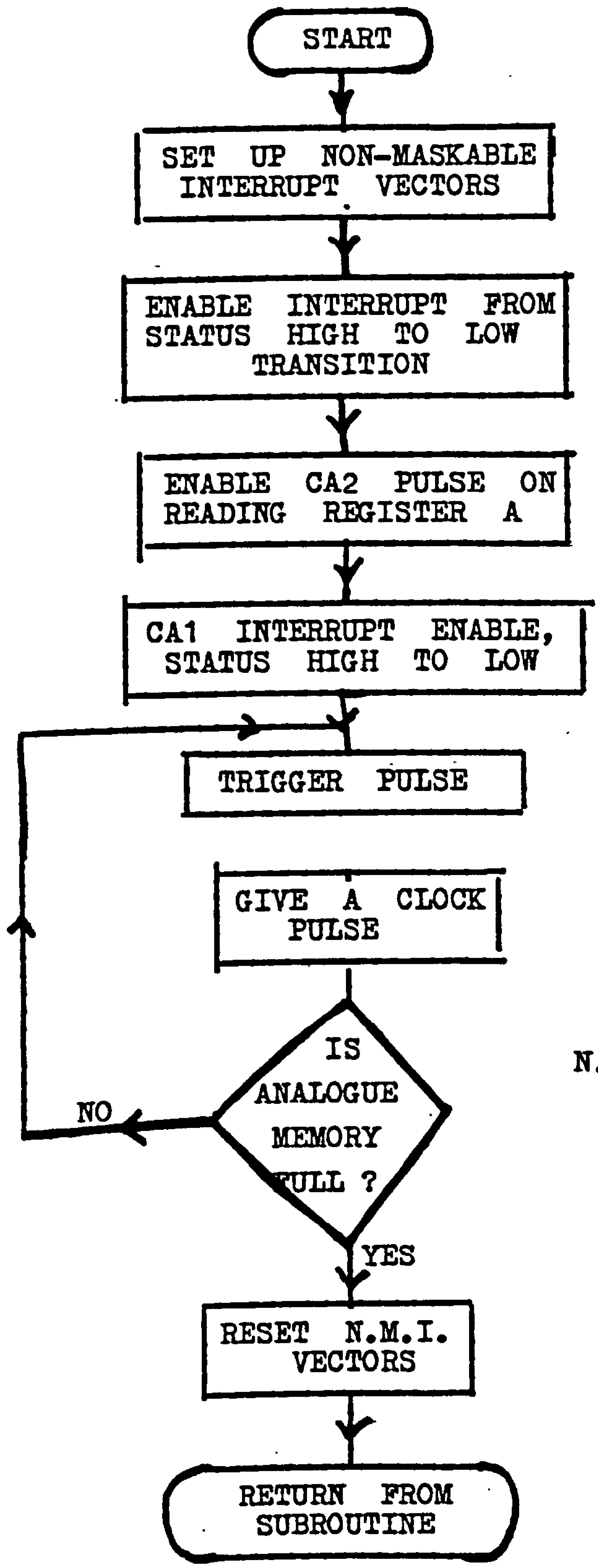

N.B. THIS DECISION IS UNDER HARDWARE CONTROL (SEE TEXT)

Fig. A.1 Servicing of Kemo Analogue Memory

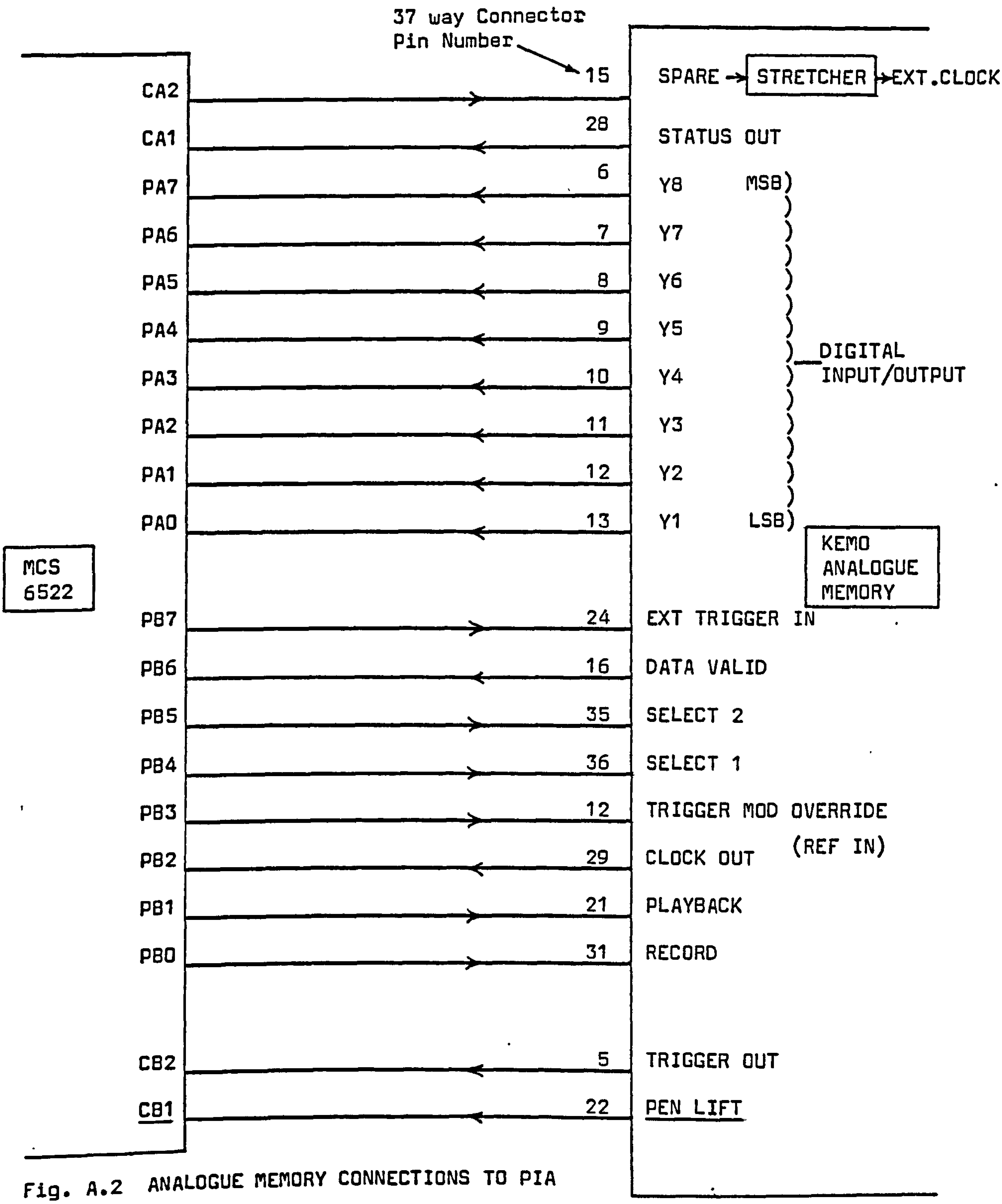

Fig. A.2 ANALOGUE MEMORY CONNECTIONS TO PIA

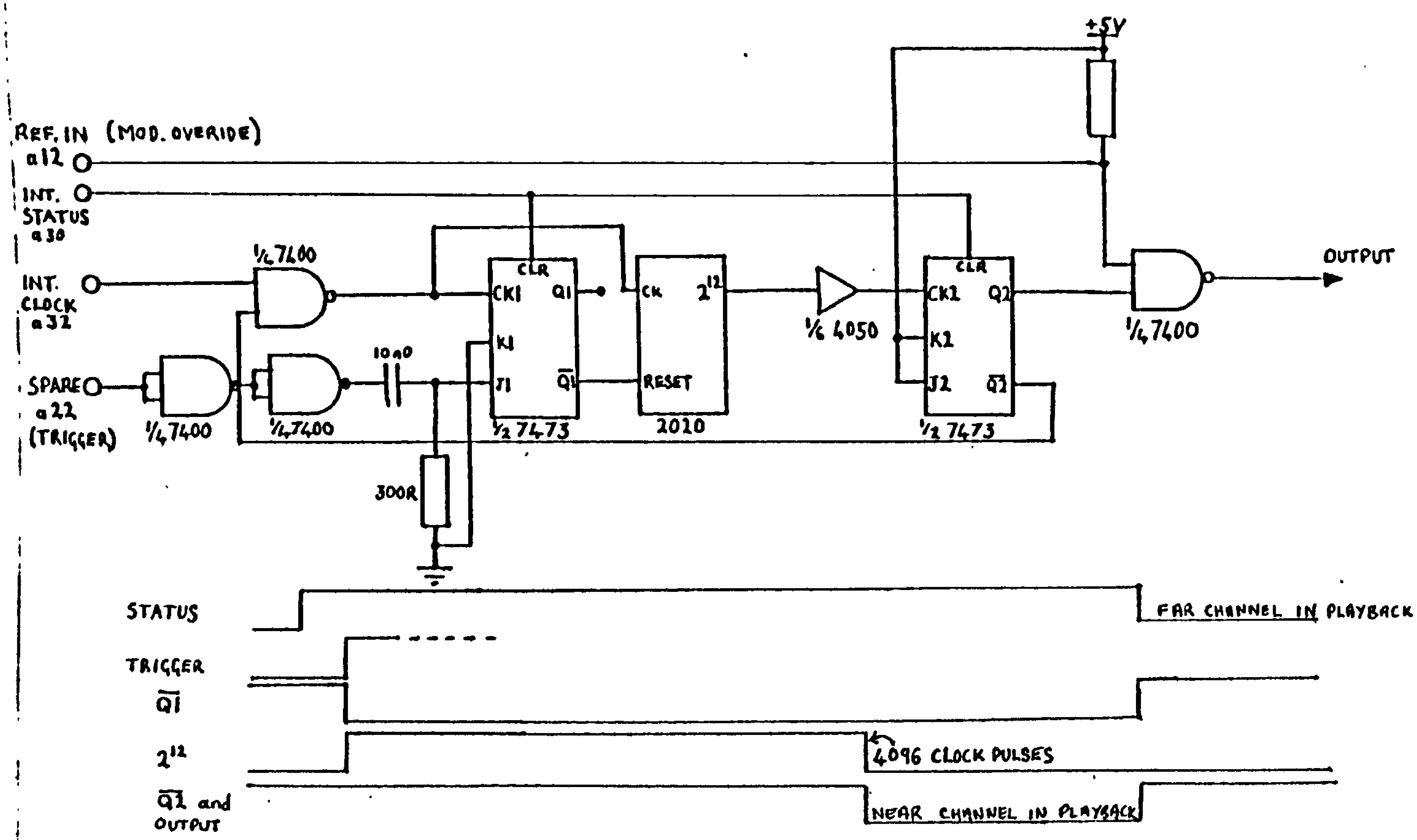

Fig A.3 Independent Triggering Modification to Kemo Analogue Memory

Note that the switch must be kept in its central position to avoid the outputs of two logic gates being connected together.

The REFERENCE IN input was used to over-ride the action of this modification, such as required in the setting up of the auto-attenuator.

A.2.2 The Datalab DL901 Transient Event Recorder

The output from the hot wire anemometer was captured in a Datalab DL901 transient event recorder in coincidence with the capture of the acoustic data in the Analogue Memory. In order to achieve this the DL901 was armed prior to applying the external trigger from the microcomputer which was also responsible for initiating the sound burst. The captured data could then be transferred to the microcomputer in a separate subroutine. See flowchart in Fig. A.4.

Digital data is taken from the DL901 using the handshaking control lines available at a 24 way rear mounted connector, which are indicated in Fig. A.5. below.

The PIA used for this was a MCS6535, using port A for the data bus and port B for the control signals.

Because the event recorder has a dynamic RAM the time between consecutive word requests must be less than 1 ms or the refresh cycle will cause a time-out of about a second. To overcome the possibility of word requests greater than 1 ms the data was transferred in a block of 1024 bytes, rather than requesting and processing the data a byte at a time. The top

ARM SUBROUTINE

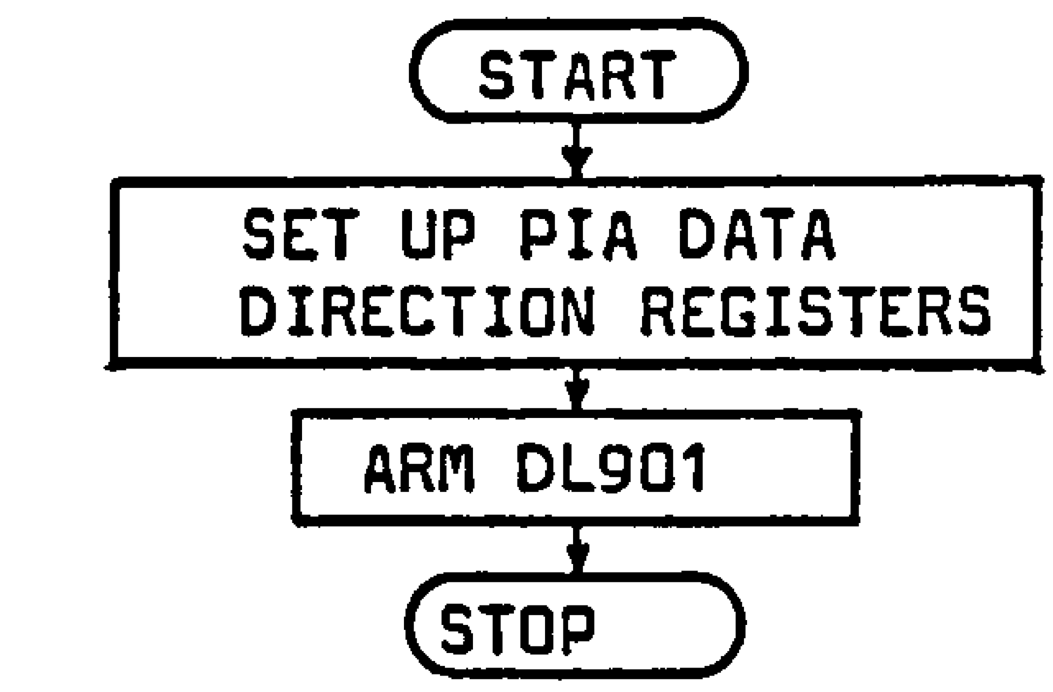

DATA TRANSFER SUBROUTINE

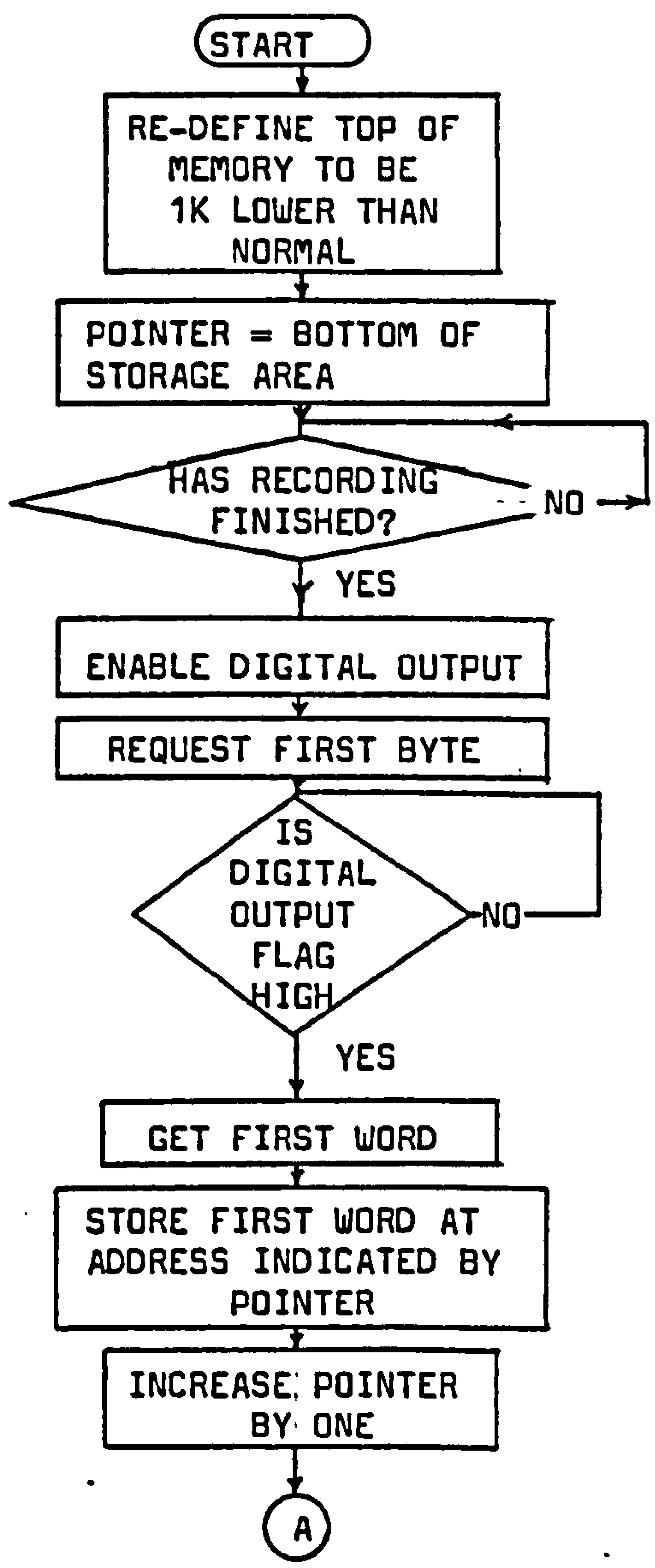

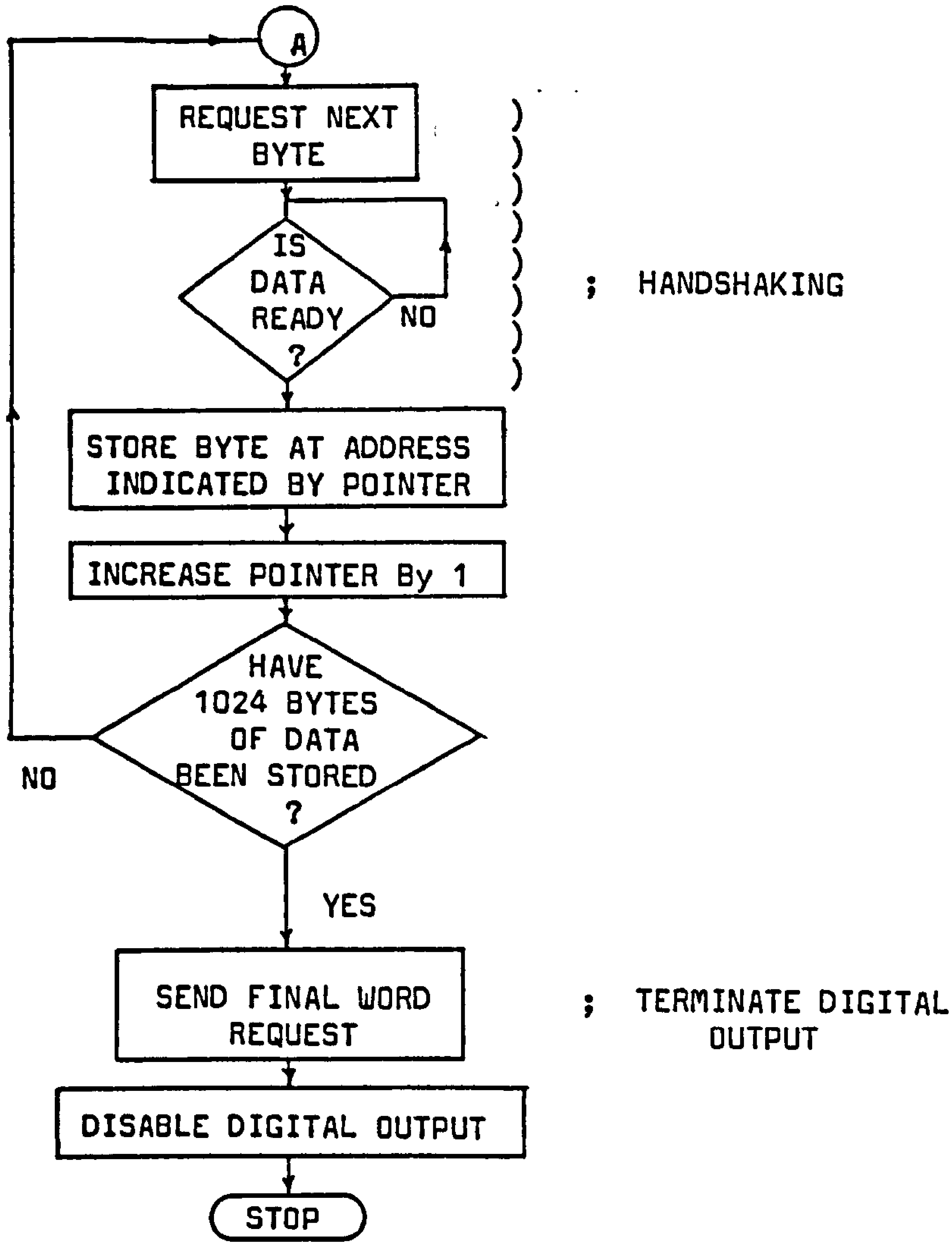

Fig. A.4 Servicing of Datalab DL901 Event Recorder.

DL 901 Signal	Input or Output	PIA Connection	Remarks
Word Request	In	PBØ	Requests new data to be put on the bus.
Data Ready	Out	PB1	Indicates valid data on the bus.
Cycle	Out	PB2	Indicates recording in progress.
Digital Output Flag	Out	PB3	Indicates digital output mode in progress.
Digital Trigger	In	PB4	Triggers the recording made if DL901 is armed.
Digital Output enable	In	PB5	Allows data to be output to data bus.
Digital Output request	In	PB6	After enable, this initiates output.
Digital Arm	In	PB7	Arms DL901 ready for triggering.

Fig. A.5 Signals for Datalab DL901 Event Recorder.

1K of the microcomputer memory was used to house the captured data and was protected against encroachment from the operating system be re-defining the top-of-memory vectors.

A.3 The Wind Direction Indicator

The description of this device appears in Section 5.6. Using an MCS 6522 PIA the reference pulse is detected on the CB2 control line after which the pulses from the reflective optodevice are allowed to decrease a pre-set value stored in timer 2 of the PIA through the PB6 line. The pulses are counted until the coincidence pulse is detected on the CB1 control line. The value in timer 2 is then subtracted from the pre-set value, the result being half the angular displacement in degrees from the reference point to the wind direction. (The pulses appear every 2^o). This value is stored, but doubled on recall in the calculation programme.

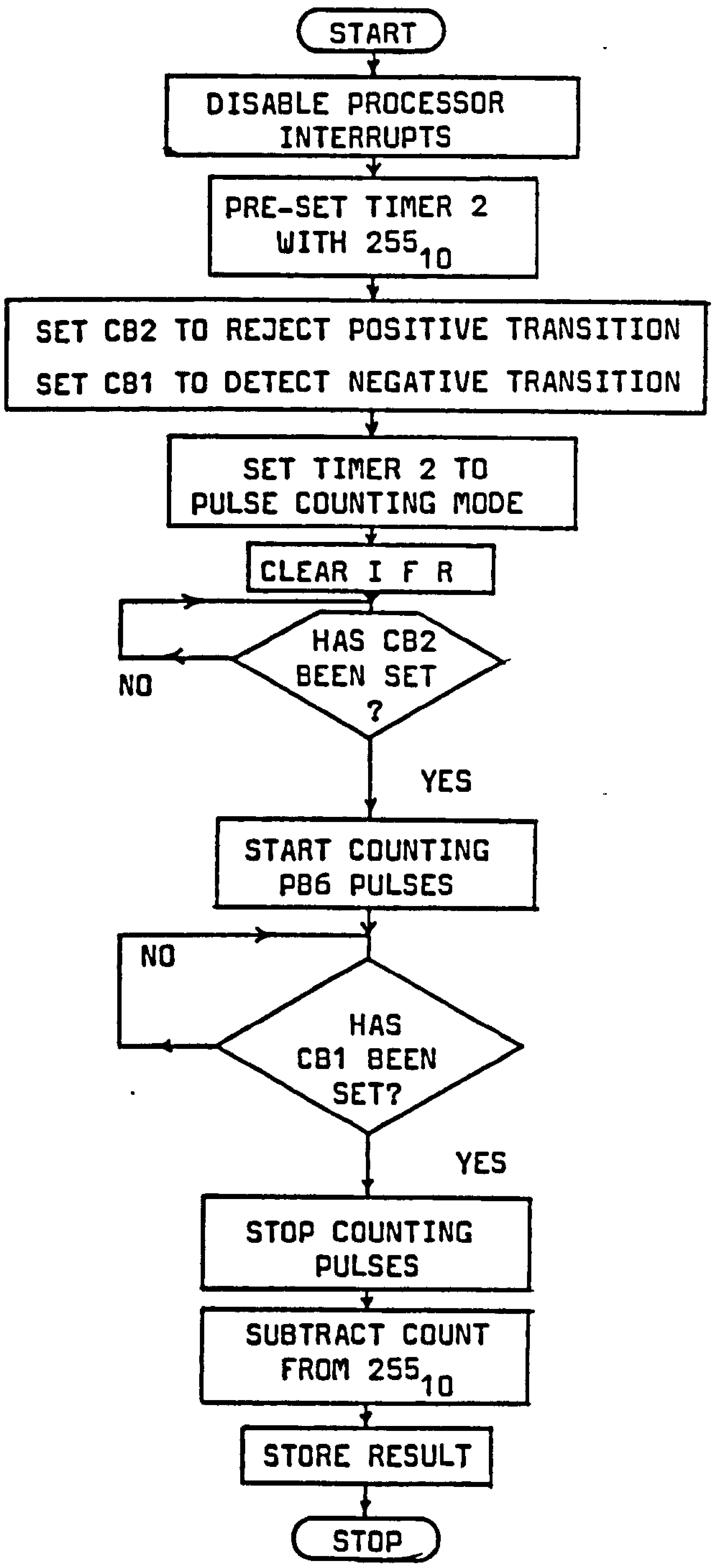

Fig. A.6 Wind Direction Sensor Flowchart.

A.4 The Electronic Thermometer

As for the wind direction sensor, an MCS 6522 in a pulse counting mode was employed to record the frequency of the output of the thermometer. Pulses were counted for one second, the duration of which was timed by counting 60 (i.e. sixtieths of a second) "jiffies" on the microcomputer's timer.

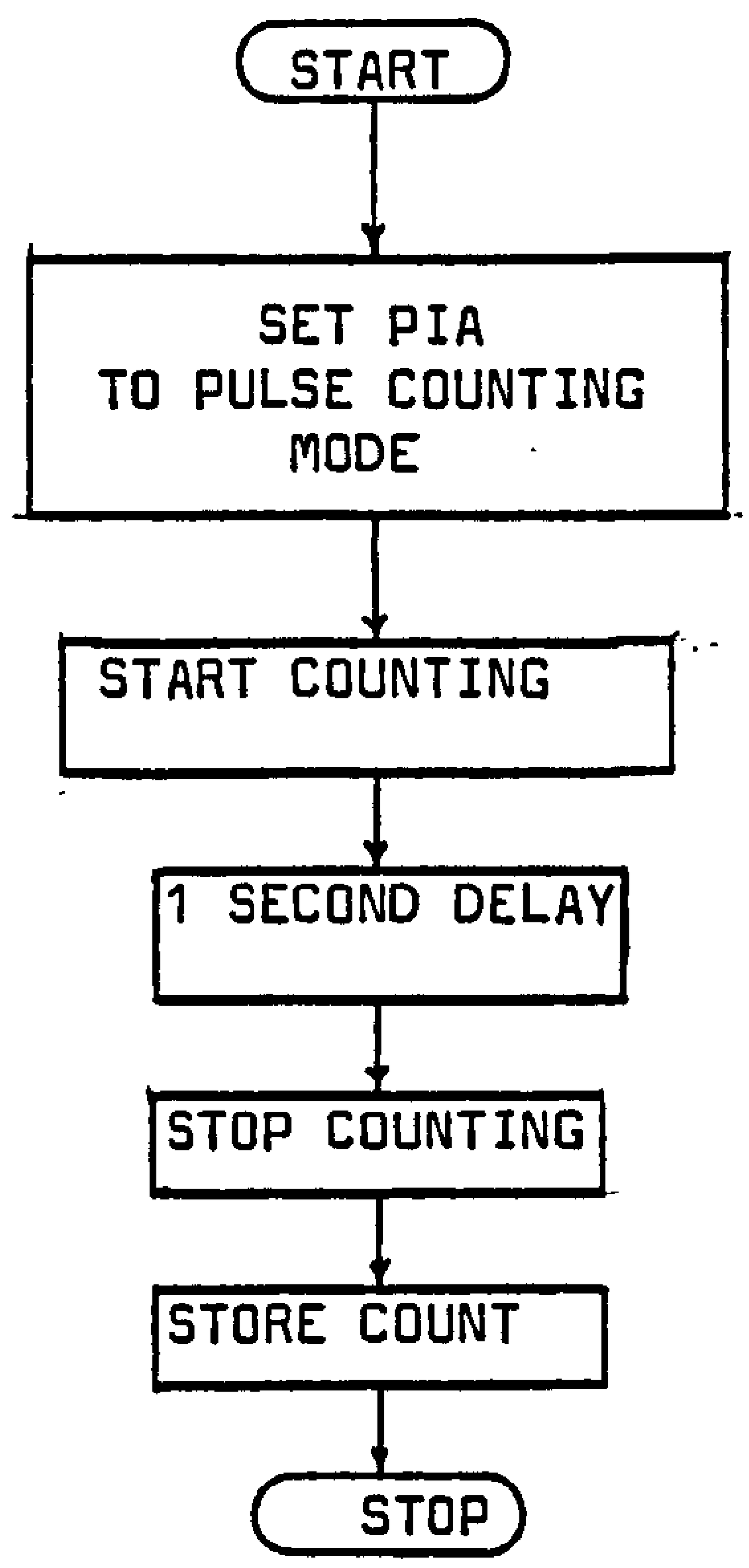

Fig. A.7 Electronic Thermometer Flowchart.

A.5 Microcomputer Control of the PIA's

The PIA's were incorporated into the PET system by using the Memory Expansion Port, which makes available the address and data bus and the various control lines used by the microprocessor.

As with the PIA's already used by the microcomputer, the additional ones were incorporated into the memory map in order to appear as RAM to the microprocessor. A convenient area was that reserved for expansion (See Fig. 5.9), although certain modifications to the microcomputer's logic circuitry were necessary in order to achieve this: Data is transferred between RAM and the microprocessor through tri-state buffers. When ROM is addressed, logic circuitry holds these buffers in a floating state, allowing data to be read directly from the addressed memory cell. The extra logic circuitry was needed to open up a block of expansion ROM in order to provide bi-directional communications for PIA's. Block 9 (i.e. memory locations 9000_{16} to $9FFF_{16}$) was used, leaving blocks A and B for expansion ROM to allow for the use of commercial ROM chips, such as Kingston Computer's NETKIT which was required to communicate with the DEC 20 mainframe as discussed in Section 12.1.2 .

Addressing the PIA's

On connecting the data part of the PIA to the system data bus, two-way communications between the various internal registers and central processor unit (CPU) are possible only if the required register is correctly addressed. Depending on the type to be used (in this project either the MCS 6535 or MCS 6522) the PIA has two or three chip select (CS) lines, to which must be applied the specified logic high or low before the individual registers internal to the PIA are addressed using register select (RS) lines.

Within the Commodore system the top four of the sixteen address lines are connected to the inputs of a so-called "1-out-of-16" multiplexer integrated circuit type SN74150. Only one of the sixteen outputs on the device will go low, a different one for each of the 16 possible combinations of input signals. These outputs then form the "block select lines" used in selecting various memory circuits, the low output indicating in which 4K block the addressed memory resides. They are available in a buffered form on the memory expansion port. Because the additional PIA's were to be located in block 9, then signal called "BS9" was connected to one of the chip select lines on each PIA added. This circuitry was duplicated externally using the next four most significant address lines as inputs. The low output of the demultiplexer indicates in which page within a block the addressed memory resides. Connecting one demultiplexer output to the spare chip select line, up to sixteen additional PIA's could be supported within the memory block 9, leaving the eight least significant address lines to select individual registers. It should be noted that, although the MCS6535 requires all of the eight least significant lines, the MCS 6522 needs only four and so this system can be wasteful of memory capacity. However, once block 9 has been committed to input/output facilities it can not easily be partly used for anything else, and sixteen PIA's were more than sufficient for the work reported here.

Nine interface adaptors were added to the PET system and housed in a 19" rack module connected to the Memory Expnasion Port by overall screened multicore cable. Each PIA was housed on a printed circuit board which slotted into the rack and engaged with a back plane via its edge connectors.

One of these boards also contained the "page select" demultiplexer circuit and so had to be in place in the rack at all times. That board also contained the Reset circuit shown in Appendix B, Fig. B.1.

Appendix B   Microcomputer control of the PIA's

Two types of interface adapter are used in the measurement system reported in this thesis: the MCS 6522 and MCS 6532. These are both in the same family of support chips for the MCS 6502 which is the microprocessor used in the PET. The reader is referred to data sheets published by MOS Technology Inc., for details of DC and timing characteristics for these devices. In addition interface adapters,including the MCS 6522, are discussed in more detail in the "PET Revealed"(52).

B.1 The MCS 6522

The structure of this device can be broken down into three main parts: a processor interface, a peripheral interface and a series of internal registers controlling some inbuilt features of this chip.

B.1.1. The Processor Interface.

This consists of an eight bit bi-directional data bus, some control lines and addressing lines. In general the data bus and control lines are connected directly to the corresponding system lines available at the Memory Expansion Port. They are summarised below.

DB0-DB7	The bi-directional data bus. The direction of data flow is controlled by the R/W line.
R/W	Read/Write line. If this is low data will be transferred into the addressed register (Write operation), or if it is high data will be transferred out of the MCS 6522 (Read operation).

$\overline{IRQ}$ Interrupt Request. This will go low if one of several events occur, (see later), signalling to the microprocessor that the MCS 6522 needs service.

$\overline{RES}$ Reset. This clears all internal registers to zero, putting peripheral interface lines in the input state. A reset circuit was added to the PET system, see Fig. B.1, as a means of resetting the computer without the need to power down.

Ø2 Phase two clock. Data transfers take place when the phase two clock is high. It also forms a time base for the chips internal timers and shift registers, etc. (see later).

The chip is addressed by means of two chip select lines (CS1, $\overline{CS2}$) with four register select lines (RSØ-RS3) to address one of the sixteen internal registers. Addressing of the PIA's is discussed in Appendix A, Section A.6.

B.1.2 The Peripheral Interface

This contains two eight bit bi-directional data ports (PA0-PA7 and PB0-PB7), each line being configured as an input or output under the control of data direction registers (DDRA and DDRB). Each line represents one TTL load in the input mode or will drive one TTL load in the output mode, although the port B lines will also drive a Darlington transistor switch.

Each port has two control lines CA1, CA2 and CB1, CB2 which act as interrupt inputs or handshaking outputs. Port A lines can handshake data on both a read or write operation and the Port B lines can handshake data in a write operation only.

8.1.3 In-built Features

The special features of this chip include two internal timers, a shift register and two interrupt control registers. The facilities are under the control of the Auxiliary Control Register (ACR) and the Peripheral Control Register (PCR).

(a) The Serial Register

It is possible to configure the shift register (SR) to accept input data or to output its contents. Data movement is clocked under the control of Timer 2, at system clock rate or by external pulses. The shift register mode is controlled by bits 2 to 4 of the auxiliary control register.

(b) Timer 1

Timer 1 has two eight bit latches and a 16 bit counter, the latches being used to store data to be loaded into the counter which then decrements at system clock rate. Upon reaching zero an interrupt flag may be set and the timer will then disable further interrupts (one-shot mode) or will transfer the contents of the latches into the counter and will continue to decrement. In addition the timer can be instructed to invert the output on PB7. The mode of Timer 1 is controlled by lines 6 and 7 of the Auxiliary Control Register.

(c) Timer 2

Under the control of bit 5 of ACR, Timer 2 can act in the "one-shot mode" as Timer 1 or can count pulses applied to PB6. In each case an interrupt will occur on reaching zero.

(d) Interrupt Control

There are six events capable of causing an interrupt to the processor. Should one of these events occur a bit is set in the interrupt flag register (IFR)

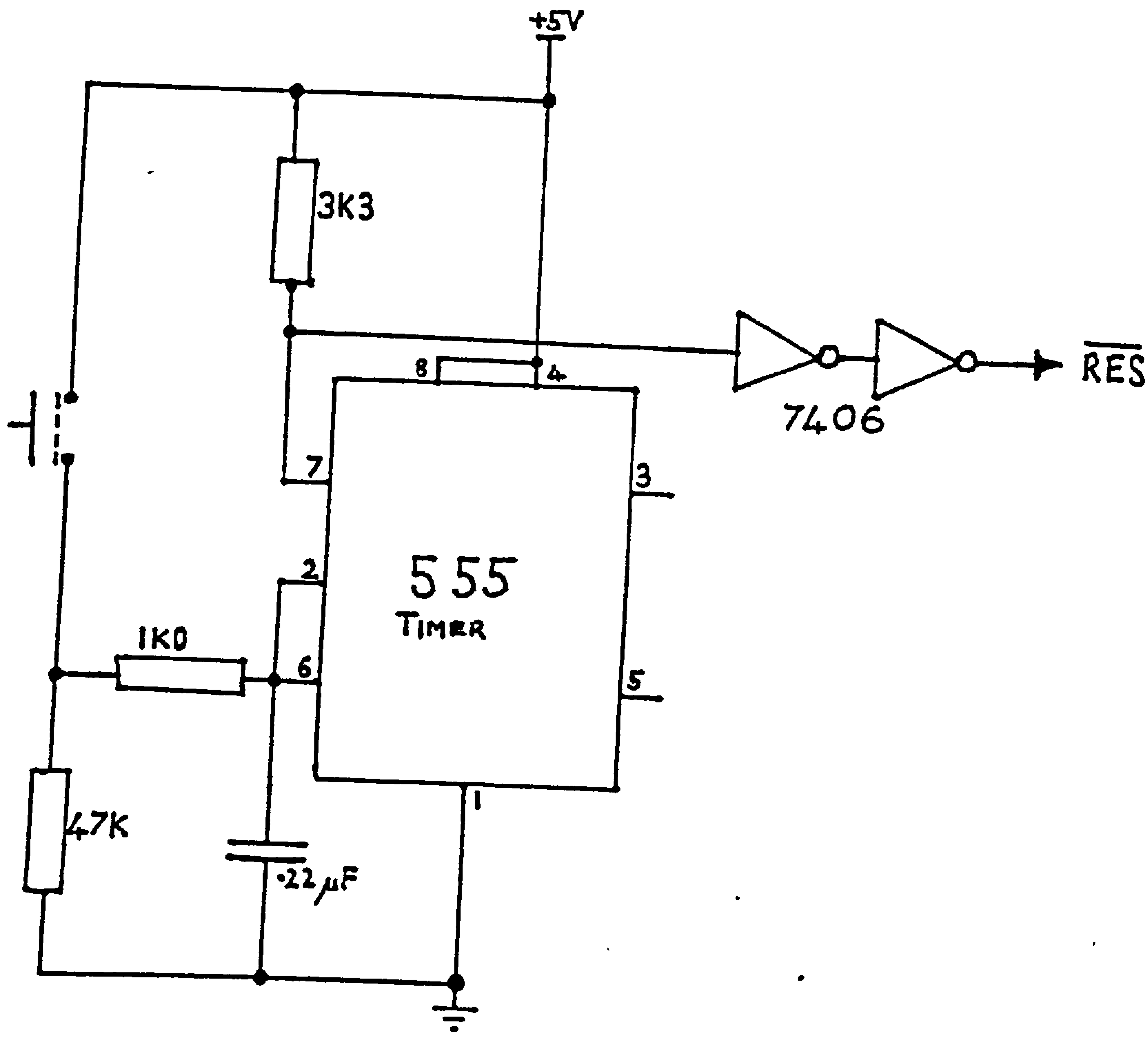

Fig. B.1 System RESET circuit.

However, the $\overline{IRQ}$ line is not pulled low unless the corresponding bit in the interrupt enable register (IER) has been previously set (under programme control).

The possible interrupt events and the bit in the IFR are:

IFRØ	Active transition on CA2
IFR1	" " " CA1
IFR2	Completion of eight shifts in the shift register.
IFR3	Active transition on CB2
IFR4	" " " CB1
IFR5	Time-out of Timer 2
IFR6	" " Timer 1
IFR7	$\overline{IRQ}$. Set if an interrupt event occurs and the corresponding Interrupt Enable bit is set.

An active transition on the control lines defined by the Peripheral Control Register.

B.2 The MCS 6532

This chip has processor and peripheral interfaces similar to those described for the MCS 6522. It does not have the in built facilities of that chip but has instead 128 bytes of RAM. In order to address the two peripheral ports, their data direction registers and the RAM there are eight register select lines.

PAGE

NUMBERING

AS ORIGINAL

Appendix C. HOT WIRE PROBE CALIBRATION

The output voltage from the anemometer is related to the fluid velocity across the hot wire probe according to King's Law:

$$V^2 = V_o^2 + BU^n$$

$$\log (V^2 - V_o^2) = \log B + n \log u$$

Where V_o is the "no-flow" voltage and B and n are constants for a particular probe. Each probe used was calibrated by plotting $V^2 - V_o^2$ against U on logarithmic axes, giving a slope of n and an ordinate intercept of log B. The source of variable air flow was a standard laboratory device consisting of a fan drawing air into a 0.2 m diameter cylinder, uniform for 4.5 m and then decreasing by 30% at the mouth of the tube to provide laminar flow. The hot-wire probe of the anemometer was centrally placed within 0.01 m of the probe, and connected to an inclined manometer, was used to determine the wind speed, U, whilst the anemometer output voltage. V was read from a digital voltmeter. A typical calibration appears in Fig C.1.

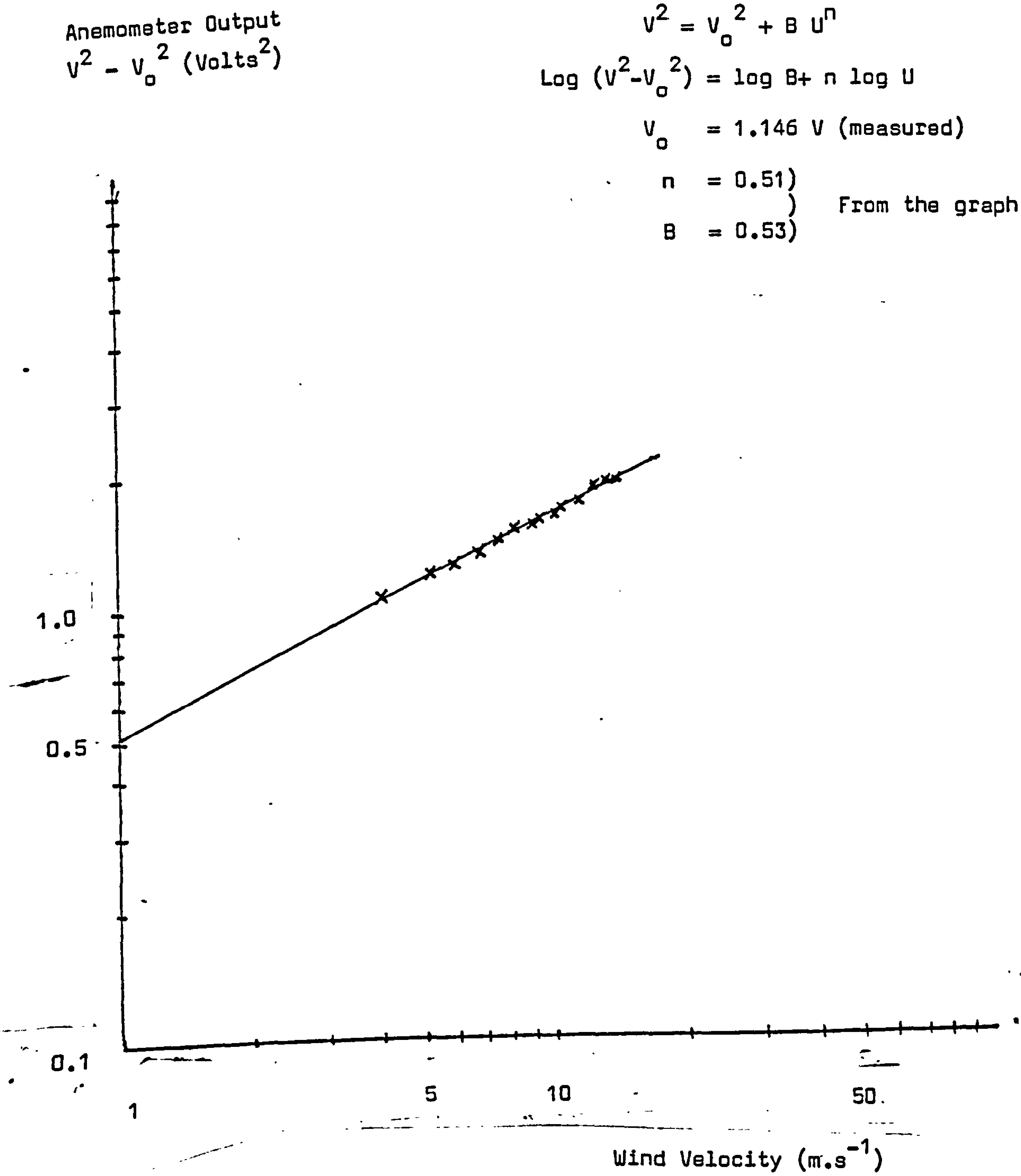

Fig. C.1 Typical Hot wire anemometer Calibration Curve.

	dB Level Diff.	Wind Turb.	Wind Speed	Temp.	Wind Dir.
	0.2365	1.3398	2.6903	25.6152	134
	1.8665	3.5226	4.5541	0.0288	54
	0.2135	2.0055	5.0715	25.7472	50
	2.7033	1.2313	7.9954	25.8932	28
	1.0429	4.1409	7.2091	26.1988	38
	2.0723	4.8310	5.9558	0.2908	38
	0.5072	4.9659	3.2977	1.0616	72
	0.2211	1.5119	1.8418	0.9136	102
4K	0.6438	4.3559	1.5316	1.2856	108
	1.8938	5.5824	2.8653	1.4416	106
	2.0479	14.8544	1.9215	1.1368	166
	1.7414	9.5383	1.9381	1.5808	168
	0.8280	5.2240	5.2156	0.3140	168
	1.3407	3.1956	4.9511	26.0312	168
	0.4923	18.2474	1.8519	25.8448	154
	1.2756	1.0801	4.9780	25.9040	186
	1.1319	1.4773	6.6469	26.1380	172
	1.4707	17.5561	3.1404	24.0612	168
	1.0982	13.8172	4.8308	24.1242	172
	1.1650	10.7945	6.7752	24.1672	178
	5.9964	[illegible]	6.7595	0.0296	190
	7.4511	14.9936	5.8606	25.9132	188
	6.9741	2.1333	7.6457	25.9204	170
	6.7138	7.7200	5.7794	25.8236	156
	6.2893	15.3067	4.7911	25.9304	244
	7.3447	4.1857	5.6132	25.9856	228
	7.0803	4.5054	8.1348	25.2312	222
	7.0053	2.0343	7.6476	25.2732	160
	7.9346	9.0194	2.4979	25.5800	160
	7.0211	1.4767	1.8712	25.7016	160
	6.9882	1.2148	2.3850	25.8464	188
	7.0956	1.1586	4.0842	25.6440	204
	6.5207	2.9914	5.6697	25.6080	214
2K	6.7265	1.5214	4.3852	25.2008	204
	6.9895	2.6316	7.3496	25.5684	174
	7.4945	1.6520	6.7639	26.0520	200
	5.4738	2.8948	5.2866	25.5192	200
	6.2105	1.4868	6.3722	25.6900	204
	7.4170	3.0558	5.4680	25.5580	208
	6.5481	[illegible]	4.7594	25.7048	210
	[illegible]	[illegible]	8.3217	25.5940	210
	7.4963	2.7342	6.5524	25.4724	186
	7.3824	1.7772	6.6588	25.7200	172
	7.1715	3.4754	6.6304	0.1588	194
	7.7643	1.0927	4.1053	0.0316	200
	7.2277	10.2957	6.2089	0.2380	218
	7.6355	3.0587	6.6720	0.1364	194
	7.8270	3.3315	6.1787	0.0720	186
	7.1669	3.0448	6.4902	0.3408	208
	7.4469	1.4390	6.4090	0.3008	198
	8.2247	2.5496	4.1492	0.2252	210
	7.7365	1.6691	6.2691	0.2108	212
	7.9494	1.1018	4.0695	0.1924	208
	6.9448	2.2150	5.2894	0.4024	208
1K	8.0926	0.9404	4.9943	25.8252	258
	7.2777	1.8501	4.9572	25.5460	260
	7.5028	1.4510	3.8391	25.9516	176
	7.0111	0.7952	5.0271	25.4228	208
	7.6451	0.4038	3.2625	0.0996	208
	9.0915	1.7473	4.2185	25.6694	210
	[illegible]	[illegible]	4.0319	25.7760	190
	5.5528	1.4601	5.9558	25.6196	214
	8.9467	3.0816	5.7336	25.9020	212
	6.0228	3.5327	7.4521	0.1448	226
	6.7454	1.4898	5.0761	26.1492	222
	7.7424	0.7952	4.6256	25.6460	234
	4.2748	5.1314	6.4749	25.7784	254
	6.1094	0.9074	7.8428	26.1464	262
	5.1160	3.9226	6.9568	0.7748	266
	6.0638	2.0586	10.9719	0.8648	264
	7.9243	2.9096	9.5030	0.6030	248
500	6.6513	2.8297	5.1941	0.6728	214
	5.5082	3.3142	3.9558	0.1484	206
	5.0048	2.7727	5.1778	25.9868	184
	6.1534	4.0239	2.2868	25.6908	218
	7.0916	5.4149	3.0128	25.3936	218
	5.2173	1.4064	6.3114	25.5484	208
	5.4744	1.8804	6.8129	25.2420	202
	5.1482	6.0281	4.1849	25.5160	178
	6.1426	7.0621	7.2305	25.5302	224
	[illegible]	[illegible]	6.6496	26.0500	246
	12.9775	1.8717	6.2067	25.6524	206
	17.1793	1.4308	6.1114	25.3980	184
	15.7448	0.7269	4.5153	25.6544	178
	12.0820	19.7373	2.9166	25.3576	164
	8.5036	2.2496	2.9656	25.5568	164
250	5.2416	1.3414	2.9008	25.2796	164
	13.9677	1.3595	2.4015	25.1617	168
	17.2127	1.8776	3.0932	25.7404	182
	11.7176	8.9164	1.5965	25.3668	186
	13.2691	15.4315	2.0773	25.3927	180
	14.2794	7.5401	4.3559	25.8948	174
	10.3771	2.0684	5.3766	25.9736	198
	11.4080	1.2575	4.9480	0.4192	192

	dB Level Diff.	Wind Turb.	Wind Speed	Temp.	Wind Dir.
	11.4080	1.2575	4.9493	0.4192	192
	12.4081	2.3487	5.1478	25.1412	166
	10.0454	1.3821	4.9804	0.7830	219
	11.0862	2.4895	6.7274	0.0210	178
	9.9019	2.6938	6.0852	26.1076	194
250	12.1847	1.7900	4.5072	0.6144	198
	11.4753	[illegible]	[illegible]	[illegible]	[illegible]
	0.1469	1.4407	2.9289	19.5848	224
	0.3940	4.9713	5.1696	19.5478	248
	0.4866	2.2976	4.7883	19.7952	278
	1.4345	1.5561	5.8363	19.5708	276
	1.8200	1.4416	4.0905	19.4684	264
	0.5851	5.5816	2.6909	19.3248	250
	1.3379	2.4974	5.5964	18.9452	206
	0.2561	2.5053	4.3494	18.8048	208
	2.8338	2.9658	7.9321	18.6198	292
	1.3482	4.1431	5.7378	18.4568	244
4K	1.5929	1.9174	10.7669	18.4928	232
	2.4962	6.7491	5.1689	19.1720	224
	0.9998	4.2565	6.0050	19.2332	236
	0.5946	3.1789	11.0487	19.7060	254
	0.3584	7.1955	3.8759	19.3430	14
	0.8806	6.0414	3.3450	19.4916	296
	0.9592	5.8479	6.2957	19.7984	324
	0.8554	25.5672	2.3461	19.4356	34
	0.6499	10.5857	2.2478	19.5412	50
	1.3954	3.2280	6.9257	[illegible]	324
	[illegible]	1.5558	3.0921	19.4712	304
	5.5764	14.7070	3.7150	19.6684	238
	4.7421	5.8232	4.7524	19.4156	262
	5.7454	8.7711	5.6595	19.4552	194
	5.6521	5.1732	8.0179	19.9384	206
	5.4014	2.7914	5.7428	20.3136	284
	5.6507	1.4013	5.8112	20.0044	246
	5.9342	2.7042	7.3111	19.7136	258
	5.8602	4.4484	5.2882	19.4744	256
	6.6378	4.2257	5.8439	19.2548	246
2K	6.4065	2.4650	7.8077	19.3640	260
	5.4456	5.8557	6.5106	19.2208	254
	4.6395	14.3560	2.2480	19.1112	260
	5.5487	3.3086	8.1491	18.7884	258
	5.4170	3.4513	11.3888	18.9912	270
	4.8842	1.0687	7.5795	18.8524	276
	5.5380	5.3165	6.9912	18.9670	284
	5.8423	2.7512	6.4364	19.1596	266
	5.3183	1.5771	6.1788	18.9428	252
	6.2091	[illegible]	6.1920	19.6228	236
	[illegible]	1.9545	11.3607	18.8376	244
	7.1983	11.1359	8.2607	19.2976	270
	7.4434	1.9106	6.5980	19.5116	248
	7.9220	2.8129	7.5669	19.7274	240
	6.6911	2.1994	6.0078	19.6500	246
	7.4997	8.1721	5.1002	19.5888	234
	6.7466	4.1282	8.5869	19.3295	218
	7.5318	4.7917	7.5188	19.0968	202
	7.4502	9.0627	9.0445	19.0956	242
	8.3606	5.6619	8.4515	18.9700	252
1K	6.6547	1.9647	5.9557	19.3760	238
	7.0522	4.2833	5.4516	19.3404	246
	7.1319	6.8446	6.3755	19.3580	258
	6.6751	5.9503	6.0007	19.4394	178
	7.5584	3.6707	2.8721	19.2272	272
	7.9651	3.2161	6.5090	19.3055	234
	7.6078	6.2904	8.6159	19.2832	242
	6.8666	5.7535	8.6518	18.9599	152
	7.1004	5.1101	9.1543	18.9900	102
	6.3542	9.4112	10.0005	19.3560	298
	2.2850	[illegible]	4.6677	17.4560	100
	5.9966	4.2093	7.2271	19.4568	332
	5.1559	7.4577	6.6062	19.3396	346
	6.0177	12.6497	4.5387	19.4772	214
	3.9633	8.5959	9.3118	19.3044	104
	3.4594	5.2909	5.5067	19.1392	204
500	3.7709	2.4755	4.0095	[illegible]	264
	8.0497	7.4718	2.6218	20.0048	236
	6.1859	2.3717	5.2052	20.3591	208
	4.5593	4.2375	5.9680	21.2960	224
	7.3459	1.6108	5.6406	22.3140	[illegible]
	6.4946	3.7693	7.8069	22.3444	228
	7.8295	5.3900	3.0286	22.0856	292
	6.9450	1.2018	1.0936	21.8592	204
	5.7111	2.1561	5.3544	22.2076	222
	7.6565	1.9114	4.5049	22.0904	200
	5.2474	7.9351	6.8097	[illegible]	322
	5.1674	4.0994	9.8460	22.1224	226
	4.7905	7.4382	4.3314	22.0396	224
	6.9339	5.1866	5.7441	[illegible]	292
	[illegible]	[illegible]	3.1197	[illegible]	352
	11.1510	[illegible]	3.3342	21.6708	236
	12.5305	4.7166	5.1606	21.6948	136
	17.1249	3.7217	9.9249	21.6792	226
	12.0471	9.1075	9.1258	21.4656	244
	16.4169	4.0109	6.4549	[illegible]	254
	13.5797	[illegible]	6.1424	21.5640	222
				[illegible]	208

	dB Level Diff.	Wind Turb.	Wind Speed	Temp.	Wind Dir.
	0.2465	1.3298	5.4961	25.4152	134
	1.8465	3.5226	4.5541	0.0288	54
	0.2135	2.0455	5.0715	25.7672	50
	2.7033	1.7314	7.8954	25.8932	28
	1.0629	4.1409	7.2091	26.1988	38
	2.0773	4.8310	5.9558	0.2908	38
	0.5872	4.9459	3.2977	1.0616	72
	0.2711	1.5119	1.8418	0.9136	102
4K	0.4378	4.3558	1.5316	1.2856	108
	1.8938	5.5824	2.8652	1.4416	106
	2.0679	14.8444	1.9215	1.1368	164
	1.7414	9.5383	1.9381	1.5808	168
	[illegible]	5.2240	5.2156	0.3140	168
	1.7407	3.1954	4.9511	26.0312	168
	6.4923	18.7474	1.8519	25.8448	154
	1.7754	1.0001	4.9780	25.9040	186
	1.1319	1.4773	6.4484	26.1380	172
	1.4767	17.5541	3.1404	25.0612	168
	1.0997	13.8172	4.8308	26.1232	172
	[illegible]	[illegible]	[illegible]	[illegible]	178
	[illegible]	[illegible]	[illegible]	0.0296	190
	7.4511	14.9936	5.8606	25.9132	188
	6.9741	2.1333	7.4457	25.9204	170
	8.7138	7.7200	5.7794	25.8236	156
	6.7883	15.3067	4.7911	25.9304	244
	7.3447	4.1857	5.4137	25.9856	228
	7.0803	4.5054	8.1348	25.2312	222
	7.0053	7.0343	7.4476	25.2732	160
	7.9346	9.0194	7.4979	25.5800	160
	7.0211	1.4767	1.8712	25.7016	160
	6.9987	1.7148	7.3850	25.8464	188
	7.0956	1.1584	4.0842	25.6440	204
	6.5207	2.9916	5.4497	25.6080	214
2K	6.7765	1.5214	6.3952	25.3008	204
	6.9895	2.4316	7.3446	25.5684	174
	7.4945	1.4520	6.7659	26.0520	200
	5.4738	2.8948	5.7866	25.5192	200
	4.2105	1.4846	4.3722	25.6900	204
	7.4176	3.6558	5.4480	25.5586	208
	[illegible]	[illegible]	[illegible]	[illegible]	210
	[illegible]	[illegible]	6.4012	25.5940	210
	7.4561	2.7342	6.5524	25.4724	186
	7.3824	1.7772	6.6588	25.7700	172
	7.1715	3.4754	6.6304	0.1588	194
	7.7643	1.0927	6.1053	0.0316	200
	7.2777	10.2957	6.2089	0.2380	218
	7.6355	3.0542	6.4720	0.1364	194
	7.8270	3.3315	6.1787	0.0720	186
	7.1669	3.0448	6.4902	0.3408	208
	7.4469	1.4390	6.4090	0.3008	198
	8.2747	2.5496	6.1492	0.2252	210
	7.7365	1.4491	6.2491	0.2108	212
	7.9494	1.1818	4.0655	0.1924	208
	6.9648	2.2150	5.3894	0.4024	208
	8.0976	0.9484	4.9943	25.8252	258
1K	7.2777	1.8501	4.3577	25.5460	260
	7.5678	1.4510	3.8391	25.9516	176
	7.8111	0.7952	5.0271	25.6228	208
	7.6450	0.4018	3.2625	0.0996	208
	[illegible]	[illegible]	[illegible]	[illegible]	210
	[illegible]	[illegible]	4.0319	25.7760	190
	5.5798	1.4401	5.9558	25.6196	214
	8.9467	3.0816	5.7336	25.9020	212
	6.0778	1.7137	7.4571	0.1448	226
	6.7454	1.4998	5.0741	26.1492	222
	7.7454	0.7897	4.4754	25.6460	234
	4.5748	5.1314	4.4769	25.7784	254
	6.1698	0.9874	7.8428	26.1464	262
	5.1140	1.5986	4.9558	0.7748	266
	6.0638	7.0586	10.9719	0.8648	264
	[illegible]	1.0364	4.5630	0.6020	248
500	[illegible]	2.8797	5.1941	0.6728	214
	5.5087	3.1147	3.9528	0.1464	206
	5.6046	[illegible]	5.1778	25.9840	184
	6.1574	4.0319	2.2068	25.6908	218
	7.0914	5.4149	3.0178	25.3976	218
	6.2121	1.4944	2.3114	25.5484	208
	5.4744	1.8804	4.8179	25.2420	202
	[illegible]	4.6781	4.1649	25.4160	178
	[illegible]	[illegible]	[illegible]	[illegible]	224
	[illegible]	[illegible]	[illegible]	25.0300	246
	[illegible]	1.8517	[illegible]	25.4524	206
	11.1703	1.4104	4.1111	25.3980	184
	11.7448	0.7669	4.9153	25.6544	178
	11.0820	19.7373	5.9164	25.3576	164
	8.5036	2.7494	7.7656	25.5168	164
250	12.7416	1.3414	7.6008	25.7796	164
	13.9477	1.3585	7.4015	25.1412	168
	11.7177	1.8715	7.3637	25.7404	182
	11.7176	8.9174	1.5985	25.4660	186
	[illegible]	19.4775	3.0973	25.3999	180
	[illegible]	[illegible]	4.1974	25.4940	174
	[illegible]	[illegible]	5.0174	25.9734	198
	[illegible]	[illegible]	4.9880	0.4192	192

	dB Level Diff.	Wind Turb.	Wind Speed	Temp.	Wi Di
	11.4080	1.2575	4.9480	0.4192	1
	12.4081	2.3687	5.1478	26.1412	1
	10.0454	1.3821	4.9804	0.2820	[illegible]
	11.0867	2.6895	6.7274	0.0320	1
	9.9019	2.6938	6.0852	26.1076	1
250	12.1847	1.9900	4.5072	0.6144	1
	[illegible]	[illegible]	[illegible]	[illegible]	[illegible]
	0.1409	1.3307	2.9289	19.5868	2
	0.3940	4.9713	5.1696	19.5428	2
	0.4866	2.2976	4.7863	19.7852	2
	1.4345	1.5561	5.8363	19.5708	2
	1.8200	1.4416	4.0905	19.4684	2
	0.5851	5.5816	2.6909	19.3248	2
	1.3379	2.4975	5.5964	18.9452	2
	0.2561	2.5053	4.3496	18.8048	2
	2.8338	2.9656	7.9321	18.6198	2
	1.3682	4.1431	5.7378	18.4468	2
4K	1.5929	1.9124	10.7669	18.8920	2
	2.6967	6.7491	5.1689	19.1720	2
	0.9998	4.2565	6.0050	19.2332	2
	0.5846	3.1789	11.0487	19.3060	2
	0.3584	7.1955	3.8750	19.3780	
	0.8806	6.0414	3.4450	19.4916	2
	0.9592	5.8479	6.2257	19.7984	3
	0.8554	25.5672	2.3461	19.6356	
	0.6499	10.5857	2.2478	19.5412	
	1.3954	3.2280	4.9757	19.7044	3
	[illegible]	[illegible]	3.0921	19.4742	3
	5.5764	14.7070	3.7150	19.6084	2
	4.7621	5.8232	4.7524	19.6156	2
	5.7354	8.7711	5.6595	19.6352	1
	5.6521	5.1732	8.0178	19.9284	2
	5.4014	2.7914	5.7428	20.3136	[illegible]
	5.6507	1.4013	5.8412	20.0044	2
	5.9342	2.7042	7.3111	19.7136	[illegible]
	5.8602	4.4484	5.2887	19.4764	2
	6.6328	4.2257	5.8439	19.7848	2
2K	6.4065	2.4650	7.8077	19.3640	2
	5.4356	5.8557	6.6106	19.2208	2
	4.6305	14.3560	2.2280	19.1112	2
	5.5487	3.3086	8.1491	18.7884	2
	5.4170	1.4513	11.3888	18.9912	2
	4.8842	4.0687	7.5795	18.8524	2
	5.5580	5.3165	6.9912	18.9520	2
	5.8423	2.7512	6.4364	19.1596	2
	5.3183	1.5771	8.1788	18.9628	2
	[illegible]	[illegible]	[illegible]	[illegible]	[illegible]
	[illegible]	1.9545	11.4607	18.9376	[illegible]
	7.1983	11.1359	8.2607	19.2076	2
	7.4434	1.9106	6.5980	19.5116	[illegible]
	7.9270	2.8129	7.5669	19.7276	2
	6.6911	2.1994	6.0028	19.4500	2
	7.4997	8.1721	5.1002	19.5888	2
	6.7466	4.1292	8.5869	19.3296	2
	7.5318	4.7817	7.5188	19.0968	2
	7.4502	9.0627	9.0445	19.0956	2
	8.3606	5.6610	8.4515	18.9760	2
1K	6.6567	1.9644	5.9557	19.3260	2
	7.0522	4.2893	5.4516	19.3404	2
	7.1319	4.8448	6.3755	19.3580	2
	6.6751	5.9503	6.0007	19.4396	1
	7.5584	3.6787	2.8721	19.2272	[illegible]
	7.9651	3.2161	6.5080	19.3056	2
	7.6078	6.2904	8.6159	19.2832	2
	6.8666	5.7535	8.4518	18.9508	1
	7.1004	5.1101	9.1543	18.9900	1
	[illegible]	[illegible]	10.3805	19.3580	[illegible]
	[illegible]	[illegible]	4.6677	19.4560	1
	5.9966	3.2093	7.2771	19.4568	3
	5.1559	7.4577	6.6062	19.3396	3
	6.0177	12.6497	4.5307	19.4792	2
	3.9633	8.5959	9.3118	19.3044	1
	3.4584	5.2909	5.5064	19.1392	[illegible]
500	[illegible].7709	2.4755	4.0095	19.7368	2
	8.0497	7.4718	2.4918	20.0048	2
	6.1859	2.3712	5.2053	20.3592	[illegible]
	4.5593	4.2475	5.9680	21.7960	2
	7.3459	1.6108	5.6480	22.3140	2
	6.4946	4.7093	7.8062	22.3464	2
	7.8725	5.3900	3.0283	22.0856	2
	6.9450	1.2018	3.0926	21.8592	2
	5.7111	2.1541	5.3564	22.0076	[illegible]
	7.6565	1.8114	4.5049	22.0984	2
	5.2476	7.9451	4.8097	22.3992	3
	5.1674	4.0494	9.8660	22.1724	2
	4.7905	7.4382	4.3314	22.0396	[illegible]
	[illegible]	8.1807	5.7448	21.7542	[illegible]
	[illegible]	[illegible]	3.5197	21.9552	3
	11.1410	7.4469	9.4342	21.6708	2
	12.6305	4.7166	5.1402	21.6948	1
	17.1239	3.5217	9.9249	21.6792	2
	12.0471	9.1075	9.1258	21.6556	2
	16.4569	4.0109	6.4549	21.6364	2
	[illegible]	[illegible]	6.1174	21.4680	2
	[illegible]	[illegible]	[illegible]	21.5590	2

	dB Level Diff.	Wind Turb.	Wind Speed	Temp.	Wind Dir.
	0.2365	1.3398	2.6903	25.6152	134
	1.8665	3.5226	4.5541	0.0288	54
	0.2135	2.0055	5.0715	25.7672	50
	2.7033	1.2314	7.8954	25.8932	28
	1.0629	4.1409	7.2091	26.1988	38
	2.0723	4.8310	5.9558	0.2908	38
	0.5872	4.9659	3.2977	1.0616	72
	0.2211	1.5119	1.8418	0.9136	102
4K	0.6438	4.3558	1.5316	1.2856	108
	1.8938	5.5824	2.8652	1.4416	106
	2.0679	14.8644	1.8215	1.1368	166
	1.7614	9.5383	1.9381	1.5808	168
	0.8280	5.2240	5.2156	0.3140	168
	1.3407	3.1956	4.9511	26.0312	168
	0.4823	18.2474	1.8519	25.8448	154
	1.2756	1.0801	4.9780	25.9040	186
	1.1319	1.4773	6.6469	26.1380	172
	1.4707	12.5561	3.1404	26.0612	168
	1.0982	13.8172	4.8308	26.1232	172
	1.1650	10.7240	6.7762	26.1672	178
	6.9964	2.0107	6.7396	0.0296	190
	7.6511	14.9936	5.8606	25.9132	188
	6.9741	2.1333	7.6457	25.9204	170
	6.7138	7.7200	5.7794	25.8236	156
	6.2883	15.3062	4.7911	25.9304	244
	7.3447	4.1857	5.6132	25.9856	228
	7.0803	4.5054	8.1348	25.2312	222
	7.0053	2.0343	7.6476	25.2732	160
	7.9346	9.0194	2.4979	25.5800	160
	7.0211	1.4267	1.8712	25.7016	160
	6.9882	1.2148	2.3850	25.8464	188
	7.0956	1.1586	4.0842	25.6440	204
	6.5207	2.9916	5.6697	25.6080	214
2K	6.7265	1.5214	6.3852	25.7008	204
	6.9895	2.6316	7.3496	25.5684	174
	7.4945	1.6520	6.7639	26.0520	200
	5.4738	2.8948	5.2866	25.5192	200
	6.2105	1.4868	6.3722	25.6900	204
	7.4170	3.0558	5.4680	25.5580	208
	6.5381	3.8513	4.7594	25.7048	210
	6.8851	1.1111	8.3212	25.5940	210
	7.4963	2.7342	6.5524	25.4724	186
	7.3824	1.7772	6.6588	25.7200	172
	7.1715	3.4754	6.6304	0.1588	194
	7.7643	1.0927	6.1053	0.0316	200
	7.2277	10.2957	6.2089	0.2380	218
	7.6355	3.0582	6.6720	0.1364	194
	7.8270	3.3315	6.1787	0.0720	186
	7.1669	3.0448	6.4902	0.3408	208
	7.4469	1.4390	6.4090	0.3008	198
	8.2247	2.5696	4.1492	0.2252	210
	7.7365	1.6691	6.2691	0.2108	212
	7.9494	1.1018	4.0695	0.1924	208
	6.9648	2.2150	5.2894	0.4024	208
	8.0926	0.9404	4.9943	25.8252	258
1K	7.2777	1.8501	4.9572	25.5460	260
	7.5028	1.4510	3.8391	25.9516	176
	7.0111	0.7952	5.0271	25.6228	208
	7.6451	0.4038	3.2625	0.0996	208
	8.0815	1.7673	4.2185	25.6684	210
	7.3121	6.2144	4.0319	25.7760	190
	5.5528	1.4601	5.9558	25.6196	214
	8.9467	3.0816	5.7336	25.9020	212
	6.0228	3.5327	7.4521	0.1448	226
	6.7454	1.4898	5.0761	26.1492	222
	7.7424	0.7852	4.6256	25.6460	234
	4.2748	5.1314	6.4769	25.7784	254
	6.1094	0.9074	7.8428	26.1464	262
	5.1160	3.9286	6.9568	0.7748	266
	6.0638	2.0586	10.9719	0.8648	264
	2.9243	2.9096	9.5030	0.6020	248
500	6.6513	2.8297	5.1941	0.6728	214
	5.5082	3.3142	3.9558	0.1484	206
	5.0048	2.3727	5.1778	25.9868	184
	6.1534	4.0239	2.2868	25.6908	218
	7.0916	5.4149	3.0128	25.3976	218
	5.2173	1.4064	6.3114	25.5484	208
	5.4744	1.8804	6.8129	25.2420	202
	5.1482	6.0281	4.1849	25.6160	178
	6.1426	3.0924	7.2305	25.6308	224
	9.9947	1.9208	6.6406	26.0500	246
	12.9275	1.8217	6.2067	25.6524	206
	17.1793	1.4308	6.1114	25.3980	184
	15.7448	0.7069	4.9153	25.6544	178
	12.0820	19.7373	2.9166	25.3576	164
	8.5036	2.2496	2.9656	25.5568	164
250	15.2416	1.3614	2.9008	25.2796	164
	13.9677	1.3585	2.4015	25.1612	168
	12.2127	1.8776	3.0932	25.7404	182
	11.7176	8.9124	1.5985	25.3668	186
	13.2691	15.4315	2.0773	25.3992	180
	14.2794	2.5803	4.8929	25.8948	174
	10.7771	2.0684	5.3786	25.9736	198
	11.4080	1.2575	4.9480	0.4192	192

	dB Level Diff.	Wind Turb.	Wind Speed	Temp.	Wind Dir.
	11.4080	1.2575	4.9480	0.4192	192
	12.4081	2.3687	5.1478	26.1412	166
	10.0454	1.3821	4.9804	0.2820	218
	11.0862	2.6895	6.7274	0.0220	178
	9.9019	2.6938	6.0852	26.1076	194
250	12.1847	1.9900	4.5072	0.6144	198
	[illegible]	[illegible]	5.4138	[illegible]	[illegible]
	0.1409	1.3307	2.9289	19.5868	224
	0.3940	4.9713	5.1696	19.5428	248
	0.4866	2.2976	4.7883	19.7852	278
	1.4345	1.5561	5.8363	19.5708	276
	1.8200	1.4616	4.0905	19.4684	264
	0.5851	5.5816	2.6909	19.3248	250
	1.3379	2.4974	5.5964	18.9452	206
	0.2561	2.5052	4.3496	18.8048	208
	2.8338	2.9656	7.9321	18.6188	292
	1.3682	4.1431	5.7378	18.4468	244
4K	-1.5929	1.9124	10.7669	18.8928	232
	2.6962	6.7491	5.1689	19.1720	278
	0.9998	4.2565	6.0050	19.2332	236
	0.5846	3.1789	11.0482	19.3060	254
	0.3584	7.1955	3.8750	19.3280	14
	0.8806	6.0414	3.3450	19.6916	296
	0.9592	5.8479	6.2257	19.7984	324
	0.8554	25.5672	2.3461	19.6356	34
	0.6499	10.5857	2.2478	19.5412	50
	1.3954	3.2280	6.9757	19.3064	326
	6.0589	1.5358	3.0921	19.4732	304
	5.5764	16.7070	3.7150	19.6084	238
	4.7621	5.8232	4.7524	19.6156	262
	5.7354	8.7711	5.6595	19.6352	194
	5.6521	5.1732	8.0178	19.9284	206
	5.4014	2.7914	5.7428	20.3136	284
	5.6507	1.4013	5.8412	20.0044	246
	5.9342	2.7042	7.3111	19.7136	258
	5.8602	4.4484	5.2887	19.4764	256
	6.6328	4.2257	5.8439	19.2848	266
2K	6.4065	2.4650	7.8077	19.3640	260
	5.4356	5.8657	6.6106	19.2208	254
	4.6305	14.3660	2.2280	19.1112	260
	5.5487	3.3086	8.1491	18.7884	258
	5.4170	3.4513	11.3888	18.9912	270
	4.8842	4.0687	7.5795	18.8524	276
	5.5380	5.3165	6.9912	18.9620	284
	5.8423	2.7512	6.4364	19.1596	266
	5.3183	1.5771	8.1788	18.9628	252
	6.2091	3.2924	6.2820	18.6248	236
	7.9825	1.9545	11.4607	18.8376	244
	7.1983	11.1359	8.2607	19.2076	270
	7.4434	1.9106	6.5980	19.5116	248
	7.9220	2.8129	7.5669	19.7276	240
	6.6911	2.1994	6.0028	19.6500	246
	7.4997	8.1721	5.1002	19.5888	236
	6.7466	4.1282	8.5869	19.3296	218
	7.5318	4.7817	7.5188	19.0968	202
	7.4502	9.0627	9.0445	19.0956	242
	8.3606	5.6610	8.4515	18.9700	252
1K	6.6567	1.9647	5.9557	19.3260	238
	7.0522	4.2883	5.4516	19.3404	246
	7.1319	6.8446	6.3755	19.3580	258
	6.6751	5.9503	6.0007	19.4396	178
	7.5584	3.6787	2.8721	19.2272	272
	7.9651	3.2161	6.5080	19.3056	234
	7.6078	6.2904	8.6159	19.2832	242
	6.8666	5.7535	8.6518	18.9508	152
	7.1004	5.1101	9.1543	18.9900	102
	6.3542	9.4117	10.8805	19.3580	298
	2.2650	5.5322	4.6677	19.4560	100
	5.9966	3.2093	7.2721	19.4568	332
	5.1559	7.4577	6.6062	19.3396	346
	6.0177	12.6497	4.5387	19.4792	214
	3.9633	8.5959	9.3118	19.3044	104
	3.4584	5.2909	5.5067	19.1392	204
500	5.7709	2.4755	4.0095	19.7368	266
	8.0497	7.4718	2.6918	20.0048	236
	6.1859	2.3717	5.2053	20.3592	208
	4.5593	4.2375	5.9680	21.7960	224
	7.3459	1.6108	5.6480	22.3140	212
	6.4946	4.7093	7.8069	22.3464	228
	7.8225	5.3900	3.0286	22.0856	292
	6.9450	1.2018	3.0926	21.8592	204
	5.7111	2.1561	5.3564	22.0076	222
	7.6565	1.8114	6.5049	22.0984	220
	5.2476	7.9351	6.8097	22.3992	322
	5.1674	4.0894	9.8660	22.1724	226
	4.7905	7.4382	4.3314	22.0396	238
	6.9208	8.1803	5.7444	21.7548	292
	[illegible]	[illegible]	[illegible]	21.9552	352
	11.1310	7.4365	9.3342	21.6708	236
	12.6305	4.7164	5.1608	21.6948	138
	17.1239	3.5217	9.9249	21.6792	226
	12.0471	9.1075	9.1258	21.6656	246
	16.4569	4.0100	6.4549	21.6344	254
	[illegible]	[illegible]	6.1424	21.6680	222
				[illegible]	208

	dB Level Diff.	Wind Turb.	Wind Speed	Temp.	Wind Dir.
	8.0497	7.4718	2.6918	20.0048	236
500	6.1859	2.3717	5.2053	20.3592	208
	4.5593	4.2375	5.9680	21.2960	224
	7.3459	1.6108	5.6480	22.3140	212
	6.4946	4.7093	7.8069	22.3464	228
	7.8275	5.3900	3.0286	22.0856	292
	6.9450	1.2018	3.0926	21.8592	204
	5.7111	2.1561	5.3564	22.0076	222
	7.6565	1.8114	6.5049	22.0984	220
	5.2476	7.9351	6.8097	22.3992	322
	5.1674	4.0894	9.8660	22.1724	226
	4.7905	7.4382	4.3314	22.0396	238
	6.9208	8.1803	5.7444	21.7548	292
	11.0182	2.7881	2.5197	21.9552	352
	11.1310	7.4365	8.3342	21.6708	236
250	12.6305	4.7164	5.1608	21.6948	138
	17.1239	3.5217	9.9249	21.6792	226
	12.0471	9.1075	9.1258	21.6656	246
	16.4569	4.0100	6.4549	21.6364	254
	13.5326	1.1869	6.1424	21.6680	222
	10.8259	1.3739	8.0784	21.5580	208
	12.0613	3.1131	6.5780	21.6648	234
	13.1000	2.2900	9.8182	21.6868	232
	13.0793	4.1785	9.3177	22.0652	240
	11.3096	7.1997	4.7713	22.2460	66
	7.3787	4.1453	6.7797	22.3932	116
	13.7250	3.0085	3.4722	22.6020	272
	12.4950	3.2887	2.9301	22.9344	266
	11.4436	2.7940	6.8174	22.5812	264
	15.5184	2.2220	10.9562	22.4128	144
	14.9026	7.0947	8.1063	22.3028	34
	13.2710	7.2729	5.3068	22.2164	198
	15.7982	3.2099	2.4960	22.1952	150
	-0.2416	6.2509	24.5241	22.7380	324
	-0.1442	8.5788	15.7413	22.3012	342
	0.4287	2.4669	24.7589	22.8108	278
	0.7778	17.2895	19.2558	22.6264	330
	1.3991	9.4138	24.4452	23.7468	278
4K	0.2639	6.2832	21.3156	22.5492	274
	0.5478	0.0000	25.5216	22.9420	310
	0.6826	16.4556	20.8005	22.9484	360
	1.6456	18.4296	18.6673	23.2564	274
	0.1819	16.5421	20.2299	24.0392	282
	0.7869	16.3406	18.4227	22.6932	270
	-0.1375	9.0851	24.1864	23.3208	252
	-1.9887	15.2945	12.7170	22.9032	284
	2.5969	0.0000	25.5216	23.0480	284
	0.7060	12.6426	23.5727	24.2724	332
	0.5779	0.0000	25.5216	23.1588	26
	1.0248	16.5582	22.3499	23.2436	324
	0.3814	5.4037	10.1876	23.4968	322
	1.2817	7.9871	20.4464	23.2156	374
	1.7742	4.4124	18.7548	24.4268	244
	5.4659	17.9620	15.9453	23.1116	276
	4.7442	7.0637	9.9990	23.2100	298
	4.8623	2.7472	19.4573	23.4088	214
	5.4218	1.4134	14.4992	23.3584	270
	4.4217	14.4117	10.0378	24.4408	248
	5.0888	6.7619	14.1081	23.4892	360
2K	4.6407	8.1982	16.2052	23.7008	276
	4.4178	4.3133	24.9961	23.3612	258
	4.4217	3.3629	18.8992	23.5956	306
	5.6370	26.1966	16.7760	24.9344	292
	5.0939	16.7726	11.2440	24.1204	290
	5.4003	13.1658	22.1950	24.0724	328
	5.6661	15.1007	19.4105	23.6220	300
	4.9787	8.4383	24.4219	23.5080	254
	4.9349	11.6954	14.5403	24.4372	284
	4.4270	15.0218	21.7377	24.1080	256
	6.3107	1.6999	22.6925	24.3648	260
	4.9919	21.9648	18.5621	24.0264	338
	5.8355	7.1312	12.2786	23.7284	276
	5.6065	13.8111	15.4286	24.9332	296
	7.9760	2.7891	17.7009	24.4320	254
	7.4243	14.6030	16.2511	24.0608	284
	7.7888	10.0909	22.5946	23.8508	304
	6.9605	2.8751	16.8977	24.2200	346
	6.2362	0.2159	25.5110	25.4256	298
	7.4462	3.3139	25.1149	24.0284	244
	7.5024	12.3929	21.1796	24.5580	262
1K	7.2533	11.5695	21.7669	24.0500	234
	7.0046	4.7033	15.8017	24.8216	204
	7.5589	12.9055	20.8459	25.0596	300
	8.5208	10.1252	14.1055	24.7944	258
	6.8373	2.9376	25.0237	24.6620	236
	7.2868	15.9925	15.8677	24.3652	262
	7.0132	3.9114	25.0808	24.8796	246
	7.2655	6.3422	23.6273	25.4288	242
	7.5939	13.5774	11.6114	24.5352	276
	7.6772	15.6362	12.4850	24.6012	234
	7.9063	14.5953	13.1280	24.7984	276
	7.5230	4.3184	24.4946	24.7640	290
	8.2779	20.8788	12.2521	25.9400	256
	5.3068	4.5328	18.1793	25.1800	232
	5.2989	8.7214	10.3893	24.9868	282
	7.0143	17.6028	13.9427	25.1932	236
	5.2484	2.1654	17.2147	25.1364	280
	5.4766	15.3297	16.2190	25.6520	304
	9.6307	11.5521	22.8691	24.8896	282
	7.7036	12.2647	20.4959	25.1812	234
	9.8619	8.8037	17.5102	25.6812	224
	7.5442	4.0654	9.2320	25.2048	250
	8.2237	0.0000	[illegible]	0.1016	250

	Db Level Diff.	Wind Turb.	Wind Speed	Temp.	Wind Dir.
	5.6068	4.5328	18.1793	25.1800	232
500	5.2989	8.7214	10.3893	24.9868	282
	7.0143	17.6028	13.9427	25.1932	236
	5.2484	2.1654	17.2147	25.1364	280
	5.4766	15.3297	16.2190	25.6520	304
	9.6307	11.5521	22.8691	24.8896	282
	7.7036	12.2647	20.4959	25.1812	234
	9.8619	8.8037	17.5102	25.6812	224
	7.5442	4.0654	9.2320	25.2048	250
	8.2237	0.0000	25.5216	0.1016	250
	7.5149	3.7131	18.7215	25.0840	212
	5.1885	2.9053	25.0228	25.3460	280
	8.1464	15.7507	12.8674	25.1392	274
	5.7228	1.1814	13.9180	25.7828	254
	6.4125	15.3272	11.0899	0.1296	236
	4.6838	12.3279	10.0058	25.9784	258
	7.5124	8.8383	9.7182	25.2756	282
	6.7983	3.5967	12.3194	25.5372	346
	8.0831	4.2334	15.3832	26.1528	322
	6.4460	4.2977	14.2870	0.2148	302
	9.0581	14.3264	9.0812	25.7724	262
250	10.5387	13.5624	14.2258	25.8320	294
	6.6189	8.6560	24.2925	25.8932	294
	9.4527	0.0000	25.5216	25.7916	336
	13.3520	1.1003	22.1731	1.0940	324
	12.5500	16.6677	13.4500	0.2268	238
	11.4283	3.3739	9.8653	26.0428	274
	11.2794	16.7240	12.4887	25.9372	292
	10.2824	14.4638	17.3555	25.8184	298
	9.5945	4.9268	10.3318	0.5688	346
	7.6697	10.5664	20.4681	25.7240	310
	13.2913	10.9268	9.5798	0.0072	290
	9.4051	11.3662	12.0274	25.8952	12
	13.2302	5.7529	19.2541	26.1680	350
	12.5549	3.1650	20.7669	0.5596	288
	7.5569	8.8480	12.3972	25.8524	260
	10.5153	3.1912	15.8034	25.7252	198
	13.1719	3.4567	17.1134	25.5356	284
	8.7192	5.1221	15.3560	26.0192	262
	9.2005	14.2914	16.9275	0.3172	278
	1.0552	17.4426	18.7581	17.9548	262
	-0.7010	14.1291	13.1971	17.0332	256
	-0.0062	0.0000	25.5216	16.7188	238
	0.0426	16.9343	20.5960	17.3408	244
	0.9273	0.0000	25.5216	17.2440	232
	4.1989	2.0108	21.2995	17.9340	244
	-0.6010	2.0267	23.0451	16.9412	220
4K	-0.7378	6.3394	18.4536	17.4840	216
	0.8102	16.6077	11.0639	16.8188	258
	0.7717	0.0000	25.5216	17.2928	244
	0.1870	0.0000	25.5216	18.1640	238
	-0.8480	26.6870	19.5391	17.2536	262
	-0.2197	0.0000	25.5216	17.1416	224
	1.1739	6.0391	19.5589	17.4484	216
	0.4549	20.1025	19.3978	17.4900	268
	0.4110	8.5883	22.7044	18.0312	258
	-0.4369	7.8757	21.0981	17.2972	244
	-0.2011	2.8090	25.3470	17.1636	240
	1.6355	0.0000	25.5216	17.7620	222
	0.1759	13.1884	23.3521	17.3692	250
	4.1432	9.3738	13.3506	18.1400	248
	5.7100	3.8667	24.1783	17.8244	282
	5.7230	18.6957	10.8228	17.5772	268
	5.2198	14.5431	15.9215	17.4932	266
	5.1097	17.6333	16.7645	17.5092	268
2K	4.4170	0.0000	25.5216	18.2444	260
	5.2850	18.9681	19.4461	17.9316	264
	5.8779	0.0000	25.5216	17.9756	228
	5.5801	14.9132	22.9093	18.0268	238
	4.3375	0.0000	25.5216	17.7564	240
	6.0615	4.3695	25.1143	18.4656	250
	4.8046	0.0000	25.5216	17.9592	256
	5.3235	0.0000	25.5216	18.1436	234
	4.3116	9.8863	20.5897	18.2360	216
	5.6188	0.0000	25.5216	17.9572	236
	5.1216	13.0330	23.4397	18.7044	250
	3.9879	0.0000	25.5216	17.8880	226
	4.0435	13.3733	17.7647	18.1364	238
	5.2660	3.6006	23.4014	18.4056	204
	6.2700	0.0000	25.5216	18.0852	256
	7.3001	4.4934	23.6898	19.1652	226
	6.7227	19.0139	16.1672	18.3180	296
	7.4117	8.3526	24.0750	18.0684	288
	7.2165	11.7298	11.6456	18.5552	312
	7.0821	10.5990	15.5437	18.1244	286
	6.7540	6.4009	21.6827	19.1120	262
	7.2862	23.2885	19.9660	18.2564	260
1K	8.8418	0.0000	25.5216	18.3812	302
	6.7053	18.6718	12.1447	18.5488	326
	10.0031	8.2260	24.0068	18.5676	340
	7.8296	0.0000	25.5216	19.1632	192
	7.1843	15.8117	14.0595	18.4360	324
	8.0769	1.6812	8.4194	19.0004	318
	7.3788	8.6543	11.0877	19.0696	234
	6.8649	13.0258	12.7301	18.9648	270
	7.0784	13.3945	19.9316	19.8512	250
	7.4001	22.2963	17.6593	18.6452	274
	6.8373	17.1127	16.4089	18.7900	278
	6.6202	2.7143	25.1643	18.8480	248
	7.5485	9.3847	18.4821	18.6276	220
	6.0845	3.7882	24.5922	19.0132	230
	6.5032	0.0000	25.5216	18.7748	244
	10.1807	[illegible]	[illegible]	19.2956	216

	dB Level Diff.	Wind Turb.	Wind Speed	Temp.	Wind Dir.
	[illegible]	0.0000	25.5216	18.1436	234
	4.3116	9.8863	20.5897	18.2360	216
	5.6188	0.0000	25.5216	17.9572	236
	5.1216	13.0330	23.4397	18.7044	250
	3.9879	0.0000	25.5216	17.8880	226
	4.0435	13.3733	17.7647	18.1364	238
2K	5.2660	3.6006	23.4014	18.4056	204
	6.2200	0.0000	25.5216	18.0852	256
	7.3001	[illegible]	23.6898	19.1652	226
	6.7227	19.0139	16.1672	18.3180	296
	7.4117	8.3526	24.0750	18.0684	288
	7.2165	11.7298	11.6456	18.5552	312
	7.0821	10.5990	15.5437	18.1244	286
	6.7540	6.4009	21.6827	19.1120	262
	7.2862	23.2885	19.9660	18.2564	260
	8.8418	0.0000	25.5216	18.3812	302
	6.7053	18.6718	12.1447	18.5488	326
	10.0031	8.2260	24.0068	18.5676	340
	7.8296	0.0000	25.5216	19.1632	192
1K	7.1843	15.8117	14.0595	18.4360	324
	8.0769	1.6812	8.4194	19.0004	318
	7.3788	8.6543	11.0877	19.0696	234
	6.8649	13.0258	12.7301	18.9648	270
	7.0784	13.3945	19.9316	19.8512	250
	7.4001	22.2963	17.6593	18.6452	274
	6.8373	17.1127	16.4089	18.7900	278
	6.6202	2.7143	25.1643	18.8480	248
	7.5485	8.3847	18.4821	18.6276	220
	6.0845	3.7882	24.5922	19.0132	230
	6.5032	0.0000	25.5216	18.7748	244
	10.1807	11.2325	16.2684	19.2956	236
	6.1154	0.0000	25.5216	[illegible]	240
500	8.6339	0.0000	25.5216	19.3028	244
	5.8073	1.3433	25.4349	18.9892	234
	9.1988	0.0000	25.5216	19.1096	250
	8.7744	11.8779	19.8858	18.9768	258
	10.2723	4.2929	25.1198	19.4580	260
	8.8388	20.1774	16.8136	19.2280	246
	7.0758	13.0818	18.4328	19.0972	232
	6.7081	6.3654	10.7780	19.2184	232
	9.3145	8.8070	8.6894	19.4340	260
	8.8259	3.9899	21.6672	19.6484	278
	6.2149	12.6111	15.8590	19.9416	224
	5.0076	20.9550	16.7062	19.5672	254
	7.0872	2.0436	16.9917	19.9168	282
	9.1272	10.5446	19.5543	20.0592	252
	7.2376	10.2556	14.5978	19.8512	264
	4.9121	6.4004	11.3443	19.7124	326
	8.2130	3.3084	17.9781	20.3836	300
	11.5054	2.0757	18.8017	20.1832	292
	9.7132	4.2617	20.8112	20.5340	314
	10.3169	5.5662	17.0601	20.0324	336
250	8.1267	2.0691	21.3433	19.9940	268
	8.9215	5.5673	18.8041	20.6060	320
	8.1412	5.2859	16.5430	20.7300	232
	12.3677	8.6085	10.7503	20.7792	70
	14.3136	2.9677	12.5408	20.2864	6
	10.6842	1.4000	10.8848	20.9956	262
	10.3578	5.7341	16.6515	21.1524	292
	8.6470	11.8599	12.6195	20.8568	326
	6.9393	4.3499	16.0796	21.0740	210
	8.4225	10.0568	18.1574	21.4968	288
	16.3761	5.8033	24.3740	21.6668	320
	10.5628	3.3933	20.0545	21.8276	310
	10.1384	12.8395	14.8722	21.5052	272
	10.2418	3.4940	24.8584	22.2620	324
	11.3488	14.1490	18.3342	21.9728	344
	13.4780	18.7066	10.5354	22.4000	262

	dB Level Diff.	Wind Turb.	Wind Speed	Temp.	Wind Dir.
	5.7935	10.0071	4.9419	24.6452	154
	4.1599	9.2432	5.0421	24.4620	130
	4.0926	5.0670	5.0303	24.0004	110
	4.9109	3.3154	7.3950	24.0940	112
	4.7783	12.7141	3.5320	24.7704	122
	6.0034	3.0002	5.0400	24.2750	100
	4.9210	2.1002	7.9571	24.1700	102
4K	5.5700	4.3000	6.2002	24.3576	132
	4.4319	0.3099	4.4036	23.9200	122
	5.2505	1.1503	0.5414	23.5560	92
	3.9741	2.7357	4.0179	24.1604	74
	4.7742	2.0543	5.9215	24.3472	116
	0.6450	3.9924	9.0700	24.0232	108
	4.3716	3.0026	0.3033	24.4324	110
	4.0900	5.1244	6.0455	24.0732	94
	0.1750	1.4360	0.7109	24.5012	126
	5.7007	1.0093	9.4553	24.7404	114
	7.7514	10.0017	8.4201	25.3000	108
	4.0772	2.5993	11.3052	24.7928	116
	3.1227	5.3107	6.4207	24.9080	108
	9.0717	23.3349	6.2420	25.4330	134
	10.8604	3.5085	7.0620	24.7024	120
	11.5047	4.1623	0.5000	24.5032	112
	10.8757	1.5623	8.4688	24.7612	118
	10.4059	5.0000	0.2911	25.0400	122
	10.4040	5.3665	6.5009	24.0704	62
	10.0790	1.6500	3.7100	24.7520	60
	11.2627	1.1375	4.6437	24.1504	90
2K	10.0695	9.4570	1.0237	24.3176	124
	9.9732	1.7300	1.4200	24.1756	132
	9.8199	9.1102	3.0220	24.0092	132
	10.4681	20.5911	0.0262	24.7384	110
	10.4077	4.0670	4.0597	24.1036	58
	10.9816	2.0667	2.9714	23.9436	58
	10.6625	1.3390	4.1653	23.5940	60
	10.9591	0.2699	3.5009	23.0016	100
	10.5241	1.0140	5.7271	23.9000	108
	10.2019	9.3000	6.6376	25.0156	118
	11.1865	2.3765	7.5605	24.0924	68
	10.1419	2.7054	5.0834	24.9600	102
	10.1404	2.9255	5.3961	26.0944	60
	10.5101	1.4707	4.8622	26.1980	60
	9.9120	1.6716	4.0534	26.0792	54
	9.0002	1.1130	3.5774	25.9910	54
	9.6400	0.3459	4.0357	25.9748	60
	11.5463	2.2397	4.7466	25.5748	74
1K	9.7901	1.3074	7.1676	25.4332	86
	10.6500	4.7004	3.7771	25.3936	78
	9.4410	5.0152	5.6092	25.1000	94
	9.9004	1.5746	6.4410	24.9200	08
	9.5290	1.3985	5.7108	24.9004	80
	10.8267	9.1219	4.9473	25.0596	86
	10.3311	4.0058	4.5763	25.2040	96
	9.2010	3.2498	5.1900	25.4432	90
	10.7097	2.3024	7.3920	25.6116	104
	8.4001	2.4233	6.8300	25.1000	94
	9.7236	1.4040	8.4159	25.2256	90
	11.7344	2.1960	7.1325	24.0044	92
	9.2770	0.1249	4.0004	24.2120	92
	11.5153	0.0963	7.5177	23.6332	110
	12.5144	1.3990	9.7730	24.3072	112
	12.7473	2.4330	9.4007	24.4764	118
	9.5315	2.0003	11.1697	24.5120	118
	13.7504	7.3020	9.2017	24.7948	136
	12.0020	1.0935	7.6034	24.1620	124
	12.0231	1.0524	8.9121	24.5412	120
	15.1930	5.9652	0.6250	24.0416	96
500	12.3231	14.4372	7.7210	24.0040	130
	12.3793	20.2020	2.7969	24.4732	132
	11.9052	27.0200	3.5231	24.0004	132
	14.2215	14.1057	4.0402	25.0226	128
	12.9419	4.2255	6.1399	25.4390	112
	14.4542	1.4205	7.8491	25.5032	122
	13.0434	5.3653	8.0700	25.0630	60
	10.9535	0.2270	5.9303	25.4544	40
	13.6300	4.7160	5.2547	25.2300	94
	12.1407	2.5144	6.6110	24.0300	70
	10.3743	1.0108	0.2987	24.0612	60
	13.4230	1.3765	9.0301	25.3350	00
	12.5503	1.2422	10.3619	25.0072	90
	14.3221	0.4071	10.7402	25.0500	50
	14.3573	3.1339	0.1321	25.0920	50
	11.4577	0.0434	4.9901	0.1250	00
	11.4905	1.2439	7.7619	25.0388	64
	0.0425	1.9330	0.7474	25.4050	60
	13.1979	1.3909	10.0703	25.7344	66
250	9.0010	1.4491	7.0390	0.0644	44
	10.3245	1.3495	5.9712	26.0000	62
	6.7094	1.5605	9.4747	25.9920	54

	dB Level Diff.	Wind Turb.	Wind Speed	Temp.	Wind Dir.
	12.2869	2.7141	4.0070	26.0976	62
	11.7610	1.0214	5.1477	25.0000	78
	14.2101	1.5269	9.0009	25.0724	74
	14.0104	1.1543	7.7194	0.2064	60
	12.2099	1.2367	0.4093	0.2244	52
	14.4703	0.2930	6.0925	26.0000	100
250	11.2842	12.5500	5.6147	25.0092	132
	11.9232	0.9044	5.7256	25.0096	100
	9.2796	0.5390	3.0500	24.9440	62
	12.4751	3.2532	2.6567	25.1944	62
	6.9931	2.0463	2.6714	25.2100	00
	2.7791	1.9238	6.3912	0.0012	202
	3.7500	6.7822	2.7603	0.0012	274
	4.7470	4.0299	9.6376	0.0012	276
	2.1104	5.1645	4.1004	0.0012	260
	3.5002	0.0305	2.4001	0.0012	298
	1.0650	2.0467	4.9200	0.0012	224
	1.3431	0.5063	6.7112	0.0012	266
	1.6310	0.3236	6.5653	0.0012	244
	4.3672	3.1963	7.0244	0.0012	200
	2.6958	1.3202	0.0716	0.0012	242
	3.0911	5.7413	4.7132	0.0012	264
	3.0771	2.7910	0.7465	0.0012	282
	3.2623	3.0257	0.9150	0.0012	236
4K	3.4200	3.1915	10.3457	0.0012	234
	1.3077	4.5576	4.0014	0.0012	264
	2.5310	1.2930	6.0594	0.0012	270
	3.6179	5.1117	10.4227	0.0012	250
	2.7237	3.5673	12.5059	0.0012	248
	2.0979	3.3566	11.0202	0.0012	276
	1.4726	5.9557	0.7512	0.0012	244
	9.2010	0.3150	4.9059	0.0012	310
	9.9382	3.5270	9.3939	0.0012	290
	9.5100	5.3003	8.5730	0.0012	270
	10.4121	2.0247	6.4140	0.0012	304
	9.9900	3.5016	5.1120	0.0012	220
	9.7967	7.0390	5.0320	0.0012	300
	10.0727	9.0550	7.0500	0.0012	254
	9.0445	1.5444	9.1096	0.0012	254
	9.0535	4.5425	5.4131	0.0012	250
	9.7207	2.3300	7.0130	0.0012	230
2K	9.0970	0.7715	3.9037	0.0012	240
	9.4005	2.2063	0.3310	0.0012	234
	9.0005	4.7454	0.5712	0.0012	260
	10.1750	2.4117	10.4300	0.0012	240
	10.5139	3.2275	5.9110	0.0012	260
	9.0005	3.3454	7.0254	0.0012	230
	9.0023	2.1344	7.5900	0.0012	244
	9.9670	4.1430	9.0239	0.0012	300
	10.4507	13.7655	7.5703	0.0012	246
	9.5675	0.9529	13.0217	0.0012	270
	9.9830	2.0100	0.1400	0.0012	202
	4.0114	7.7409	5.3425	0.0012	266
	10.2002	0.2072	6.2052	0.0012	254
	0.9290	1.3640	7.0743	0.0012	272
	10.2090	1.0130	6.0744	0.0012	252
	10.2003	1.1090	7.6559	0.0012	290
	9.6136	6.0705	3.7763	0.0012	204
	9.0443	10.0637	4.7940	0.0012	230
	4.1150	1.0090	10.5670	0.0012	270
1K					
	0.7920	3.4050	11.0007	0.0012	250
	10.5090	7.2301	0.0432	0.0012	270
	10.0094	0.0786	6.0000	0.0012	200
	11.7412	4.0536	9.0002	0.0012	162
	0.5500	2.2326	6.3400	0.0012	300
	9.9070	0.2311	5.5894	0.0012	212
	9.0755	3.5177	7.4112	0.0012	224
	0.7627	2.5211	1.9322	0.0012	254
	0.9914	1.5624	0.6110	0.0012	260
	0.1700	2.5371	7.4255	0.0012	270
	9.9942	9.6721	5.7000	0.0012	290
	12.0052	1.1300	7.9715	0.0012	230
	14.6500	0.3600	5.8302	0.0012	282
	4.6500	1.9073	9.9214	0.0012	250
	12.3761	5.9774	7.4039	0.0012	300
	11.4673	4.9101	9.0062	0.0012	274
	10.1976	4.7634	9.1841	0.0012	332
	13.0741	3.4211	6.7591	0.0012	300
	11.5700	0.2312	0.9001	0.0012	252
	12.3722	3.1604	6.9434	0.0012	262
	14.3577	1.0554	10.7731	0.0012	300
	11.2472	2.1327	0.5690	0.0012	332
	14.3503	0.7665	7.2102	0.0012	280
500	14.0222	2.4150	7.6521	0.0012	236
	13.5249	2.2913	6.3692	0.0012	276
	15.2444	3.0043	6.0094	0.0012	262
	12.7601	4.7004	10.6005	0.0012	242
	12.7136	2.9116	6.4373	0.0012	242
	12.2031	1.9700	6.3603	0.0012	244
	12.5219	3.7749	5.0061	0.0012	256
	11.4693	2.9999	4.0014	0.0012	[illegible]

	dB Level Diff.	Wind Turb.	Wind Speed	Temp.	Wind Dir.
	12.7001	4.7009	10.6685	0.0012	242
	12.7136	2.9116	6.0373	0.0012	242
	12.2031	1.9760	6.3003	0.0012	244
	12.5219	3.7749	5.0001	0.0012	256
	13.4693	7.9999	4.8014	0.0012	276
	12.1727	3.3760	10.1310	0.0012	244
	14.5503	1.4133	3.2932	0.0012	290
	11.7055	2.5002	4.5990	0.0012	260
	14.0075	2.4796	7.0096	0.0012	352
	0.8752	1.0738	1.6000	0.0012	262
	12.3722	5.5617	2.0092	0.0012	138
	12.4071	3.0221	2.0044	0.0012	266
	10.9900	9.1266	4.7231	0.0012	234
	12.5015	4.0214	6.0160	0.0012	252
	14.9300	0.9552	3.2319	0.0012	242
	11.4004	4.0633	4.0017	0.0012	236
	12.5108	2.9063	5.0965	0.0012	252
	15.0709	1.3975	5.9733	0.0012	248
	10.7249	4.9115	0.5500	0.0012	258
	10.4752	4.0156	5.9305	0.0012	244
250	10.4002	2.7031	0.1002	0.0012	284
	15.5559	3.5496	9.4904	0.0012	270
	10.0115	2.2571	5.1773	0.0012	194
	13.6505	3.2723	7.5766	0.0012	200
	14.1151	2.9958	0.3422	18.9604	192
	4.3319	2.0734	25.5204	24.6540	264
	4.0002	20.1178	20.3139	23.9152	270
	3.0427	5.0900	17.7314	24.0296	272
	5.0732	18.4690	19.1996	24.0804	306
	4.0359	12.9271	12.0076	23.3760	260
	3.1944	13.0351	13.5204	23.0900	278
	2.6447	3.7460	25.2011	23.1766	270
4K	3.1611	24.0318	19.5898	22.1260	236
	4.1701	0.9246	25.4921	22.0296	262

	3.0059	10.2307	20.1042	21.4340	270
	5.2737	17.2501	21.0392	20.0900	270
	4.1198	13.9097	22.0007	20.0224	280
	2.3253	0.0000	25.5210	20.0416	294
	3.4114	20.0113	19.9971	21.0760	276
	3.7000	15.0013	18.6400	19.0000	290
	5.5516	0.0000	25.5210	19.7700	304
	4.2502	15.0913	22.1120	19.2596	274
	4.3822	19.7369	10.4030	16.5620	260
	4.3374	4.0013	17.3020	18.7004	274
	4.3135	12.0059	10.1147	16.1910	236
	9.9014	1.0210	16.1901	17.0904	270
	9.7200	20.2700	16.2765	17.7544	320
	9.9600	10.0002	14.2325	16.4230	290
	10.0315	0.2597	25.5001	16.9552	220
2K	10.2462	1.2321	25.4545	16.0120	332
	9.2323	3.3942	21.5924	15.0604	4
	11.6190	15.1617	12.3909	15.0304	310
	9.3795	23.4618	15.7473	15.5000	260
	10.6500	29.6539	17.5259	15.0112	270
	9.4296	1.9000	24.1079	13.0024	234
	0.7200	6.5005	15.5401	13.0776	254
	9.6101	2.0770	25.3325	13.2200	226
	0.0011	0.0000	25.5216	13.0972	240
	10.7223	9.0000	11.7077	13.7360	250
	11.0000	19.9790	19.5750	13.4300	300
	10.7216	11.4306	19.9157	13.2572	320
	10.4025	1.3552	22.5002	13.1708	96
	10.1015	13.3947	12.5532	12.0040	164
	9.0129	12.1469	14.0469	13.1220	314
	10.6008	16.4762	14.0175	12.3552	210
	0.3994	0.1949	14.0735	11.9032	352
	7.3107	23.6965	20.5003	11.5724	314
	0.2243	4.0033	14.7904	12.0320	202
	0.0559	2.7002	10.2349	11.9532	320
	0.5727	2.0262	0.9492	11.3220	352
1K	9.5544	2.0094	12.0536	11.2412	354
	7.3967	2.2720	11.3550	11.2760	312
	9.0209	9.2775	16.7203	11.0204	298
	0.9727	15.1520	11.0100	10.9720	270
	0.5259	15.0709	14.0014	9.7332	220
	9.4041	10.0000	17.0400	9.4440	298
	7.1220	0.8585	25.4749	0.0090	230
	9.2900	3.1377	19.9050	0.7400	276
	0.0120	2.7720	17.3701	0.5312	204
	7.1094	3.0350	21.2005	0.0340	200
	0.2400	0.0000	25.5210	0.9500	310
	9.2070	0.2000	25.5210	7.3220	206
	0.1615	15.0362	18.8750	0.9016	276
	0.4007	0.0000	25.5210	0.9100	334
	9.2205	19.1755	19.3200	5.0010	320
	13.0109	0.0000	25.5210	5.1024	346
	13.0312	2.4170	25.2913	4.0132	350
	15.1990	19.0696	17.7056	4.9120	324
	13.1403	2.3015	25.2180	4.9172	310
	17.3102	2.1500	25.5100	4.0370	354
	14.2060	5.2357	11.0400	3.0356	330
500	12.0219	0.0202	12.2077	2.5924	322
	13.9002	7.4090	20.0754	3.0004	294
	13.0010	2.2037	15.9963	3.6160	250

	dB Level Diff.	Wind Turb.	Wind Speed	Temp.	Wind Dir
	12.6730	2.3255	14.1037	3.1066	244
	13.0715	12.3105	9.4005	2.1556	240
	13.9212	6.0700	9.0032	1.0056	310
	15.1014	11.5110	11.3405	0.1050	310
	14.6219	23.5403	16.2091	25.9012	262
	13.0107	19.5970	16.1343	24.9920	280
	13.5101	17.3732	18.0260	25.3220	270
500	17.4301	9.5941	23.1137	24.0410	280
	15.0052	0.0533	16.2075	25.0016	298
	15.3043	1.0027	25.4393	25.5704	320
	14.5337	2.1302	21.4316	17.9228	260
	9.1226	1.2711	25.3735	17.5372	272
	13.2540	15.0002	13.1610	17.2060	298
	5.5252	16.5006	20.3611	16.0720	250
	13.4322	13.4415	17.2512	17.3496	266
	0.7247	2.1001	24.4030	17.0050	222
	9.6405	5.7358	21.4191	17.0000	270
	11.5771	16.7150	18.0441	17.0024	270
	9.2672	7.4050	24.1095	17.0900	234
	10.1021	0.0000	25.5210	17.4360	222
250	6.7521	16.0027	12.2676	17.4412	274
	0.4594	20.5742	17.7320	17.6324	262
	9.2065	13.0935	13.9350	18.0496	268
	10.4725	15.3741	17.0901	17.7706	256
	12.1394	2.0765	15.7200	18.1904	204
	7.0634	0.0000	25.5216	18.6900	240
	9.2733	22.1975	13.0546	18.7100	302
	11.2699	1.5055	25.3069	18.4404	240
	10.4902	2.7043	19.1120	18.4210	216
	11.0906	6.2262	12.7020	18.9392	220
	9.9060	2.0007	21.1723	18.0024	212
	4.1603	13.0063	11.0992	13.7990	282
	4.2370	7.4536	14.3091	13.5632	266
	4.2320	12.1014	12.0270	13.0244	244
	2.4300	10.0547	16.1003	14.0752	280
	3.3094	0.0000	25.5216	14.4012	300
	3.4283	5.0033	21.4357	16.0620	230
	3.0160	7.7274	24.7375	14.1096	296
	2.7347	0.0000	25.5216	14.0304	276
	2.0985	0.0000	25.5216	13.0000	304
	4.9500	22.2337	13.0990	14.5090	310
4K	4.9115	16.3075	15.1000	14.0449	304
	2.0641	2.5656	17.6260	13.9000	260
	4.1350	3.0121	22.9630	14.3244	236
	3.0070	15.4391	14.2615	14.4200	262
	4.5004	0.0000	25.5210	14.9360	294
	5.7815	4.0670	20.4039	14.4472	312
	4.5300	4.5570	24.1679	14.5332	336
	4.4182	3.7400	18.0705	14.0760	2
	2.0273	6.0452	9.0773	14.3212	296
	7.3307	0.4017	12.7407	14.0128	284
	9.4351	0.3004	23.0175	14.2312	238
	9.7410	2.4040	25.1902	14.4300	242
2K	9.0375	2.5671	21.4357	14.1772	204
	0.6576	6.7981	23.6159	14.1096	252
	9.3100	7.4095	23.1009	15.1092	282
	9.0003	20.3020	13.5730	14.4100	200
	10.3030	1.4721	24.9052	14.1064	254
	10.1307	3.4343	10.0149	14.0530	240
	9.0950	15.6025	12.0002	14.2004	274

	9.6504	20.3479	12.0007	15.5190	282
	9.0950	1.7100	25.3270	14.4600	240
	9.5035	29.1000	18.2120	14.4130	310
	11.0045	0.7477	25.4142	14.4430	296
	10.4514	18.2449	17.5722	14.7000	262
	9.0025	4.0990	19.7593	15.2504	302
	10.0556	4.2661	6.2607	14.5330	270
	9.5170	13.4112	15.2627	15.0336	242
	9.0000	3.2751	19.0079	14.5030	230
	9.1377	2.7180	16.3021	14.0972	190
	9.3553	11.2905	18.6500	15.4540	8
	2.3870	18.0362	17.0107	15.0920	234
	0.0070	0.7210	25.4924	15.0956	240
1K	0.3677	1.5206	20.9054	15.1000	210
	0.2305	0.0000	25.5210	14.0370	270
	7.0001	15.9332	14.2030	15.4360	292
	9.3059	18.1597	14.0206	15.0104	282
	0.2221	13.2057	21.7147	15.2952	278
	0.0123	0.0000	25.5210	15.3912	296
	9.0371	15.4511	20.3069	15.0556	272
	7.0230	2.0191	25.4566	16.1492	272
	0.6403	14.9360	22.2205	15.5232	258
	0.5601	3.0227	23.2262	14.9564	16
	0.1000	6.2326	18.0725	15.2104	300
	9.4202	9.0221	14.5490	15.4000	316
	0.1339	11.1152	0.7270	15.9330	322
	9.0991	1.0154	25.4030	15.0204	264
	7.8150	12.5620	13.9110	15.3952	280
	0.9175	13.9638	19.0004	15.4740	250
	10.9720	15.2945	15.0225	15.4000	240
	9.1772	13.4904	14.0334	15.5052	256
	13.0973	12.1294	20.1325	15.2752	230
	15.5650	14.3042	23.3312	15.3300	270
	13.0196	1.3574	25.4577	15.0900	250
	13.0092	0.2000	25.5216	15.4000	242

	dB Level Diff.	Wind Turb.	Wind Speed	Temp.	Wind Dir.
	6.2076	0.7218	25.4924	15.0956	240
	8.3677	1.5266	20.9654	15.1000	218
	8.7365	0.0000	25.5216	14.8376	276
	7.8601	15.9332	14.2836	15.4300	292
	9.3059	16.1597	14.0266	15.0164	282
	8.2221	13.2657	21.7147	15.2952	278
	6.0123	0.0000	25.5216	15.3912	296
	9.0371	15.4511	24.3069	15.0556	272
	7.6238	2.0191	25.4566	16.1492	272
1K	8.0483	14.3306	22.2245	15.5232	258
	8.5601	3.0227	23.2262	14.9564	14
	6.1840	6.2320	18.0725	15.2164	300
	9.4202	9.0221	14.5496	15.4080	316
	6.1339	11.1152	8.7278	15.9336	322
	9.0991	1.0154	25.4036	15.0264	264
	7.8150	12.5620	13.9110	15.3952	288
	8.9175	13.9038	19.0064	15.4748	250
	10.9726	15.2945	15.0225	15.4800	248
	9.1777	13.4564	14.0334	15.5052	256
	13.0973	12.1254	20.1325	15.2752	230
	15.5650	14.3042	23.3312	15.3300	270
	13.0198	1.3574	25.4577	15.8968	258
	13.0092	0.2000	25.5216	15.4600	242
	13.0690	2.0540	23.1626	15.7852	274
	15.0831	0.0000	25.5216	15.3280	242
	12.9776	16.8834	16.6271	15.3780	238
	14.9440	4.3055	15.3112	15.7704	268
	15.2981	2.0070	25.4026	15.5792	252
500	14.2236	24.7297	18.9100	15.4812	284
	13.9676	5.1465	24.0136	15.4996	284
	13.2435	12.0124	26.7779	15.8464	278
	13.7946	0.0000	25.5216	15.0612	278
	13.7352	10.5191	10.5903	15.7756	228
	15.0399	4.3121	23.5444	15.6980	238
	13.2949	0.3362	25.5146	15.6276	296
	12.3404	0.7327	25.4600	15.0648	292
	14.4747	22.0525	19.2596	15.9936	280
	10.2305	7.6063	18.6275	16.3680	236
	17.0409	0.0000	25.5216	16.3508	240
	7.5035	15.7693	19.9152	16.0056	270
	6.1290	21.4260	17.2204	15.9368	278
	10.5004	13.3226	10.2145	16.3044	230
	12.2794	14.7740	15.6712	15.9628	244
	8.2944	24.0131	18.5260	15.0596	330
	10.7230	4.0096	10.4191	15.9104	294
	9.0355	6.9836	13.0129	16.2176	246
	11.1967	10.0047	13.5626	16.4152	222
	5.7655	15.4179	17.7526	16.1024	290
250					
	8.9004	9.7081	11.2973	16.4368	252
	13.3653	25.3802	16.3719	16.1716	256
	8.2257	16.0923	15.7000	16.1400	240
	7.9292	12.1200	15.1734	16.4292	280
	12.3940	2.0556	25.0828	16.6748	278
	6.1203	0.0000	25.5216	16.2772	272
	10.1689	3.8776	25.2988	16.5916	310
	9.4690	22.7071	15.3515	16.0664	330
	11.3052	17.1190	23.5519	16.7052	316
	11.4457	11.9414	12.1063	16.9132	318
	11.4267	6.3924	16.0751	16.9064	298

	dB Level Diff.	Wind Turb.	Wind Speed	Temp.	Wind Dir.
	12.4132	2.2172	8.8430	1.1540	306
	21.8470	5.2597	5.2900	0.0012	246
	23.2273	4.7140	10.0691	0.0012	228
	22.3080	2.0817	10.2047	0.0012	244
	22.2134	2.0938	14.3219	0.0012	248
	21.0810	4.4478	9.0505	0.0012	234
	22.3511	2.9842	6.5797	0.0012	286
	21.3800	2.7382	6.2150	0.0012	258
	21.9707	4.0834	4.4317	0.0012	250
	22.2177	3.4078	4.2068	0.0012	242
	21.1289	1.1108	5.7624	0.0012	254
	21.0452	1.9737	4.2406	0.0012	242
4K	23.0116	2.0967	8.3077	0.0012	242
	22.9315	1.2981	12.1401	0.0012	300
	24.8040	2.1500	11.1018	0.0012	268
	23.9980	1.6495	6.3982	0.0012	240
	22.3126	2.4425	6.4969	0.0012	262
	~~12.9139~~	2.2193	7.2395	0.0012	242
	23.0089	2.5483	8.1769	0.0012	224
	22.5815	4.1303	8.3214	0.0012	252
	12.1497	3.7555	9.9090	0.0012	244
	11.1600	2.8687	6.5018	0.0012	324
	13.0000	2.1401	8.5762	0.0012	272
	12.6911	2.3175	8.7717	0.0012	252
2K	14.0538	7.2355	5.4660	0.0012	290
	11.7353	6.6241	6.3304	0.0012	220
	12.9266	1.5379	7.2597	0.0012	184
	12.9134	1.1227	7.0105	0.0012	262
	12.5417	2.0054	8.2493	0.0012	256

	15.0723	2.8787	12.0053	0.0012	250
	12.6070	3.0323	9.4533	0.0012	270
	12.7439	3.3923	7.0012	0.0012	258
	12.5003	0.1201	9.0524	0.0012	262
	12.2095	2.1353	7.7960	0.0012	252
	13.1741	1.5183	6.0655	0.0012	272
	12.1990	4.6612	8.1014	0.0012	286
	12.0854	3.4833	8.3951	0.0012	280
	12.3524	2.4397	10.0747	0.0012	270
	13.8875	3.8742	4.2158	0.0012	238
	12.5493	2.4607	11.0716	0.0012	246
	7.8317	1.3136	10.5673	0.0012	274
	10.4054	8.0775	7.3916	0.0012	288
	9.7830	1.4394	13.0266	0.0012	268
	10.7000	5.4888	7.2208	0.0012	222
	9.3582	4.4797	4.9168	0.0012	304
	9.8870	1.5695	11.2029	0.0012	216
	10.2776	10.2841	8.4786	0.0012	264
	11.3801	0.8807	14.3403	0.0012	286
	10.0200	1.8171	12.3164	0.0012	192
K	11.2401	0.0897	4.3173	0.0012	200
	10.0793	0.3018	5.0204	0.0012	240
	12.4289	1.6416	11.6580	0.0012	236
	8.9381	13.1574	8.3101	0.0012	274
	10.8774	5.0820	2.9769	0.0012	270
	11.0501	3.9433	5.5036	0.0012	252
	10.8002	4.9184	5.8810	0.0012	268
	8.8290	1.8285	7.2120	0.0012	264
	9.4598	1.0280	5.8449	0.0012	254
	10.1470	3.3300	7.3407	0.0012	264
	10.6233	2.8925	10.4333	0.0012	262
	17.2453	3.2765	4.5401	0.0012	234
	19.0891	2.8032	2.8753	0.0012	180
	10.3343	4.0050	3.1489	0.0012	272
	14.9018	1.7249	7.9782	0.0012	292
	14.7150	4.8182	9.4278	0.0012	238
	10.0104	4.9427	4.0036	0.0012	214
	14.7238	5.0959	8.8794	0.0012	200
	15.7800	1.3703	6.4516	0.0012	160
0	14.7097	3.8322	3.2736	0.0012	276
	10.1370	1.9780	6.2740	0.0012	290
	10.2548	4.0957	7.1100	0.0012	214
	17.9372	1.2050	5.0091	0.0012	232
	10.3445	5.4457	5.7009	0.0012	246
	10.9694	2.0604	9.4100	0.0012	250
	19.2993	1.0000	10.0319	0.0012	320
	13.0495	4.3501	10.0901	0.0012	352
	15.3406	6.1533	10.3695	0.0012	254
	18.1475	4.7405	11.5704	0.0012	294
	18.0467	10.6889	5.1774	17.7016	260
	15.3520	3.3653	10.6383	0.0012	294
	15.3234	3.3844	9.7526	0.0012	218
	10.5887	2.0251	3.0010	0.0012	294
	20.0222	3.2983	4.7236	0.0012	268
	18.5620	4.3238	4.9250	0.0012	256
	18.2750	1.3855	8.5357	0.0012	270
	17.1655	1.3225	9.7319	0.0012	248
	10.4527	2.9786	7.3467	0.0012	256
	14.4234	5.3427	9.7105	0.0012	272
	17.5268	5.0263	10.4719	0.0012	298

	dB Level Diff.	Wind Turb.	Wind Speed	Temp.	Wind Dir.
	[illegible]	[illegible]	[illegible]	[illegible]	[illegible]
	18.0467	10.6889	5.1774	17.7016	260
	15.3520	3.3653	10.6383	0.0012	294
	15.3234	3.3844	9.7526	0.0012	218
	10.5887	2.0251	3.0010	0.0012	294
	20.0222	3.2983	4.7236	0.0012	268
250	18.5620	4.3238	4.9250	0.0012	256
	18.2750	1.3855	8.5357	0.0012	270
	17.1655	1.3225	9.7319	0.0012	248
	10.4527	2.9786	7.3467	0.0012	256
	14.4234	5.3427	9.7105	0.0012	272
	17.5268	5.0263	10.4719	0.0012	298

	13.1943	2.8482	15.4292	0.0012	284
	17.4242	3.2781	9.8054	0.0012	234
	14.8024	2.8261	6.9069	0.0012	266
	19.1509	4.3721	8.5715	0.0012	236
	16.3303	2.2330	10.9651	0.0012	246
	19.5929	5.8820	5.8859	0.0012	250
	21.3779	2.9817	4.9326	0.0012	258
	14.8791	1.4183	5.5175	0.0012	278
	11.9261	4.4621	6.3815	0.0012	208
	10.8564	1.3453	8.6472	0.0012	262
	14.3197	5.4990	7.0204	0.0012	256
	20.1391	4.3563	21.9059	17.1316	298
	21.8077	21.0147	18.6162	17.0928	244
	18.9310	14.8957	20.7616	17.5972	226
	6.0709	22.1931	16.2004	17.7828	250
	22.2802	7.8403	23.8181	17.8268	254
	21.2585	6.7311	24.0099	17.7660	242
4K	4.3964	15.8491	16.1611	18.2216	272
	10.6947	16.9156	19.6518	17.9988	260
	7.8829	15.4329	20.7026	16.9720	286
	12.6201	9.0273	23.9371	17.1452	268
	19.7105	15.6550	20.8166	17.4416	272
	7.6516	16.7694	17.8367	17.6540	232
	5.8929	8.2140	24.1845	18.6060	240
	19.3998	13.2253	13.6415	18.7536	268
	20.4494	19.1395	15.9264	18.0068	288
	21.3196	4.5392	16.8880	18.1028	232
	7.4427	0.0000	25.5216	17.8344	220
	19.9333	2.3746	17.9887	18.1120	242
	19.0604	5.2476	17.3218	17.8632	224
	20.8556	15.4140	16.7970	18.0732	240
	14.2627	-11.8591	13.5903	18.0188	254
	12.5702	5.6021	20.8232	17.9356	308
	11.9795	1.2593	21.4082	17.7256	52
	12.3623	-14.9097	16.8110	17.2408	262
	12.3427	-15.8000	12.7004	16.7784	302
	14.4205	-16.5041	16.5495	16.7584	268
	13.1256	-19.3047	19.7961	16.8084	298
	12.1380	0.0000	25.5216	16.9536	330
2K	12.5587	5.3076	19.3976	16.7044	2
	8.8728	9.3148	17.3204	16.4060	230
	12.7783	-10.4075	21.5514	16.0220	328
	11.4173	1.2038	25.4297	17.4016	240
	12.9789	-15.9364	15.8905	17.7104	304
	12.5042	3.0036	24.9350	17.6892	342
	12.9678	1.4031	13.3213	17.3040	252
	11.3884	7.1009	12.3798	17.7300	218
	13.0035	7.9350	24.8403	18.5300	312
	13.2373	6.7459	15.4557	18.8936	290
	11.5426	-20.3244	21.8058	18.9340	288
	11.8876	-17.0001	22.1628	18.5676	336
	11.4019	0.0000	25.5216	17.5192	202
	10.8215	0.0000	25.5216	17.2652	242
	11.4809	0.0000	25.5216	17.1236	240
1K	10.3006	0.0000	25.5216	17.1132	228
	11.2937	0.0000	25.5216	17.4144	262
	12.0614	18.5567	18.7122	17.8476	238
	11.1741	1.2905	17.4332	16.5328	272
	10.4865	10.7747	21.4714	17.9040	268
	9.3095	4.5346	17.9269	17.4456	224

	11.0002	0.0000	25.5216	17.0760	224
	10.9809	-10.8301	23.9100	17.0592	252
	10.0391	0.0423	24.2008	17.2564	262
	9.7849	-12.9512	10.3821	17.1472	318
	10.0640	-14.3362	12.5778	17.5744	268
	10.1601	9.3477	24.2166	17.0444	236
	10.6951	5.6956	17.4001	18.4656	224
	10.2311	4.0041	16.3743	18.0300	246
	10.4380	0.3682	14.0428	17.9236	254
	11.2990	5.7849	22.1737	17.9028	238
	12.2931	-15.6142	15.5763	17.7700	282

8

	dB Level Diff.	Wind Turb.	Wind Speed	Temp.	Wind Dir.
	[illegible]	[illegible]	[illegible]	[illegible]	[illegible]
	16.8990	-18.9220	14.0816	17.6048	242
	17.4579	15.6671	22.0502	17.7248	254
	17.1331	0.0000	25.5216	17.0408	272
	16.8767	-16.5906	18.5104	17.2336	276
	19.2581	-11.0806	22.7956	17.0816	282
	16.1802	-20.8677	17.2631	17.2664	264
500	16.9757	0.2643	25.5125	17.9900	224
	20.8972	0.1337	24.2369	17.7268	230
	18.7994	0.0000	25.5216	17.5096	248
	18.3625	-20.2425	19.2250	17.3572	276
	16.6460	5.9788	25.0468	17.4528	256
	16.3441	18.5198	15.9860	17.5104	282
	19.6582	19.1773	14.1801	17.0836	284
	21.6404	9.3690	13.7786	17.2176	264
	16.2788	-18.6916	19.2333	17.3488	278
	20.0896	4.9259	24.3757	18.0828	272
	16.7956	14.0149	23.6839	18.1352	258
	17.0642	0.0000	25.5216	17.7520	316
	[illegible]	13.1625	13.5091	17.9216	254
	7.5583	0.0000	25.5216	17.4932	264
	10.4439	0.0000	25.5216	18.0016	220
	10.1006	10.6597	14.9240	17.7596	240
	11.6948	1.1379	25.4892	17.4692	256
	13.6763	0.0000	25.5216	17.4304	232
	14.1946	6.1732	24.9287	17.4436	250
	14.1871	8.3343	10.5135	17.5876	294
	6.2851	21.2932	21.5791	18.3688	252
	12.2087	8.9645	11.0121	17.8508	208
250	15.3695	7.0998	14.5065	17.6072	242
	12.9777	2.4980	23.1467	17.1440	246
	7.8475	0.0365	25.5213	17.1784	336
	24.0137	18.0433	11.9095	17.1408	292
	12.4483	7.4859	24.6455	16.9960	258
	15.2823	16.7666	15.9744	17.7372	288
	13.9873	19.3227	16.5335	17.4996	248
	13.2201	4.4163	16.8307	17.0304	268
	14.8765	14.8764	20.3219	17.4306	266
	9.5183	0.0000	25.5216	17.2556	234
	14.6734	0.0000	25.5216	17.3804	218
	7.3752	20.3391	10.8898	11.0152	272
	20.9965	9.4842	10.1841	11.4424	300
	9.1449	16.5676	10.0807	11.1916	244
	3.9561	13.6566	19.0164	10.9932	252
	3.9613	0.0000	25.5216	11.4148	264
	13.5679	1.5500	25.4256	10.9932	328
	4.2027	3.7264	23.4623	11.2272	272
4K	5.4706	5.6472	12.9541	11.1346	40
	22.7905	5.1415	9.3010	11.2900	348

3'''

	dB Level Diff.	Wind Turb.	Wind Speed	Temp.	Wind Dir.
	5.4981	13.1324	13.8371	11.4736	274
	14.2911	3.4166	19.3679	11.5164	282
	4.7495	13.7266	20.5084	11.3380	338
	20.0373	3.7836	12.5362	11.3700	270
	20.3459	21.2735	17.2165	11.2656	316
	5.8020	19.8461	18.1527	11.1248	330
	5.3747	17.5216	17.6149	11.4784	290
	19.8849	11.2850	13.4130	11.6064	260
	20.0757	8.1975	17.0574	11.1692	320
	7.7691	2.5267	24.9817	11.3736	306
	20.0688	21.2211	16.9244	11.2052	322
	12.7884	9.9823	15.4479	11.3408	30
	12.8718	2.6126	13.3138	11.7000	304
	11.3983	-25.4579	17.8487	11.8304	270
	11.7058	9.9000	22.5072	11.5776	328
	12.3057	5.8987	18.1076	11.4508	258
	12.4303	-19.3832	12.7960	11.7292	274
	12.1148	8.1579	23.3215	11.7368	232
	12.9103	-13.9949	12.4333	11.3236	238
2K	12.2618	11.1422	8.9574	11.6068	328
	13.1682	3.3780	19.5178	11.5144	294
	13.5642	1.9849	8.7859	11.7876	204
	13.2123	3.5392	14.2858	11.5368	336
	12.9862	12.0270	18.4246	11.9208	324
	13.0977	1.9736	25.0393	11.5688	280
	10.5875	2.7617	24.9849	11.7972	250
	11.9616	2.3000	24.9845	11.7872	232
	12.4608	1.4654	21.9772	11.8420	236
	12.0270	0.0000	25.5216	11.5532	244
	13.6366	-19.5895	11.5129	12.0676	252
	12.4139	-10.6142	14.0778	11.5596	252
	9.0097	2.5523	9.3240	11.7972	228
	10.9137	9.8635	11.4946	12.0620	232
	10.6547	4.3436	23.8644	11.8496	188
	10.0884	0.0000	25.5216	11.9152	232
	10.2501	3.0250	8.6493	12.0796	252
	9.8805	4.3519	9.0677	11.5916	106
1K	11.0236	29.4391	15.4068	12.2080	250
	8.3755	2.0720	20.8789	11.9840	302
	10.2106	0.0000	25.5216	11.8368	296
	10.8335	19.7863	12.8523	12.2260	274

	dB Level Diff.	Wind Turb.	Wind Speed	Temp.	Wind Dir.
	10.9137	9.8635	11.4946	12.0620	232
	10.6547	4.3436	23.8644	11.8496	188
	10.0884	0.0000	25.5216	11.9152	232
	10.2501	3.0250	8.6493	12.0796	252
	9.8805	4.3519	9.0677	11.5916	106
	11.0236	29.4391	15.4068	12.2080	250
1K	8.3755	2.0720	20.8789	11.9840	302
	10.2106	0.0000	25.5216	11.8368	296
	10.8335	19.7863	12.8523	12.2260	274
	10.4438	3.1593	19.6956	11.9220	332
	9.7994	13.7561	14.6697	11.8152	282
	11.4737	3.3561	19.3166	12.0424	240
	10.9078	0.0000	25.5216	11.7224	264
	10.7438	9.4282	15.9294	12.3324	282
	9.6531	0.0000	25.5216	12.2328	314
	10.6676	10.3047	21.6042	11.8576	258
	9.3475	7.3979	7.8800	12.3056	274
	11.2013	4.9215	10.0974	12.0824	274
	10.0477	4.0885	17.5262	11.9968	244
	17.6536	4.7835	15.6984	12.3540	274
	15.3664	3.7125	8.1667	11.9124	276
	16.2892	17.9046	13.9562	12.2448	274
	19.1873	21.6100	15.5384	12.4736	254
	16.8765	13.9231	21.6402	12.0128	264
	15.5162	7.6565	19.6615	12.4628	302
	16.6656	20.7596	15.6538	12.4492	274
	16.8558	5.4633	8.4952	12.1636	254
	16.0475	12.6601	13.0899	12.1720	248
500					
	16.1719	5.2600	21.2648	12.4372	288
	19.2094	4.7600	20.0388	12.1692	302
	16.2567	4.8165	10.1462	11.9632	242
	17.2990	-20.0300	16.6610	12.2236	276
	17.1817	6.3372	22.5443	12.2736	256
	16.8391	0.5021	25.5081	12.3452	248
	16.5778	-15.6243	17.4080	12.5848	280
	16.5259	0.0000	25.5216	12.4056	308
	21.3535	2.1146	10.2713	12.0052	220
	17.2858	6.6760	18.1467	12.6604	254
	16.6432	11.6124	20.4969	12.3332	264
	13.1311	9.8821	21.8584	12.6728	264
	11.6804	5.4375	13.7665	12.4156	226
	13.1444	20.4437	14.6081	12.4056	262
	13.6965	14.5545	17.6366	12.6076	284
	14.1033	0.0000	25.5216	12.5212	308
	9.9763	5.5363	20.6462	12.2176	320
250	15.0764	13.5797	13.2295	12.4748	346
	12.2215	4.0518	11.1677	12.6200	234
	18.2103	1.4188	25.3162	12.0004	306
	12.2627	6.7663	24.6245	12.6752	304
	13.8107	25.1339	17.9323	12.7684	318
	11.5635	9.4984	20.0356	12.4464	292
	15.7033	12.4662	12.5729	12.6400	262
	11.0710	4.2137	15.3966	12.0264	300
	11.7201	4.3868	11.3915	13.0152	270
	13.9319	16.0322	16.8653	12.0332	240
	15.4927	8.4361	21.1252	12.5372	234
	16.6225	6.6176	24.5196	12.6100	282
	14.8487	9.6322	14.0416	12.0704	288
	16.0193	-1.8100	22.0627	12.6120	292

	dB Level Diff.	Wind Turb.	Wind Speed	Temp.	Wind Dir.
	6.2134	2.0745	11.9785	3.5328	68
	4.7109	2.7448	10.3365	3.5020	86
	6.2433	1.4481	10.4494	3.3248	96
	6.1692	2.4002	8.4099	3.5948	52
	6.9236	2.6577	5.9191	4.0148	40
	6.6509	0.4603	5.5587	3.9140	56
	7.2258	1.4653	5.3803	3.2420	54
	8.9942	1.0317	6.1236	2.7336	48
4K	9.1201	2.9292	8.0465	2.9704	54
	5.5750	2.6941	8.4432	2.7000	50
	11.3216	1.2440	8.5430	2.1752	64
	6.0955	2.9784	9.0352	0.1196	58
	7.9287	1.6795	7.3448	25.9348	66
	7.4137	2.7385	9.2462	25.2572	64
	6.8618	2.1354	12.0201	26.1412	64
	6.4537	4.1541	9.5709	25.7164	64
	7.9436	1.0969	8.9189	25.7204	80
	6.1896	1.2637	8.9545	25.4592	74
	4.7455	2.9872	9.0329	25.9596	106
	11.6910	4.3980	6.1019	26.0972	116
	14.2553	2.1458	6.2912	26.1820	34
	13.8147	2.1994	5.8055	25.8816	34
	13.1696	1.4558	6.0200	25.5732	32
	14.5212	1.1237	7.8550	25.4392	54
	17.3881	2.7686	8.2095	25.2852	76
	12.4966	1.7531	9.0423	25.5072	96
	15.1302	6.3122	10.1302	25.3668	102
	14.1981	0.7456	5.4236	25.4372	118
	12.9835	5.3422	3.0643	25.0604	118

2K

	dB Level Diff.	Wind Turb.	Wind Speed	Temp.	Wind Dir.
	12.6273	6.0200	7.5840	25.7364	90
	13.3585	0.8019	6.5319	25.0468	52
	14.2152	4.9690	5.4381	25.4056	62
	12.7251	3.5359	5.6358	25.3024	62
	12.0802	0.5025	8.5226	25.8472	72
	13.5315	1.5027	5.7671	0.0172	54
	15.3700	2.7788	7.3268	25.7980	68
	12.7696	1.2302	6.3470	25.3240	78
	15.2636	1.0994	6.3116	24.9184	70
	13.1243	2.3902	6.1950	24.8492	86
	14.5540	6.2262	7.0915	24.9688	92
	13.7601	1.2320	6.6173	25.6900	92
	10.3444	1.5949	7.4959	25.3716	80
	13.0840	1.3166	8.9842	24.9924	88
	13.2254	3.6777	7.0411	24.9500	76
	13.0503	2.2032	8.5094	24.7904	78
	13.2782	1.7314	10.4258	24.6752	76
1K	12.2642	5.8511	7.7164	25.0772	92
	12.0497	1.6335	11.4621	25.5072	96
	11.5566	1.4012	10.4299	26.1868	112
	12.3798	1.8180	5.9202	0.0700	116
	13.5814	4.4257	8.0312	0.0488	72
	13.1221	1.2394	10.1830	26.2000	92
	13.0049	1.5983	10.2011	0.0272	86
	13.7911	4.5797	8.9497	25.9084	80
	12.3843	5.0047	8.5192	0.0796	96
	13.1881	1.4214	8.9050	0.2108	74
	12.9800	3.3995	9.1256	0.2348	84
	12.5983	3.1917	7.4036	25.9692	88
	14.9574	5.3832	9.4738	0.1676	96
	12.1869	3.8351	10.1762	0.4672	114
	18.1736	3.5191	9.4674	25.5760	100
	16.3855	3.0888	10.3096	25.9848	88
	17.5276	0.2296	9.9254	25.8316	80
	21.3199	1.7848	8.5742	25.3364	96
	19.7790	1.1708	7.0134	24.9136	80
	18.1584	1.2343	9.9972	25.2564	94
	16.7072	1.5907	8.7134	25.7184	86
	20.1805	2.4263	9.4087	25.5080	74
	17.3372	4.7808	6.7239	25.0016	88
500	19.7390	1.4183	10.7305	25.8828	102
	18.6755	4.5063	7.4345	25.5176	96
	19.2044	0.9087	10.5045	25.1228	90
	20.3076	2.1806	8.4562	25.2372	138
	17.7592	1.9240	8.9826	24.9800	88
	20.1613	1.5301	8.1264	25.4908	66
	24.0003	2.6391	8.2526	25.6536	76
	17.3974	0.9911	10.4204	25.7036	76
	17.7879	2.2192	10.7129	25.3068	82
	22.9304	1.5887	10.5086	25.2292	60
	[illegible]	1.5439	6.8590	25.3972	66
	17.7144	4.2293	6.3206	25.4576	68
	17.6377	2.0389	7.6164	25.1276	90
	18.8186	4.0131	4.4006	24.8480	92
	15.4995	6.0970	8.2464	24.8900	96

	dB Level Diff.	Wind Turb.	Wind Speed	Temp.	Wind Dir.
	18.1706	1.9013	5.6087	25.3964	102
	18.8849	1.4293	6.6151	25.5340	94
	16.9183	22.1602	3.4916	25.3084	86
	18.8460	1.6020	5.5034	25.7328	60
	17.6074	4.2556	4.8830	25.6700	88
250	19.3685	0.6185	2.3765	24.9546	120
	11.3812	15.4316	2.6096	24.3460	142
	16.0794	1.2292	4.9790	24.7792	114
	13.9295	2.4070	6.6155	24.0116	98
	12.6394	3.1662	7.6296	24.5168	92
	15.0942	1.2159	11.4951	[illegible]	90
	11.8604	2.6099	10.2188	18.8412	266
	20.1802	0.1991	7.6954	18.9032	276
	20.0711	11.4748	3.3552	19.4460	270
	17.0442	2.9371	0.5030	19.4204	228
	20.7369	5.2810	7.0575	19.5904	126
	20.1004	4.2131	4.3220	19.4148	250
	20.2303	3.7402	5.0131	19.1128	256
	18.5596	11.7377	5.3517	19.2508	260
4K	20.3346	5.0595	8.0600	18.6872	278
	20.9103	3.2787	6.7084	19.0236	242
	20.9274	4.9797	10.2700	19.0412	206
	3.3689	5.5202	7.4236	18.0280	236
	19.5874	2.5981	9.8737	19.1260	234
	19.6125	0.2040	9.0323	18.6500	258
	22.2605	3.1084	6.7144	19.0476	276
	21.3900	4.7328	6.7710	19.2488	264
	20.5564	3.2949	5.1291	19.3806	276
	19.5097	2.7404	6.0433	19.7060	228
	22.5686	5.0004	7.9107	19.5864	186
	[illegible]	3.6544	7.8397	19.4484	194
	15.6102	1.5796	7.1489	19.6744	250
	13.6428	34.9445	3.3912	19.3196	114
	14.0577	10.0232	3.7399	19.0096	102
	13.5266	12.1097	4.4515	18.9060	256
	14.0709	2.2018	11.0090	19.3200	260
	14.3617	5.7918	4.6091	19.2056	232
	14.3520	1.0463	7.4934	19.1932	264
	12.2740	12.2003	1.6018	19.3084	286
2K	12.1339	3.8939	3.4239	19.3564	264
	12.5395	2.0200	3.7127	19.3012	248
	15.0278	2.2592	4.3643	19.1972	224
	14.4860	3.1189	6.6979	19.3060	248
	15.6348	2.0200	6.0760	19.3044	252
	15.7199	3.8084	4.7199	19.4976	252
	15.1862	3.7021	2.5919	19.5452	86
	12.4134	1.1036	1.5942	19.5936	252
	14.7103	1.9993	4.2070	19.3444	256
	11.5509	7.4884	3.9898	19.7488	234
	14.1875	7.9423	2.7632	19.0708	266
	14.3843	7.5974	4.3405	19.9272	294
	11.2303	3.9236	5.9408	19.6908	314
	12.1940	14.1927	4.8962	19.8004	292
	11.6963	2.9581	6.9921	19.7444	310
	12.0314	1.4783	4.0310	19.2720	258
	11.5532	3.7598	6.0994	18.9744	308
	11.0555	3.2619	0.3125	19.1696	260
	11.8444	2.0405	7.2900	19.3004	310
	10.9916	6.0597	4.7989	19.3076	362
	11.9387	5.2034	6.5139	19.0276	42

1K

	dB Level Diff.	Wind Turb.	Wind Speed	Temp.	Wind Dir.
	12.6823	1.5269	9.0954	19.3420	64
	11.4861	3.3649	3.2602	19.3412	304
	11.8866	3.0227	5.2293	19.0060	244
	12.4904	5.5298	7.2732	19.2732	242
	11.1385	4.9548	0.2025	19.2100	284
	11.5163	4.0769	13.1671	19.1004	344
	11.3126	3.2054	5.5594	19.5004	274
	11.7200	1.0028	6.6712	19.5952	264
	10.5237	3.7805	7.1207	19.0528	200
	13.0448	4.1011	5.4039	19.7908	156
	12.0450	4.5996	5.7134	19.3060	268
	20.4322	2.1967	5.3116	19.0300	264
	20.0306	0.8900	5.2591	19.0300	272
	21.9183	2.5761	0.0069	19.2176	264
	19.2635	0.9457	10.4950	18.9300	272
	19.0840	3.4080	9.3201	18.0512	282
	19.5203	7.2192	7.3584	18.8852	244
	19.6001	1.5730	6.7771	19.2908	328
500	18.1760	1.7971	4.9559	19.9092	294
	18.0501	3.5004	5.3550	19.3260	278
	17.7519	0.1897	10.5750	19.4368	338
	21.0535	3.0286	5.2407	19.2796	216
	19.7817	2.3743	4.7233	19.1772	260
	19.0218	0.5764	0.3795	19.6112	270

	dB Level Diff.	Wind Turb.	Wind Speed	Temp.	Wind Dir.
	21.9183	2.5701	8.0069	19.2176	264
	19.2835	0.9457	10.4950	18.9380	272
	19.0640	3.4080	9.3201	18.8512	282
	19.5203	7.2192	7.3584	18.8852	244
	19.0801	1.5730	6.7771	19.2908	328
500	[illegible].1700	1.7971	4.9559	19.9892	294
	16.6501	3.5604	5.3558	19.3260	278
	17.7519	0.1097	10.5750	19.4368	338
	21.0535	3.8280	5.2407	19.2796	216
	19.7817	2.3743	4.7233	19.1772	260
	19.0210	8.5764	8.3795	19.6112	278
	18.0487	3.3622	5.8161	19.0068	270
	22.3858	4.4450	7.2820	18.8332	282
	16.3611	4.1960	8.8571	19.3120	256
	20.1433	3.6530	6.0836	19.4296	286
	16.3702	2.5682	8.4599	19.7904	254
	20.7700	3.1715	5.4840	19.5312	260
	19.0591	5.3384	5.8029	19.2720	348
	21.0229	1.0292	5.6074	19.7016	242
	15.6973	7.3134	5.4746	19.7536	248
	16.5089	3.3936	6.2297	19.6672	274
	22.1196	7.2091	9.6448	19.1960	252
	15.8447	4.0211	8.4206	19.0012	270
	26.2602	2.9305	9.9199	18.8856	262
	14.8803	3.2713	6.4698	19.4308	266
	15.2701	4.0573	9.5732	19.7296	250
	16.7770	1.3139	10.8850	18.9800	262
250	16.0457	3.8865	9.9363	19.0376	250
	16.1490	3.0123	9.4173	18.9600	282
	16.8505	2.7554	5.9323	18.8968	282
	15.7082	4.0520	9.8846	19.3200	242
	15.6452	7.5047	12.3437	18.5916	292
	20.9044	2.5580	14.6948	18.7092	260
	19.0334	3.3311	11.0882	18.7052	246
	17.0072	2.0123	7.9556	18.7600	260
	23.8375	3.7295	16.4087	19.2892	272
	19.5574	8.5027	12.9771	19.1608	278
	14.0015	5.2711	12.3414	19.0148	246
	11.3878	16.8816	13.8127	16.9460	286
	12.8677	14.4325	17.7666	17.1736	230
	24.4089	1.4716	25.4241	17.1168	196
	16.4310	0.0000	25.5216	17.3044	220
	22.9023	22.1842	16.7280	17.5216	236
	5.8805	0.4375	25.5046	17.2828	232
	17.0144	0.0000	25.5216	17.2804	214
	21.0482	0.0000	25.5216	17.4948	218
	23.4465	3.2731	24.0010	17.6144	194

4K

	21.4849	1.8205	18.2948	17.8032	260
	20.0560	9.0501	20.2567	17.4604	234
	23.3771	8.4896	13.1607	17.4616	230
	21.2819	11.5108	22.3374	17.6584	258
	23.6048	14.3545	17.4042	17.3588	262
	18.5606	5.2124	17.6302	17.4092	224
	22.0512	2.8769	24.9273	17.3820	232
	21.0211	3.2021	21.8445	17.2304	254
	23.0513	1.1327	19.1798	17.0344	230
	23.1048	0.0821	22.9066	17.2016	220
	8.3101	1.3453	25.4550	16.9768	250
	10.8900	15.6748	15.3529	16.4728	244
	10.5995	0.0000	25.5216	16.9704	246
	12.2175	9.7168	14.0463	16.9104	272
	14.0004	2.9027	24.8925	16.6236	312
	11.7953	18.5076	13.8211	16.9324	208
	11.0686	3.7834	19.6474	17.5416	322
2K	11.2986	9.4516	17.2154	17.3372	262
	14.2863	5.5938	10.7638	17.7332	208
	12.9777	17.3262	22.0118	17.9016	290
	13.0594	17.3674	17.9076	17.9368	272
	11.9084	10.3016	11.0106	17.6096	260
	13.1944	0.0000	25.5216	18.1956	220
	10.0195	2.2702	20.5507	18.5404	228
	13.0810	1.5985	21.5940	18.3096	188
	12.9905	6.0571	13.6181	18.1724	188
	11.0658	2.0821	18.7391	18.2540	210
	13.0199	2.0334	24.1842	18.2308	204
	12.5668	2.7449	13.3724	18.0844	208
	13.1443	11.0013	13.5170	17.6384	198
	11.0487	13.3320	22.9362	17.8860	234
	11.4142	3.5390	18.1702	18.0856	184
	12.2676	3.7987	20.3815	18.1196	212
	14.2830	9.7356	10.8203	18.2516	234
	11.6082	17.0996	14.7761	18.2376	246
	11.0017	4.4355	9.6895	18.3648	270
	11.7717	1.9764	23.6681	18.2532	306
	12.6439	11.3324	13.3397	18.1564	282

	dB Level Diff.	Wind Turb.	Wind Speed	Temp.	Wind Dir.
	12.2676	3.7987	20.3015	18.1196	212
	14.0830	9.7356	10.8203	18.2516	234
	11.6082	17.0996	14.7761	18.2376	246
	11.0017	4.4355	9.6895	18.3648	270
	11.7717	1.9764	23.6681	18.2532	306
1K	12.6439	11.3324	13.3397	18.1564	282
	11.7085	13.8452	21.5157	17.8708	276
	13.5839	9.6988	16.0588	17.1916	282
	10.3076	3.1185	19.7300	17.4252	224
	14.6180	4.2070	11.0762	17.9824	240
	13.9131	3.7662	11.8851	17.7156	316
	13.6780	5.8681	11.0103	17.0412	262
	12.4411	4.3680	12.1044	17.5804	252
	12.0473	19.8924	13.0951	17.0300	240
	11.7221	11.8361	15.0793	17.3712	244
	12.2327	0.0000	25.5216	17.1424	274
	14.1695	5.5191	19.6499	17.5000	224
	12.2151	4.8871	18.8860	18.0264	266
	13.0179	23.5400	18.5149	18.0012	254
	16.0585	6.0632	21.0526	17.4920	234
	20.6627	17.5209	15.7343	17.3196	254
	17.8903	3.9267	25.0944	17.1876	240
	19.3503	0.0000	25.5216	17.3496	210
	20.4399	0.0000	25.5216	17.0056	296
	20.0594	0.1209	25.5189	16.9404	234
500	16.9207	17.7407	17.6133	17.2012	242
	21.5349	2.2422	23.7137	17.3372	220
	19.8956	12.4044	12.4745	17.6160	238

	19.2397	3.0039	20.2597	17.3916	260
	18.0276	13.5017	15.2323	16.7504	272
	18.9850	10.9405	18.4762	16.5396	282
	19.7651	0.0000	25.5216	16.5056	260
	20.3878	4.9300	23.6034	16.7492	258
	21.5603	3.0950	17.7604	16.5024	224
	20.7861	19.5131	19.7017	16.4592	236
	20.0977	5.9403	17.9300	16.4424	256
	22.2003	0.0000	25.5216	16.3324	248
	22.4300	16.3427	22.5804	16.4340	256
	18.0221	22.5190	20.4936	16.1076	316
	14.0030	14.0035	22.1742	16.3160	292
	11.5856	24.4060	16.9703	16.9984	270
	15.5344	5.2081	25.1230	17.4120	322
	14.4720	13.0035	20.9185	17.1730	314
	15.6081	9.9330	15.5047	16.4740	314
	15.8397	19.5569	14.6714	16.4948	254
	18.0899	17.8309	12.6812	16.4060	238
	15.0336	9.6489	23.0560	16.2748	296
250	16.7439	7.9633	16.4004	15.7552	290
	14.8804	0.0000	25.5216	15.9052	294
	15.0945	2.7771	9.3738	16.1296	266
	12.3987	9.0216	14.0690	16.7992	290
	14.2098	0.0000	25.5216	16.3604	314
	14.0113	9.5207	21.3511	16.1340	298
	17.0725	16.4476	22.6307	16.2952	344
	15.7828	14.7430	23.2133	16.5672	278
	20.7453	5.0344	17.9195	17.2148	246
	13.0445	7.5408	20.0229	17.5536	252
	18.3937	17.0089	16.3555	17.4120	282
	15.0745	18.2530	16.3104	16.8068	256
	8.9559	13.5003	9.4303	0.0012	278
	23.0546	14.9614	16.9327	0.0012	266
	22.9567	0.9630	25.4862	0.0012	266
	22.0134	0.2714	25.5052	0.0012	228
	22.0713	11.5265	11.9343	0.0012	260
4K	24.3901	6.2077	25.5108	0.0012	234
	22.2524	2.7237	25.3279	0.0012	250
	23.0117	19.2330	13.4405	0.0012	232
	21.9901	2.0629	24.2414	0.0012	250
	8.8445	1.6518	24.8974	0.0012	242
	13.3588	15.0727	12.7523	0.0012	252
	24.1356	4.4025	15.9926	0.0012	312
	13.5242	2.0047	19.8422	0.0012	266
	22.9724	14.1696	10.0230	0.0012	320
	22.1342	7.9711	15.2103	0.0012	306
	9.0079	14.0970	14.0425	0.0012	282
	12.3173	3.2254	11.1552	0.0012	234
	23.7401	12.0290	11.9577	0.0012	232
	9.2977	4.8879	9.2107	0.0012	320
	21.0944	1.7585	15.2350	0.0012	324
	13.0182	1.5034	19.7273	0.0012	352
	13.1789	16.3100	10.0500	0.0012	342
	13.5135	11.0237	12.9719	0.0012	310
	13.0141	6.6515	25.5210	0.0012	318
	11.2509	0.5780	12.0155	0.0012	284
	12.6114	4.1900	0.4124	0.0012	254

Appendix E: Programme Listings

This appendix shows the BASIC and Assembler programmes used in the work reported in this thesis. They are:

MASTER SRC . Source code listing of the individual service routines called from a BASIC control programme.

MASTER SRC/4 Version of the above for use with scale models.

MASTER BSC BASIC control programme for full size outdoor experiments. Uses MASTER SRC.

DATA BSC Picks up data stored on floppy disc at the time of an outdoor experiment and prints results to a local printer.

DEC BSC Calculates results from floppy disc but transfers the data to the DEC 20 mainframe via the NETKIT system. It executes a Forbran programme on the DEC 20 called PETP.FOR.

DEC 20/5SRC Source code listing of the Assembler routine to transfer data via the NETKIT system to the DEC 20. This is used by DEC BSC, above. Note that the NETKIT ROM is located in Block A of the PET memory map.

```
0000                    ;REVISED DEC-20 LINK - USES HALF DUPLEX AND THE "$" IS DETECTED IN IRQ
0000                    ;*************REDIRECT IRQ VECTOR
0000                    STATUS=$AFF1          ; UART STATUS
0000                    RXBUFF=$AFF0
0000                           *=$0280
0280  00                STORE  .BYTE 00
0281  78                       SEI
0282  A9 8C                    LDA #<NIRQ
0284  85 90                    STA $90
0286  A9 02                    LDA #>NIRQ
0288  85 91                    STA $91
028A  58                       CLI
028B  60                       RTS
028C                    ;*************DETECT RX DATA
028C  AD F1 AF          NIRQ   LDA STATUS
028F  29 08                    AND #$08       ;TEST FOR RX BUFFER FULL
0291  F0 09                    BEQ END        ;IF EMPTY THEN BRANCH
0293  AD F0 AF                 LDA RXBUFF     ;GET RX CHARACTER
0296  8D 80 02                 STA STORE
0299  8D 00 80                 STA $8000      ;TOP R.H. OF SCREEN
029C  4C 2E E6          END    JMP $E62E      ;CONTINUE WITH NORMAL IRQ SERVICE ROUTINE
029F                    ;************RESTORE IRQ VECTOR
029F  78                REST   SEI
02A0  A9 2E                    LDA #$2E
02A2  85 90                    STA $90
02A4  A9 E6                    LDA #$E6
02A6  85 91                    STA $91
02A8  58                       CLI
02A9  60                       RTS
02AA  20 F6 A3                 JSR $A3F6      ;CLEAR STATUS, ETC.
02AD  20 E9 DC                 JSR $DCE9      ;FL. PT. ACC#1 TO ASCII STRING
02B0  A2 00                    LDX #$00
02B2  BD 00 01          DEC2   LDA $0100,X    ;GET ASCII CHAR.
02B5  F0 07                    BEQ DEC1       ;00 SIGNIFIES LAST CHAR.
02B7  20 83 A3                 JSR $A383      ;TRANSMIT DATA
02BA  E8                       INX
02BB  4C B2 02                 JMP DEC2
```

O:DEC20/SSRC......PAGE 0002

LINE# LOC CODE LINE

```
02BE  A9 2C             DEC1   LDA #',        ;SEPARATE DATA BY COMMAS
02C0  20 83 A3                 JSR $A383
02C3  60                       RTS
02C4                    ;************SET UP SERIAL PORT
02C4  20 00 A0                 JSR $A000
02C7  A9 0E                    LDA #$0E
02C9  8D 4C E8                 STA $E84C      ;LOWER CASE
02CC  A9 60                    LDA #$60
02CE  8D 64 02                 STA $0264
02D1  A9 00                    LDA #$00
02D3  8D 6E 02                 STA $026E
02D6  A9 45                    LDA #$45
02D8  8D F2 AF                 STA $AFF2      ;COMMAND REGISTER
02DB  A9 38                    LDA #$38
02DD  8D F3 AF                 STA $AFF3      ;CONTROL REGISTER
02E0  60                       RTS
02E1                           .END
```

ERRORS = 0000

SYMBOL TABLE

SYMBOL VALUE

DEC1	02BE	DEC2	02B2	END	029C	NIRQ	028C
REST	029F	RXBUFF	AFF0	STATUS	AFF1	STORE	0280

END OF ASSEMBLY

```
0001  0000                ;CONTROL PROGRAMME
0002  0000                      .LIB 0:MASTSRC
0003  0000                ;CALIBRATION SUBROUTINE
0004  0000                EXP1=$5E
0005  0000                EXP2=$66
0006  0000                ORB=$9600
0007  0000                IRA=$9601
0008  0000                DDRA=$9603
0009  0000                DDRB=$9602
0010  0000                T2LL=$9608
0011  0000                T2CH=$9609
0012  0000                ACR=$960B
0013  0000                PCR=$960C
0014  0000                IFR=$960D
0015  0000                IER=$960E
0016  0000                CALN=$0FF6
0017  0000                CALF=$0FFB
0018  0000                OVER=$0FF5
0019  0000                      *=$1000
0020  1000  A2 F6               LDX #<CALN      ;ENTRY FOR NEAR CAL.
0021  1002  A9 15               LDA #$15
0022  1004  A0 BB               LDY #$BB
0023  1006  4C 0F 10            JMP ENT1
0024  1009  A2 FB               LDX #<CALF      ;ENTRY FOR FAR CAL.
0025  100B  A9 25               LDA #$25
0026  100D  A0 BB               LDY #$BB
0027  100F  8C 02 96     ENT1   STY DDRB
0028  1012  86 1F               STX $1F
0029  1014  8D 00 96            STA ORB
0030  1017  A9 0F               LDA #>CALN
0031  1019  85 20               STA $20
0032  101B  A9 90               LDA #$90
0033  101D  85 5E               STA EXP1
0034  101F  A9 00               LDA #$00
0035  1021  8D 03 96            STA DDRA
0036  1024  85 5F               STA EXP1+1      ;INITIALISE ACC#1
0037  1026  85 60               STA EXP1+2
```

0:MASTERSRC......PAGE 0002

```
LINE# LOC CODE LINE

0038  1028  85 61               STA EXP1+3
0039  102A  85 62               STA EXP1+4
0040  102C  A9 7F               LDA #$7F
0041  102E  8D 0E 96            STA IER
0042  1031  A9 0A               LDA #$0A
0043  1033  8D 0C 96            STA PCR         ;CA2 PULSE ON READ IRA,CA1 & CA2 -VE TRANSITION
0044  1036  AD 01 96            LDA IRA         ;SYNCHRONISING PULSE
0045  1039  AD 00 96            LDA ORB
0046  103C  09 02               ORA #$02        ;RESTORE PB PULSE
0047  103E  8D 00 96            STA ORB
0048  1041  A0 00               LDY #$00
0049  1043  20 59 10            JSR RMS         ;ACC#1 =SIGMA(X*X)/4096
0050  1046  A5 1F               LDA $1F
0051  1048  48                  PHA
0052  1049  A5 20               LDA $20
0053  104B  48                  PHA
0054  104C  20 5E DE            JSR $DE5E       ;ACC#1=RMS
0055  104F  68                  PLA
0056  1050  85 20               STA $20
0057  1052  68                  PLA
0058  1053  85 1F               STA $1F
0059  1055  20 E7 DA            JSR $DAE7       ;ACC1 TO MEMORY
0060  1058  60                  RTS
0061  1059  98           RMS    TYA
0062  105A  F0 0C               BEQ RMSA
0063  105C  AD 01 96            LDA IRA         ;GET A BYTE OF DATA
0064  105F  F0 04               BEQ RMS1        ;TEST FOR -VE OVERLOAD
0065  1061  C9 FF               CMP #$FF        ;  "    "  +VE    "
0066  1063  D0 06               BNE RMSB
0067  1065  4C 9D 10     RMS1   JMP ERR
0068  1068  AD 01 96     RMSA   LDA IRA
0069  106B  38           RMSB   SEC
0070  106C  E9 7F               SBC #$7F        ;SUBTRACT GND LEVEL
0071  106E  85 66               STA EXP2
0072  1070  B0 06               BCS JUMP6       ;TEST FOR RESULT -VE.
0073  1072  A9 01               LDA #$01        ;2'S COMP.
0074  1074  E5 66               SBC EXP2
```

```
1076  85 66              STA EXP2
1078  85 6B      JUMP6   STA EXP2+5
107A  20 FC 10           JSR SUM           ;ACC1=(SIGMA X*X)
107D  A9 10              LDA #$10
107F  2C 0D 96           BIT IFR           ;TEST FOR 4K COMPLETED (PEN LIFT HIGH TO LOW)
1082  F0 D5              BEQ RMS
1084  A5 5F              LDA EXP1+1
1086  30 0D      LOOP5   BMI JUMP7         ;TEST FOR NON-NORMALISED RESULT
1088  C6 5E              DEC EXP1
108A  06 62              ASL EXP1+4
108C  26 61              ROL EXP1+3
108E  26 60              ROL EXP1+2
1090  26 5F              ROL EXP1+1
1092  4C 86 10           JMP LOOP5
1095  38         JUMP7   SEC
1096  A5 5E              LDA EXP1
1098  E9 0C              SBC #$0C          ;DIVIDE BY 4096
109A  85 5E              STA EXP1
109C  60                 RTS
109D  48         ERR     PHA
109E  A2 08              LDX #$08
10A0  BD B1 10   ERR3    LDA ERR1,X
10A3  20 D2 FF           JSR $FFD2         ;OUTPUT A CHARACTER
10A6  CA                 DEX
10A7  D0 F7              BNE ERR3
10A9  A9 FF      ERR2    LDA #$FF
10AB  85 63              STA $63           ;O/L INDICATION BY NEGATING RESULT
10AD  68                 PLA
10AE  4C 6B 10           JMP RMSB
10B1  00         ERR1    .BYTE $00
10B2  44                 .BYTE $44
10B3  41                 .BYTE $41
10B4  4F                 .BYTE $4F
10B5  4C                 .BYTE $4C
10B6  52                 .BYTE $52
10B7  45                 .BYTE $45
10B8  56                 .BYTE $56
```



```
LINE# LOC CODE LINE

10B9  4F                 .BYTE $4F
10BA             ;DELAY SUBROUTINE
10BA  58         DELY    CLI
10BB  A9 00              LDA #$00
10BD  85 8F              STA $8F
10BF  E4 8F      WAIT1   CPX $8F
10C1  D0 FC              BNE WAIT1
10C3  78                 SEI
10C4  60                 RTS
10C5             ;RECORD DATA IN ANALOGUE MEMORY
10C5  A9 F0      REC     LDA #<NMI
10C7  85 94              STA $94
10C9  A9 10              LDA #>NMI
10CB  85 95              STA $95
10CD  A9 0A              LDA #$0A
10CF  8D 0C 96           STA PCR           ;CA2 PULSE ON READ IRA
10D2  A9 BB              LDA #$BB
10D4  8D 02 96           STA DDRB
10D7  A9 82              LDA #$82
10D9  8D 0E 96           STA IER           ;CA1 INTERRUPT ENABLE(STATUS HIGH TO LOW)
10DC  A9 3A              LDA #%00111010
10DE  8D 00 96           STA ORB           ;GATE OPEN
10E1  AD 01 96           LDA IRA           ;SINGLE PULSE
10E4  A9 BB              LDA #%10111011
10E6  8D 00 96           STA ORB
10E9  78                 SEI               ;TO PREVENT SERVICE EVERY 1/60 SEC.
10EA  AD 01 96   LOOP1   LDA IRA
10ED  4C EA 10           JMP LOOP1         ;GIVE CLOCK PULSES TILL INTERRUPT OCCURS
10F0  A9 89      NMI     LDA #$89          ;RESTORE VECTOR
10F2  85 94              STA $94
10F4  A9 C3              LDA #$C3
10F6  85 95              STA $95
10F8  68                 PLA               ;RESTORE STACK FOR RTS INSTRUCTION
10F9  68                 PLA
10FA  68                 PLA
10FB  60                 RTS
10FC             ;SUBROUTINE TO ACCUMULATE SQUARED DATA IN ACC#1
```

```
10FC  A9 00       SUM    LDA #$00       ;RESET RESULT STORES
10FE  85 67              STA EXP2+1     ;RESULT HIGH
1100  85 68              STA EXP2+2     ;RESULT LOW
1102  A2 08              LDX #$08
1104  18          LOOP2  CLC
1105  46 66              LSR EXP2       ;DATA1
1107  90 06              BCC JUMP1
1109  A5 6B              LDA EXP2+5     ;DATA2
110B  18                 CLC
110C  4C 11 11           JMP JUMP2
110F  A9 00       JUMP1  LDA #$00
1111  65 67       JUMP2  ADC EXP2+1
1113  6A                 ROR A
1114  85 67              STA EXP2+1
1116  66 68              ROR EXP2+2
1118  CA                 DEX
1119  D0 E9              BNE LOOP2
111B  A9 00              LDA #$00
111D  85 69              STA EXP2+3
111F  85 6A              STA EXP2+4
1121  A2 90              LDX #$90
1123  E4 5E       LOOP3  CPX EXP1       ;ADJUST ACC2 TO ACC1
1125  F0 0C              BEQ JUMP3
1127  E8                 INX
1128  46 67              LSR EXP2+1
112A  66 68              ROR EXP2+2
112C  66 69              ROR EXP2+3
112E  66 6A              ROR EXP2+4
1130  4C 23 11           JMP LOOP3
1133  A2 04       JUMP3  LDX #$04
1135  18                 CLC
1136  B5 5E       LOOP4  LDA EXP1,X     ;ADD ACC2 TO ACC1
1138  75 66              ADC EXP2,X
113A  95 5E              STA EXP1,X
113C  CA                 DEX
113D  D0 F7              BNE LOOP4
113F  90 0A              BCC JUMP4      ;TEST FOR OVERFLOW
```

0:MASTERSRC......PAGE 0006

LINE# LOC CODE LINE

```
1141  E6 5E              INC EXP1
1143  66 5F              ROR EXP1+1
1145  66 60              ROR EXP1+2
1147  66 61              ROR EXP1+3
1149  66 62              ROR EXP1+4
114B  60          JUMP4  RTS
114C                     .END
114C                     .LIB 0:MFILTSRC
114C              PA=$9180
114C              PADD=$9181
114C              PB=$9182
114C              PBDD=$9183
114C  00          LF     .BYTE 0
114D  00          LRGE   .BYTE 0
114E  00          UF     .BYTE 0
114F  00          URGE   .BYTE 0
1150  78          FILT   SEI
1151  A9 FF              LDA #$FF
1153  8D 81 91           STA PADD       ;PA0-7=O/P
1156  A9 7F              LDA #$7F
1158  8D 83 91           STA PBDD       ;PB7 ONLY=I/P
115B                                   ;SET UPPER CUT-OFF FREQUENCY
115B  38                 SEC
115C  A9 FF              LDA #$FF
115E  ED 4E 11           SBC UF
1161  8D 80 91           STA PA
1164  38                 SEC
1165  A9 FF              LDA #$FF
1167  ED 4F 11           SBC URGE
116A  0A                 ASL A          ;RANGE=PB1-5
116B  09 41              ORA #%01000001 ;PB6=ADDRESS
116D  8D 82 91           STA PB         ;PB0=STROBE
1170  CE 82 91           DEC PB         ;ENTER STROBE
1173  AD 82 91    WAIT3  LDA PB
1176  30 FB              BMI WAIT3      ;ACKNOWLEDGE RESPONSE
1178  EE 82 91           INC PB
117B                                   ;SET LOWER CUT-OFF FREQUENCY
```

```
0223  117B  38              SEC
0224  117C  A9 FF           LDA #$FF
0225  117E  ED 4C 11        SBC LF
0226  1181  8D 80 91        STA PA
0227  1184  38              SEC
0228  1185  A9 FF           LDA #$FF
0229  1187  ED 4B 11        SBC LRGE
0230  118A  0A              ASL A
0231  118B  09 01           ORA #%00000001
0232  118D  29 BF           AND #%10111111   ;ADDRESS=0
0233  118F  8D 82 91        STA PB
0234  1192  CE 82 91        DEC PB
0235  1195  AD 82 91  WAIT2 LDA PB
0236  1198  30 FB           BMI WAIT2
0237  119A  EE 82 91        INC PB
0238  119D  60              RTS
0239  119E                  .END
0240  119E                  .LIB O:ATTSRC
0241  119E            ;SET AUTOMATIC ATTENUATOR (EARLY) FROM OVERLOAD DETECTION FROM THE KEMO
0242  119E            RATN=$9282       ;RECIEVE ATTENUATOR
0243  119E  A9 FF           LDA #$FF
0244  11A0  8D 83 92        STA RATN+1       ;DATA DIRECTION
0245  11A3  A9 01           LDA #$01
0246  11A5  8D 82 92        STA RATN         ;SET ATTEN. MINIMUM
0247  11A8  A9 BB           LDA #%10111011
0248  11AA  8D 02 96        STA DDRB
0249  11AD  A9 00           LDA #$00
0250  11AF  8D 03 96        STA DDRA
0251  11B2  8D 08 96        STA T2LL
0252  11B5  A9 7F           LDA #$7F
0253  11B7  8D 0E 96        STA IER          ;CLEAR INT. ENABLE
0254  11BA  A9 0A           LDA #$0A
0255  11BC  8D 0C 96        STA PCR          ;CA2 PULSE EVERY READ IRA INSTRUCTION
0256  11BF  A9 20           LDA #$20
0257  11C1  8D 0B 96        STA ACR          ;T2 PULSE COUNTING MODE(COUNTS DATA VALID)
0258  11C4  A9 A2           LDA #%10100010
0259  11C6  8D 00 96        STA ORB          ;REC MODE, Y1 SELECT,EXT TRIG HIGH,OVER-RIDE ACTIVE
```



```
LINE# LOC CODE LINE

0260  11C9  AD 01 96        LDA IRA          ;SINGLE PULSE
0261  11CC  A9 A0     EAT3  LDA #$A0
0262  11CE  8D 09 96        STA T2CH         ;INITIALISE COUNTER FOR NO. OF UNDERLOADED SAMPLES
0263  11D1  AD 01 96  EAT2  LDA IRA          ;SINGLE PULSE
0264  11D4  F0 15           BEQ EAT1         ;TEST FOR $00
0265  11D6  18              CLC
0266  11D7  69 01           ADC #$01
0267  11D9  F0 10           BEQ EAT1         ;TEST FOR $FF
0268  11DB  A9 20           LDA #%00100000
0269  11DD  2C 0D 96        BIT IFR          ;TEST FOR T2 INTERRUPT
0270  11E0  F0 EF           BEQ EAT2
0271  11E2  A9 3B           LDA #%00111011   ;GATE CLOSED,OVER-RIDE INACTIVE
0272  11E4  8D 00 96        STA ORB
0273  11E7  AD 01 96        LDA IRA          ;SINGLE PULSE
0274  11EA  60              RTS
0275  11EB  0E 82 92  EAT1  ASL RATN         ;INCREASE ATTENUATION
0276  11EE  AD 01 96        LDA IRA          ;SINGLE PULSE
0277  11F1  A2 80           LDX #$80         ;2 SEC. DELAY
0278  11F3  20 BA 10        JSR DELY         ;1 SEC. DELAY
0279  11F6  4C CC 11        JMP EAT3         ;RE-INITIALISE COUNTER AND CONTINUE
0280  11F9                  .END
0281  11F9                  .LIB O:ACCSRC
0282  11F9            POINTL=$0FF3
0283  11F9            POINTH=$0FF4
0284  11F9  A9 15     SD1   LDA #$15         ;Y2 SELECT (I.E. NEAR MICROPHONE)
0285  11FB  2C A9 25        BIT $25A9        ;2ND ENTRY- Y1 SELECT
0286  11FE  8D 00 96        STA ORB
0287  1201  A2 0F     SD8   LDX #$0F
0288  1203  A9 00           LDA #$00
0289  1205  95 5E     SD9   STA EXP1,X
0290  1207  CA              DEX
0291  1208  D0 FB           BNE SD9
0292  120A  A9 90           LDA #$90
0293  120C  85 5E           STA EXP1
0294  120E  AD 01 96        LDA IRA          ;SYNCHRONISING PULSE
0295  1211  AD 00 96        LDA ORB
0296  1214  09 02           ORA #$02
```

```
1216  8D 00 96          STA ORB         ;RESTORE PB PULSE
1219  A0 01             LDY #$01
121B  20 59 10          JSR RMS         ;ACC#1=RMS
121E  AD F3 0F          LDA POINTL
1221  38                SEC
1222  E9 05             SBC #$05
1224  8D F3 0F          STA POINTL
1227  AA                TAX
1228  B0 03             BCS SD10
122A  CE F4 0F          DEC POINTH
122D  AC F4 0F    SD10  LDY POINTH
1230  20 E3 DA          JSR $DAE3       ;RMS TO STORE
1233  60                RTS
1234                    .END
1234                    .LIB 0:BGROUNDSRC
1234              ;TEST BACKGROUND LEVEL
1234  A9 BB             LDA #$BB
1236  8D 02 96          STA DDRB
1239  A9 08             LDA #$08
123B  8D 0E 96          STA IER         ;INHIBIT CB2 INTERRUPT
123E  A9 4A             LDA #$4A
1240  8D 0C 96          STA PCR         ;CB2 +VE TRANS,CA2 PULSE O/P
1243  A9 3A       BGD1  LDA #$3A
1245  8D 00 96          STA ORB         ;ARM KEMO BY SETTING RECORD MODE
1248  AD 01 96          LDA IRA         ;SINGLE CLOCK PULSE
124B  A9 3B             LDA #$3B
124D  8D 00 96          STA ORB         ;RESET RECORD PULSE AND CLEAR CB2 INTERRU
1250  58                CLI
1251  A9 00             LDA #$00
1253  85 8F             STA $8F         ;RESET JIFFY CLOCK
1255  A9 08       BGD2  LDA #$08
1257  2C 0E             BIT IER         ;TEST FOR TRIGGER
125A  D0 E7             BNE BGD1        ;IF TRIGGER THEN RESTART
125C  A9 3C             LDA #$3C
125E  C5 8F             CMP $8F
1260  B0 F3             BCS BGD2        ;IF JIFFY < 1SEC. THEN RETEST FOR TRIGGER
1262  78                SEI
```


LINE# LOC CODE LINE

```
1263  60                RTS
1264                    .END
1264                    .LIB 0:MADATASRC
1264              ;TAKE DATA FROM THE ADC AND STORE AT $3C00 - $3FFF
1264              PCRA=$900C
1264              IFRA=$900D
1264              BASE=$3C00
1264              IERA=$900E
1264              IRAA=$9001
1264  A9 08             LDA #$08
1266  8D 0C 90          STA PCRA        ;CA2 HANDSHAKE O/P  - CA1 -VE TRANS.
1269  A9 03             LDA #$03
126B  8D 0E 90          STA IERA        ;DISABLE CA1 & CA2 INTERRUPTS
126E  A9 3C             LDA #>BASE
1270  85 FF             STA $FF         ;HIGH POINTER FOR STORAGE
1272  85 35             STA $35         ; "      "      "  LIMIT OF BASIC MEMORY
1274  A9 00             LDA #<BASE
1276  85 FE             STA $FE         ;LOW POINTER FOR STORAGE
1278  85 34             STA $34         ; "      "      "  LIMIT OF BASIC MEMORY
127A  A0 00             LDY #$00
127C  AD 01 90          LDA IRAA        ;START FIRST CONVERSION
127F  A9 02       AD1   LDA #$02
1281  2C 0D 90    AD2   BIT IFRA
1284  F0 FB             BEQ AD2         ;WAIT FOR EOC PULSE HIGH TO LOW
1286  AD 01 90          LDA IRAA        ;GET DATA - START NEXT CONVERSION
1289  91 FE             STA ($FE),Y
128B  C8                INY
128C  D0 F1             BNE AD1         ;TEST FOR END OF PAGE
128E  E6 FF             INC $FF
1290  A5 FF             LDA $FF
1292  C9 40             CMP #$40
1294  D0 E9             BNE AD1
1296                    .END
1296                    .LIB 0:MAVESRC
1296              ;SUBROUTINE TO CALCULATE THE MEAN OF 1K OF DATA ($3C00-$3FFF)
1296              TOTAL=$0054
1296  A9 00             LDA #<BASE
```

```
1298  85 FE            STA $FE
129A  A9 3C            LDA #>BASE
129C  85 FF            STA $FF
129E  A9 00            LDA #$00
12A0  A2 0F            LDX #$0F
12A2  95 5E      AVE1  STA EXP1,X
12A4  CA               DEX
12A5  D0 FB            BNE AVE1
12A7  A9 88            LDA #$88
12A9  85 5E            STA EXP1
12AB  A0 00            LDY #$00
12AD  A9 00      AVE5  LDA #$00
12AF  85 68            STA EXP2+2
12B1  85 69            STA EXP2+3
12B3  85 6A            STA EXP2+4
12B5  B1 FE            LDA ($FE),Y
12B7  85 67            STA EXP2+1
12B9  A2 88            LDX #$88
12BB  E4 5E      AVE3  CPX EXP1
12BD  F0 0C            BEQ AVE2
12BF  46 67            LSR EXP2+1
12C1  66 68            ROR EXP2+2
12C3  66 69            ROR EXP2+3
12C5  66 6A            ROR EXP2+4
12C7  E8               INX
12C8  4C BB 12         JMP AVE3
12CB  A2 04      AVE2  LDX #$04
12CD  18               CLC
12CE  B5 5E      AVE4  LDA EXP1,X
12D0  75 66            ADC EXP2,X
12D2  95 5E            STA EXP1,X
12D4  CA               DEX
12D5  D0 F7            BNE AVE4
12D7  90 0A            BCC AVE7         ;TEST FOR OVERFLOW
12D9  E6 5E            INC EXP1
12DB  66 5F            ROR EXP1+1
12DD  66 60            ROR EXP1+2
```


LINE# LOC CODE LINE

/4

```
12DF  66 61            ROR EXP1+3
12E1  66 62            ROR EXP1+4
12E3  C8         AVE7  INY
12E4  D0 C7            BNE AVE5
12E6  E6 FF            INC $FF
12E8  A5 FF            LDA $FF
12EA  C9 40            CMP #$40
12EC  90 BF            BCC AVE5
12EE  A5 5F            LDA EXP1+1
12F0  30 0D      AVE8  BMI AVE6         ;TEST FOR NON-NORMALISED RESULT
12F2  C6 5E            DEC EXP1
12F4  06 62            ASL EXP1+4
12F6  26 61            ROL EXP1+3
12F8  26 60            ROL EXP1+2
12FA  26 5F            ROL EXP1+1
12FC  4C F0 12         JMP AVE8
12FF  A5 5E      AVE6  LDA EXP1
1301  38               SEC
1302  E9 0A            SBC #$0A         ;DIVIDE BY 1024
1304  85 5E            STA EXP1
1306  A9 88            LDA #$88         ;LOAD ACC#2 WITH 247(BASE10)
1308  85 66            STA EXP2
130A  A9 F7            LDA #$F7
130C  85 67            STA EXP2+1
130E  A9 00            LDA #$00
1310  85 68            STA EXP2+2
1312  85 69            STA EXP2+3
1314  85 6A            STA EXP2+4
1316  20 7B D7         JSR $D77B        ;ADD OFFSET TO RESULT
1319  38               SEC
131A  AD F3 0F         LDA POINTL
131D  E9 05            SBC #$05
131F  8D F3 0F         STA POINTL
1322  B0 03            BCS AVE9
1324  CE F4 0F         DEC POINTH
1327  AE F3 0F   AVE9  LDX POINTL
132A  AC F4 0F         LDY POINTH
```

```
0445  132D  20 E3 DA          JSR $DAE3
0446  1330  38                SEC
0447  1331  AD F3 0F          LDA POINTL
0448  1334  E9 05             SBC #$05
0449  1336  8D F3 0F          STA POINTL
0450  1339  B0 03             BCS AVE18
0451  133B  CE F4 0F          DEC POINTH
0452  133E  A2 04      AVE18  LDX #$04
0453  1340  A9 00             LDA #$00
0454  1342  95 54      AVE24  STA TOTAL,X
0455  1344  CA                DEX
0456  1345  D0 FB             BNE AVE24
0457  1347  A9 92             LDA #$92
0458  1349  85 54             STA TOTAL
0459  134B  A9 00             LDA #<BASE      ;CALCULATE SIGMA(X*X)
0460  134D  85 FE             STA $FE
0461  134F  A9 3C             LDA #>BASE
0462  1351  85 FF             STA $FF
0463  1353  A0 00             LDY #$00
0464  1355  A9 00      AVE12  LDA #$00
0465  1357  85 66             STA EXP2
0466  1359  85 60             STA EXP1+2
0467  135B  85 68             STA EXP2+2
0468  135D  85 61             STA EXP1+3
0469  135F  85 69             STA EXP2+3
0470  1361  85 62             STA EXP1+4
0471  1363  85 6A             STA EXP2+4
0472  1365  B1 FE             LDA ($FE),Y
0473  1367  18                CLC
0474  1368  69 F7             ADC #$F7
0475  136A  6A                ROR A
0476  136B  85 67             STA EXP2+1
0477  136D  85 5F             STA EXP1+1
0478  136F  90 5F          BCC AVE25
***UNDEFINED SYMBOL********
0479  1371  A9 80             LDA #$80
0480  1373  85 60             STA EXP1+2
```

D:MASTERSRC......PAGE 0014

LINE# LOC CODE LINE

```
0481  1375  85 68             STA EXP2+2
0482  1377  A9 92             LDA #$92
0483  1379  85 5E             STA EXP1
0484  137B  98                TYA
0485  137C  48                PHA
0486  137D  20 3F D9          JSR $D93F       ;ACC#1=(X+OFFSET).
0487  1380  68                PLA
0488  1381  A8                TAY
0489  1382  A6 5E             LDX EXP1
0490  1384  E4 54      AVE20  CPX TOTAL       ;COMPARE ACC#1 WITH TOTAL
0491  1386  F0 0C             BEQ AVE19
0492  1388  46 5F             LSR EXP1+1
0493  138A  66 60             ROR EXP1+2
0494  138C  66 61             ROR EXP1+3
0495  138E  66 62             ROR EXP1+4
0496  1390  E8                INX
0497  1391  4C 84 13          JMP AVE20
0498  1394  A2 04      AVE19  LDX #$04        ;ADD ACC#1 TO TOTAL
0499  1396  18                CLC
0500  1397  B5 5E      AVE21  LDA EXP1,X
0501  1399  75 54             ADC TOTAL,X
0502  139B  95 54             STA TOTAL,X
0503  139D  CA                DEX
0504  139E  D0 F7             BNE AVE21
0505  13A0  90 0A             BCC AVE23       ;TEST FOR OVERFLOW
0506  13A2  E6 54             INC TOTAL
0507  13A4  66 55             ROR TOTAL+1
0508  13A6  66 56             ROR TOTAL+2
0509  13A8  66 57             ROR TOTAL+3
0510  13AA  66 58             ROR TOTAL+4
0511  13AC  C8         AVE23  INY
0512  13AD  D0 A6             BNE AVE12       ;TEST FOR END OF PAGE
0513  13AF  E6 FF             INC $FF
0514  13B1  A5 FF             LDA $FF
0515  13B3  C9 40             CMP #$40        ;TEST FOR END OF 1K
0516  13B5  90 9E             BCC AVE12
0517  13B7  A5 55             LDA TOTAL+1     ;TEST FOR NON-NORMALISED RESULT
```

```
13B9  30 0D        AVE14  BMI AVE13
13BB  C6 54               DEC TOTAL
13BD  06 58               ASL TOTAL+4
13BF  26 57               ROL TOTAL+3
13C1  26 56               ROL TOTAL+2
13C3  26 55               ROL TOTAL+1
13C5  4C B9 13            JMP AVE14
13C8  38           AVE13  SEC
13C9  A5 54               LDA TOTAL
13CB  E9 0A               SBC #$0A        ;DIVIDE BY 1024
13CD  85 54               STA TOTAL
13CF  AD F3 0F            LDA POINTL
13D2  85 1F               STA $1F
13D4  AD F4 0F            LDA POINTH
13D7  85 20               STA $20
13D9  A0 04               LDY #$04
13DB  B9 54 00     AVE22  LDA TOTAL,Y
13DE  91 1F               STA ($1F),Y
13E0  88                  DEY
13E1  D0 F8               BNE AVE22
13E3  A5 54               LDA TOTAL
13E5  91 1F               STA ($1F),Y
13E7                      .END
13E7                      .LIB O:MDIRSRC
13E7               ;PROGRAMME TO COUNT PULSES FROM WIND DIRECTION SENSOR
13E7               ORBB=$9000
13E7               IERB=$900E
13E7               T2LLB=$9008
13E7               PCRB=$900C
13E7               ACRB=$900B
13E7               IFRB=$900D
13E7               T2CHB=$9009
13E7  4C EB 13            JMP DIR0
13EA  00           COUNTL .BYTE 00
13EB  A9 18        DIR0   LDA #$18
13ED  8D 0E 90            STA IERB        ;DISABLE CB1/CB2 INTERRUPTS
13F0  A9 FF               LDA #$FF
```



```
13F2  8D 08 90            STA T2LLB
13F5  A9 40               LDA #$40
13F7  8D 0C 90            STA PCRB        ;CB2 +VE TRANS.,CB1 -VE
13FA  A9 20               LDA #$20
13FC  8D 0B 90            STA ACRB        ;T2 PULSE COUNT MODE
13FF  AD 00 90            LDA ORBB        ;CLEAR IFR
1402  A9 08               LDA #$08
1404  2C 0D 90     DIR1   BIT IFRB
1407  F0 FB               BEQ DIR1        ;WAIT FOR CB2 - I.E. START COUNT PULSE
1409  A9 00               LDA #$00
140B  8D 09 90            STA T2CHB       ;T2=$00FF - START COUNT
140E  AD 00 90            LDA ORBB        ;CLEAR IFR
1411  A9 10               LDA #$10
1413  2C 0D 90     DIR2   BIT IFRB
1416  F0 FB               BEQ DIR2        ;WAIT FOR CB1 - I.E COINCIDENCE PULSE
1418  AD 08 90            LDA T2LLB       ;GET COUNT
141B  8D EA 13            STA COUNTL
141E  A9 FF               LDA #$FF
1420  38                  SEC
1421  ED EA 13            SBC COUNTL      ;COMPLIMENT COUNT
1424  8D EA 13            STA COUNTL
1427  A0 00               LDY #$00
1429  38                  SEC
142A  AD F3 0F            LDA POINTL
142D  E9 01               SBC #$01
142F  8D F3 0F            STA POINTL
1432  85 1F               STA $1F
1434  AD F4 0F            LDA POINTH
1437  E9 00               SBC #$00
1439  8D F4 0F            STA POINTH
143C  85 20               STA $20
143E  AD EA 13            LDA COUNTL
1441  91 1F               STA ($1F),Y
1443                      .END
1443                      .LIB O:MTEMPSRC
1443               ;COUNT PULSES FROM TEMPERATURE SENS USING 6522 @ $9700 - $970F
1443               ORBT=$9700
```

```
0592  1443  4C 48 14          JMP TEMO
0593  1446  00        TEMPL   .BYTE 00
0594  1447  00        TEMPH   .BYTE 00
0595  1448  58        TEMO    CLI
0596  1449  A9 20             LDA #$20
0597  144B  8D 0B 97          STA ORBT+11      ;ACR-T2 PULSE COUNT MODE
0598  144E  A9 FF             LDA #$FF
0599  1450  8D 08 97          STA ORBT+8       ;T2LL
0600  1453  A2 3C             LDX #$3C         ;1 SEC. DELAY
0601  1455  A9 FF             LDA #$FF
0602  1457  8D 09 97          STA ORBT+9       ;START COUNTING
0603  145A  20 BA 10          JSR DELY
0604  145D  AD 0B 97          LDA ORBT+11
0605  1460  29 DF             AND #%11011111   ;STOP PULSE COUNTING
0606  1462  AD 08 97          LDA ORBT+8
0607  1465  8D 46 14          STA TEMPL
0608  1468  AD 09 97          LDA ORBT+9
0609  146B  8D 47 14          STA TEMPH
0610  146E  38                SEC              ;SUBTRACT FROM $FFFF
0611  146F  A9 FF             LDA #$FF
0612  1471  ED 46 14          SBC TEMPL
0613  1474  8D 46 14          STA TEMPL
0614  1477  A9 FF             LDA #$FF
0615  1479  ED 47 14          SBC TEMPH
0616  147C  8D 47 14          STA TEMPH
0617  147F  38                SEC
0618  1480  AD F3 0F          LDA POINTL
0619  1483  E9 02             SBC #$02
0620  1485  8D F3 0F          STA POINTL
0621  1488  85 1F             STA $1F
0622  148A  AD F4 0F          LDA POINTH
0623  148D  E9 00             SBC #$00
0624  148F  8D F4 0F          STA POINTH
0625  1492  85 20             STA $20
0626  1494  A0 01             LDY #$01
0627  1496  AD 46 14          LDA TEMPL
0628  1499  91 1F             STA ($1F),Y
```



```
LINE# LOC CODE LINE

0629  149B  88                DEY
0630  149C  AD 47 14          LDA TEMPH
0631  149F  91 1F             STA ($1F),Y
0632  14A1  60                RTS
0633  14A2                    .END
0634  14A2                    .LIB 0:MSAVESRC
0635  14A2            ;SUBROUTINE TO SAVE DATA
0636  14A2  A2 08             LDX #$08
0637  14A4  86 D4             STX $D4          ;DEVICE NO. (8 FOR DISC)
0638  14A6  CA                DEX
0639  14A7  86 B4             STX $B4          ;BUFFER CHARACTER (SIMULATES SAVE INSTRUCTION)
0640  14A9  A9 00             LDA #$00
0641  14AB  85 9D             STA $9D          ;LOAD/VERIFY FLAG
0642  14AD  A0 02             LDY #$02
0643  14AF  18                CLC
0644  14B0  B1 2A             LDA ($2A),Y
0645  14B2  69 02             ADC #$02
0646  14B4  85 D1             STA $D1          ;FILE NAME LENGTH
0647  14B6  AD F3 0F          LDA $0FF3
0648  14B9  C8                INY
0649  14BA  38                SEC
0650  14BB  B1 2A             LDA ($2A),Y
0651  14BD  E9 02             SBC #$02
0652  14BF  85 DA             STA $DA          ;FILE NAME ADDRESS LOW
0653  14C1  C8                INY
0654  14C2  B1 2A             LDA ($2A),Y
0655  14C4  E9 00             SBC #$00
0656  14C6  85 DB             STA $DB          ;FILE NAME ADDRESS HIGH
0657  14C8  A0 00             LDY #$00
0658  14CA  A9 30             LDA #'0          ;FOR DISK DRIVE NO. 0
0659  14CC  91 DA             STA ($DA),Y
0660  14CE  C8                INY
0661  14CF  A9 3A             LDA #':          ;DELIMITER
0662  14D1  91 DA             STA ($DA),Y
0663  14D3  85 FB             STA $FB          ;START ADDRESS LOW
0664  14D5  AD F4 0F          LDA $0FF4
0665  14D8  85 FC             STA $FC          ;START ADDRESS HIGH
```

```
14DA  A9 00           LDA #$00
14DC  85 C9           STA $C9          ;END ADDRESS LOW
14DE  A9 3C           LDA #$3C
14E0  85 CA           STA $CA          ;END ADDRESS HIGH
14E2  20 A4 F6        JSR $F6A4        ;PERFORM SAVE
14E5  60              RTS
14E6                  .END
14E6                  .END
```

```
ERRORS = 0001
```

```
SYMBOL TABLE

SYMBOL VALUE
 ACR      960B    ACRD     900B    AD1      127F    AD2      1281
 AVE1     12A2    AVE12    1355    AVE13    13C8    AVE14    13B9
 AVE18    133E    AVE19    1394    AVE2     12CB    AVE20    1384
 AVE21    1397    AVE22    13DB    AVE23    13AC    AVE24    1342
 AVE3     12BB    AVE4     12CE    AVE5     12AD    AVE6     12FF
 AVE7     12E3    AVE8     12F0    AVE9     1327    BASE     3C00
 BGD1     1243    BGD2     1255    CALF     0FFB    CALN     0FF6
 COUNTL   13EA    DDRA     9603    DDRB     9602    DELY     10BA
 DIR0     13EB    DIR1     1404    DIR2     1413    EAT1     11EB
 EAT2     11D1    EAT3     11CC    ENT1     100F    ERR      109D
 ERR1     10B1    ERR2     10A9    ERR3     10A0    EXP1     005E
 EXP2     0066    FILT     1150    IER      960E    IERA     900E
 IERB     900E    IFR      960D    IFRA     900D    IFRB     900D
 IRA      9601    IRAA     9001    JUMP1    110F    JUMP2    1111
 JUMP3    1133    JUMP4    114B    JUMP6    1078    JUMP7    1095
 LF       114C    LOOP1    10EA    LOOP2    1104    LOOP3    1123
 LOOP4    1136    LOOP5    1086    LRGE     114B    NMI      10F0
 ORB      9600    ORBD     9000    ORBT     9700    OVER     0FF5
 PA       9180    PADD     9181    PB       9182    PBDD     9183
 PCR      960C    PCRA     900C    PCRD     900C    POINTH   0FF4
```

```
SYMBOL TABLE

SYMBOL VALUE
 POINTL   0FF3    RATN     9282    REC      10C5    RMS      1059
 RMS1     1065    RMSA     1068    RMSB     106B    SD1      11F9
 SD10     122D    SD8      1201    SD9      1205    SUM      10FC
 T2CH     9609    T2CHB    9009    T2LL     9608    T2LLB    9008
 TEMO     1448    TEMPH    1447    TEMPL    1446    TOTAL    0054
 WF       114E    URGE     114F    WAIT1    10BF    WAIT2    1195
 WAIT3    1173
END OF ASSEMBLY
```

```
0000                    ;CONTROL PROGRAMME.VERSION/4 FOR USE WITH MODELS. DATA SENT TO DEC/20
0000                           .LIB O:MASTSRC/4
0000                    ;VERSION /4 FOR USE WITH MODELS
0000                    EXP1=$5E
0000                    EXP2=$66
0000                    ORB=$9600
0000                    IRA=$9601
0000                    DDRA=$9603
0000                    DDRB=$9602
0000                    T2LL=$9608
0000                    T2CH=$9609
0000                    ACR=$960B
0000                    PCR=$960C
0000                    IFR=$960D
0000                    IER=$960E
0000                    OVER=$0FFB
0000                    ;CALCULATE AND SAVE CALIBRATIONS
0000                           *=$1000
1000  A0 02                    LDY #$02        ;ENTRY FOR NEAR CAL.
1002  A2 15                    LDX #$15
1004  4C 0B 10                 JMP ENT1
1007  A0 09                    LDY #$09        ;ENTRY FOR FAR CAL.
1009  A2 25                    LDX #$25
100B  A9 BB             ENT1   LDA #$BB
100D  8D 02 96                 STA DDRB
1010  8E 00 96                 STX ORB
1013  84 1F                    STY $1F         ;DETERMINE LOCATION OF APPROPRIATE VARIABLE (CN OR CF)
1015  18                       CLC
1016  A5 2A                    LDA $2A
1018  65 1F                    ADC $1F
101A  48                       PHA
101B  A5 2B                    LDA $2B
101D  69 00                    ADC #$00
101F  48                       PHA
1020  A9 01                    LDA #$01
1022  8D 80 92                 STA $9280
1025  8D 82 92                 STA $9282
```

O:MASTERSRC/4......PAGE 0002

LINE# LOC CODE LINE

```
1028  A9 FF                    LDA #$FF
102A  8D 81 92                 STA $9281
102D  8D 83 92                 STA $9283
1030  A9 90                    LDA #$90
1032  85 5E                    STA EXP1
1034  A9 00                    LDA #$00
1036  8D 03 96                 STA DDRA
1039  85 5F                    STA EXP1+1      ;INITIALISE ACCM1
103B  85 60                    STA EXP1+2
103D  85 61                    STA EXP1+3
103F  85 62                    STA EXP1+4
1041  A9 7F                    LDA #$7F
1043  8D 0E 96                 STA IER
1046  A9 0A                    LDA #$0A
1048  8D 0C 96                 STA PCR         ;CA2 PULSE ON READ IRA,CA1 & CA2 -VE TRANSITI
104B  AD 01 96                 LDA IRA         ;SYNCHRONISING PULSE
104E  AD 00 96                 LDA ORB
1051  09 02                    ORA #$02        ;RESTORE PB PULSE
1053  8D 00 96                 STA ORB
1056  A0 00                    LDY #$00
1058  A9 10                    LDA #$10
105A  85 FE                    STA $FE
105C  A9 00                    LDA #$00
105E  8D FB 0F                 STA OVER
1061  A9 0C                    LDA #$0C
1063  8D DA 10                 STA RMSC+1
1066  20 84 10                 JSR RMSE        ;ACCM1 =SIGMA(X*X)/4096
1069  20 5E DE                 JSR $DE5E       ;ACCM1=RMS
106C  68                       PLA
106D  85 20                    STA $20
106F  68                       PLA
1070  85 1F                    STA $1F
1072  20 E7 DA                 JSR $DAE7       ;ACC1 TO MEMORY
1075  60                       RTS
1076  A9 04             RMS    LDA #$04
1078  85 FE                    STA $FE
107A  A9 C0                    LDA #$C0
```

```
107C  8D FB 0F          STA OVER
107F  A9 0A             LDA #$0A
1081  8D DA 10          STA RMSC+1
1084  A9 00      RMSE   LDA #$00
1086  85 FF             STA $FF
1088  98         RMSD   TYA
1089  F0 0C             BEQ RMSA
108B  AD 01 96          LDA IRA         ;GET A BYTE OF DATA
108E  F0 04             BEQ RMS1        ;TEST FOR -VE OVERLOAD
1090  C9 FF             CMP #$FF        ;  "    "  +VE    "
1092  D0 06             BNE RMSB
1094  4C DE 10   RMS1   JMP ERR
1097  AD 01 96   RMSA   LDA IRA
109A  38         RMSB   SEC
109B  E9 80             SBC #$80        ;SUBTRACT GND LEVEL
109D  85 66             STA EXP2
109F  B0 06             BCS JUMP6       ;TEST FOR RESULT -VE.
10A1  A9 01             LDA #$01        ;2'S COMP.
10A3  E5 66             SBC EXP2
10A5  85 66             STA EXP2
10A7  85 6B      JUMP6  STA EXP2+5
10A9  20 45 11          JSR SUM         ;ACC1=(SIGMA X*X)
10AC  E6 FF             INC $FF
10AE  D0 D8             BNE RMSD
10B0  C6 FE             DEC $FE
10B2  D0 D4             BNE RMSD
10B4  AD FB 0F          LDA OVER
10B7  F0 0C             BEQ RMSF
10B9  AD 01 96   RMSG   LDA IRA
10BC  E6 FF             INC $FF
10BE  D0 F9             BNE RMSG
10C0  CE FB 0F          DEC OVER
10C3  D0 F4             BNE RMSG
10C5  A5 5F      RMSF   LDA EXP1+1
10C7  30 0D      LOOP5  BMI JUMP7       ;TEST FOR NON-NORMALISED RESULT
10C9  C6 5E             DEC EXP1
10CB  06 62             ASL EXP1+4
```


LINE# LOC CODE LINE

```
10CD  26 61             ROL EXP1+3
10CF  26 60             ROL EXP1+2
10D1  26 5F             ROL EXP1+1
10D3  4C C7 10          JMP LOOP5
10D6  38         JUMP7  SEC
10D7  A5 5E             LDA EXP1
10D9  E9 0A      RMSC   SBC #$0A
10DB  85 5E             STA EXP1
10DD  60                RTS
10DE  48         ERR    PHA
10DF  A2 08             LDX #$08
10E1  BD F2 10   ERR3   LDA ERR1,X
10E4  20 D2 FF          JSR $FFD2       ;OUTPUT A CHARACTER
10E7  CA                DEX
10E8  30 F7             BMI ERR3
10EA  A9 FF      ERR2   LDA #$FF
10EC  85 63             STA $63         ;O/L INDICATION BY NEGATING RESULT
10EE  68                PLA
10EF  4C 9A 10          JMP RMSB
10F2  20         ERR1   .BYTE $20
10F3  44                .BYTE $44
10F4  41                .BYTE $41
10F5  4F                .BYTE $4F
10F6  4C                .BYTE $4C
10F7  52                .BYTE $52
10F8  45                .BYTE $45
10F9  56                .BYTE $56
10FA  4F                .BYTE $4F
10FB                    ;DELAY SUBROUTINE
10FB  58         DELY   CLI
10FC  A9 00             LDA #$00
10FE  85 8F             STA $8F
1100  E4 8F      WAIT1  CPX $8F
1102  D0 FC             BNE WAIT1
1104  78                SEI
1105  60                RTS
1106                    ;RECORD DATA IN ANALOGUE MEMORY
```

```
1106  A9 31     REC    LDA #<NMI
1108  85 94            STA $94
110A  A9 11            LDA #>NMI
110C  85 95            STA $95
110E  A9 0A            LDA #$0A
1110  8D 0C 96         STA PCR         ;CA2 PULSE ON READ IRA
1113  A9 BB            LDA #$BB
1115  8D 02 96         STA DDRB
1118  A9 82            LDA #$82
111A  8D 0E 96         STA IER         ;CA1 INTERRUPT ENABLE(STATUS HIGH TO LOW)
111D  A9 3A            LDA #%00111010
111F  8D 00 96         STA ORB         ;GATE OPEN
1122  AD 01 96         LDA IRA         ;SINGLE PULSE
1125  A9 BB            LDA #%10111011
1127  8D 00 96         STA ORB
112A  78               SEI             ;TO PREVENT SERVICE EVERY 1/60 SEC.
112B  AD 01 96  LOOP1  LDA IRA
112E  4C 2B 11         JMP LOOP1       ;GIVE CLOCK PULSES TILL INTERRUPT OCCURS
1131  A9 89     NMI    LDA #$89        ;RESTORE VECTOR
1133  85 94            STA $94
1135  A9 C3            LDA #$C3
1137  85 95            STA $95
1139  68               PLA             ;RESTORE STACK FOR RTS INSTRUCTION
113A  68               PLA
113B  68               PLA
113C  A9 3B            LDA #$3B        ;CLOSE GATE
113E  8D 00 96         STA ORB
1141  AD 01 96         LDA IRA         ;CLOCK PULSE
1144  60               RTS
1145            ;SUBROUTINE TO ACCUMULATE SQUARED DATA IN ACC#1
1145  A9 00     SUM    LDA #$00        ;RESET RESULT STORES
1147  85 67            STA EXP2+1      ;RESULT HIGH
1149  85 68            STA EXP2+2      ;RESULT LOW
114B  A2 08            LDX #$08
114D  18        LOOP2  CLC
114E  46 66            LSR EXP2        ;DATA1
1150  90 06            BCC JUMP1
```

O:MASTERSRC/4......PAGE 0006

LINE# LOC CODE LINE

```
1152  A5 6B            LDA EXP2+5      ;DATA2
1154  18               CLC
1155  4C 5A 11         JMP JUMP2
1158  A9 00     JUMP1  LDA #$00
115A  65 67     JUMP2  ADC EXP2+1
115C  6A               ROR A
115D  85 67            STA EXP2+1
115F  66 68            ROR EXP2+2
1161  CA               DEX
1162  D0 E9            BNE LOOP2
1164  A9 00            LDA #$00
1166  85 69            STA EXP2+3
1168  85 6A            STA EXP2+4
116A  A2 90            LDX #$90
116C  E4 5E     LOOP3  CPX EXP1        ;ADJUST ACC2 TO ACC1
116E  F0 0C            BEQ JUMP3
1170  E8               INX
1171  46 67            LSR EXP2+1
1173  66 68            ROR EXP2+2
1175  66 69            ROR EXP2+3
1177  66 6A            ROR EXP2+4
1179  4C 6C 11         JMP LOOP3
117C  A2 04     JUMP3  LDX #$04
117E  18               CLC
117F  B5 5E     LOOP4  LDA EXP1,X      ;ADD ACC2 TO ACC1
1181  75 66            ADC EXP2,X
1183  95 5E            STA EXP1,X
1185  CA               DEX
1186  D0 F7            BNE LOOP4
1188  90 0A            BCC JUMP4       ;TEST FOR OVERFLOW
118A  E6 5E            INC EXP1
118C  66 5F            ROR EXP1+1
118E  66 60            ROR EXP1+2
1190  66 61            ROR EXP1+3
1192  66 62            ROR EXP1+4
1194  60        JUMP4  RTS
1195                   .END
```

```
1195                   .LIB 0:ATTSRC/4
1195              ;SET FAR CHANNEL AUTO-ATTENUATOR BY OVERLOAD DETECTION DURING TONE-BURSTS
1195              RATN=$9282
1195  A9 FF            LDA #$FF
1197  8D 83 92         STA RATN+1
119A  A0 01            LDY #$01
119C  8C 82 92         STY RATN       ;SET MIN. ATTENUATION
119F  20 06 11  ATT3   JSR REC        ;RECORD DATA
11A2  A9 25            LDA #%00100101
11A4  8D 00 96         STA ORB        ;PLAYBACK MODE. SELECT FAR CHANNEL
11A7  AD 01 96         LDA IRA
11AA  A9 27            LDA #%00100111
11AC  8D 00 96         STA ORB
11AF  A9 04            LDA #$04
11B1  85 FE            STA $FE
11B3  A9 00            LDA #$00
11B5  85 FF            STA $FF
11B7  AD 01 96  ATT2   LDA IRA
11BA  F0 10            BEQ ATT1       ;TEST FOR -VE OVERLOAD
11BC  C9 FF            CMP #$FF
11BE  F0 0C            BEQ ATT1       ;TEST FOR +VE OVERLOAD
11C0  E6 FF            INC $FF
11C2  D0 F3            BNE ATT2
11C4  C6 FE            DEC $FE
11C6  D0 EF            BNE ATT2
11C8  88               DEY
11C9  10 07            BPL ATT4       ;CAPTURE ANOTHER BURST TO MAKE SURE OF ATTENUATOR SETTING
11CB  60               RTS
11CC  0E 82 92  ATT1   ASL RATN       ;INC ATTENUATION
11CF  AD 01 96         LDA IRA
11D2  A2 3C     ATT4   LDX #$3C
11D4  20 FB 10         JSR DELY       ;1 SEC. DELAY
11D7  4C 9F 11         JMP ATT3
11DA                   .END
11DA                   .LIB 0:SET901SRC/3
11DA              ;ARM DL901 READY FOR EXTERNAL TRIGGER
11DA              PAB=$9380
```


LINE# LOC CODE LINE

```
11DA              DDRAB=$9381
11DA              PBB=$9382
11DA              DDRBB=$9383
11DA              BASE=$7C00
11DA  A9 00            LDA #$00
11DC  8D 84 93         STA $9384
11DF  8D 81 93         STA DDRAB      ;ALL I/P
11E2  A9 B1            LDA #$B1
11E4  8D 83 93         STA DDRBB      ;PB0,4,5,7 O/P
11E7  A9 B0            LDA #$B0       ;ARM,DOE&DOR ALL HIGH
11E9  8D 82 93         STA PBB
11EC  A9 30            LDA #$30       ;ARM LOW
11EE  8D 82 93         STA PBB
11F1  60               RTS
11F2                   .END
11F2                   .LIB 0:BGROUNDSRC
11F2              ;TEST BACKGROUND LEVEL
11F2  A9 BB            LDA #$BB
11F4  8D 02 96         STA DDRB
11F7  A9 08            LDA #$08
11F9  8D 0E 96         STA IER        ;INHIBIT CB2 INTERRUPT
11FC  A9 4A            LDA #$4A
11FE  8D 0C 96         STA PCR        ;CB2 +VE TRANS,CA2 PULSE O/P
1201  A9 3A     BGD1   LDA #$3A
1203  8D 00 96         STA ORB        ;ARM KEMO BY SETTING RECORD MODE
1206  AD 01 96         LDA IRA        ;SINGLE CLOCK PULSE
1209  A9 3B            LDA #$3B
120B  8D 00 96         STA ORB        ;RESET RECORD PULSE AND CLEAR CB2 INTERRUPT
120E  58               CLI
120F  A9 00            LDA #$00
1211  85 8F            STA $8F        ;RESET JIFFY CLOCK
1213  A9 08     BGD2   LDA #$08
1215  2C 0D 96         BIT IFR        ;TEST FOR TRIGGER
1218  D0 E7            BNE BGD1       ;IF TRIGGER THEN RESTART
121A  A9 3C            LDA #$3C
121C  C5 8F            CMP $8F
121E  B0 F3            BCS BGD2       ;IF JIFFY < 1SEC. THEN RETEST FOR TRIGGER
```

```
1220  78                SEI
1221  60                RTS
1222                    .END
1222                    .LIB O:ACCSRC/3
1222              POINTL=$0FFE
1222              POINTH=$0FFF
1222  A2 15       SD1   LDX #$15       ;Y2 SELECT (I.E. NEAR CHANNEL)
1224  A0 10             LDY #$10
1226  4C 2D 12          JMP SD2
1229  A2 25             LDX #$25
122B  A0 17             LDY #$17
122D  8E 00 96    SD2   STX ORB
1230  84 1F             STY $1F
1232  18                CLC
1233  A5 2A             LDA $2A
1235  65 1F             ADC $1F
1237  48                PHA
1238  A5 2B             LDA $2B
123A  69 00             ADC #$00
123C  48                PHA
123D  A2 0F       SD8   LDX #$0F
123F  A9 00             LDA #$00
1241  95 5E       SD9   STA EXP1,X
1243  CA                DEX
1244  D0 FB             BNE SD9
1246  A9 90             LDA #$90
1248  85 5E             STA EXP1
124A  AD 01 96          LDA IRA        ;SYNCHRONISING PULSE
124D  AD 00 96          LDA ORB
1250  09 02             ORA #$02
1252  8D 00 96          STA ORB        ;RESTORE PB PULSE
1255  A0 01             LDY #$01
1257  20 76 10          JSR RMS        ;ACC#1=RMS^2
125A  AD FE 0F          LDA POINTL
125D  38                SEC
125E  E9 05             SBC #$05
1260  8D FE 0F          STA POINTL
```

O:MASTERSRC/4......PAGE 0010

LINE# LOC CODE LINE

```
1263  AA                TAX
1264  B0 03             BCS SD10
1266  CE FF 0F          DEC POINTH
1269  AC FF 0F    SD10  LDY POINTH
126C  20 E3 DA          JSR $DAE3      ;RMS TO STORE
126F  68                PLA
1270  85 20             STA $20
1272  68                PLA
1273  85 1F             STA $1F
1275  20 E7 DA          JSR $DAE7      ;RMS TO 'RN' OR 'RF'
1278  60                RTS
1279                    .END
1279                    .LIB O:DATA901SRC
1279  A9 00             LDA #<BASE
127B  85 FE             STA $FE
127D  85 34             STA $34
127F  A9 7C             LDA #>BASE
1281  85 FF             STA $FF
1283  85 35             STA $35
1285  A0 01             LDY #$01
1287  A9 40             LDA #$40
1289  2C 82 93    WAIT4 BIT PBB        ;WAIT FOR CYCLE LOW
128C  D0 FB             BNE WAIT4      ;(I.E. RECORD ENDS)
128E  A9 10             LDA #$10       ;DOE LOW
1290  8D 82 93          STA PBB
1293  A9 00             LDA #$00       ;DOR LOW
1295  8D 82 93          STA PBB
1298  A9 08             LDA #$08
129A  2C 82 93    WAIT5 BIT PBB        ;WAIT FOR DOF HIGH
129D  F0 FB             BEQ WAIT5
129F  AD 80 93          LDA PAB        ;GET 1ST WORD
12A2  8D 00 7C          STA BASE
12A5  EE 82 93    LOOP6 INC PBB
12A8  CE 82 93          DEC PBB        ;WORD REQUEST
12AB  A9 02             LDA #$02
12AD  2C 82 93    WAIT6 BIT PBB        ;WAIT FOR DATA READY
12B0  F0 FB             BEQ WAIT6
```

```
12B2  AD 80 93          LDA PAD
12B5  91 FE             STA ($FE),Y      ;STORE @ $3C01 UP
12B7  C8                INY
12B8  D0 EB             BNE LOOP6
12BA  E6 FF             INC $FF
12BC  A5 FF             LDA $FF
12BE  C9 80             CMP #$80         ;TEST FOR END OF TRANSFER
12C0  90 E3             BCC LOOP6
12C2  EE 82 93          INC PBD
12C5  CE 82 93          DEC PBD          ; LAST WORD REQUEST
12C8  A9 20             LDA #$20
12CA  8D 82 93          STA PBD          ;DISABLE DL901 O/P
12CD  A9 7C             LDA #>BASE
12CF  85 FF             STA $FF          ;RE-INITIALISE ADDRESS POINTER
12D1                    .END
12D1                    .LIB 0:WAVESRC/3
12D1              ;SUBROUTINE TO CALCULATE THE MEAN OF 1K OF DATA ($7C00-$7FFF)
12D1              TOTAL=$0054
12D1              LEAST=$0FFC
12D1              MOST=$0FFD
12D1  A9 FF             LDA #$FF
12D3  8D FC 0F          STA LEAST
12D6  A9 00             LDA #$00
12D8  8D FD 0F          STA MOST
12DB  A2 0F             LDX #$0F
12DD  95 5E       AVE1  STA EXP1,X
12DF  CA                DEX
12E0  D0 FB             BNE AVE1
12E2  A9 88             LDA #$88
12E4  85 5E             STA EXP1
12E6  A0 00             LDY #$00
12E8  A9 00       AVE5  LDA #$00
12EA  85 68             STA EXP2+2
12EC  85 69             STA EXP2+3
12EE  85 6A             STA EXP2+4
12F0  B1 FE             LDA ($FE),Y
12F2  AA                TAX              ;CONVERT VOLTAGE TO WIND SPEED
```


LINE# LOC CODE LINE

34

```
12F3  BD 00 7B          LDA $7B00,X
12F6  CD FD 0F          CMP MOST
12F9  90 03             BCC AVE10        ;BRANCH IF A < MOST
12FB  8D FD 0F          STA MOST
12FE  CD FC 0F    AVE10 CMP LEAST
1301  B0 03             BCS AVE11        ;BRANCH IF A >= LEAST
1303  8D FC 0F          STA LEAST
1306  85 67       AVE11 STA EXP2+1
1308  A2 88             LDX #$88
130A  E4 5E       AVE3  CPX EXP1
130C  F0 0C             BEQ AVE2
130E  46 67             LSR EXP2+1
1310  66 68             ROR EXP2+2
1312  66 69             ROR EXP2+3
1314  66 6A             ROR EXP2+4
1316  E8                INX
1317  4C 0A 13          JMP AVE3
131A  A2 04       AVE2  LDX #$04
131C  18                CLC
131D  B5 5E       AVE4  LDA EXP1,X
131F  75 66             ADC EXP2,X
1321  95 5E             STA EXP1,X
1323  CA                DEX
1324  D0 F7             BNE AVE4
1326  90 0A             BCC AVE7         ;TEST FOR OVERFLOW
1328  E6 5E             INC EXP1
132A  66 5F             ROR EXP1+1
132C  66 60             ROR EXP1+2
132E  66 61             ROR EXP1+3
1330  66 62             ROR EXP1+4
1332  C8          AVE7  INY
1333  D0 B3             BNE AVE5
1335  E6 FF             INC $FF
1337  A5 FF             LDA $FF
1339  C9 80             CMP #$80
133B  90 AB             BCC AVE5
133D  A5 5F             LDA EXP1+1
```

```
133F  30 0D      AVE8   BMI AVE6       ;TEST FOR NON-NORMALISED RESULT
1341  C6 5E             DEC EXP1
1343  06 62             ASL EXP1+4
1345  26 61             ROL EXP1+3
1347  26 60             ROL EXP1+2
1349  26 5F             ROL EXP1+1
134B  4C 3F 13          JMP AVE8
134E  A5 5E      AVE6   LDA EXP1
1350  38                SEC
1351  E9 0A             SBC #$0A       ;DIVIDE BY 1024
1353  85 5E             STA EXP1
1355  38                SEC
1356  AD FE 0F          LDA POINTL
1359  E9 05             SBC #$05
135B  8D FE 0F          STA POINTL
135E  B0 03             BCS AVE9
1360  CE FF 0F          DEC POINTH
1363  AE FE 0F   AVE9   LDX POINTL
1366  AC FF 0F          LDY POINTH
1369  20 E3 DA          JSR $DAE3
136C  18                CLC
136D  A5 2A             LDA $2A
136F  69 1E             ADC #$1E
1371  85 1F             STA $1F
1373  A5 2B             LDA $2B
1375  69 00             ADC #$00
1377  85 20             STA $20
1379  20 E7 DA          JSR $DAE7
137C  38                SEC            ;CALCULATE RMS OF 1K OF DATA
137D  AD FE 0F          LDA POINTL
1380  E9 05             SBC #$05
1382  8D FE 0F          STA POINTL
1385  B0 03             BCS AVE18
1387  CE FF 0F          DEC POINTH
138A  A2 04      AVE18  LDX #$04
138C  A9 00             LDA #$00
138E  95 54      AVE24  STA TOTAL,X
```

O:MASTERSRC/4......PAGE 0014

LINE# LOC CODE LINE

```
1390  CA                DEX
1391  D0 FB             BNE AVE24
1393  A9 90             LDA #$90
1395  85 54             STA TOTAL
1397  A9 00             LDA #<BASE     ;CALCULATE SIGMA(X*X)
1399  85 FE             STA $FE
139B  A9 7C             LDA #>BASE
139D  85 FF             STA $FF
139F  A0 00             LDY #$00
13A1  A9 00      AVE12  LDA #$00
13A3  85 66             STA EXP2
13A5  85 60             STA EXP1+2
13A7  85 68             STA EXP2+2
13A9  85 61             STA EXP1+3
13AB  85 69             STA EXP2+3
13AD  85 62             STA EXP1+4
13AF  85 6A             STA EXP2+4
13B1  B1 FE             LDA ($FE),Y
13B3  AA                TAX
13B4  BD 00 7B          LDA $7B00,X
13B7  85 67             STA EXP2+1
13B9  85 5F             STA EXP1+1
13BB  A9 90      AVE25  LDA #$90
13BD  85 5E             STA EXP1
13BF  98                TYA
13C0  48                PHA
13C1  20 3F D9          JSR $D93F      ;ACCN1=X*X
13C4  68                PLA
13C5  A8                TAY
13C6  A6 5E             LDX EXP1
13C8  E4 54      AVE20  CPX TOTAL      ;COMPARE ACCN1 WITH TOTAL
13CA  F0 0C             BEQ AVE19
13CC  46 5F             LSR EXP1+1
13CE  66 60             ROR EXP1+2
13D0  66 61             ROR EXP1+3
13D2  66 62             ROR EXP1+4
13D4  E8                INX
```

```
13D5  4C C8 13          JMP AVE20
13D8  A2 04      AVE19  LDX #$04        ;ADD ACC#1 TO TOTAL
13DA  18                CLC
13DB  B5 5E      AVE21  LDA EXP1,X
13DD  75 54             ADC TOTAL,X
13DF  95 54             STA TOTAL,X
13E1  CA                DEX
13E2  D0 F7             BNE AVE21
13E4  90 0A             BCC AVE23       ;TEST FOR OVERFLOW
13E6  E6 54             INC TOTAL
13E8  66 55             ROR TOTAL+1
13EA  66 56             ROR TOTAL+2
13EC  66 57             ROR TOTAL+3
13EE  66 58             ROR TOTAL+4
13F0  C8         AVE23  INY
13F1  D0 AE             BNE AVE12       ;TEST FOR END OF PAGE
13F3  E6 FF             INC $FF
13F5  A5 FF             LDA $FF
13F7  C9 80             CMP #$80        ;TEST FOR END OF 1K
13F9  90 A6             BCC AVE12
13FB  A5 55             LDA TOTAL+1     ;TEST FOR NON-NORMALISED RESULT
13FD  30 0D      AVE14  BMI AVE13
13FF  C6 54             DEC TOTAL
1401  06 58             ASL TOTAL+4
1403  26 57             ROL TOTAL+3
1405  26 56             ROL TOTAL+2
1407  26 55             ROL TOTAL+1
1409  4C FD 13          JMP AVE14
140C  38         AVE13  SEC
140D  A5 54             LDA TOTAL
140F  E9 0A             SBC #$0A        ;DIVIDE BY 1024
1411  85 54             STA TOTAL
1413  AD FE 0F          LDA POINTL
1416  85 1F             STA $1F
1418  AD FF 0F          LDA POINTH
141B  85 20             STA $20
141D  18                CLC
```


LINE# LOC CODE LINE

```
141E  A5 2A             LDA $2A
1420  69 25             ADC #$25
1422  85 1F             STA $1F
1424  A5 2B             LDA $2B
1426  69 00             ADC #$00
1428  85 20             STA $20
142A  AD FE 0F          LDA POINTL
142D  85 FE             STA $FE
142F  AD FF 0F          LDA POINTH
1432  85 FF             STA $FF
1434  A0 04             LDY #$04
1436  B9 54 00   AVE22  LDA TOTAL,Y
1439  91 1F             STA ($1F),Y
143B  91 FE             STA ($FE),Y
143D  88                DEY
143E  10 F6             BPL AVE22
1440  38                SEC
1441  AD FE 0F          LDA POINTL
1444  E9 02             SBC #$02
1446  8D FE 0F          STA POINTL
1449  85 1F             STA $1F
144B  AD FF 0F          LDA POINTH
144E  E9 00             SBC #$00
1450  8D FF 0F          STA POINTH
1453  85 20             STA $20
1455  A0 01             LDY #$01
1457  AD FD 0F          LDA MOST
145A  91 1F             STA ($1F),Y
145C  88                DEY
145D  AD FC 0F          LDA LEAST
1460  91 1F             STA ($1F),Y
1462  60                RTS
1463                    .END
1463                    .LIB O:SAVESRC/3
1463             ;SUBROUTINE TO SAVE DATA
1463  A2 08             LDX #$08
1465  86 D4             STX $D4         ;DEVICE NO. (8 FOR DISC)
```

```
0593  1467  CA              DEX
0594  1468  86 B4           STX $B4         ;BUFFER CHARACTER (SIMULATES SAVE INSTRUCTION)
0595  146A  A9 00           LDA #$00
0596  146C  85 9D           STA $9D         ;LOAD/VERIFY FLAG
0597  146E  18              CLC
0598  146F  A5 2A           LDA $2A
0599  1471  69 2C           ADC #$2C
0600  1473  85 1F           STA $1F
0601  1475  A5 2B           LDA $2B
0602  1477  69 00           ADC #$00
0603  1479  85 20           STA $20
0604  147B  A0 00           LDY #$00
0605  147D  18              CLC
0606  147E  B1 1F           LDA ($1F),Y
0607  1480  69 02           ADC #$02
0608  1482  85 D1           STA $D1         ;FILE NAME LENGTH
0609  1484  C8              INY
0610  1485  38              SEC
0611  1486  B1 1F           LDA ($1F),Y
0612  1488  E9 02           SBC #$02
0613  148A  85 DA           STA $DA         ;FILE NAME ADDRESS LOW
0614  148C  C8              INY
0615  148D  B1 1F           LDA ($1F),Y
0616  148F  E9 00           SBC #$00
0617  1491  85 DB           STA $DB         ;FILE NAME ADDRESS HIGH
0618  1493  A0 00           LDY #$00
0619  1495  A9 30           LDA #'0         ;FOR DISK DRIVE NO. 0
0620  1497  91 DA           STA ($DA),Y
0621  1499  C8              INY
0622  149A  A9 3A           LDA #':         ;DELIMITER
0623  149C  91 DA           STA ($DA),Y
0624  149E  AD FE 0F        LDA POINTL
0625  14A1  85 FB           STA $FB         ;START ADDRESS LOW
0626  14A3  AD FF 0F        LDA POINTH
0627  14A6  85 FC           STA $FC         ;START ADDRESS HIGH
0628  14A8  A9 00           LDA #$00
0629  14AA  85 C9           STA $C9         ;END ADDRESS LOW
```



```
LINE# LOC CODE LINE

0630  14AC  A9 7C           LDA #$7C
0631  14AE  85 CA           STA $CA         ;END ADDRESS HIGH
0632  14B0  20 A4 F6        JSR $F6A4       ;PERFORM SAVE
0633  14B3  60              RTS
0634  14B4                  .END
0635  14B4                  .END

ERRORS = 0000

SYMBOL TABLE

SYMBOL VALUE
 ACR     960B    ATT1    11CC    ATT2    11B7    ATT3    119F
 ATT4    11D2    AVE1    12DD    AVE10   12FE    AVE11   1306
 AVE12   13A1    AVE13   140C    AVE14   13FD    AVE18   138A
 AVE19   13D8    AVE2    131A    AVE20   13C8    AVE21   13DB
 AVE22   1436    AVE23   13F0    AVE24   138E    AVE25   13BB
 AVE3    130A    AVE4    131D    AVE5    12EB    AVE6    134E
 AVE7    1332    AVE8    133F    AVE9    1363    BASE    7C00
 BGD1    1201    BGD2    1213    DDRA    9603    DDRAB   9381
 DDRB    9602    DDRBB   9383    DELY    10FB    ENT1    100B
 ERR     10DE    ERR1    10F2    ERR2    10EA    ERR3    10E1
 EXP1    005E    EXP2    0066    IER     960E    IFR     960D
 IRA     9601    JUMP1   1158    JUMP2   115A    JUMP3   117C
 JUMP4   1194    JUMP6   10A7    JUMP7   10D6    LEAST   0FFC
 LOOP1   112B    LOOP2   114B    LOOP3   116C    LOOP4   117F
 LOOP5   10C7    LOOP6   12A5    MOST    0FFD    NMI     1131
 ORB     9600    OVER    0FFB    PAB     9380    PBB     9382
 PCR     960C    POINTH  0FFF    POINTL  0FFE    RATN    9282
 REC     1106    RMS     1076    RMS1    1094    RMSA    1097
 RMSB    109A    RMSC    10B9    RMSD    1088    RMSE    1084
 RMSF    10C5    RMSG    10B9    SD1     1222    SD10    1269
 SD2     122D    SD8     123B    SD9     1241    SUM     1145
 T2CH    9609    T2LL    9608    TOTAL   0054    WAIT1   1100
```

```
1000 A$=""
1100 F=F+1:IFF>1GOTO1300
1200 LOAD"1:MASTERMC",8
1300 PRINT"DO YOU REQUIRE A CALIBRATION"
1400 GETA$:IFA$=""GOTO1400
1500 IFA$="Y"THEN GOSUB7400
1510 PRINT"SET FILTERS TO 250HZ.":PRINT"SET TIGGER TO 'INT'"
1600 INPUT"HOW MANY PASSES AT EACH OCTAVE BAND     (1 TO 80)";N
1700 IFN<1ORN>80THENPRINT"OUT OF RANGE":GOTO1600
1800 POKE4083,0:POKE4084,60
1900 FORX=0TO4
2000 POKE37505,255:POKE37504,2^(4-X)
2100 F=(2^X)*250*2^-.5:D=1:Y=0
2200 IF1>FGOTO2400
2300 F=F/10:D=D*2:GOTO2200
2400 G=INT(F*100)
2500 G=INT(G/10)*16+INT(G-INT(G/10)*10)
2600 POKE4428+Y,G:POKE4429+Y,D/2
2700 IFY=2GOTO2900
2800 F=F*2:Y=2:GOTO2200
2900 SYS(4432):REM FILTER
3000 SYS(4510):REM ATTENUATOR
3100 POKE38400,PEEK(38400)AND253
3200 Z=PEEK(38401)
3300 POKE38400,PEEK(38400)OR2
3400 Z=PEEK(38401)
3500 FORZ=0TO1000:NEXT
3600 FORZ=1TON
3650 SYS(4660):REM BACKGROUND
3700 SYS(4293):REM RECORD
3800 SYS(4601):REM NEAR CHANNEL
3900 SYS(4604):REM FAR CHANNEL
4000 SYS(4708):REM MET. DATA
4100 F=PEEK(4083)-2
4200 IFF<0THENF=256+F:POKE4084,(PEEK(4084)-1)
4250 POKE(4083),F
4300 POKE(PEEK(4084)*256+PEEK(4083)+1),PEEK(37504):REM RECORD FILTER SETTING
4400 POKE(PEEK(4084)*256+PEEK(4083)),PEEK(37506):REM RECORD ATTEN. SETTING
4500 NEXT
4600 POKE36866,1
4700 FORA=1TO3
4800 POKE36864,(PEEK(36864)AND254)
4900 FORZ=0TO30:NEXT
5000 POKE36864,(PEEK(36864)OR1)
5100 FORZ=0TO30:NEXT
5200 NEXT
5300 NEXT
5400 A=PEEK(4084)*256+PEEK(4083)-10:REMSAVE CALIBRATIONS
5500 FORZ=0TO9
5600 POKE(A+Z),PEEK(4086+Z)
5700 NEXT
5800 POKE(A-1),N
5900 GOSUB6700
6000 F=PEEK(4083)-11
6100 IFF<0THENF=256+F:POKE4084,(PEEK(4084)-1)
6150 POKE(4083),F
6200 POKE52,0:POKE53,64
6300 POKE48,0:POKE49,64
6400 INPUT"INPUT DATA FILENAME";A$
6500 SYS(5282)
6600 END
6700 FORA=0TO34:REM FILTER SET 4K TO 250 HZ
6800 POKE36864,(PEEK(36864)AND254)
6900 FORZ=0TO30:NEXT
7000 POKE36864,(PEEK(36864)OR1)
7100 FORZ=0TO30:NEXT
7200 NEXT
7300 RETURN
7400 PRINT"SET FILTERS TO 1K":PRINT"SET TRIGGER TO 'EXT'"
7410 PRINT"NEAR MIC. FIRST. PRESS A KEY  TO CONTINUE"
7500 GETA$:IFA$=""GOTO7500
7600 SYS(4293)
7700 SYS(4096):REM CALIBRATE NEAR MIC.
7800 PRINT"NOW 2ND. MIC. PRESS A KEY  TO CONTINUE"
7900 GETA$:IFA$=""GOTO7900
8000 SYS(4293)
8100 SYS(4105)
8200 RETURN
READY.
```

```
1000 CN=0:CF=0:TU=0:WS=0:RF=0:RN=0
1010 INPUT"CALIBRATION LEVEL ON FAR CHANNEL";L
1020 INPUT"HOW MANY PASSES PER BAND";P
1030 P=15360-P*125-11
1040 OPEN4,4
1050 N=PEEK(P):REM***********NO. PASSES/BAND
1060 P=P+1:REM**************POINTER TO DATA
1062 PRINT"INPUT CALIBRATIONS (Y OR N)"
1064 GET A$:IFA$=""GOTO1064
1067 IF A$="Y"GOTO1094
1070 FORB=0TO7STEP7
1080 GOSUB5000:REM**********CALIBRATION
1090 NEXT
1092 GOTO 1100
1094 P=P+10
1097 INPUT"NEAR CHANNEL,FAR CHANNEL";CN,CF
1100 PRINT#4,"NEAR CHANNEL CALIBRATION=";CN,"FAR CHANNEL CALIBRATION=";CF
1200 FORX=0TO4:REM***********FILTER COUNTER
1205 C=0:D=0:MN=0:MF=0
1210 PRINT#4:PRINT#4
1250 PRINT#4,CHR$(13):GOSUB8000
1260 PRINT#4,CHR$(124);" CENTRE FREQUENCY="250*2^(4-X);TAB(10);
1265 PRINT#4,"NO. OF PASSES =";N;TAB(74);CHR$(124)
1267 GOSUB8000
1270 PRINT#4,CHR$(124);" NEAR CHANNEL";TAB(28);CHR$(124); " FAR CHANNEL";
1275 PRINT#4,TAB(29);CHR$(124);" MET. DATA";TAB(31);CHR$(124)
1277 GOSUB8000
1280 PRINT#4,CHR$(124);" RMS (DB)";TAB(4);CHR$(124);" RUN.AVE (DB)";
1285 PRINT#4,CHR$(124);" STD.DEV (DB)";
1290 PRINT#4,CHR$(124);" RMS (DB)";TAB(4);CHR$(124);" RUN.AVE (DB)";
1295 PRINT#4,CHR$(124);" STD.DEV (DB)";
1297 PRINT#4,CHR$(124);" %TURBULENCE ";CHR$(124);" TEMP(C)";TAB(5);CHR$(124);
1298 PRINT#4," W.DIR.(DEG) ";CHR$(124)
1299 GOSUB8000
1300 FORZ=1TON
1400 AT=PEEK(P)-1:P=P+1:REM*****ATTENUATOR SETTING
1500 IFPEEK(P)<>2^XTHENPRINT"ERROR"
1600 P=P+1
1610 TP=(PEEK(P)*256+PEEK(P+1))/2500:P=P+2:REM**TEMP. IN DEG. C
1700 WD=PEEK(P)*2:P=P+1:REM****WIND DIRECTION IN DEGREES
1800 FORB=14TO35STEP7
1900 GOSUB5000
2000 NEXT
2100 IFRN<0THENPRINT#4,"OVERLOAD ON NEAR CHANNEL":RN=-RN
2200 IFRF<0THENPRINT#4,"OVERLOAD ON FAR CHANNEL":RF=-RF
2600 RN=SQR(RN):RF=SQR(RF)
2700 DN=20*LOG(RN/CN)/LOG(10)+94
2800 DF=20*LOG(RF/CF)/LOG(10)+L+AT
2850 IFF<0GOTO3800
2900 C=(C+RN)
2910 MN=(MN+RN*RN)
3000 D=(D+RF)
3010 MF=(MF+RF*RF)
3100 AN=20*LOG(C/(Z*CN))/LOG(10)+94
3200 AF=20*LOG(D/(Z*CF))/LOG(10)+L+AT
3250 IFZ=1GOTO3770
3300 SN=SQR((MN/Z)-(C/Z)^2)
3400 SN=-20*LOG(1-(SN*Z)/C)/LOG(10)
3600 SF=SQR((MF/Z)-(D/Z)^2)
3700 SF=-20*LOG(1-(SF*(Z+F))/D)/LOG(10)
3750 GOTO3800
3770 SN=0:SF=0
3800 TU=SQR(-TU-WS*WS)
3805 TR=400*WS*TU/(WS*WS-346*346)
3810 Y=DN:GOSUB7000:Y=AN:GOSUB7000:Y=SN:GOSUB7000
3820 Y=DF:GOSUB7000:Y=AF:GOSUB7000:Y=SF:GOSUB7000
3830 Y=TR:GOSUB7000:Y=TP:GOSUB7000:Y=WD:GOSUB7000
3900 PRINT#4,CHR$(124);CHR$(27);CHR$(120);CHR$(13)
4000 NEXT
4050 FORQ=0TO2000:NEXT:GOSUB8000
4100 NEXT
4900 END
5000 FORA=2TO6
5200 POKE(PEEK(43)*256+PEEK(42)+A+B),PEEK(P):P=P+1
5300 NEXT
5600 RETURN
7000 PRINT#4,CHR$(124);CHR$(27);CHR$(108);INT(Y*1000)/1000;CHR$(13);TAB(13);
7100 RETURN
8000 FORQ=0TO127:PRINT#4,"-";:NEXT:PRINT#4,CHR$(13)
8100 RETURN
READY.
```

```
500 IFDA>0GOTO905
600 CN=0:CF=0:TU=0:US=0:RF=0:RN=0
700 REM VERSION      TO PRODUCE DATA.FILE ;20PASSES,5FREQS,NDAYS
800 DA=1
810 INPUT"DRIVE NO. (3=END)";A$
815 IF A$="3"THEN END
820 INPUT"FILE NAME";B$
830 A$=A$+":"+B$:LOADA$,8
905 REM EXE PETP.FOR
910 DATA 69,88,69,32,80,69,84,80,46,70,79,82,13,-1
920 READA
930 IFA<0THEN970
940 POKE165,A
950 SYS(41889)
960 GOTO920
970 SYS(805)
980 POKE1,0:POKE2,3
1010 INPUT"CALIBRATION LEVEL ON FAR CHANNEL";L
1020 INPUT"NO. PASSES/BAND";XX
1030 REMP=12849:REM START OF DATA
1040 P=3*4096+12*256-XX*125-11
1050 N=PEEK(P):REM**********NO. PASSES/BAND
1060 P=P+1:REM**************POINTER TO DATA
1062 PRINT"INPUT CALIBRATIONS (Y OR N)"
1064 GET A$:IFA$=""GOTO1064
1067 IF A$="Y"GOTO1094
1070 FORB=0TO7STEP7
1080 GOSUB5000:REM**********CALIBRATION
1090 NEXT
1092 GOTO 1100
1094 P=P+10
1097 INPUT"NEAR CHANNEL,FAR CHANNEL";CN,CF
1100 PRINT"NEAR CHANNEL CALIBRATION=";CN,"FAR CHANNEL CALIBRATION=";CF
1200 FORX=0TO4:REM***********FILTER COUNTER
1205 C=0:D=0:MN=0:MF=0
1300 FORZ=1TO10
1400 AT=LOG(PEEK(P))/LOG(2):P=P+1:REM*****ATTENUATOR SETTING
1500 IFPEEK(P)<>2^(4-X)THENPRINT"ERROR"
1600 P=P+1
1608 REM TP=(PEEK(P)*256+PEEK(P+1))/2500
1610 P=P+2:REM BY-PASS TEMP.DATA
1800 FORB=14TO35STEP7
1900 GOSUB5000
2000 NEXT
2040 REM WD=PEEK(P)*2:REM****WIND DIRECTION IN DEGREES
2050 P=P+1:REM BY-PASS W.DIR. DATA
2100 IFRN<0THENPRINT"OVERLOAD ON NEAR CHANNEL":RN=-RN
2200 IFRF<0THENPRINT"OVERLOAD ON FAR CHANNEL":RF=-RF
2600 RN=SQR(RN):RF=SQR(RF)
2700 DN=20*LOG(RN/CN)/LOG(10)+94
2800 DF=20*LOG(RF/CF)/LOG(10)+L+AT
3800 TU=SQR(-TU-US*US):TV=(US*US-346*346)
3805 TR=400*US*TU/TV
3810 WV=(TV/(.44*309*309))^2
3820 D=USR(DN-DF):D=USR(TR):D=USR(WV):REM:D=USR(WD):D=USR(TP)
3830 SYS(3*256+26)
3840 SYS(805)
4000 NEXT
4100 NEXT
4200 GOTO810
5000 FORA=2TO6
5200 POKE(PEEK(43)*256+PEEK(42)+A+B),PEEK(P):P=P+1
5300 NEXT
5600 RETURN
READY.
```